

# **Sex-Specific Biology of *Plasmodium falciparum***

Melanie Claire Ridgway

May, 2019

A thesis submitted for the degree of Doctor of  
Philosophy of The Australian National University



**Australian  
National  
University**

© Copyright by Melanie Claire Ridgway 2019  
All Rights Reserved

## Declaration

The work presented in this thesis is my own with the exception of the generous contributions acknowledged below.

Phuong Tran generated the gABCG2-GFP *P. falciparum* parasite line, made the plasmids for the disruption of sphingomyelin synthase genes and prepared the culture medium samples for lipidomics. Harpreet Vohra and Michael Devoy provided assistance with sorting male and female gametocytes. Daniela Cihalova conducted part of the experiment yielding Supplementary Figure 4. Manuel Rauch prepared *P. berghei* samples for lipidomics and counted the number of cells per mosquito salivary gland. Simon Brown performed the direct infusion MSMS lipidomics measurements on all samples. Library preparation and whole genome bisulfite sequencing was commercially performed at the Ramaciotti Centre for Genomics. Aaron Jex performed the bioinformatics analysis of the bisulfite sequences.

The word count for this thesis excluding tables, figures, bibliographies and appendices is 40,489 words.

Melanie Claire Ridgway  
May, 2019

## **Acknowledgement**

Thank you to my supervisor Alexander Maier for supporting my pursuit of a well-rounded PhD experience and to my associate supervisors Aaron Jex, Kevin Saliba and Giel van Dooren for their thoughtful guidance and encouragement.

This thesis would not have been possible without the generous contributions from Aaron Jex, Simon Brown, Manuel Rauch, Harpreet Vohra, Michael Devoy, Phuong Tran and Daniela Cihalova. Thank you for your time dedicated to this project and for making it such a pleasure to work with you.

To the other Maier lab students past and present, Babette Beher, Merryn Fraser, Julie-Anne Gabelich, Richa Harnal, François Korbmacher, Ben Lodder, Mrinalini Pratap, Prince Sebastian, Mona Shahali, Cameron Tate, Emma Wisdom, Renate Zelger and Meng Zhang: thank you for passing on your wisdom, sharing lab duties and for entertaining me through hours of culturing.

I would like to acknowledge the Australian Government for my Research Training Program Scholarship and The Australian National University (ANU) Research School of Biology for my supplementary scholarship. I am also grateful to the Australian Society for Parasitology, the Burroughs Wellcome Fund, the European Molecular Biology Laboratories Australia and the Alexander von Humboldt Foundation for generously funding travel related to my PhD.

My PhD also benefited from the broader ANU parasitology community who provided insightful feedback throughout my project. I am particularly grateful to Adele Lehane and Kiaran Kirk for introducing me to parasitology and for their continued mentorship. Thanks also to my parasitology friends Adelaide Dennis, Sanduni Hapuarachchi, Esther Rajendran, James Rosling, Edwin Tjhin and Erick Tjhin, for both helping and distracting me from my research.

And last but not least, thank you to my friends and family for cheering me on.

## Abstract

Malaria, caused by *Plasmodium* parasites, is responsible for almost 500,000 deaths annually. Disease transmission requires the parasite to differentiate into male and female gametocytes in human red blood cells prior to sexual reproduction upon ingestion by a mosquito. This thesis addresses fundamental questions about the sex-specific development of *Plasmodium* gametocytes to guide transmission-blocking antimalarial interventions.

Although *Plasmodium* depends on host nutrients to survive, the lifecycle of the malaria parasite spans radically different host environments, particularly in terms of lipid composition. In culture, asexual *P. falciparum* proliferation is accompanied by stage-specific lipid modifications such as increasing phosphatidylcholine during membrane biogenesis. *In vivo* *P. berghei* lifecycle progression in the mouse and mosquito is accompanied by changes in lipid composition, with gametocytes apparently synthesising lipids *de novo* in preparation for transmission. Parasite species-specific lipid changes to the host red blood cell reflect differences in the lipid composition of their respective host species, suggesting host-parasite co-evolution of lipid metabolism.

Investigation of gametocyte biology in a sex-specific manner required the development of a novel method to sort male and female gametocytes. The technique is applied to validate novel sex-specific gametocyte markers. The role of DNA methylation in sex determination and differentiation in *P. falciparum* is also investigated as a fundamental biology application of this technique.

Lipid metabolism of *P. falciparum* gametocytes is next investigated in a sex-specific manner. Female gametocytes stockpile neutral lipids and sphingolipids, consistent with female gametocytes being the main contributor of resources for zygote development immediately after fertilisation. Specific lipids appear to be imported from the host and may be essential culture medium supplements for gametocytes. Finally, the biological significance of *de novo* synthesis of key sex-specific gametocyte lipids is investigated by genetic and chemical inhibition of parasite lipid metabolism.

Overall this thesis highlights gametocyte and sex-specific *Plasmodium* traits that could assist with monitoring and blocking malaria transmission.

## List of abbreviations

AC	adenylyl cyclase
ACAT	acetyl CoA: cholesterol acyltransferase
ANOVA	analysis of variance
AP2-G	activating enhancer binding protein 2 gamma
APC-Cy7	allophycocyanin-cyano dye 7
AT	adenosine/thymine
ATP	adenosine triphosphate
bp	base pair
°C	degrees Celsius
CDP	cytidine diphosphate
CE	cholesteryl ester
Cer	ceramide
CL	cardiolipin
cm	centimetre
cm <sup>2</sup>	centimetre squared
CoA	co-enzyme A
CpG	cytosine-guanine
°C/s	degrees Celsius per second
Da	Dalton
DAG	diacylglycerol
DHCer	dihydroceramide
DHSM	dihydrosphingomyelin
DIG-dUTP	alkali-labile digoxigenin deoxyuridine triphosphate
DMSO	dimethyl sulfoxide
DNA	deoxyribonucleic acid
FC	free cholesterol
FAE	fatty acid elongation
FACS	fluorescence activated cell sorting
FAS	fatty acid synthesis
FITC	fluorescein isothiocyanate
×g	gravitational force equivalent
gABCG2	gametocyte ATP-binding cassette transporter family member 2

GFP.....	green fluorescent protein
GO.....	gene ontology
GPI.....	glycosylphosphatidylinositol
h.....	hour
hDHFR.....	human dihydrofolate reductase
HEPES.....	4-(2-hydroxyethyl)-1-piperazineethanesulfonic acid
hpi.....	hours post invasion
kb.....	kilo base pairs
KO.....	knock out
LCAT.....	lecithin : cholesterol acyltransferase
LPC.....	lysophosphatidylcholine
M.....	moles per litre
mg/kg.....	milligram per kilogram
mg/mL.....	milligram per millilitre
min.....	minutes
mJ/cm <sup>2</sup> .....	milliJoules per centimetre squared
mL.....	millilitre
mm.....	millimetre
mM.....	millimoles per litre
mRNA.....	messenger ribonucleic acid
m/s.....	metres per second
MS.....	mass spectrometry
MSMS.....	tandem mass spectrometry
μF.....	microFaraday
μg.....	microgram
μg/mL.....	microgram per millilitre
μL.....	microlitre
μm.....	micrometre
μM.....	micromoles per litre
NADH.....	nicotinamide adenine dinucleotide (reduced)
NADP.....	nicotinamide adenine dinucleotide phosphate
nm.....	nanometre
nM.....	nanomoles per litre
P25 or <i>pfs25</i> .....	ookinete surface protein (PF3D7_1031000)

P230 or <i>pfs230p</i> .....	6 cystein protein (PF3D7_0208900)
PBLAST.....	protein basic local alignment search tool
PBS.....	phosphate buffered saline
PC.....	phosphatidylcholine
PCR.....	polymerase chain reaction
PE.....	phosphatidylethanolamine
PG.....	phosphatidylglycerol
PHIST.....	<i>Plasmodium</i> helical interspersed subtelomeric
PlasmoDB.....	<i>Plasmodium</i> Genomics Resource
PS.....	phosphatidylserine
PVM.....	parasitophorous vacuole membrane
qPCR.....	quantitative polymerase chain reaction
qRTPCR.....	quantitative reverse transcriptase polymerase chain reaction
RBC.....	red blood cell
RNA.....	ribonucleic acid
RPMI.....	Roswell Park Memorial Institute
rRNA.....	ribosomal ribonucleic acid
s.....	second
SCC.....	sodium chloride/citric acid buffer
SM.....	sphingomyelin
SMS.....	sphingomyelin synthase
TAG.....	triacylglycerol
TBE.....	Tris/boric acid/ethylenediaminetetraacetic acid
TE.....	Tris base/ethylenediaminetetraacetic acid
tRNA.....	transfer ribonucleic acid
U/mL.....	enzyme unit per millilitre
UV.....	ultra violet
V.....	volts
v/v.....	volume per volume
WT.....	wild type
w/v.....	weight per volume



## Table of contents

<b>Sex-specific biology of <i>Plasmodium falciparum</i></b> .....	<b>1</b>
<b>Declaration</b> .....	<b>3</b>
<b>Acknowledgement</b> .....	<b>4</b>
<b>Abstract</b> .....	<b>5</b>
<b>List of abbreviations</b> .....	<b>6</b>
<b>Table of contents</b> .....	<b>9</b>
<b>Introduction</b> .....	<b>11</b>
<b>1. Malaria disease and diagnostics</b> .....	<b>12</b>
<b>2. <i>Plasmodium</i>, causative agent of malaria</b> .....	<b>13</b>
2.1. <i>Plasmodium</i> species and the origin of human malaria.....	13
2.2. <i>Plasmodium</i> lifecycle and targets for antimalarial interventions .....	15
<b>3. Sex and sex determination</b> .....	<b>18</b>
3.1. Definition of sex .....	18
3.2. Models of sex determination .....	19
3.3. Sex determination in <i>Plasmodium</i> .....	20
<b>4. The host environments of <i>Plasmodium</i> gametocytes</b> .....	<b>21</b>
<b>5. Lipid structures, functions and sources</b> .....	<b>23</b>
5.1. Lipid classes and cellular functions .....	23
5.2. Lipid sources.....	27
5.3. Lipid metabolism.....	30
<b>6. Research Aims</b> .....	<b>35</b>
<b>Materials and Methods</b> .....	<b>37</b>
<b>1. Materials</b> .....	<b>38</b>
1.1. Chemical reagents.....	38
1.2. Ethics approvals and biological reagents .....	38
<b>2. Methods</b> .....	<b>39</b>
2.1. Solution preparation .....	39
2.2. Culturing techniques .....	40
2.3. Microscopy and cell counting .....	43
2.4. Generation of transgenic <i>P. falciparum</i> cell lines .....	43
2.5. Flow cytometry measurements.....	45
2.6. Molecular biology techniques.....	48
2.7. Lipidomic analysis.....	55
2.8. Bisulfite sequencing .....	60
<b>Result Chapter 1</b> .....	<b>61</b>
<b><i>Plasmodium</i> lipid dynamics in the mammalian host and mosquito vector</b> .....	<b>61</b>
<b>Overview</b> .....	<b>62</b>
<b>Part 1: Lipid dynamics during asexual blood stage <i>P. falciparum</i> replication</b> .....	<b>63</b>
Introduction.....	63
Results .....	66
Discussion .....	76
<b>Part 2: Lipid dynamics over the lifecycle of <i>P. berghei</i></b> .....	<b>79</b>
Introduction.....	79
Results .....	80
Discussion .....	102

<b>Part 3: Lipid scavenging in asexual blood stage <i>Plasmodium</i> parasites.....</b>	<b>106</b>
Introduction.....	106
Results .....	107
Discussion .....	109
<b>Conclusion .....</b>	<b>112</b>
<b>Result Chapter 2 .....</b>	<b>114</b>
<b>Novel method and applications for the separation of male and female gametocytes ....</b>	<b>114</b>
<b>Overview .....</b>	<b>115</b>
<b>Part 1: Novel method for the separation of male and female gametocytes .....</b>	<b>116</b>
Introduction.....	116
Results .....	119
Discussion .....	124
<b>Part 2: Sex-specific DNA methylation in <i>P. falciparum</i> .....</b>	<b>127</b>
Introduction.....	127
Results .....	129
Discussion .....	142
<b>Conclusion .....</b>	<b>145</b>
<b>Result Chapter 3 .....</b>	<b>146</b>
<b>Sex-specific lipid metabolism in <i>Plasmodium</i> gametocytes .....</b>	<b>146</b>
<b>Overview .....</b>	<b>147</b>
<b>Part 1: Sex-specific lipid metabolism in <i>P. falciparum</i> gametocytes .....</b>	<b>148</b>
Introduction.....	148
Results .....	149
Discussion .....	170
<b>Part 2: Lipid scavenging in <i>Plasmodium</i> gametocytes .....</b>	<b>178</b>
Introduction.....	178
Results .....	179
Discussion .....	193
<b>Conclusion .....</b>	<b>196</b>
<b>Discussion .....</b>	<b>197</b>
1. Summary of results.....	198
2. Lipidomics as a tool to study parasite biology.....	199
3. Lipid scavenging and synthesis by <i>Plasmodium</i> parasites .....	200
4. The cost of sex for <i>Plasmodium</i> parasites .....	202
5. Confirmation of anisogamy in a unicellular organism .....	203
6. Conclusion .....	204
<b>Supplementary figures .....</b>	<b>205</b>
<b>References .....</b>	<b>218</b>

# Introduction

## 1. Malaria disease and diagnostics

Malaria, caused by infection with *Plasmodium* parasites, is one of the most important parasitic diseases in the world (White et al. 2014; Ashley et al. 2018). In 2017 there were 219 million cases of malaria worldwide, 435,000 of which were lethal (World Malaria Report, 2018). In addition an estimated 12-20 % of stillbirths in Africa, equivalent to 132,000 to 221,000 stillbirths a year, may be attributed to malaria (Moore et al. 2017). The incidence of malaria decreased from 2010 to 2015 but has since stabilised (World Malaria Report, 2018). Global efforts are now switching to eradicating the disease altogether (Snow 2015).

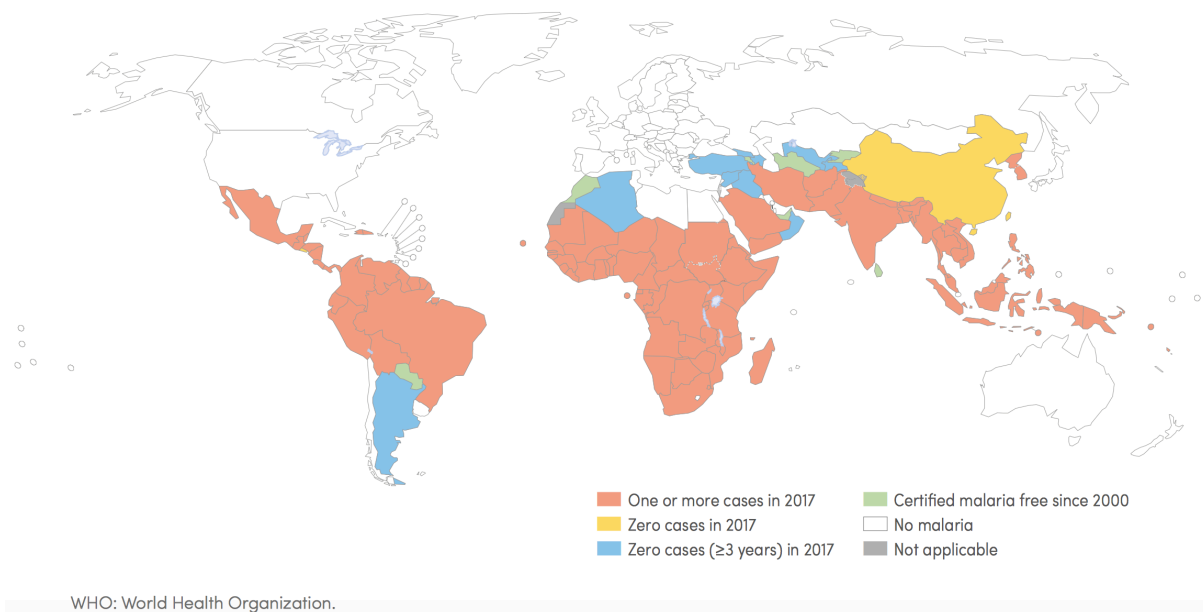


**Figure 1:** Map of current global distribution of malaria cases and progress towards malaria eradication since 2000 (World Malaria Report, 2018).

The latest World Malaria Report based on data collected in 2017 indicates that most cases of malaria (92 %) occur in Africa (Figure 1), followed by South-East Asia (5 % of cases). Four African countries (Nigeria, Democratic Republic of Congo, Mozambique and Uganda), together with India, account for almost half of the global malaria burden. Within these endemic countries, children under the age of 5 accounted for 61 % of malaria-related deaths in 2017 (World Malaria Report, 2018).

Clinical manifestations of malaria include flu-like symptoms such as headache, fatigue, muscle aches, abdominal discomfort and fever (White et al. 2014; Ashley et al. 2018). Frequently symptoms also include vomiting, nausea and hypotension. Mild anaemia, enlarged spleen (especially in children) and liver dysfunction (mostly in adult patients) can occur. Infection with *Plasmodium falciparum* (see section 2) can lead to severe malaria

characterised by seizures and coma (cerebral malaria) or placental malaria in pregnant women, which can lead to foetal growth retardation or stillbirth.

The gold standard for diagnosis of malaria is microscopic detection of *Plasmodium* parasites by Giemsa-stained thick smear. However, the sensitivity of this method depends on adequate microscopist training and is around 10 times less sensitive than molecular testing (Hofmann et al. 2015). Rapid diagnostic tests detect circulating *Plasmodium* antigens and are easy to use (Pham et al. 2018). In 2017 an estimated 75 % of malaria tests were conducted with rapid diagnostic tests (World Malaria Report, 2018). However, rapid diagnostic tests have several limitations including insufficient sensitivity to detect low parasite numbers in asymptomatic individuals, qualitative results rather than quantification of the parasite burden and inability to distinguish between *Plasmodium* species (Pham et al. 2018). Nucleic acid based tests such as quantitative polymerase chain reaction (qPCR) are the most sensitive diagnostic tools currently available and address the aforementioned limitations of rapid diagnostic tests (Pham et al. 2018). However, qPCR is challenging in resource-limited settings since the reagents are heat sensitive and adequate distribution of qPCR machines is economically impractical. The principal application of nucleic acid tests such as qPCR is therefore laboratory-based monitoring of parasite field samples, rather than point of care diagnostics.

## **2. *Plasmodium*, causative agent of malaria**

### **2.1. *Plasmodium* species and the origin of human malaria**

Alphonse Laveran originally identified parasites in the blood of malaria patients as the cause of malaria in the late nineteenth century (Laveran, 1881). Today six species of *Plasmodium* parasites are known to infect humans: *P. falciparum* and *P. vivax* are the most common, although *P. malariae*, two subspecies of *P. ovale* and *P. knowlesi* also cause malaria (White et al. 2014; Ashley et al. 2018). *P. falciparum* is the most virulent parasite and is responsible for the majority of malaria-related deaths (World Malaria Report, 2018). The two subspecies of *P. ovale* were most recently identified: *P. o. curtis* and *P. o. wallikeri* (Sutherland et al. 2010). *P. vivax* and *P. ovale* parasites can lay dormant in the human host and cause malaria relapses years after the initial infection (Krotoski et al. 1982). *P. knowlesi* was originally described as a monkey parasite until widespread human *P. knowlesi* infection was reported in South-East Asia (Cox-Singh et al. 2008).

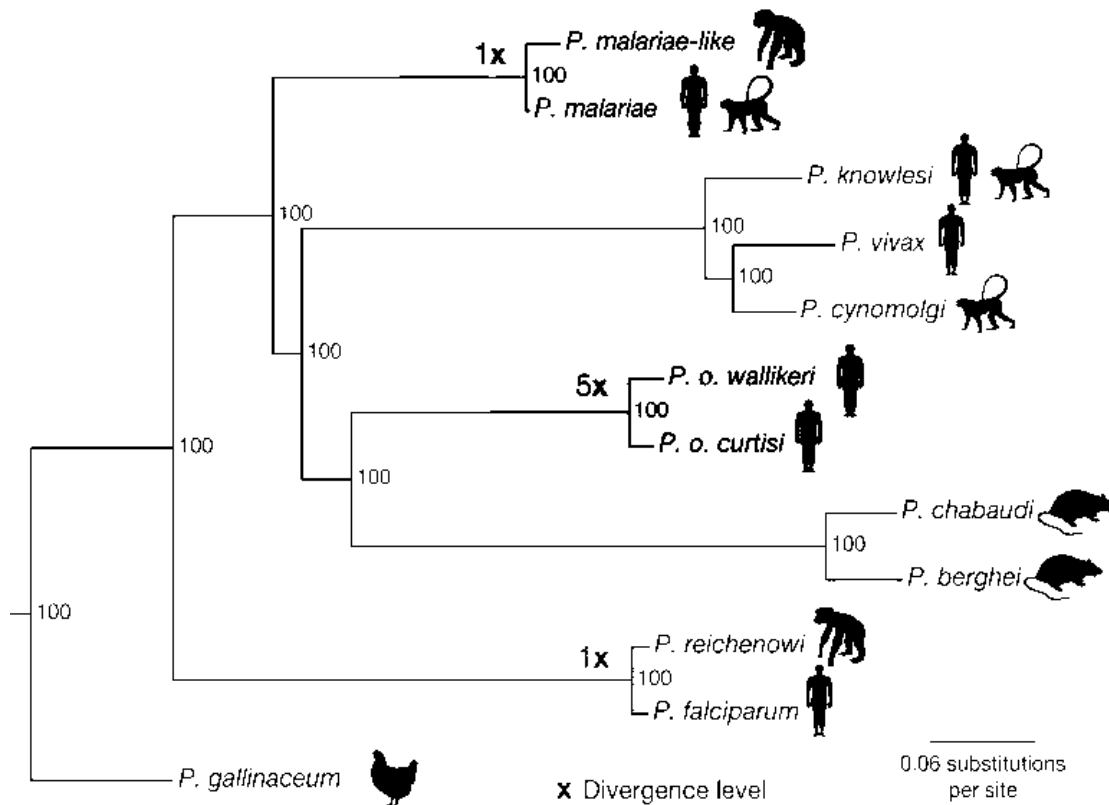


**Figure 2:** Phylogeny of 12 *Plasmodium* species with their vertebrate hosts. Maximum likelihood tree indicates divergence levels normalised to that of *P. falciparum* and *P. reichenowi*, and branching point bootstrap values (Rutledge et al. 2017).

*Plasmodium* parasites can indeed infect a broad range of vertebrates, although each species of *Plasmodium* has a limited range of potential hosts. *P. falciparum* exclusively infects humans but is more closely related to ape *Plasmodium* species such as *P. reichenowi* than other human malaria parasites (Figure 2). Phylogeny suggests *P. falciparum* emerged from host switching of gorilla parasites whereas the ancestor of *P. vivax* could infect gorillas, chimpanzees and humans (Loy et al. 2017). Comparison of the *P. falciparum* genome to current chimpanzee parasites *P. reichenowi* and *P. gaboni* offers insights into the parasite's evolution. On one hand, conserved invasion machinery genes may have enabled cross species infection of the common ancestor of these parasite species (Sundararaman et al. 2016). On the other hand, the proliferation of ape parasite-specific host cell remodelling genes suggests host-specific adaptive parasite evolution. Similarly *P. falciparum* exerts a strong selective pressure on human traits that impact susceptibility to malaria (Kwiatkowski 2005). For example haemoglobin S allele that confers resistance to *P. falciparum* malaria but also causes sickle cell anaemia is much more prevalent in malaria endemic countries (Piel et al. 2010). Overall it appears that host and parasite have co-evolved in a manner that limits zoonotic *Plasmodium* infection.

Although this is promising from a clinical perspective, the fact that *P. falciparum* is both lethal and exclusive to humans limits ethical *in vivo* experimentation to highly controlled clinical trials. Rodent malaria parasite species such as *P. berghei* can infect lab rodents, making them practical models for *in vivo* studies of *Plasmodium* throughout the parasite lifecycle. *Plasmodium* parasites belong to the same Apicomplexa phylum as *Toxoplasma gondii*, an obligate intracellular parasite at times used as a reference in this thesis where *Plasmodium* evidence is lacking.

## 2.2. *Plasmodium* lifecycle and targets for antimalarial interventions

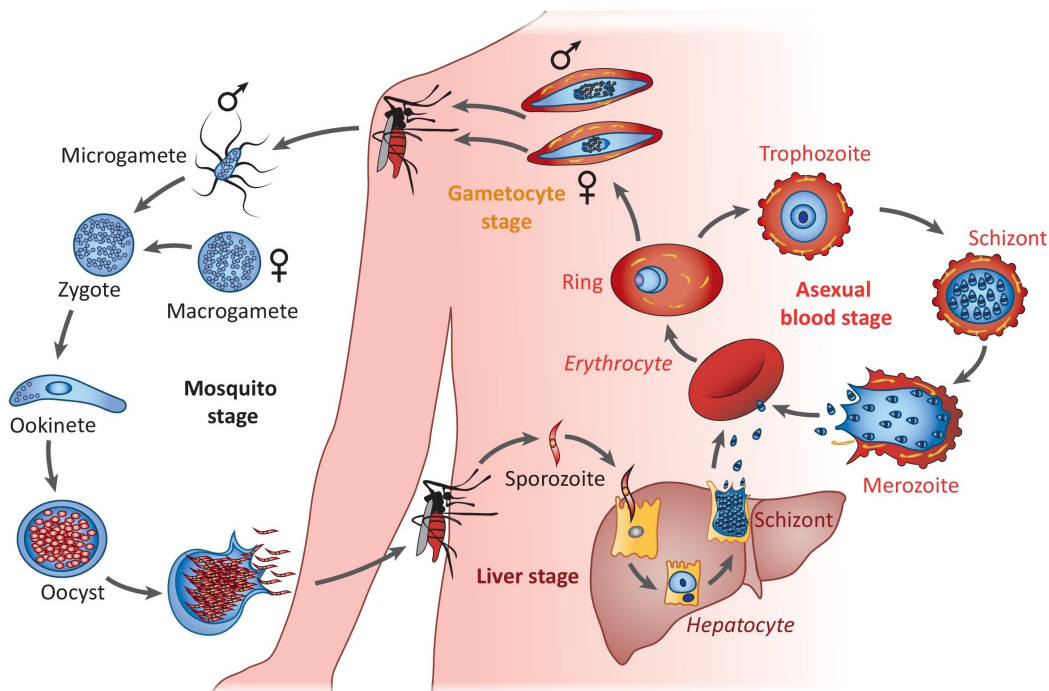


**Figure 3:** *P. falciparum* lifecycle from Maier et al. (2018). Mosquitos transfer *Plasmodium* parasites at sporozoite stage to humans during a blood meal. Sporozoites invade hepatocytes in the liver where they replicate asexually into many merozoites. Upon rupture of the host hepatocyte, merozoites are released into the blood stream and invade erythrocytes. In the erythrocyte, most parasites replicate asexually and transit through ring, trophozoite then schizont stage before releasing daughter merozoites that invade other erythrocytes. A subset of merozoites commits to sexual reproduction and differentiates into male and female gametocytes. Gametocytes are ingested by the mosquito during a blood meal and rapidly activate into male and female gametes that form a zygote after fertilisation. Soon afterwards the ookinete encysts in the mosquito midgut wall, forming an oocyst where many sporozoites are produced by asexual proliferation. Sporozoites migrate to the mosquito salivary gland for transmission back to a human host during a mosquito blood meal.

*Plasmodium* parasites are transmitted to humans *via* mosquito vectors (Figure 3). Sporozoite stage parasites are transmitted from the mosquito to the human host during a blood meal.

Sporozoites migrate to the liver where they invade hepatocytes and replicate asexually. Merozoite release from the hepatocytes into the human host blood stream initiates cyclic asexual proliferation in the blood. Merozoites invade red blood cells (RBC) where they mature through ring, trophozoite and schizont stages before rupturing the host RBC and releasing up to 32 daughter merozoites that will invade other RBC. A minority of asexual blood stage parasites instead differentiate into male and female gametocytes, the sexually committed blood stage parasites. Only gametocytes can survive ingestion by the mosquito during a blood meal. In the mosquito midgut gametocytes activate and form mature gametes capable of sexual reproduction. Female gametocytes egress from the host RBC upon activation to form a spherical immobile macrogamete. Male gametocytes instead divide into eight flagellated microgametes that migrate to and fertilise a macrogamete. The resulting zygote forms a motile ookinete that encysts in the mosquito midgut wall to generate an oocyst. Many sporozoites emerge from the oocyst and migrate to the salivary gland, poised for transmission back to the human host.

Symptoms of malaria appear once blood stage parasitemia reaches about 100 parasites per  $\mu\text{L}$  (Ashley et al. 2018). *P. falciparum* is particularly virulent due to sequestration of parasites in blood vessels that enable the parasite to avoid clearance by the spleen, but also results in obstruction of the host's blood vessels. Adherence of the infected RBC to endothelial cells or uninfected RBC (known as rosetting) is mediated by *P. falciparum* erythrocyte membrane protein 1 expressed at the surface of the infected RBC in so-called knobs (Smith et al. 1995; Baruch et al. 1995; Su et al. 1995). Severe malaria results from obstruction of blood vessels in vital organs including the brain (cerebral malaria) or the placenta (placental malaria) (Ashley et al. 2018). Asexual blood stage proliferation is therefore the target of curative malaria therapies.

The current World Health Organisation recommended course of treatment for *P. falciparum* or *P. knowlesi* malaria is the administration of an artemisinin combination therapy. Artemisinin rapidly clears blood stage parasites but given its short half-life, it is prescribed in combination with longer lasting antimalarials. As well as adequately clearing residual parasites, combination therapies should prevent or delay the development of drug resistant parasites (Ashley et al. 2018). *P. vivax*, *P. malariae* and *P. ovale* infection is treated with chloroquine except in Indonesia and Oceania where *P. vivax* chloroquine resistance is widespread and infection is therefore treated with artemisinin combination therapies.



Unfortunately artemisinin combination therapy failure is now frequent in Cambodia, Thailand and Vietnam due to the emergence of artemisinin resistant parasites (Phyo et al. 2016; Thanh et al. 2017; Imwong et al. 2017). In the absence of adequate alternative treatments for malaria, the spread of parasite resistance to artemisinin combination therapies is the current greatest threat to controlling malaria.

Although other lifecycle stages are asymptomatic, they are essential for parasite lifecycle progression and transmission of malaria. The lifecycle of the malaria parasite consists of waves of clonal population expansion punctuated with bottlenecks in parasite numbers. As illustrated in Figure 3, asexual parasite proliferation occurs in the hepatocyte, RBC and in the mosquito midgut. By contrast, massive loss of parasites occurs as sporozoites migrate from the midgut wall to the salivary gland, and from the human skin to the liver, or by ingestion of a few gametocytes by the mosquito and subsequent sexual reproduction between one male microgamete and one female macrogamete. The natural parasite population bottlenecks (sporozoite stage and sexual stage) are attractive targets for disrupting the parasite lifecycle and blocking disease transmission (Sinden 2017).

At present malaria treatment options that target parasites other than asexual blood stages are limited. Vaccine candidates targeting various parasite lifecycle stages in the human host have so far proven ineffective at providing long term sterile immunity (Matuschewski 2017). Primaquine is the only available antimalarial drug effective at killing either dormant liver stages of *P. vivax* and *P. malariae* or *P. falciparum* gametocytes (Recht et al. 2018). However, it can cause dose dependent haemolysis in the case of glucose 6-phosphate dehydrogenase deficiency, which is common in malaria-endemic regions (Hockwald et al. 1952; Dern et al. 1954; Recht et al. 2018). In the face of growing resistance to current antimalarial drugs, and with renewed interest in preventing malaria transmission, candidate next generation antimalarial drugs developed by the Medicines for Malaria Venture are now required to have anti-gametocyte activity in addition to killing asexual blood stage parasites (Burrows et al. 2017).

In terms of malaria prevention, current strategies consist of prophylaxis drug regimens in vulnerable populations and interventions to reduce the frequency of mosquito bites. The World Health Organisation recommends the intermittent preventative treatment in pregnancy with sulfadoxine-pyrimethamine in malaria-endemic regions of Africa. Seasonal malaria

chemoprevention programmes target children in malaria-endemic countries. However, these interventions are far from covering all of the eligible population at risk (World Malaria Report, 2018). Between 2000 and 2015, an estimated 69 % of the 1.2 billion averted cases of malaria were due to the distribution of insecticide treated bed nets and 10 % were the result of indoor residual spraying of insecticides (Cibulskis et al. 2016). This progress is threatened by the widespread mosquito resistance to the main insecticide classes pyrethroids, organochlorines, carbamates and organophosphates. Novel mosquito vector focused intervention strategies such as co-infection with *Enterobacter bacterium* (Cirimotich et al. 2011) or gene drives that inhibit parasite development in the mosquito may soon be applied in the field to control malaria transmission (Shaw & Catteruccia 2018).

Together these interventions have significantly reduced both the incidence and morbidity of malaria. Blocking disease transmission is paramount in the current context of disease eradication. This thesis focuses on gametocytes that are the parasite lifecycle stage responsible for human to mosquito transmission.

### **3. Sex and sex determination**

Male and female gametocytes are the precursors of *Plasmodium* gametes and sexual reproduction in the mosquito vector. Although morphological differences between male and female gametocytes are subtle, gametocyte activation to form gametes is highly sex-specific: the female gametocyte egresses from the host RBC to become a round immobile macrogamete whereas the male gametocyte divides into eight flagellated microgametes. The speed of gametocyte activation contrasts with the much slower gametocyte maturation in the vertebrate host. In *P. falciparum*, gametocytes mature over 10-12 days but activate within 30 minutes (min) of ingestion by a mosquito. This suggests that preparation for sex-specific activation occurs in gametocytes and that gametocyte biology is similarly sex-specific. In this thesis the biology of gametocytes is not only contrasted to that of other parasite lifecycle stages, but is also investigated in a sex-specific manner.

#### **3.1. Definition of sex**

When it comes to sex, size matters: the sex of gametes is based on morphology. If sexual reproduction occurs between gametes of the same size (isogamy), sexually compatible gametes are referred to as mating types rather than males and females. By contrast, anisogamy involves gametes of different size: male gametes are by definition the smaller

gamete while females are the larger. In rare cases where size difference is subtle, the male gamete refers to the motile gamete, whereas the female gamete is immobile. In some organisms not all male and female gametes are compatible (for example gametes from the same parent), so both gamete sex and mating types are juxtaposed. In *Plasmodium*, anisogamy clearly defines male microgametes from female macrogametes, although the size difference between gametocytes is subtler. Self-fertilisation between *Plasmodium* gametes from the same asexual parent is possible.

Eukaryotic sexual lifecycle typically alternates between haploid and diploid stages through meiosis (diploid to haploid transition) and syngamy (fusion of haploid gametes forms a diploid cell). Sex determination and mitotic cell proliferation occurs in the diploid lifecycle stage of humans. By contrast, asexual proliferation and parasite sex is determined in the haploid stage of *Plasmodium*.

### **3.2. Models of sex determination**

Although the fundamental aspects of sexual reproduction are conserved among eukaryotes, a huge variety of mechanisms of sex determination have evolved including genetic sex determination and environmental sex determination. In the case of genetic sex determination, sex depends on the inheritance of a sex-determining region, which sometimes consists of dedicated sex chromosomes. For example, human sex determination follows the XY system of genetic sex determination where the sex of the zygote is determined by the sex-determining region carried in the sperm (X makes a female and Y makes a male) (Mignerot & Coelho 2016). By contrast, environmental sex determination is driven by perception of environmental factors such as temperature, social queues and hormones. Temperature-dependent sex determination has been described in many reptile species, whereby the temperature range at which the eggs are incubated biases the sex ratio of the hatch (Quinn et al. 2009; Holleley et al. 2015). Genetic and environmental sex-determination are not mutually exclusive, and frequent variation of the mechanism of sex determination is observed between closely related organisms (Mork et al. 2014; Gamble et al. 2015).

The molecular mechanism of sex determination was originally modelled on the sex-specific expression of a molecular switch that regulated a cascade of downstream effector genes similar to the *sry* master regulator of sex determination in humans (Sinclair et al. 1990). However, sex determination in other organisms more closely resembles a

parliamentary decision among many genes. The binary decision to become either male or female sexual stages is sometimes the result of a single molecular switch, but in other organisms a threshold to which multiple factors contribute is more likely. Regardless of the molecular determinant of sex, antagonistic signals that promote one sex while inhibiting development of the other are a common feature and may explain the evolutionary plasticity of the mechanism of sex determination (Capel 2017).

### **3.3. Sex determination in *Plasmodium***

In *Plasmodium*, the mechanism of sex determination is unclear. Asexual blood stage parasites, males and females are haploid and share the same genome, which rules out any model of genetic sex determination. Environmental sex determination is theoretically possible, although temperature-dependent sex determination is unlikely. Indeed, sex determination occurs in the endothermic vertebrate host and the sex ratio varies in temperature controlled *in vitro* gametocytogenesis.

One theory of sex determination suggests that gametocyte sex ratio is self-regulated. The gametocyte population is generally female biased, consistent with the fact that male gametocytes give rise to 8 flagellated gametes unlike female gametocytes that only yield one female macrogamete. However, in polyclonal infections, the sex ratio is more male biased (Paul & Coulson, et al. 2000; Nee et al. 2002; Sowunmi et al. 2009). The proportion of gametocytes of a given genotype appears to impact the sex ratio of *Plasmodium* gametocytes according to Hamilton's theory of local mate competition (Hamilton 1967) rather than Fisher's hypothesis on natural selection (Fisher 1930). In the context of non-random mate competition, Hamilton proposed the sex ratio would become more female biased to reduce competition among males for fertilising the same female egg. The sex ratio of *P. chabaudi* gametocytes of a given genotype is proportional to the fraction of total gametocytes with the same genotype (Reece et al. 2008). This implies not only a mechanism of recognition of kin, but also a means of determining the proportion of genetically identical gametocytes in the population (Knowles & Sheldon 2008). However, the mechanism of such recognition is unclear and injection of lysed *P. chabaudi* of a different genotype only slightly increased the gametocyte sex ratio (Carter et al. 2014).

In the context of an endoparasite such as *Plasmodium*, environmental sex determination infers a mechanism of host-parasite interaction. The sex ratio of gametocytes appears to be

modified by anaemia experimentally in avian and rodent *Plasmodium* parasites (Paul & Coulson, et al. 2000; Paul et al. 2002; Reece et al. 2008; Carter et al. 2014) and in *P. falciparum* infected humans (Robert et al. 2003; Gbotosho et al. 2011). Stimulation of erythropoiesis in chickens and injection of recombinant mouse erythropoietin in mice increased the proportion of male gametocytes relative to females in *P. gallinaceum* and *P. vinckei* respectively (Paul & Coulson, et al. 2000). A protein kinase signalling cascade triggered by erythropoietin binding to its receptor has been hypothesised but not experimentally proven as the molecular mechanism of sex determination in *Plasmodium* (Paul & Doerig, et al. 2000). The *P. falciparum* gametocyte sex ratio is impacted by drug treatment in malaria patients (Sowunmi et al. 2008; Stone et al. 2017; Dicko et al. 2018), although this could be the result of sex-specific gametocyte drug sensitivity as previously reported *in vitro* (Delves et al. 2013). In summary, there are many (host) environmental factors that contribute to the sex ratio of *Plasmodium* gametocytes, potentially indicating a role in parasite sex determination.

#### **4. The host environments of *Plasmodium* gametocytes**

Unlike asexual blood stage parasites, gametocytes have the remarkable ability to thrive in three different host extracellular environments. Gametocytes mature through five morphologically defined stages, stage V being the most mature. Sexually committed rings, stage I and stage V gametocytes circulate in the mammalian host blood stream, effectively bathing in nutrients but at risk of immune clearance. Stage II to IV gametocytes on the other hand are sequestered in the human host bone marrow (Aguilar et al. 2014; Joice et al. 2014; Obaldia et al. 2018; De Niz et al. 2018). In the bone marrow, gametocytes mature alongside blood cells undergoing haematopoiesis and energy-rich marrow adipose tissue. The skeletal bone marrow is a major contributor to glucose and fatty acid clearance *in vivo*, likely making this a nutrient rich niche for the parasite (Bartelt et al. 2017). Finally, the mature gametocyte is ingested by a mosquito and rapidly activates to form gametes in response to a drop in temperature, xanthuric acid and a rise in pH (Billker et al. 1998). The only environmental constant in the gametocyte lifespan is the surrounding host RBC.

While *P. falciparum* resides in mature RBC, other species including *P. vivax* and *P. berghei* prefer the circulating precursors of RBC known as reticulocytes. Neither host cell is nucleated, although reticulocytes contain mitochondria and are more metabolically active than

mature RBC (Srivastava et al. 2017). Despite being devoid of most organelles, the host blood cell is a source of nutrients for *Plasmodium* parasites. For example, blood stage parasites scavenge amino acids from host cell haemoglobin to synthesise parasite proteins (Sherman 1977; Divo et al. 1985; Jun Liu et al. 2006). However, given that RBC and reticulocytes are enucleated, the resources of the host cell are relatively finite.

Compared to asexual blood stage parasites that reinvade a host RBC every two days, *P. falciparum* gametocytes inhabit their host cell for at least two weeks until they are ready for ingestion by a mosquito. Gametocytes were long thought to be metabolically dormant and able to survive off the nutrients available in the host RBC (Canning & Sinden 1975; Sinden et al. 1978). However, more recent discoveries indicate that parasite metabolism varies with lifecycle stage and is active in gametocytes (MacRae et al. 2013; Gulati et al. 2015; Ke et al. 2015; Tran et al. 2016). This suggests that the host cell nutrient pool is insufficient for gametocytogenesis.

Indeed, parasite proliferation *in vivo* and *in vitro* is dependent on extracellular nutrient availability. In culture, asexual *P. falciparum* requires an extracellular source of nutrients for continuous culture (Divo et al. 1985; Mi-Ichi et al. 2006; Mi-Ichi et al. 2007). Serum lipids are modified *in vivo* upon infection with *P. falciparum* (Visser et al. 2013) and lysophosphatidylcholine depletion in serum triggers gametocytogenesis (Brancucci et al. 2017). *In vivo* caloric restriction of the host reduces blood stage parasite proliferation and virulence (Mancio-Silva et al. 2017). In addition, it has been proposed that the unique diet of the Fulani ethnic group may contribute to their natural resistance to malaria (Zuzarte-Luis et al. 2017). Cholesterol availability in the plasma and blood stage parasite proliferation may be correlated: of the three variants of apolipoprotein E that transports cholesterol and triglycerides in the blood, variant  $\epsilon 4$  is associated with higher plasma cholesterol levels and higher *Plasmodium* density (Rougeron et al. 2013). Overall, it appears that asexual parasite proliferation and commitment to gametocytogenesis are related to nutrient availability in the host, including nutrients beyond the host cell.

The mechanism by which *Plasmodium* perceives and responds to changes in the host environment is unclear, although blood stage parasites extensively remodel their host cell in part to access extra-cellular nutrients. Gametocyte stage *P. falciparum* host cell remodelling is distinct to asexual stage RBC modifications (Tibúrcio et al. 2015). Asexual blood stage

parasites, but not gametocytes, express new permeability pathways on the surface of the infected RBC that allow selective exchange of solutes (Ginsburg et al. 1983). The tubulovesicular membrane network creates a hydrophobic bridge between the host RBC plasma membrane and the intracellular parasite (Behari & Haldar 1994) that may facilitate lipid exchange between the parasite and host. Together these modifications enable the parasite to scavenge nutrients from beyond their host cell. The stage-specific modifications of the host cell may reflect different nutrient requirements between asexual and sexual blood stage parasites, or may reflect adaptations to their different host environments.

In addition to scavenging nutrients from the host, the parasite encodes its own metabolic enzymes outlined here briefly (Gardner et al. 2002). The parasite is capable of glycolysis but lacks enzymes required for gluconeogenesis and synthesis of carbohydrate stores such as trehalose or glycogen. Enzymes for the pentose phosphate pathway and the tricarboxylic acid cycle are present in the *P. falciparum* genome. However, parts of the mitochondrial adenosine triphosphate (ATP) synthase and the electron transport chain are missing. Parasites are incapable of *de novo* essential amino acid synthesis, although machinery for para-aminobenzoate and folate synthesis is encoded in the genome. In terms of nucleotide synthesis, parasites can only synthesise pyrimidine *de novo*, from which purine and deoxyribonucleotides can be derived with parasite enzymes. Finally, mevalonate independent isoprenoid synthesis and fatty acid synthesis type II occurs in the apicoplast, a plastid-like parasite organelle. These metabolic pathways complement the parasite's ability to scavenge nutrients, likely enabling the parasite to survive in various host environments.

In summary, *Plasmodium* thrives in distinct host environments by scavenging some nutrients from the host and synthesising others *de novo*. Gametocyte stage parasites span particularly distinct host environments perhaps by perceiving and adapting to change. The focus of this thesis is the metabolism and scavenging of lipids during the switch from asexual blood stage proliferation to gametocytogenesis and transmission to the mosquito vector.

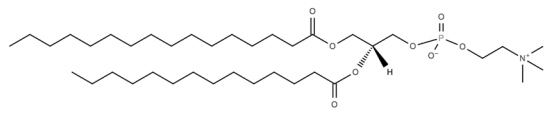
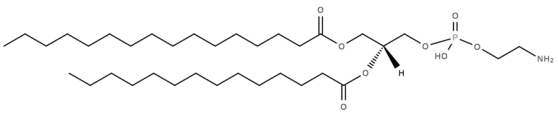
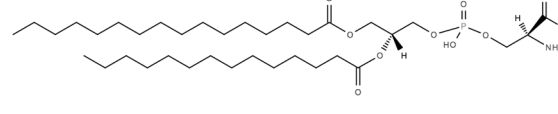
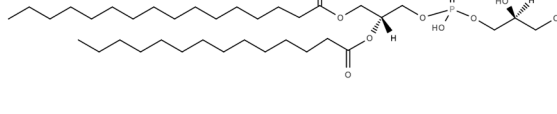
## **5. Lipid structures, functions and sources**

### **5.1. Lipid classes and cellular functions**

Lipids are generally defined as molecules that are insoluble in water but soluble in organic solvents. Given the significant structural diversity of lipids, there are multiple classification

schemes for these molecules (Fahy et al. 2011). The complete lipid profile of a cell, the lipidome, is a subset of the metabolome. In this thesis the lipidome is categorised as per Tran et al. (2016) into phospholipids, neutral lipids, free cholesterol and sphingolipids. The structural definition of each of these lipid categories and their general biological functions are described below.

**Table 1:** Examples of phospholipid structures

Phospholipid category	Name	Structure
Phosphatidylcholine	PC 30:0	
Phosphatidylethanolamine	PE 30:0	
Phosphatidylserine	PS 30:0	
Phosphatidylglycerol	PG 30:0	

Phospholipids contain two fatty acyl chains joined to a hydrophilic head group (Table 1). Phospholipids are categorised based on their head group as phosphatidylcholine (PC), phosphatidylethanolamine (PE), phosphatidylserine (PS) or phosphatidylglycerol (PG). Phosphatidylinositol, although important for intracellular signalling pathways, is excluded from this study since the time scale of signalling pathway dynamics is significantly different to the lifecycle stages compared in this thesis. Within each phospholipid category the length and number of double bonds in the fatty acyl chain distinguishes many phospholipid species. For example, the fatty acyl chains of PC 34:1 contain 34 carbons and one double bond.

Phospholipids are amphiphilic and mostly form lipid bilayers in an aqueous environment. The phospholipid composition impacts the biophysical properties of the membrane, with saturated phospholipid-rich membranes being less fluid than membranes with unsaturated phospholipids (Los & Murata 2004). Some organisms increase the proportion of saturated phospholipids and/or decrease the average acyl chain length of their membranes in response



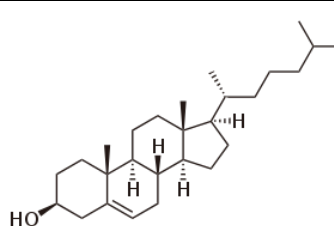
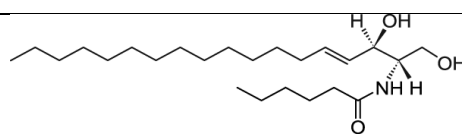
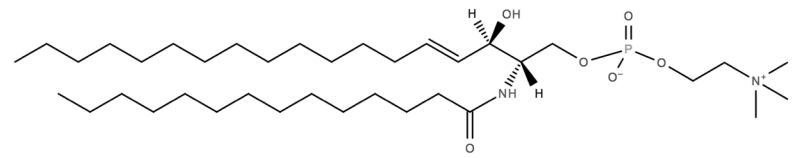
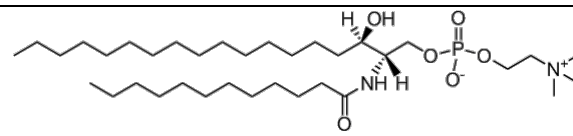
to a drop in temperature to maintain membrane fluidity (de Kroon et al. 2013). In addition, the shape of phospholipids impacts the stability of membranes: while the cylindrical shape of PC forms stable bilayers, PE is more conical and thus facilitates membrane bending events such as fission and fusion (Cullis & de Kruijff 1979). Finally, the overall shape of the phospholipid affects the distribution of lateral pressure in the membrane, which can impact the function of transmembrane proteins such as mechano-sensitive  $\text{Ca}^{2+}$  channels (van den Brink-van der Laan et al. 2004; Loukin et al. 2007). PC is also a source of numerous intracellular signalling molecules including phosphatidic acid, diacylglycerol (DAG), lysophosphatidylcholine (LPC) and free fatty acids (Exton 1994). PS is not essential in yeast but in higher eukaryotes it functions as a specific activator of protein kinase C (Vance & Steenbergen 2005). PG is the precursor of cardiolipin (CL), an exclusively mitochondrial lipid mostly found in the inner membrane (Daum 1985; de Kroon et al. 1999; Gebert et al. 2009). CL has been proposed as a proton trap for oxidative phosphorylation due to its negative head group charge (Haines & Dencher 2002). The conical shape of CL (similar to PE) could facilitate mitochondrial membrane fission and fusion (DeVay et al. 2009; Joshi et al. 2012). PG also has a negatively charged head group but lacks the conical shape of CL.

**Table 2:** Examples of neutral lipid structures with R representing a hydrocarbon chain

Neutral lipid category	Structure
Triacylglycerol	
Diacylglycerol	
Cholesteryl ester	

Neutral lipids include triacylglycerol (TAG), DAG and cholesteryl ester (CE). Unlike phospholipids that contain a polar head group, fatty acyl chains in neutral lipids are linked to neutral glycerol or cholesterol. In general, neutral lipids function as molecular stores of energy and membrane lipid components. Given that *Plasmodium* is incapable of  $\beta$ -oxidation however, neutral lipids likely function as lipid rather than energy stores for the parasite. They form the hydrophobic core of lipid droplets (the surface being made of amphiphilic molecules such as phospholipids or proteins with their polar region facing outwards). In other organisms, lipid droplets are involved in protein maturation and sequestering hydrophobic precursors to intracellular signalling molecules (Welte & Gould 2017). In *T. gondii* neutral lipids sequester otherwise toxic free fatty acids (Nolan et al. 2018). DAG itself is also a key intracellular signalling molecule. Female *P. falciparum* gametocytes contain a neutral lipid store, which potentially represents a lipid reserve for the human to mosquito transition and zygote development (Tran et al. 2014). In asexual blood stage parasites, lipid droplets rich in neutral lipids may mediate haemozoin crystal formation, which is essential for the detoxification of haem (Papalexis et al. 2001; Jackson et al. 2004).

**Table 3:** Examples of cholesterol and sphingolipid structures

Lipid category	Structure
Free cholesterol	
Ceramide	
Sphingomyelin	
Dihydrosphingomyelin	

Free cholesterol (FC), together with sphingomyelin (SM), forms detergent resistant membrane domains referred to here as lipid rafts. Lipid rafts are rigid membrane domains

that mediate intracellular signalling and organise membrane proteins (Rietveld & Simons 1998; Lingwood & Simons 2010). In mammalian sexual reproduction, lipids play a key role in sperm capacitation and acrosome exocytosis (Martínez & Morros 1996). As the sperm transits through the female genital tract, cholesterol is removed from the acrosomal membrane of the spermatozoid. This destabilises the membrane and increases calcium permeability, ultimately leading to acrosome exocytosis and enabling spermatozoid binding and fusion with the female egg. *Plasmodium* is unable to synthesise cholesterol *de novo* and must scavenge it from the host environment (Sherman 1979). Three metabolically related sphingolipids are addressed in this thesis: SM, ceramide (Cer) and dihydrosphingomyelin (DHSM). Sphingolipids are involved in vesicle mediated protein trafficking (Klemm et al. 2009; Gillon et al. 2012) and some, including ceramide, function as signalling molecules (Hannun & Obeid 2008; Dickson 2008).

Given the many functions of lipids in the cell, the localisation, abundance and nature of lipids are tightly regulated. As a parasite, *Plasmodium* can synthesise some lipids *de novo* but is dependent on scavenging other lipids from the host. The *Plasmodium* lipidome therefore reflects both major cellular processes and parasite-host interactions.

## **5.2. Lipid sources**

*Plasmodium* has the ability to scavenge some lipids from the host environment rather than synthesise all lipids *de novo*. Monitoring parasite uptake of exogenously supplied labelled lipids has shed light on the source of parasite lipids (Table 4). Parasite encoded lipid synthesis pathways are detailed in section 5.3.

**Table 4:** Source of major lipids in *Plasmodium* parasites.

Lipid		<i>De novo</i> synthesis	Direct scavenge	Scavenge and remodelling
Phospholipids	PC	Yes (van Meer et al. 2008; Gibellini & Smith 2010; Flammersfeld et al. 2018; Wein et al. 2018)	Yes (Moll et al. 1988)	Yes from PE (Moll et al. 1988)
	PE	Yes (Elabbadi et al. 1997; Choi et al. 2016; Wein et al. 2018)	Yes (Moll et al. 1988)	Yes from PS (Moll et al. 1988) and PC (Grellier et al. 1991)
	PS	Yes (Elabbadi et al. 1997; Wein et al. 2018)	Yes (Moll et al. 1988)	
	PG	Possible (Ramakrishnan et al. 2013)		
Neutral lipids	DAG	Yes (Vielemeyer et al. 2004; Ramakrishnan et al. 2013)	Yes (Vielemeyer et al. 2004)	Yes from oleic acid (Nawabi et al. 2003)
	TAG	Yes (Vielemeyer et al. 2004; Ramakrishnan et al. 2013)		Yes from DAG, oleic acid and palmitic acid (Nawabi et al. 2003; Vielemeyer et al. 2004; Palacpac et al. 2004)
	CE	No (Nawabi et al. 2003; Vielemeyer et al. 2004)		Not from oleic acid or cholesterol (Nawabi et al. 2003; Vielemeyer et al. 2004)
Sphingolipids	Cer	Yes (Gerold & Schwarz 2001)		Yes from SM (Lauer et al. 2001)
	SM	Yes (Gerold & Schwarz 2001)	Yes (Hsiao et al. 1991; Lauer et al. 2000)	
	DHSM	Yes (Gerold & Schwarz 2001)		
Cholesterol		No (Sherman 1979)	Yes (Vielemeyer et al. 2004)	

*P. falciparum* incorporates exogenous phospholipids, including PC, from high density lipoproteins in human serum. Rather than internalising the lipoprotein by endocytosis,

phospholipids are transported by flip-flop from the outer leaflet to the inner leaflet of the host RBC plasma membrane *via* a parasite-encoded protein (Haldar et al. 1989; Grellier et al. 1991; Haldar & Uyetake 1992; Berman et al. 1994). A fraction of the internalised PC is converted to PE in the parasite (Grellier et al. 1991). *P. knowlesi*-infected RBC also incorporate exogenously supplied PC, PS and PE (Moll et al. 1988). In this study PC was not modified by the parasite, whereas PE was converted to PC, and PS was converted to PE after uptake. In the mosquito, oocyst stage parasites take up mosquito lipophorin, the main lipid transporter in mosquito haemolymph, and sporozoites incorporate lipophorin phospholipids (Atella et al. 2009). PG uptake has not been directly investigated in *Plasmodium*, although given that the lipid is specific to mitochondria and RBC are devoid of mitochondria, it is unlikely to be scavenged by blood stage *P. falciparum* parasites. In summary, the host is a rich source of most phospholipids for *Plasmodium*.

In terms of neutral lipid scavenging, incorporation of exogenous labelled oleic and palmitic acid in TAG has been reported in trophozoite and schizont stage *P. falciparum* (Palacpac et al. 2004). Another study identified oleic acid incorporation in both TAG and DAG, but not CE (Nawabi et al. 2003). *P. falciparum* imports exogenous oleate, DAG and cholesterol (Vielemeyer et al. 2004). *P. falciparum* acyl-Co-enzyme-A:diacylglycerol acyltransferase is proposed to synthesise TAG from exogenous DAG and oleate, but CE synthesis appears to be absent in asexual blood stages (Vielemeyer et al. 2004). In *P. berghei*, host RBC glycerol, a precursor for neutral lipid synthesis, is taken up by the parasite *via* *P. berghei* aquaglyceroporin (62 % identical to the *P. falciparum* homologue) on the parasite plasma membrane (Promeneur et al. 2007). In human RBC, aquaglyceroporin 3 is the main glycerol channel, whereas mouse RBC acquire glycerol through aquaglyceroporin 9 (Yangjian Liu et al. 2007). Parasite neutral lipids are therefore both sourced from the host environment and synthesised by the parasite from host-derived precursors.

As for the source of parasite sphingolipids, *de novo* glycosphingolipid synthesis from exogenous serine and glucosamine has been demonstrated in *P. falciparum* (Gerold & Schwarz 2001) in addition to internalisation of host cell SM and glycosphingolipids (Maguire et al. 1991; Hsiao et al. 1991; Lauer et al. 2000). SM is apparently internalised by diffusion from the host cell plasma membrane to the tubulovesicular membrane network and the parasite plasma membrane (Lauer et al. 2001). Parasite-encoded sphingomyelinase hydrolyses exogenously supplied SM to form ceramide in the extra-parasitic compartment of

the infected RBC, potentially in the tubulovesicular membrane network (Lauer et al. 2001). Import of fluorescently labelled glycosphingolipids into the parasite after saponin isolation from the host RBC was also observed in *P. falciparum* by microscopy (Essaka et al. 2010). Direct import of DHSM has not been investigated. Overall, *Plasmodium* can apparently incorporate most sphingolipids available in the host environment.

Asexual blood stage *P. falciparum* imports exogenous cholesterol (Vielemeyer et al. 2004) since it is unable to synthesise cholesterol *de novo* (Sherman 1979). Cholesterol and sphingomyelin from the host RBC plasma membrane are incorporated in the parasitophorous vacuole membrane (PVM, Lauer et al. 2000). A homolog of a human protein required for cholesterol and sphingolipid transport, *P. falciparum* Niemann-Pick Type C1-Related protein, is required for digestive vacuole formation and modulation the lipid composition of the parasite plasma membrane (Istvan et al. 2019). In the liver, *P. falciparum* also scavenges cholesterol synthesised by the host hepatocyte and imported by the hepatocyte from circulating low density lipoproteins (Labaied et al. 2011). The mosquito host relies on the blood meal as a source of cholesterol for mosquito egg development. As such, the mosquito stage parasites are in direct competition with their host for cholesterol (Costa et al. 2018). Given that cholesterol is exclusively sourced from the host, the cholesterol content of the parasite reflects host-parasite interactions.

Lipid scavenging from the host is therefore a major source of lipids and lipid precursors for the parasite. However, lipid remodelling and *de novo* lipid synthesis complement this lipid scavenging to build the complete parasite lipidome. An overview of the lipid synthesis pathways of relevance to this thesis is presented below.

### **5.3. Lipid metabolism**

*Plasmodium* encodes enzymes for the synthesis of all of the lipid categories described above but cholesterol. The activity of these pathways contributes to the lipidome of the parasite-infected host cells. The metabolic pathways are presented here as context for the lipidome analysis in this thesis.

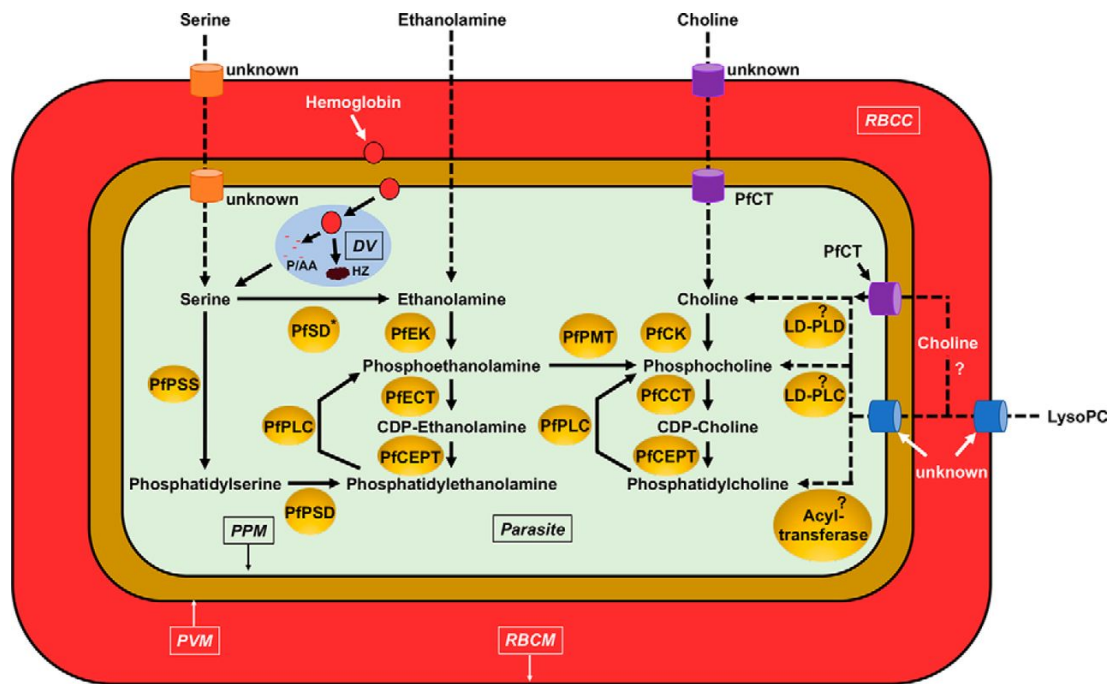


**Figure 4:** Phospholipid metabolism in *P. falciparum* (Pf) from Kilian et al. (2018). PSS: phosphatidylserine synthase; SD: serine decarboxylase; PLC: phospholipase C; PSD: phosphatidylserine decarboxylase; EK: ethanolamine kinase; ECT: citidine diphosphate-phosphoethanolamine cytidyltransferase; CEPT: choline/ethanolamine phosphotransferase; PMT: phosphoethanolamine methyltransferase; CK: choline kinase; CCT: citidine triphosphate-phosphocholine cytidyltransferase; LD-PLD: lysophosphatidylcholine-dependent phospholipase D; LD-PLC: lysophosphatidylcholine-dependent phospholipase C; CT: choline transporter; LysoPC: lysophosphatidylcholine; RBCC: red blood cell cytosol; PVM: parasitophorous vacuole; RBCM: red blood cell membrane; DV: digestive vacuole; P/AA: peptides/amino acids; HZ: haemozoin. Dashed arrows and “?” represent putative pathways and enzymes respectively.

*Plasmodium* parasites can synthesise PC *de novo* through two pathways (Figure 4). Most PC is synthesized by the citidine diphosphate (CDP) -choline branch of the Kennedy pathway (van Meer et al. 2008; Gibellini & Smith 2010; Wein et al. 2018; Flammersfeld et al. 2018), however, PC can also be generated by triple methylation of phosphoethanolamine by phosphoethanolamine methyltransferase (Pessi et al. 2004; Witola et al. 2006; Reynolds et al. 2008). LPC in the culture medium is taken up by *Plasmodium* and converted to PC through an unknown mechanism (Brancucci et al. 2017).

PE can also be synthesised through two pathways encoded by *Plasmodium* (Figure 4): from ethanolamine *via* the CDP-ethanolamine branch of the Kennedy pathway, or by decarboxylation of PS (Elabbadi et al. 1997; Choi et al. 2016; Wein et al. 2018). Parasites may import ethanolamine and generate ethanolamine for the former pathway from serine (Elabbadi et al. 1997; Kilian et al. 2018).

PS is synthesised from serine by phosphatidylserine synthase (Elabbadi et al. 1997; Wein et al. 2018). Serine is either imported from the host, or derived from haemoglobin digestion in the digestive vacuole (Figure 4).

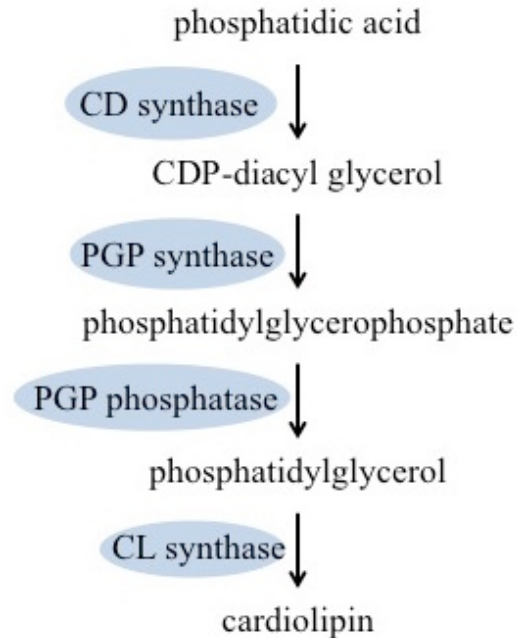


**Figure 5:** hypothetical synthesis pathway for phosphatidylglycerol (PG) and cardiolipin (CL) in the mitochondria. CD synthase: cytidine diphosphate diacylglycerol synthase; PGP: phosphatidylglycerophosphate; CDP: cytidine diphosphate. Enzymes are represented in blue.

PG is a precursor of CL that has not been studied experimentally in *Plasmodium* (Ramakrishnan et al. 2013). A hypothetical synthesis pathway is presented in Figure 5. Homologs of mammalian and yeast phosphatidylglycerophosphate synthase and prokaryote CL synthase are encoded in the *Plasmodium* genome. Prokaryote-type CL synthase uses CDP-diacylglycerol as a phosphatidyl group source for the synthesis of CL, unlike the mammalian enzyme that requires a second PG molecule. In *Trypanosoma brucei*, a protist parasite, CL synthase and phosphatidylglycerophosphate synthase localise to the mitochondria and are associated with large protein complexes (Serricchio & Bütikofer 2012; Serricchio & Bütikofer 2013). Both enzymes could in fact be in the same mitochondrial lipid synthesis complex (Ramakrishnan et al. 2013).



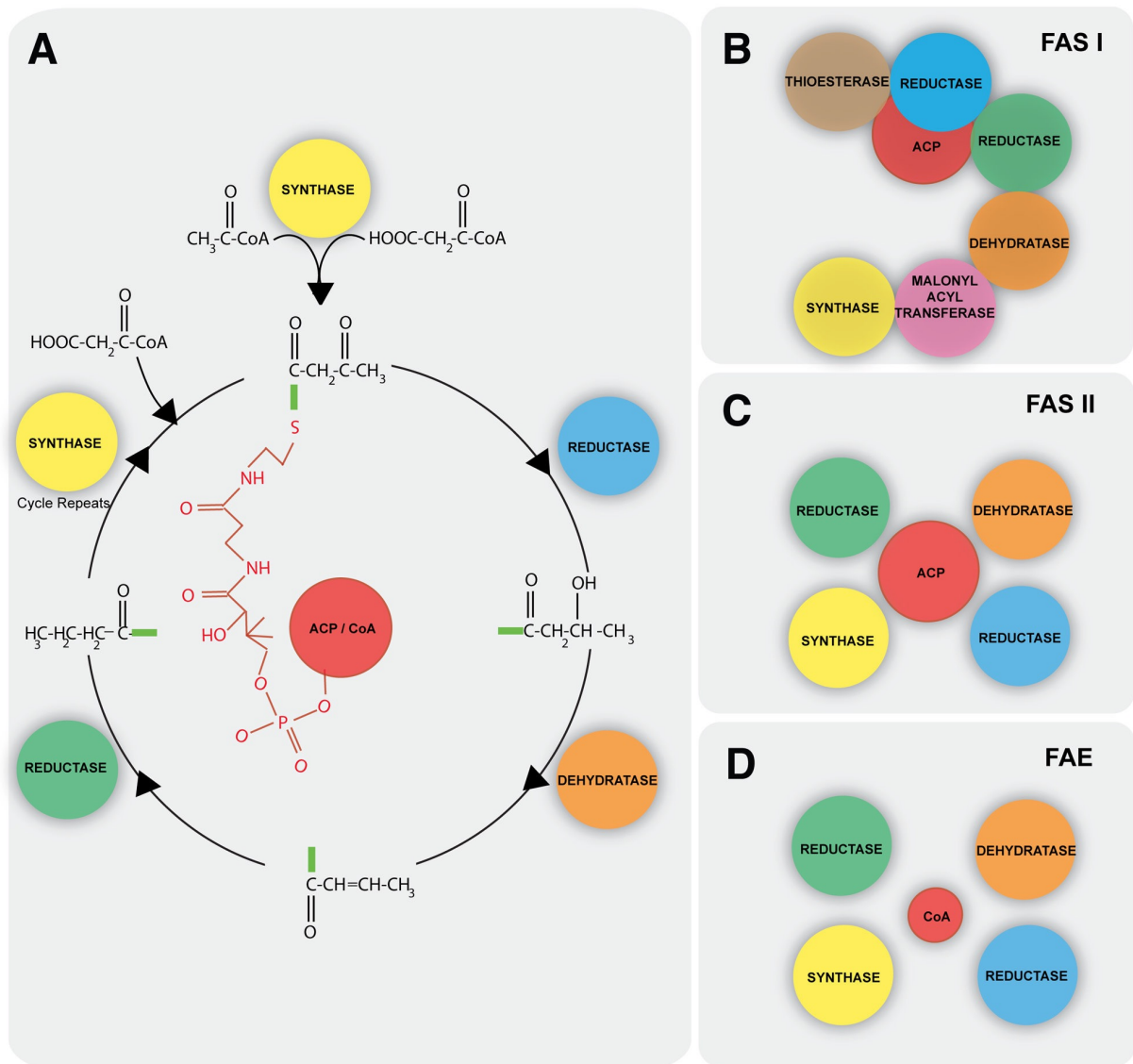


**Figure 6:** Schematic of fatty acid synthesis in *Plasmodium* (Ramakrishnan et al. 2013). A) Overview of fatty acid synthesis steps. B) Fatty Acid Synthesis I pathway (FASI) involves a large protein with multiple catalytic activities. C) Fatty Acid Synthesis II (FASII) enzymes are separate. D) Fatty acid elongation (FAE) is similar to FAS except the anchor molecule is co-enzyme A (CoA) rather than Acyl Carrier Protein (ACP).

*Plasmodium* encodes fatty acid synthesis type II (FASII) enzymes for *de novo* fatty acid synthesis (Figure 6). This pathway is not essential in blood or mosquito stages but is required for parasite development in the liver (Yu et al. 2008; Vaughan et al. 2009). It appears that the importance of the FASII pathway is relative to the availability of exogenous fatty acids, similar to observations in bacteria (Brinster et al. 2009; Parsons et al. 2011; Botté et al. 2013). FASII differs from the mammalian FASI pathway in the structure of key enzymes: FASII pathway involves multiple separate enzymes that are combined in one large protein in the FASI pathway (Figure 6 B and C).

Existing fatty acids can also be modified through the fatty acid elongation (FAE) pathway and/or desaturation in *Plasmodium*. FAE is similar to FASII except the starting molecule is much longer and co-enzyme A (CoA) is used as an anchor rather than acyl carrier proteins (Figure 6 A and D). FAE is active in *Plasmodium* blood stages (Mi-Ichi et al. 2006) and three FAE enzymes have been identified in the genome. In closely related apicomplexan parasite *T. gondii*, each of these FAE enzymes have specific substrates and products (Ramakrishnan et al. 2012). Unsaturated fatty acids are synthesised from saturated fatty acids by desaturases. Monounsaturated fatty acid synthesis by steraoyl-CoA desaturase is essential for blood stage *P. falciparum* (Gratraud et al. 2009). Polyunsaturated fatty acid synthesis is absent in apicomplexan parasites including *Plasmodium*, suggesting these fatty acids are sourced from the host (Ramakrishnan et al. 2013). Acyl CoA: cholesterol acyltransferase (ACAT) and acyl CoA: diacylglycerol acyltransferase mediate the synthesis of neutral lipids from fatty acids. *Plasmodium* encodes both enzymes, although only DAG and TAG synthesis (not CE synthesis) have previously been reported in *P. falciparum* (Vielemeyer et al. 2004).

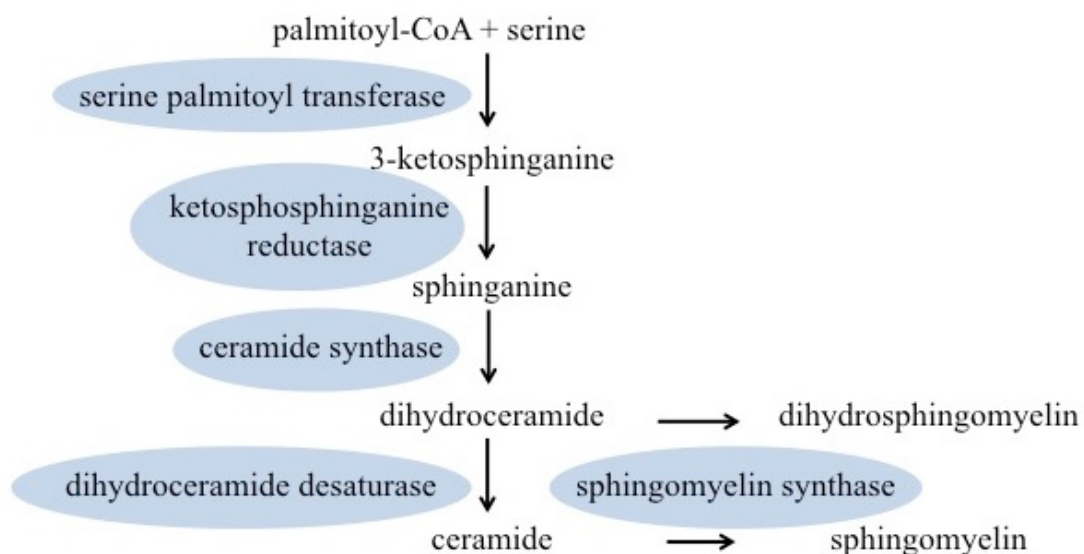


**Figure 7:** Sphingolipid synthesis pathway in *Plasmodium* with enzymes represented in blue.

SM is the most abundant sphingolipid in *Plasmodium* (similar to mammalian cells) and accumulates during gametocytogenesis (Ramakrishnan et al. 2013; Tran et al. 2014; Gulati et al. 2015). In mammalian cells, sphingolipid synthesis starts in the endoplasmic reticulum where palmitoyl-CoA and serine are used to form ceramide in four sequential reactions (Figure 7, Mullen et al. 2012). SM synthase transfers phosphocholine from PC to ceramide in the Golgi to form SM. This pathway not only generates SM, but also regulates the levels of

secondary messenger molecules ceramide and DAG (Fyrst & Saba 2010). Various complex sphingolipids are also formed by glycosylation of ceramide. SM synthesis has previously been observed in *Plasmodium* (Gerold & Schwarz 2001), although the function of the two putative sphingomyelin synthases (SMS) in the genome has yet to be experimentally verified.

In summary, *Plasmodium* parasites have conserved the ability to synthesise diverse lipids. This suggests that lipid homeostasis is critical for parasite survival throughout the parasite lifecycle that spans distinct lipid environments.

## 6. Research Aims

Given the many roles of lipids in the biology of *Plasmodium*, this thesis aims to characterise the sex-specific biology of *Plasmodium* through the lipid profile of the parasite in various host environments. Specifically the thesis addresses the following research aims:

1. Identify lipid dynamics in the infected host cell during the lifecycle of *Plasmodium* that result from parasite lipid synthesis or host lipid scavenging.

Lipidomic analysis of asexual *P. falciparum* replication in infected RBC is extended in the mouse model of malaria, *P. berghei*, from schizonts and gametocytes in the mammalian host to sporozoites in the mosquito vector. Comparison of host cell lipids and lipid dynamics during the lifecycle of *Plasmodium* parasites highlights parasite driven or host derived lipid characteristics.

2. Develop a method to separate male and female *P. falciparum* gametocytes to address clinical and fundamental research problems relating to gametocytes.

Live male and female gametocytes are separated by fluorescence activated cell sorting (FACS) based on a female-specific green fluorescent protein (GFP) tag. This method is applied to validate novel sex-specific gametocyte markers for monitoring gametocyte sex. As a proof of concept application, putative deoxyribonucleic acid (DNA) methylation patterns of male and female gametocytes collected using this method are compared to address a possible mechanism of sex-determination in *P. falciparum*.

3. Determine whether the lipid profile of *P. falciparum* gametocytes contributes to sex dimorphism via *de novo* lipid synthesis or by scavenging host lipids.

Using the method developed in aim 2, the lipidome of male and female gametocytes is compared to highlight potential sex-dimorphisms in *P. falciparum*. The source and functional significance of the main sex-specific lipid characteristics is explored through chemical and genetic disruption of *de novo* lipid metabolism in blood stage parasites. Finally, possible lipid scavenging is investigated by measuring the extracellular lipids available to gametocytes *in vitro*.

Overall, a better understanding of the fundamental biology of *Plasmodium* sexual reproduction and transmission between hosts may highlight molecular sex dimorphisms and pave the way for transmission blocking antimalarial interventions in the field.

# **Materials and Methods**

## 1. Materials

### 1.1. Chemical reagents

Chemicals were sourced from Sigma-Aldrich with the following exceptions. Gentamicin, Hoechst 33342, MitoTracker Deep Red and RPMI 1640-HEPES (Roswell Park Memorial Institute media formula 1640 with 4-(2-hydroxyethyl)-1-piperazineethanesulfonic acid) with Glutamax were purchased from Thermo Fisher Scientific. Restriction enzymes, polymerases and corresponding buffers were purchased from New England Biolabs. Quantitative PCR reagents and Southern blot probe reagents were purchased from Roche. Glybenclamide was purchased from Jomar Life Research, GT11 was purchased from Avanti Polar Lipids and Geimsa stain SNP was purchased from POCD Healthcare.

### 1.2. Ethics approvals and biological reagents

Human type O<sup>+</sup> RBC and human serum were kindly donated by the Australian Red Cross Blood Bank and approved for experimental use by the Australian National University Human Ethics Committee 2017 agreement 351 and the Australian Red Cross agreement 17-06ACT-07. RBC from two donors were pooled and stored at 4°C. Serum from at least 5 donors of the same blood type was pooled together and heat inactivated at 50°C for 1 h prior to use.

Wild type (WT) *Plasmodium falciparum* 3D7 strain parasites were originally derived from clinical isolate NF54 from a patient in the Netherlands (Ponnudurai et al. 1981; Walliker et al. 1987). 3D7 parasites expressing a GFP tagged gametocyte ATP binding cassette transporter family member 2 (gABCG2) protein (PF3D7\_1426500) were generated by Tran et al. (2014).

SWISS mice (Janvier labs) were infected with *Plasmodium berghei* ANKA strain parasites expressing GFP under elongation factor 1 $\alpha$  promoter (Janse et al. 2006). *Anopheles stephensi* mosquitos were grown in 75 % humidity with alternating 14 h light, 10 h dark cycles at 20 °C.

Mouse experiments were performed in accordance with the German Tierschutzgesetz in der Fassung von 18. Mai 2006 (BGB1. I S. 1207) implementing Directive 86/609/EEC from the European Union and the European Convention for the protection of vertebrate animals used for experimental and other scientific purposes. Protocols were approved by the ethics committee of the Max Planck Institute for Infection Biology and the Berlin state authorities (Landesamt für Gesundheit und Soziales regulation G0469/09).

## **2. Methods**

### **2.1. Solution preparation**

Powders were weighed on an Ohaus Scout or Pioneer weigh scale and solutions were prepared in milliQ water. pH was adjusted using a Cyberscan 510 pH meter fitted with a Thermo Scientific Eutech electrode calibrated to pH 4, 7 and 10 prior to each use. Solutions were sterilised by autoclaving or filtering through a Corning 0.22  $\mu\text{m}$  Polyethersulfone low-binding sterilising bottle top filter as required. Stock solutions of drugs were prepared in dimethylsulfoxide (DMSO) with the exception of 5-fluorocytosine (distributed in solution at 10 mg/mL) and artemisinin, which was dissolved in incomplete culture medium at 200  $\mu\text{M}$ .

**Table 1:** Composition of solutions

Solution	Composition
Depurination solution	0.25 M HCl
Denaturation solution	0.5 M NaOH, 1.5 M NaCl
Neutralisation solution	0.5 M Tris base, 1.5 M NaCl; pH 7.5
SCC, 20×	3 M NaCl, 0.3 M citric acid trisodium dihydrate; pH 7.0
Maleic acid buffer, 10×	1 M maleic acid, 1.5 M NaCl; pH 7.5
Washing buffer	maleic acid buffer 1×, 0.3 % (v/v) Tween-20
Blocking solution	maleic acid buffer 1×, 1 % (w/v) skim milk powder
Detection buffer	100 mM Tris-hydrochloride, 100 mM NaCl; pH 9.5
Stripping buffer	0.2 M NaOH, 0.1 % (w/v) sodium dodecyl sulphate
TBE buffer	0.1 M Tris, 0.1 M boric acid, 2 mM ethylenediaminetetraacetic acid
TE buffer	10 mM Tris base, 1 mM ethylenediaminetetraacetic acid; pH 8.0
Phosphate buffered saline (PBS), 10×	10.6 mM KH <sub>2</sub> PO <sub>4</sub> , 1.55 M NaCl, 29.7 mM Na <sub>2</sub> HPO <sub>4</sub> ; pH 7.4
Incomplete culture medium	RPMI 1640-HEPES with Glutamax
Complete culture medium	RPMI 1640-HEPES with Glutamax, 10 mM glucose, 20 µg/mL gentamicin, 480 µM hypoxanthine, 0.375 % (w/v) AlbuMAX II, 2.5 % (v/v) human serum
Cell freezing medium	28 % (v/v) glycerol, 3 % (w/v) sorbitol, 0.65 % (w/v) NaCl
Cytomix	120 mM KCl, 0.15 mM CaCl <sub>2</sub> , 10 mM K <sub>2</sub> HPO <sub>4</sub> /KH <sub>2</sub> PO <sub>4</sub> , 25 mM HEPES, 2 mM ethylene glycol-bis(β-aminoethyl ether)-tetraacetic acid, 5 mM MgCl <sub>2</sub> ; pH 7.6

## 2.2. Culturing techniques

### 2.2.1 Culture of asexual blood stage *P. falciparum*

Asexual parasites were continuously cultured as described by Trager & Jensen (1976) with modifications (Maier & Rug 2013) in Corning 150 mm × 25 mm or 100 mm × 20 mm culture dishes at 4 % haematocrit in complete culture medium. Culture medium was replaced and parasitemia was monitored at least three times a week as follows. Settled culture cells were smeared on a glass slide, air-dried, fixed by dipping in methanol, stained in Giemsa stain for 5



min and rinsed in water prior to observation under an Olympus BX41 microscope. Parasitemia was maintained at less than 5 % by replacing a fraction of the infected RBC with uninfected RBC three times a week. Cultures were otherwise incubated at 37°C in hypoxic conditions (1 % O<sub>2</sub>, 5 % CO<sub>2</sub>, 94 % N<sub>2</sub>).

### **2.2.2 Culture of male and female gametocytes**

Parasites were induced to form gametocytes as described by Fivelman et al. (2007) with modifications to reduce asexual parasite proliferation. Briefly, a sorbitol-synchronised culture containing 2 % trophozoites at 4 % haematocrit was stressed by replacing only a quarter of the culture medium on day -2 and 2/3 of the culture medium on day -1. The next day, termed day 0 of gametocytogenesis, a high parasitemia ring stage culture was treated with 5 % (w/v) sorbitol to remove asynchronous trophozoite (see 2.2.5) and magnet enrichment was applied to remove spontaneously committed mature gametocytes (see 2.2.7). On day 1 post commitment the culture was again treated with 5 % (w/v) sorbitol to remove mature asexual parasites. From day 1 onwards, the culture medium was replaced daily and supplemented with 50 mM N-acetyl-D-glucosamine to prevent asexual parasite proliferation (Gupta et al. 1985). For collection of gametocytes on day 9, the culture was treated with 5 % (w/v) sorbitol on day 7 and 8 to remove asexual parasites, and gametocytes were magnet enriched on day 8 (see 2.2.7). Gametocytes were incubated overnight in complete culture medium at 37°C in hypoxic conditions (1 % O<sub>2</sub>, 5 % CO<sub>2</sub>, 94 % N<sub>2</sub>).

### **2.2.3 Freezing *P. falciparum* parasites**

Asexual *P. falciparum* culture was pelleted at 524 ×g over 5 min and gently resuspended in two pellet volumes of cell freezing medium. One mL aliquots in Greiner bio-one 2 mL cryotubes were snap frozen by immersion in liquid nitrogen and stored in liquid nitrogen.

### **2.2.4 Thawing *P. falciparum* parasites**

Frozen aliquots of *P. falciparum*-infected RBC in cell freezing medium were thawed at 37°C in a water bath. The osmolarity of the medium was gradually decreased by adding a gradient of concentrations of NaCl solution drop wise with gentle swirling. Each 1 mL frozen aliquot was gently resuspended in 200 µL 12 % (w/v) NaCl in PBS and incubated for 5 min at room temperature, then resuspended in 10 mL 1.8 % (w/v) NaCl in PBS and 10 mL 0.9 % (w/v) NaCl, 0.2 % (w/v) glucose. Cells were pelleted at 524 ×g over 5 min and resuspended in 10 mL of 2 % haematocrit RBC in complete culture medium. Cultures were incubated at 37°C in hypoxic conditions (1 % O<sub>2</sub>, 5 % CO<sub>2</sub>, 94 % N<sub>2</sub>). The parasitemia was monitored by Giemsa-stained thin smear and culture medium was replaced daily until normal parasite proliferation resumed.

### **2.2.5 Sorbitol synchronisation of *P. falciparum* parasites**

Cultures were synchronised by selective lysis of mature asexual parasites older than 18 hours post invasion (hpi) by sorbitol treatment as described previously (Lambros & Vanderberg 1979). Sorbitol is a substrate of the parasite induced new permeability pathways that are expressed on the RBC plasma membrane by 18 hpi. Entry of sorbitol into RBC infected with mature asexual parasites, but not ring stage or gametocyte-infected RBC, induces osmotic lysis. Briefly, ring stage *P. falciparum* culture was centrifuged at 524 ×g for 5 min and the resulting pellet was resuspended in 5 % (w/v) sorbitol and incubated in a 37 °C water bath for 10 min. The culture dish was replaced or rinsed with 5 % (w/v) sorbitol. Cells were pelleted as before, resuspended in complete culture medium and returned to normal culturing conditions. Sorbitol treatment was performed twice 14 h apart to obtain parasites synchronised to within a 4 h age window.

### **2.2.6 Saponin isolation of *P. falciparum* parasites**

To isolate the parasites from their host RBC, cultures were treated with saponin that selectively disrupts the cholesterol-rich RBC plasma membrane and the PVM, leaving the parasite plasma membrane intact (Dourmashkin et al. 1962). *P. falciparum* culture was pelleted at 524 ×g for 5 min and resuspended in three pellet volumes of cold 0.15 % (w/v) saponin in PBS. After incubating on ice for 15 min, the cells were rinsed twice (or until supernatant was colourless) in cold PBS with 4,100 ×g, 1 min spins.

### **2.2.7 Magnetic enrichment of *P. falciparum* parasites**

Mature gametocytes and mature asexual parasites are magnetic due to the conversion of non-magnetic Fe<sup>2+</sup> in haem to magnetic Fe<sup>3+</sup> in the process of haemozoin crystallisation. These stages are therefore retained in a magnetic column unlike uninfected RBC or ring stage parasites present in the culture. Magnetic enrichment was performed on a Super MACS separator with CS column (Miltenyi Biotec) as per the manufacturer's instructions with some modifications. Briefly, the column was sterilised with 80 % ethanol, rinsed with PBS and equilibrated in incomplete culture medium. High density *P. falciparum* culture (approx. 10 % haematocrit) was passed through the magnetised column drop wise. For collection of the magnetic fraction, the magnetised column was rinsed with an excess of incomplete culture medium, and then mature parasites were eluted from the de-magnetised column in complete culture medium. For collection of the non-magnetic fraction, the magnetised column was instead rinsed in complete culture medium and uninfected RBC and ring stage parasites were collected in the flow through. Haematocrit was restored to 4 % with complete culture medium

for continued culture of non-magnetic flow through. After each use the column was rinsed with milliQ water then 100 % ethanol and air-dried.

### **2.3. Microscopy and cell counting**

#### **2.3.1. Giemsa-stained thin smear**

For routine parasitemia monitoring, at least 300 cells were counted on a Giemsa-stained thin smear prepared as described in 2.2.1. For gametocyte stage determination, the images below from Roncalés et al. (2012) were used as a reference.

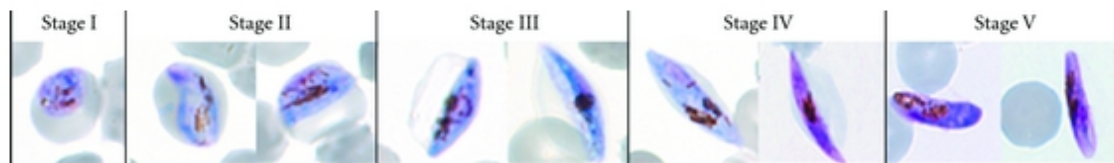


**Figure 1:** Giemsa-stained gametocyte stages observed under light microscope (Roncalés et al. 2012).

#### **2.3.2. Cell density counting with haemocytometer**

Cell density counts were performed on an Improved Neubauer haemocytometer (Hirschmann) as per the manufacturer's instructions under an Olympus BX41 microscope at 40× magnification.

#### **2.3.3. Live cell fluorescence microscopy**

For live cell fluorescence microscopy a droplet of cells suspended in PBS or culture medium was placed on a pre-cleaned clear glass slide (Hurst) and sealed under a No 1.5 coverslip (Sigma) with nail polish. Cells were observed at 100× magnification with immersion oil on a restorative widefield deconvolution microscope (DeltaVision Elite, GE Healthcare) detecting GFP (488 nm excitation/498-598 emission) and Hoechst 33342 (405 nm excitation/410-498 nm emission). Images were deconvolved using the softWoRx acquisition software (version 5.0) and were processed with the Fiji module in ImageJ 2.0 software.

### **2.4. Generation of transgenic *P. falciparum* cell lines**

#### **2.4.1. Construct preparation**

Annotated sequence of *P. falciparum* 3D7 reference strain was sourced from the *Plasmodium* Genomics Resource PlasmoDB (<http://www.plasmodb.org/>). To disrupt SMS1 (PF3D7\_0625000) by double recombination, a 5' fragment and a 3' fragment of SMS1 locus were amplified using primers a1398/a1399 and a1400/a1401 (Table 2) and cloned into a pCC-1

vector containing a human dihydrofolate reductase (hDHFR) and 5-fluorocytosine drug selection cassette (Maier et al. 2008) at SacII/SpeI and EcoRI/AvrII sites to generate pCC-1/SMS1 construct (Supplementary Figure 2). SMS2 (PF3D7\_0625100) was also disrupted by double recombination by amplifying a 5' fragment with al406/al407 primers and a 3' fragment with al408/409 primers (Table 2), which were cloned into a pCC-1 vector at SacII/SpeI and EcoRI/AvrII sites to generate pCC-1/SMS2 construct (Supplementary Figure 3). Given that SMS1 and SMS2 are adjacent genes, the pCC-1/SMS1 and 2 construct aiming to disrupt both SMS genes was generated by cloning the 5' fragment of SMS1 (amplified with al398/al399 primers) and the 3' fragment of SMS2 (amplified with al408/al409 primers) at SacII/SpeI and EcoRI/AvrII sites. Inserted DNA regions were confirmed by analytical restriction enzyme digest and sequenced to verify constructs. Plasmids were purified using Invitrogen Purelink Maxiprep kit prior to transfection.

**Table 2:** Primers for construct preparation. Lowercase letters in the primer sequences correspond to restriction enzyme sites while uppercase letters refer to the gene sequence.

Primer code	Primer description		Primer sequence
al398	SMS1 5'	forward	atcccgcggCACACATTTGTACCTCTC
al399		reverse	gatactagtATCTGAGAAATTGGAACGC
al400	SMS1 3'	forward	atcgaattcGCTGCAAGAAGATATGC
al401		reverse	gatcctaggAAAAAGAGTTTGTAGGTG
al406	SMS2 5'	forward	atcccgcggGTTTAATACACGTGAG
al407		reverse	gatactagtCGATCACTTAATGGTTGCG
al408	SMS2 3'	forward	atcgaattcTATACCTTAGATTATGCC
al409		reverse	gatcctaggAAAAACGACATTTAGGG

#### 2.4.2. Transfection and selection

*P. falciparum* 3D7 reference strain parasites were transfected as described previously (Rug & Maier 2013). Briefly, 400  $\mu$ L of 100  $\mu$ g of plasmid DNA in Cytomix was electroporated into a sorbitol synchronised ring stage culture at 5 % parasitemia by 310 V, 950  $\mu$ F pulse delivered in a 0.2 cm electrode gap cuvette placed in a BioRad Genepulser II with  $\infty$  capacitor. Transformed cells were immediately resuspended in complete culture medium with 3 % haematocrit uninfected RBC and incubated at 37°C in hypoxic conditions (1 % O<sub>2</sub>, 5 % CO<sub>2</sub>, 94 % N<sub>2</sub>) in a Corning 100 mm  $\times$  20 mm culture dish. Culture medium was

supplemented with 2 nM WR99210 from 4 h post transformation and was replaced daily for 5 days post transfection, then three times a week until parasites were observed by Giemsa-stained thin smears of the culture. In the absence of drug pressure, episomal plasmids containing drug resistance cassettes are lost during parasite proliferation, whereas integrated resistance cassettes are replicated with the parasite genome. Parasites were therefore cultured in the absence of WR99210 for 21 days before re-introducing 2 nM WR99210 to the culture medium to eliminate parasites that had lost the episomal resistance cassette. Parasites having integrated the plasmid were enriched by three such off/on drug cycles then negative selection was applied by adding 231 nM 5-fluorocytosine.

### **2.4.3. Cloning by limited dilution**

*P. falciparum* culture was diluted in a 2 % haematocrit suspension of uninfected RBC in complete culture medium to 2 and 0.5 parasites per well of a Corning flat bottom 96 well plate and incubated at 37°C in hypoxic conditions (1 % O<sub>2</sub>, 5 % CO<sub>2</sub>, 94 % N<sub>2</sub>). Gas was replaced every 2-3 days and the culture medium was replaced once a week. After 10 days, parasitemia was monitored by Giemsa-stained thin smear every second day in 10 wells of the high parasitemia plate. Once parasites were detected, all wells of both plates were monitored for parasites by Giemsa-stained thin smears. Clones were progressively expanded in complete culture medium with 4 % haematocrit uninfected RBC in 35 mm ×10 mm, 100 mm ×20 mm then 150 mm ×25 mm Corning culture dishes.

## **2.5. Flow cytometry measurements**

### **2.5.1. Sorting of male and female gametocytes by flow cytometry**

Magnet enriched 3D7 gABCG2-GFP gametocytes were incubated with 50 µg/mL Hoechst 33342 in PBS for 15 min at 37 °C, rinsed twice in PBS with 2,000 ×g, 1 min spins and resuspended in PBS for FACS. Single colour controls consisted of 3D7 WT asexual parasite culture stained with Hoechst 33342 exactly as described above and unstained 3D7 gABCG2-GFP gametocytes suspended in PBS. Unstained 3D7 WT asexual parasite culture in PBS served as the no colour control.

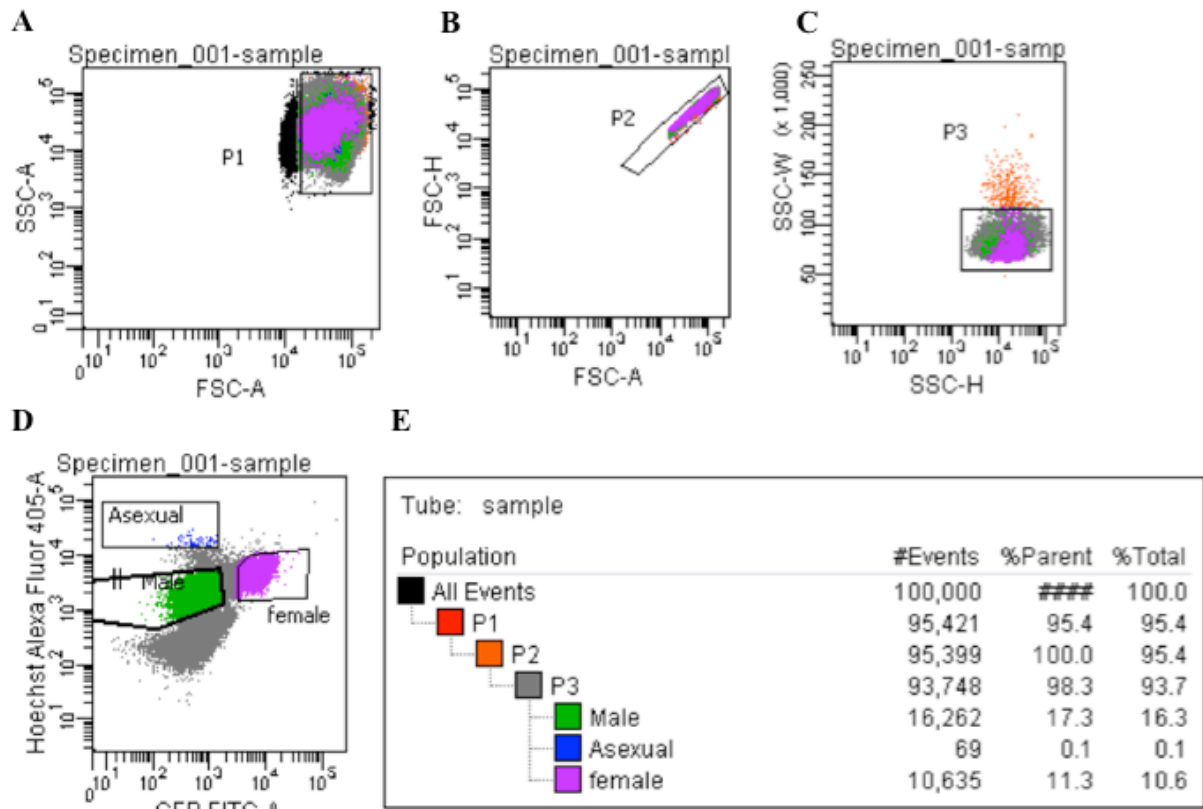


**Figure 2:** Representative full gating strategy for sorting male and female gametocytes by flow cytometry. A-C) Dot plots of sequential gating (P1-3) to exclude debris and doublet cells. D) Dot plot of gating around male gametocytes (Male), female gametocytes (Female) and activated male gametocytes or contaminating asexual parasites (Asexual). E) Corresponding population statistics. SSC-A: side scatter area; FSC-A: forward scatter area; FSC-H: forward scatter height; SSC-H: side scatter height; SSC-W: side scatter width; GFP FITC-A: green fluorescent protein fluorescein isothiocyanate area (488 nm excitation/530 nm emission); Hoechst Alexa Fluor 405-A: Hoechst 33342 Alexa Fluor 405 area (405 nm excitation/421 nm emission).

Cell sorting was performed on a BD FACS Aria I calibrated prior to each sort with the unstained and single colour controls. FACS sorting was performed at 37°C in PBS with collection in complete culture medium diluted up to 1:5 by PBS during collection (depending on the number of collected cells, each in a droplet of PBS). The gating strategy established using FACS Diva software is illustrated in Figure 2. Briefly, three gates were established to isolate whole, single cells based on forward and side scatter. Of these cells, gametocytes were identified based on the presence of Hoechst 33342 staining (405 nm excitation/421 nm emission) and females displayed an additional GFP signal (488 nm excitation/530 nm emission) from the female specific expression of gABCG2-GFP. Gametocytes of both sexes had similar Hoechst intensity given their similar DNA content. Cells with low Hoechst intensity correspond to uninfected RBC and were excluded. A low proportion of cells with

high Hoechst intensity were also excluded as they correspond to either asexual schizont stage parasites or activated male gametocytes that have replicated their DNA. Male and female gametocyte gates were conservatively drawn to prioritise purity rather than yield. Collected cells were centrifuged at  $754 \times g$  for 10 min and used immediately for experiments.

### **2.5.2. Sex-specific gametocyte viability assay**

To determine the sex-specific effect of lipid targeting drugs on gametocytes, magnet enriched gametocytes were exposed to 20  $\mu\text{M}$  of each compound, 200  $\mu\text{M}$  artemisinin (0 % viable control) or 0.1 % (v/v) DMSO (100 % viable control) for 96 h from day 2 to 4 post commitment in complete culture medium with 50 mM N-acetyl D-glucosamine in a 96 well plate at 37 °C in hypoxic conditions (1 % O<sub>2</sub>, 5 % CO<sub>2</sub>, 94 % N<sub>2</sub>).

Parasites were stained in 50  $\mu\text{g}/\text{mL}$  Hoechst 33342 and 500 nM MitoTracker Deep Red in complete culture medium supplemented with 50 mM N-acetyl D-glucosamine for 30 min at 37 °C in hypoxic conditions (1 % O<sub>2</sub>, 5 % CO<sub>2</sub>, 94 % N<sub>2</sub>). Stained cells were rinsed twice in PBS with 1000  $\times g$ , 5 min spins and resuspended in PBS. Single colour controls for flow cytometry consisted of asexual 3D7 WT culture stained with 500 nM MitoTracker Deep Red or 50  $\mu\text{g}/\text{mL}$  Hoechst 33342 for 30 min in complete culture medium and rinsed twice in PBS with 1000  $\times g$ , 1 min spins and resuspended in PBS; and unstained 3D7 gABCG2-GFP gametocytes suspended in PBS. Unstained asexual 3D7 WT parasites in PBS were used as the unstained control. Samples were analysed on a LSR II Flow Cytometer (BD Biosciences) detecting Hoechst 33342 in the Pacific Blue channel (405 nm excitation/461 nm emission), MitoTracker Deep Red in the APC-Cy7 channel (allophycocyanin-cyano dye 7, 644 nm excitation/665 nm emission) and GFP in the FITC channel (fluorescein isothiocyanate, 488 nm excitation/509 nm emission). A total of 500,000 events were recorded in each single colour control. In each sample data was recorded until 500,000 female gametocytes were counted.

The gating strategy to exclude debris, select single cells, exclude uninfected RBC and asexual parasites, and to identify male and female gametocytes is the same as in Figure 2. In addition, the mean fluorescence intensity of MitoTracker Deep Red detected on the APC-Cy7 channel was recorded for each of the gametocyte populations. Data was analysed in FlowJo and statistical significance was determined by ANOVA (analysis of variance) in GraphPad Prism. Cell viability is expressed as a percentage of the mean fluorescence intensity of MitoTracker

Deep Red in gametocytes treated with 0.1 % DMSO (100 % viable) and 200  $\mu$ M artemisinin treated gametocytes (0 % viable).

### **2.5.3. Gametocyte commitment rate assay**

To measure parasite commitment rate, gametocytes were induced as described in 2.2.2, starting with exactly 2 % trophozoites at 4 % haematocrit on day -3 of gametocytogenesis. Every second day from day 2 onwards parasitemia was measured by flow cytometry of an aliquot of culture stained with 50  $\mu$ g/mL Hoechst 33342 in PBS for 15 min at 37 °C, rinsed twice in PBS with 2000  $\times$ g, 1 min spins and resuspended in PBS. Samples were analysed on a LSR II Flow Cytometer (BD Biosciences) detecting Hoechst 33342 in the Pacific Blue channel (350 nm excitation/461 nm emission). Parasitemia was calculated as the proportion of Hoechst 33342 positive cells in 200,000 whole, single cells as gated in FACS Diva software. Statistical significance and graphing of results was performed in GraphPad Prism 7.

## **2.6. Molecular biology techniques**

### **2.6.1. DNA extraction and concentration**

Genomic DNA was extracted from saponin-isolated trophozoite stage parasites (see 2.2.6) or frozen male and female gametocyte-infected RBC sorted by FACS (see 2.5.1) using DNeasy Blood and Tissue kit (Qiagen) as per the manufacturer's instructions. For Southern blot analysis, genomic DNA was eluted twice in 200  $\mu$ L elution buffer then concentrated in 40  $\mu$ L 3 M sodium acetate and 880  $\mu$ L 100 % ethanol at 4 °C overnight. Samples were centrifuged at 17,000  $\times$ g for 30 min at 4 °C then DNA was washed twice in 70 % ethanol with 17,000  $\times$ g, 20 min spins. DNA was air dried then re-suspended in TE buffer. Genomic DNA samples prepared for bisulfite sequencing were eluted in milliQ water pH 7.0 and concentrated by SpeediVac rotary vacuum pump at 37 °C until sample volume reached approximately 20  $\mu$ L. DNA concentration and purity was measured by nanodrop.

### **2.6.2. RNA extraction**

Ribonucleic acid (RNA) was extracted from frozen saponin-isolated asexual parasites (see 2.2.6) or frozen male and female gametocyte-infected RBC sorted by FACS (see 2.5.1) using RNeasy kit (Qiagen) as per the manufacturer's instructions, without DNA digestion. RNA was eluted in 20  $\mu$ L RNase free water (provided) and re-eluted in the first eluate. RNA concentration and purity was measured by nanodrop.



## 2.6.3. Quantitative PCR

### 2.6.3.1. Primer design to quantify asexual parasites, male gametocytes and female gametocytes

A reference gene and markers for male gametocytes, female gametocytes and asexual stage parasites were selected based on RNA seq profiles (López-Barragán et al. 2011). Of the selected markers, gABCG2 (PF3D7\_1426500), P25 (ookinete surface protein, PF3D7\_1031000) and P230 (6 cysteine protein, PF3D7\_0208900) were previously described sex-specific markers. Putative female marker (PF3D7\_1447600), putative male marker 1 (PF3D7\_1477700, *Plasmodium* helical interspersed subtelomeric (PHIST) type a exported protein), putative male marker 2 (PF3D7\_1438800), putative asexual marker 1 (PF3D7\_0309500, asparagine synthetase [glutamine-hydrolysing]), putative asexual marker 2 (PF3D7\_1311900, V-type proton ATPase catalytic subunit A) and the reference gene (PF3D7\_0317300) have not been described previously.

**Table 3:** Primers to quantify female gametocytes, male gametocytes and asexual parasites relative to a reference gene. gABCG2: gametocyte ATP-binding cassette transporter family member 2; PFM: putative female marker; P25: ookinete surface protein; PMM1 and 2: putative male marker 1 and 2; P230: 6 cystein protein; PAM1 and 2: putative asexual marker 1 and 2.

Stage	Gene Target	Primers (Forward/Reverse)
Female	gABCG2	PF3D7_1426500 TGCTACCTTGCATATTTCCATTTC TTTAAGGCTTGGGACCATCTT
	PFM	PF3D7_1447600 CGAAACAGGATGTGGATGGATAG GCCACAACCACAGGTATCAA
	P25	PF3D7_1031000 CCATGTGGAGATTTTTCCAAATGTA CATTTACCGTTACCACAAGTTACATTC
Male	PMM1	PF3D7_1477700 GAGAGGAATTAAATGCTGTTCTTAGAG ATCAACCATCCCATCCCTATTG
	PMM2	PF3D7_1438800 CAATCCAATGATAATAACCACAAAGGAG TCCTTCCTAATTTCAATTGTCCTGAA
	P230	PF3D7_0208900 CCCAACTAATCGAAGGGATGAA AGTACGTTTAGGAGCATTTTTTGGTAA
Asexual	PAM1	PF3D7_0309500 CGATTAAGAAGGAAGGCCCTAAA TTGTCGTCCCATCATCATTCTC
	PAM2	PF3D7_1311900 GGGCAGAAGCCTTAAGAGAAA CCTATACGAGATGGAGAACCAATAC
Reference	PF3D7_0317300	AATAGTCGAAGCGGGAAGTG CGAATTGGATTCTCCCAAATAACC

### 2.6.3.2. Primer design for quantification of SMS1 and SMS2 transcript abundance

The expression of SMS1 and SMS2 relative to that of a reference gene was measured by quantitative reverse transcriptase polymerase chain reaction (qRT-PCR) of the gene transcripts. Where possible primers were designed to specifically amplify RNA rather than DNA, by bridging exon/exon junctions (Figure 3). SMS1 contains four exons and is alternatively spliced between the first and second exon. To quantify total SMS1 expression, primers bridging the exon 3/exon 4 junction were designed. Each alternative SMS1 transcript (SMS1.1 and SMS1.2) was specifically quantified with primers that amplified the splice-variant-specific sequence at the exon 1/exon 2 junction. Neither SMS2 nor the reference gene contain introns, so primers for these transcripts are non-RNA-specific.

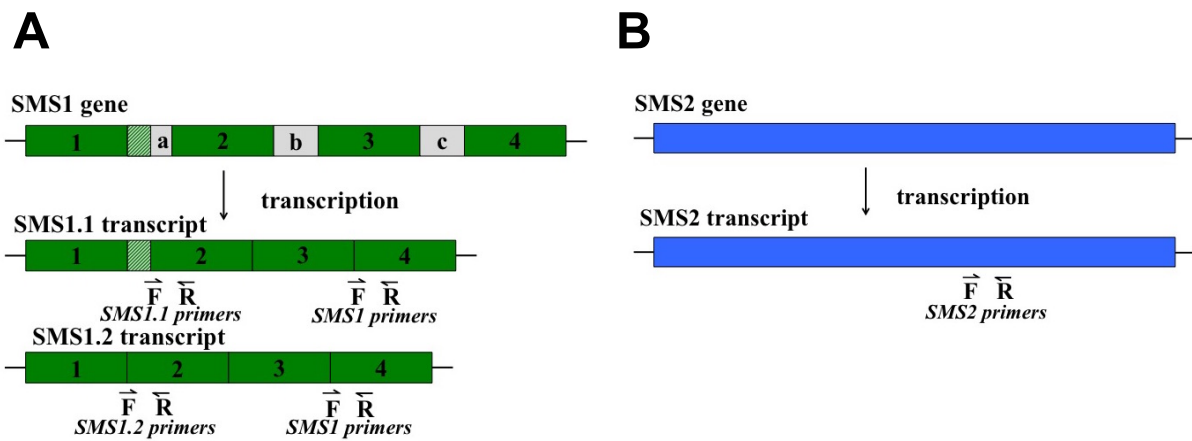


**Figure 3:** primer design for quantification of SMS1 transcripts (A) and SMS2 transcript (B). Exons are numbered 1-4 and introns are labelled a-c. F: forward, R: reverse.

**Table 4:** qRT-PCR primers for the quantification of SMS1 and SMS2 expression

Target	Gene ID	Primers (Forward/Reverse)
SMS1	PF3D7_0625000	TCATATGACAAAGAATGGAATTGT GTACCATTTCAGCGTATGAA
SMS1.1	PF3D7_0625000.1	CTTATTCTGATAATAAAGGCCAT GGTAGCACAACCAAACGC
SMS1.2	PF3D7_0625000.2	CAAATATTGGCCATTATTTTGAAG GGTAGCACAACCAAACGC
SMS2	PF3D7_0625100	ACTTCATTACCCGCAACATTAGA CCTGATACAATCAAATCAGCACATAC
Reference	PF3D7_0317300	AATAGTCGAAGCGGGAAGTG CGAATTGGATTCTCCCAAATAACC

### 2.6.3.3. Primer design for fitness competition monitoring by qPCR

The abundance of WT and knock out (KO) genotypes in co-cultures was monitored by qPCR of regions of DNA specific to each genome. SMS1 KO and SMS2 KO parasites were each quantified by primers specific to the sequence of the inserted hDHFR drug resistance cassette. WT parasites were distinguished from SMS1 KO parasites by primers specific to the region of SMS1 disrupted by homologous recombination in the SMS1 KO parasites. WT parasites in the SMS2 KO/WT co-cultures were similarly quantified by primers specific to the section of SMS2 that was removed to disrupt SMS2 in the SMS2 KO parasites. The reference gene primers amplify a gene present in both WT and KO parasites, which was quantified to normalise measurements to the same amount of DNA template.

**Table 5:** Fitness competition primers to quantify wild type (SMS1 or SMS2 “cut out”) and knock out (hDHFR) parasite genotype abundance relative to total parasite abundance (reference).

Target	Gene ID	Primers (forward/reverse)
SMS1 “cut out”	PF3D7_0625000	ACTGTTGATGTGTTAATGGGATATG ATCTTCTTGCAGCTACATCTACTA
SMS2 “cut out”	PF3D7_0625100	TTCATGCAAAGCCATTCTTTCT TGGCATAATCTAAGGTATAATTCAATCC
hDHFR		GAACTCAAGGAACCTCCACAA ACAGAACTGCCACCAACTATC
Reference	PF3D7_0317300	AATAGTCGAAGCGGGAAGTG CGAATTGGATTCTCCCAAATAACC

### 2.6.3.4. Experimental procedure

Primer pairs were designed manually or in Integrated DNA Technologies Primer Quest Tool using the 3D7 strain *P. falciparum* gene sequences from PlasmoDB. Primers were resuspended in TE buffer or autoclaved milliQ water and stored at -20°C. For qRT-PCR, genomic DNA was removed from RNA samples and complementary DNA was synthesised using Quantitect Reverse Transcription kit (Qiagen) as per the manufacturer’s instructions. For qPCR experiments, genomic DNA was used as the template for the qPCR reactions. Both qRT-PCR and qPCR were performed with Light Cycler 480 SYBR Green I Master mix (Roche) as per the manufacturer’s instructions for 10 µL reactions in a 384 well plate. Thermocycling was performed in a Light Cycler 480 with a 10 min, 95°C pre-incubation; 45 cycles of 15 s denaturation at 95°C, 15 s annealing at an assay-specific temperature and 20 s elongation at 72°C; followed by a melt curve established by denaturing at 95°C for 30 s,

annealing at 60°C for 30 s and then slowly denaturing by increasing the temperature to 95°C at 0.11°C/s. The annealing temperature was 50°C for the quantification of asexual parasites/male gametocytes/female gametocytes, or 52°C for the fitness competition qPCR and quantification of SMS1 and SMS2 expression. Melt curves were observed using Light Cycler 480 software. The exported text file was converted using Light Cycler 480 converter and Cq and PCR efficiencies were determined in LinReg. Relative quantification of transcripts was expressed as described previously (Pfaffl 2001).

For the quantification of asexual parasites/female gametocytes/male gametocytes:

$$\text{ratio} = (E_{\text{target}}^{\Delta\text{CP}_{\text{target}}(\text{female-male})}) / (E_{\text{ref}}^{\Delta\text{CP}_{\text{ref}}(\text{female-male})})$$

with:  $E_{\text{target}}$ : primer efficiency of the target gene

$E_{\text{ref}}$ : primer efficiency of the reference gene

$\Delta\text{CP}_{\text{target}}$  (female-male): difference in crossing points of target gene amplification in the female gametocyte sample and male gametocyte sample

$\Delta\text{CP}_{\text{ref}}$  (female-male): difference in crossing points of reference gene amplification in the female gametocyte sample and male gametocyte sample

For the quantification of SMS expression in WT and KO parasites:

$$\text{ratio} = (E_{\text{target}}^{\Delta\text{CP}_{\text{target}}(\text{WT-KO})}) / (E_{\text{ref}}^{\Delta\text{CP}_{\text{ref}}(\text{WT-KO})})$$

with:  $E_{\text{target}}$ : primer efficiency of the target gene

$E_{\text{ref}}$ : primer efficiency of the reference gene

$\Delta\text{CP}_{\text{target}}$  (WT-KO): difference in crossing points of target gene amplification in WT parasites and KO parasites

$\Delta\text{CP}_{\text{ref}}$  (WT-KO): difference in crossing points of reference gene amplification in WT parasites and KO parasites

For the quantification of WT and KO parasite genotypes in co-cultures:

$$\text{ratio} = (E_{\text{target}}^{\Delta\text{CP}_{\text{target}}(\text{clonal-competition})}) / (E_{\text{ref}}^{\Delta\text{CP}_{\text{ref}}(\text{clonal-competition})})$$

with:  $E_{\text{target}}$ : primer efficiency of the target gene

$E_{\text{ref}}$ : primer efficiency of the reference gene

$\Delta\text{CP}_{\text{target}}$  (clonal-competition): difference in crossing points of target gene amplification in a clonal population and the fitness competition co-culture

$\Delta\text{CP}_{\text{ref}}$  (clonal-competition): difference in crossing points of reference gene amplification in a clonal population and the fitness competition co-culture

#### 2.6.4. Southern Blot

Disruption of a gene locus by homologous recombination was confirmed by diagnostic digest with restriction enzymes followed by Southern blot probing for both the 5' and 3' homologous regions (Rug & Maier 2013). Three µg ethanol-concentrated genomic DNA or 1 ng plasmid DNA was double digested with 20 U each of either AflIII and PacI (for SMS1 KO screening) or Xmn I and Hind III- HF (for SMS2 KO screening) in Cutsmart buffer for 4 h at 37°C.

Digested DNA was run on a 0.8 % agarose gel without ethidium bromide at 90 V for 15 min then at 20 V for 18 h using BioRad gel tank and power pack. The gel was stained with 0.4 mg/mL ethidium bromide in TBE buffer for 30 min, destained in milliQ water for 20 min and imaged under ultra violet (UV) light with a ruler for scale. The gel was then rinsed as follows: 15 min in depurination solution; 3 min in milliQ water; 2× 15 min in denaturation solution; 3 min in milliQ water; 2× 15 min in neutralisation solution; 3 min in milliQ water then 5 min in 20× SCC. DNA was transferred from the gel to the membrane overnight in a capillary transfer setup.

Alkali-labile digoxigenin labelled deoxyuridine triphosphate (DIG-dUTP) was incorporated in Southern blot probes by PCR using PCR DIG Probe Synthesis kit (Roche) and a Veriti 96 Well Thermocycler (Applied Biosystems) with the following specifications. SMS2 5' and 3' probes were amplified from pCC-1/SMS2 plasmid DNA using OneTaq polymerase and Taq polymerase respectively. Due to apparent non-specific amplification of SMS1 probes, unlabelled SMS1 5' and 3' probes were first amplified from pCC-1/SMS1 plasmid using OneTaq polymerase. The respective bands of interest were then purified using a gel extraction kit (Qiagen) and used as templates for labelled probe synthesis in the same PCR conditions. All probes were synthesised in the presence of 12 µM DIG-dUTPs with the exception of SMS2 3' probe, which was amplified from 6 µM DIG-dUTPs. Thermocycling conditions consisted of initial denaturation for 30 s at 94°C; 30 cycles of 30 s at 94°C, 1 min at 45°C (SMS2 3') or 50°C (SMS2 5') or 52°C (SMS1 5') or 55°C (SMS1 3'), 1 min at 68°C; final elongation for 7 min at 68°C. Probe size was confirmed by electrophoresis at 120 V for 40 min of the PCR product on a 1 % agarose gel with ethidium bromide in TBE buffer using BioRad gel tank and power pack. Gel was imaged under UV on a Vilber Lourmat imaging system.

**Table 6:** Primers for Southern blot probe synthesis

Primer code	Primer description		Primer sequence
al 514	SMS1 5'	forward	CACACATTTGTACCTCTCTTA
al515		reverse	CCTTATGGTTGTAATGTTTGTC
al516	SMS1 3'	forward	TCACAGACAGATTCCAAGTGTT
al517		reverse	GGTACCATTTCCAGCGTATGA
al518	SMS2 5'	forward	GTAAATTAAAGACATGCACGTGAGA
al519		reverse	CGCTATCTGTTACTGACTCTTCAT
al520	SMS2 3'	forward	ACCCATAACAGAGGATAA
al521		reverse	ACGACATTTAGGGATTAAA

Following transfer, the membrane was rinsed in 2× SCC for 5 min then DNA was crosslinked to the membrane in a UV cross linker set to deliver 70 mJ/cm<sup>2</sup>. The hybridisation temperature ( $T_{hyb}$ ) was calculated as follows, with  $l$  being the length of the probe in base pairs (bp):

$$T_m = 49.82 + 0.41 (\% G + C) - (600/l)$$

$$T_{hyb} = T_m - (20 \text{ to } 25^\circ\text{C})$$

The membrane was incubated with gentle rocking in DIG Easy Hyb solution (Roche Cat. No. 11 796 895 001) at  $T_{hyb}$  for 30 min, using 1 mL per 10 cm<sup>2</sup> of membrane. The probe was denatured in 50 µL water at 95°C for 5 min, cooled quickly on ice then added to DIG Easy Hyb solution at 0.15 % (v/v) to prepare 1 mL of hybridisation solution per 10 cm<sup>2</sup> of membrane. Membrane was incubated overnight in hybridisation solution at  $T_{hyb}$  with gentle rocking. DIG Easy Hyb solution and hybridisation solution were stored at -20°C and re-used up to 3 times. Prior to re-use, hybridisation solution was warmed to 68°C for 10 min to denature probe.

Membrane was prepared for detection by rinsing in 2× SCC for 5 min; equilibrating in washing buffer for 1 min; incubating in 1 % blocking solution for 30 min; incubating in 1 % blocking solution with 1:10000 α-Digoxigenin-AP Fab fragments (Roche Cat. No. 11 093 274 910, pre-centrifuged at 17,000 ×g for 5 min to remove aggregates) for 30 min; washing membrane in washing buffer for 2× 15 min then equilibrating membrane in detection buffer for 2 min. The membrane was incubated in the dark with CSPD (Roche Cat. No. 11 655 884 001) diluted 1:100 in detection buffer for 5 min at room temperature then 10 min at 37°C.

Exposed Fuji Super RX-N Medical X-Ray film to membrane in an Amersham pharmacia biotech hypercassette and developed film in an AGFA CP1000 photo developer.

## **2.7. Lipidomic analysis**

### **2.7.1. *P. falciparum* sample preparation**

Uninfected human RBC from six donors were pooled in three independent biological replicates each from two donors and incubated at 4 % haematocrit in complete culture medium for at least 48 h at 37 °C in hypoxic conditions (1 % O<sub>2</sub>, 5 % CO<sub>2</sub>, 94 % N<sub>2</sub>). Cells were pelleted at 524 ×g over 5 min and counted on an Improved Neubauer haemocytometer (Hirschmann). Aliquots of 10<sup>7</sup> cells were resuspended in 300 µL of methanol in 2 mL tough tubes (Geneworks) and stored at -80 °C.

Male and female gametocytes were sorted live by FACS as described in 2.5.1, pelleted at 754 ×g for 10 min and resuspended in 300 µL of methanol per 10<sup>7</sup> cells (as counted during FACS) in 2 mL tough tubes (Geneworks). Each biological replicate of 10<sup>7</sup> cells is pooled from 2-5 independent gametocyte cultures.

For collection of asexual parasite stages, three independent asexual *P. falciparum* cultures were sorbitol synchronised 14 h apart to within a 4 h developmental window (assuming sorbitol is lethal to parasites from 18 hpi, as described in 2.2.5). Trophozoite-infected RBC (24-28 hpi) and schizont-infected RBC (36-40 hpi) were magnet purified to more than 98 % infected RBC (see 2.2.7), as determined by Giemsa-stained thin smear, and counted on an Improved Neubauer haemocytometer (Hirschmann). Aliquots of 10<sup>7</sup> infected RBC were resuspended in 300 µL of methanol in 2 mL tough tubes (Geneworks) and stored at -80 °C. Less synchronous mature asexual stage parasites (26-42 hpi) were prepared in the same manner to make the “asexual” sample of Result Chapter 3 part 1. Ring stage infected RBC (12-16 hpi) were stained with 50 µg/mL Hoechst 33342 for 15 min at 37 °C, rinsed twice in PBS with 2,000×g, 1 min spins and resuspended in PBS for collection by FACS. Whole, single cells were gated as illustrated in Figure 2A-C and ring-infected RBC were sorted based on parasite-specific Hoechst staining (405 nm excitation/421 nm emission). Aliquots of 10<sup>7</sup> cells (as counted by FACS) in 300 µL methanol were prepared as per gametocyte samples, except each biological repeat represents one independent asexual culture.

### **2.7.2. *P. berghei* schizont sample preparation**

Three days after mice were infected with  $10^7$  mixed stage *P. berghei* parasites by intravenous injection, blood was collected by cardiac puncture with a heparinised syringe, rinsed in transfection medium (RPMI, 50 mg/L gentamycin, 20 % (v/v) heat inactivated foetal calf serum) with 5 U/mL heparin at  $270 \times g$  for 8 min, and resuspended in transfection medium. After 15 min at room temperature, the culture was incubated at  $37^\circ C$  for 20-22 h with slow shaking. Mature schizonts were purified by density gradient centrifugation at  $320 \times g$  for 30 min in 55 % (v/v) Nycodenz in PBS. Schizonts were collected at the interface of the culture medium (top layer) and Nycodenz solution (bottom layer) and rinsed at  $320 \times g$  for 10 min in the supernatant, then counted on an Improved Neubauer haemocytometer (Hirschmann). Three independent biological replicates of  $10^7$  *P. berghei* schizont-infected mouse RBC were resuspended in 300  $\mu$ L methanol in 2 mL tough tubes (Geneworks).

### **2.7.3. *P. berghei* gametocyte sample preparation**

Gametocytes were prepared as described previously (Beetsma et al. 1998) with modifications. Briefly, mice were injected with 10 mg/L phenylhydrazine (100  $\mu$ L of 0.6 % solution) by intraperitoneal injection 24 h prior to intravenous injection of  $10^7$  blood stage *P. berghei* parasites. From day 3 onwards drinking water was supplemented with 12.5 mg/L sulfadiazine to suppress asexual blood stage parasite proliferation and gametocytemia was monitored by Giemsa-stained thin smear on day 5 or 6 post infection. Blood was collected by cardiac puncture and resuspended in RPMI with 5 U/mL heparin. White blood cells were removed by passing through a column with the following layers: cotton gauze, 3 cm cellulose, 2-3 mm acid washed 212-300  $\mu$ m glass beads. Cells were pelleted at  $320 \times g$  for 6 min and resuspended in RPMI. Gametocytes were purified by density gradient centrifugation at  $1900 \times g$  for 30 min in 48 % Nycodenz in RPMI. Gametocytes were collected at the interface and rinsed at  $7600 \times g$  for 1 min in RPMI. Gametocytemia and haematocrit was counted by Giemsa-stained thin smear and on an Improved Neubauer haemocytometer (Hirschmann) respectively. Three independent biological replicates of  $10^7$  *P. berghei* gametocyte-infected mouse RBC were resuspended in 300  $\mu$ L methanol in 2 mL tough tubes (Geneworks).

### **2.7.4. Uninfected mouse RBC sample preparation**

Blood from uninfected mice was collected by cardiac puncture in a heparinised syringe and resuspended in RPMI with 5 U/mL heparin. White blood cells were removed by passing through a column with the following layers: cotton gauze, 3 cm cellulose, 2-3 mm acid washed 212-300  $\mu$ m glass beads. Cells were pelleted at  $320 \times g$  for 6 min and resuspended in



RPMI. RBC were counted on an Improved Neubauer haemocytometer (Hirschmann) and two biological replicates of  $10^7$  uninfected RBC were resuspended in 300  $\mu\text{L}$  methanol in 2 mL tough tubes (Geneworks).

#### **2.7.5. Salivary gland sample preparation**

Blood feeding and mosquito dissection was performed as described previously (Vanderberg 1975). *Anopheles stephensi* mosquitos were killed with 70 % ethanol and washed in RPMI. Under a stereo microscope with 16 $\times$  magnification, the mosquito head was separated from the thorax and salivary glands were dissected from the head using thin needles. To estimate the average cell number per salivary gland, salivary glands were mounted on a slide with 4',6-diamidino-2-phenylindole fluoromount (DAPI, 350 nm excitation/460 nm emission) under a cover slip and dried for 1 h. Nuclei were counted in 20 salivary glands on a Zeiss axio imager.Z2 microscope. To count the number of sporozoites per salivary gland, mosquito material was ground with a pestle, centrifuged for 3 min at 9400  $\times g$  at 4  $^{\circ}\text{C}$ , resuspended in RPMI with 3 % bovine serum albumin and counted on an Improved Neubauer haemocytometer (Hirschmann). Two biological replicates of  $10^6$  *P. berghei* sporozoites were collected with mosquito salivary glands in methanol in 2 mL tough tubes (Geneworks). Each uninfected salivary gland control contained a matching amount of material to the sporozoite-infected samples. To compare sporozoite and blood stage parasite lipid abundance, the lipid profile of sporozoite-infected salivary glands was divided by the number of host cells per salivary gland.

#### **2.7.6. Media sample preparation**

Media samples for lipidomics consisted of three replicates of 300  $\mu\text{L}$  of the solutions described in Table 7 below. NB: gametocyte medium 1 is the same medium composition as complete culture medium (Table 1), which was used for all *P. falciparum* cultures, both asexual and sexual blood stages throughout this thesis. The media nomenclature described below is exclusively used for media lipidomics in Result Chapter 3.

**Table 7:** Media sample composition for lipidomics

Sample	Description
RPMI	RPMI 1640-HEPES with Glutamax
AlbuMAX II	RPMI 1640-HEPES with Glutamax, 5 % (w/v) AlbuMAX II
Serum	Heat inactivated human serum pooled from 5 donors
Asexual medium	RPMI 1640-HEPES with Glutamax, 10 mM glucose, 20 µg/mL gentamicin, 480 µM hypoxanthine, 0.5 % (w/v) AlbuMAX II
Gametocyte medium 1	RPMI 1640-HEPES with Glutamax, 10 mM glucose, 20 µg/mL gentamicin, 480 µM hypoxanthine, 0.375 % (w/v) AlbuMAX II, 2.5 % (v/v) human serum
Gametocyte medium 2	RPMI 1640 (from Gibco powder), 25 mM HEPES, 50 mg/mL hypoxanthine, 42 mL/L 5 % NaHCO <sub>3</sub> , 10 % (v/v) human serum

### 2.7.7. Lipidomics analysis by direct infusion MSMS

Lipids were extracted as described previously (Matyash et al. 2008) with modifications. Internal standards (Tran et al. 2016) in 50 µL of methanol with 0.01 % butylated hydroxytoluene were aliquoted among tubes. Internal standards and 1.4 mm beads (Geneworks) were added to tough tubes containing samples in 300 µL methanol and samples were homogenized with a bead homogenizer (FastPrep-24, MP Biomedical) at 6 m/s for 40 s and transferred to new tubes. Beads were rinsed in 100 µL of methanol, which was added to the sample in new tubes. Samples were vortexed with 1 mL of methyl-tert butyl ether at 4 °C for 1 h. Phase separation was induced by adding 300 µL of 150 mM ammonium acetate (liquid chromatography–MS grade, Fluka), vortexing for 5 min and centrifuging at 2,000 ×g for 5 min. The upper organic layer (representing around 800 µL) was transferred to a 2 mL glass vial and stored at –20 °C. Prior to MS analysis, each sample was diluted into methanol:chloroform (2:1 v/v) with 5 mM ammonium acetate.

An aliquot of each extract was hydrolyzed to remove acyl-linked lipids and re-extracted to

improve mass spectrometric analysis of sphingolipids. Two hundred  $\mu\text{L}$  of extract was added to 60  $\mu\text{L}$  of methanol containing 0.01 % butylated hydroxytoluene, 22  $\mu\text{L}$  of 10 M NaOH was added (final concentration 0.7 M), and vortexed at 800 rounds per minute on an Eppendorf Mixmate for 2 h at room temperature. Sixty  $\mu\text{L}$  of 150 mM aqueous ammonium acetate was added to induce phase separation. Tubes were vortexed and spun at  $20,000 \times g$  for 5 min to complete phase separation. The upper organic layer was removed to a new 2 mL glass vial, and diluted into methanol:chloroform (2:1 v/v) containing 5 mM ammonium acetate prior to mass spectrometric analysis.

Mass spectra was obtained with a chip-based nanoESI source (TriVersa Nanomate, Advion) and a hybrid linear ion-trap-triple quadrupole MS (QTRAP 5500, ABSCIEX). Ten  $\mu\text{L}$  of each sample extract in a sealed Eppendorf Twin-Tec 96 well plate was aspirated and delivered to the MS through a nanoESI chip. Positive ion and negative ion acquisition was obtained as described previously (Tran et al. 2016).

Data smoothing, lipid identification, removal of isotope contribution from lower mass species and correction for isotope distribution was performed in LipidView (ABSCIEX) software version 1.2. A signal to noise ratio threshold of 20 was applied for inclusion of ionized lipids. Extraction and solvent blanks were analyzed in each data acquisition batch to exclude chemical or solvent impurities. Lipids were quantified in LipidView by comparing peak area of each lipid to its class-specific internal standard after isotope correction. Where odd-chain fatty acid phospholipids or ether-linked phospholipids could not be distinguished, phospholipids were assumed to be ether linked. A correction factor of 3.45 was applied to all ether-PE species to account for the  $\sim 29\%$  difference in efficiency in the neutral loss of the 141 Da fragment from plamenyl and diacyl PE respectively (Mitchell et al. 2007; Abbott et al. 2013). Lipid species are annotated as per Liebisch et al. (2013) shorthand, except for DAG and TAG.

LipidView data was exported to Excel then imported to Markerview v1.2.1.1 (Applied Biosystems, MDS Sciex) with lipid annotation and quantification for statistical analysis of all individual lipid species. Pareto scaling without weighting was applied for unsupervised mode principal component analysis. Multiple t-tests for volcano plots were also performed in MarkerView. Grouping into lipid classes, calculation of lipid proportions and subtraction of the host cell lipid profile was performed in Microsoft Excel. For infected and uninfected mosquito salivary gland samples, the lipid abundance was divided by the number of cells per

salivary gland to obtain the lipid abundance per host cell. GraphPad Prism 7 was used to prepare final graphs and perform ANOVA with multiple comparisons on lipid class abundance.

### **2.8. Bisulfite sequencing**

One hundred ng DNA was extracted from two independent biological replicates of saponin-isolated trophozoite-infected RBC (see 2.2.6) and FACS-collected male and female gametocytes (see 2.5.1). A third trophozoite DNA sample was prepared in the same manner for an unmethylated control. Male and female gametocyte samples were pooled from 6-8 independent cultures whereas each trophozoite biological replicate is from a single *P. falciparum* culture. Bisulfite conversion was performed on all samples except the unmethylated control using EZ DNA methylation Gold kit (Zymo Research) as per the manufacturer's standard protocol. Each sample was spiked with 0.5 % unmethylated  $\lambda$  phage DNA to measure bisulfite conversion efficiency and compensate for the adenosine/thymine (AT) bias of the *P. falciparum* genome, then stored at -80 °C until library preparation. TruSeq LT library preparation as per the manufacturer's instructions followed by whole genome Illumina sequencing on a NextSeq500 Mid run with 75 bp paired end reads was performed at the Ramaciotti Centre for Genomics. Reads were aligned to *P. falciparum* 3D7 genome in BiSMark and analysed in EdgeR as per Chen et al. (2017).

# Result Chapter 1

***Plasmodium* lipid dynamics in the  
mammalian host and mosquito vector**

## Overview

In this chapter the lipid profile of *Plasmodium* parasite-infected host cells is investigated throughout the parasite lifecycle. Part 1 explores lipid dynamics over three time points of asexual blood stage *P. falciparum* replication. In Part 2 a mouse malaria parasite, *P. berghei*, is used to extend the study of lipids from schizonts to gametocytes in the blood and to sporozoites in the mosquito. Part 3 contrasts the findings in *P. berghei* and *P. falciparum* to identify species-specific lipid dynamics.

## Part 1

### Lipid dynamics during asexual blood stage *P. falciparum* replication

#### Introduction

During asexual blood stage parasite proliferation, lipids are in high demand for membrane biogenesis to surround the maturing parasite, daughter cells and organelles. Lipids also mediate parasite functions in the host RBC.

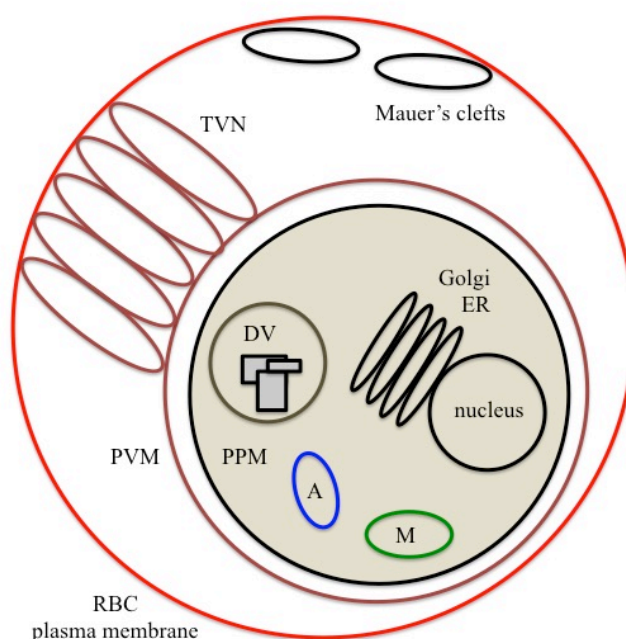


**Figure 1:** Lipid membranes in the trophozoite-infected red blood cell. The parasite (in brown) is encased in three membranes and forms membrane-bound organelles in the parasite and host cell cytoplasm. A: apicoplast; DV: digestive vacuole; ER: endoplasmic reticulum; M: mitochondria; PPM: parasite plasma membrane; PVM: parasitophorous vacuole membrane; RBC: red blood cell; TVN: tubulovesicular network.

The blood stage parasite is encased in three membranes (Figure1): the outermost RBC plasma membrane, the PVM and the internal parasite plasma membrane. The PVM progressively surrounds the invading merozoite, sourcing lipids from both the merozoite (Dluzewski et al. 1992; Dluzewski et al. 1995) and the host RBC (Haldar & Uyetake 1992). Phospholipids are the main component of membranes and are arranged in an asymmetric lipid bilayer. Whether the lipid asymmetry is modified after infection, in particular whether PS is exposed at the surface of the host RBC, is unclear (Gupta & Mishra 1981; Van der Schaft et al. 1987; Moll et al. 1990; Maguire et al. 1991; Simões et al. 1992; Sherman et al. 1997). The RBC plasma membrane is much richer in cholesterol than the parasite plasma membrane

(Tokumasu et al. 2014) – a property that allows the selective lysis of the RBC plasma membrane, but not the parasite plasma membrane with saponin (Beaumelle et al. 1987). Cholesterol and sphingomyelin in the RBC plasma membrane are clustered in detergent resistant domains, termed “lipid rafts” in this thesis (Schroeder et al. 1998). In other organisms, lipid rafts are known to be involved in protein export and function as signalling platforms (Simons & Toomre 2000). Lipid rafts may play a functional role in parasite invasion since cholesterol depletion of the host cell plasma membrane inhibits parasite invasion (Samuel et al. 2001). Only proteins in detergent resistant domains of the host RBC plasma membrane are incorporated in the PVM, presumably by a sieve-like mechanism similar to that described in *T. gondii* (Mordue et al. 1999). Lipids therefore play a structural role as components of cell membranes, but also impact protein trafficking and co-ordinate intracellular signalling pathways.

Over 48 h, the single invading merozoite multiplies into many daughter merozoites (32 in *P. falciparum*) by schizogony, requiring highly dynamic membrane biogenesis (Schrevel et al. 1977; Francia & Striepen 2014). After multiple asynchronous nuclei divisions within the same cell form a syncytium (Read et al. 1993), the last synchronised division is coupled with daughter cell assembly. In apicomplexan parasites, daughter cells are formed along the so-called pellicle that consists of a polarised microtubule scaffold and the inner membrane complex (Morrissette et al. 1997; Mann & Beckers 2001; Anderson-White et al. 2012). The inner membrane complex is comprised of a series of flattened vacuoles that derive from the Golgi apparatus and the mother parasite plasma membrane (Sheffield & Melton 1968; Agop-Nersesian et al. 2010; Anderson-White et al. 2012). The pellicle directs the segregation of organelles synthesised *de novo* into each daughter cell. Spatial segregation of proteins in the daughter cell is mediated by post-translational acylation by inner membrane complex compartment-specific acyl-transferases (Beck et al. 2010; Fung et al. 2012; De Napoli et al. 2013; Fréchal et al. 2013). After full cytokinesis of the daughter merozoites, tyrosine phosphorylation of band 3 protein breaks the bond between the lipid bilayer and the spectrin/actin cytoskeleton, thereby destabilising the host RBC plasma membrane and releasing the daughter merozoites (Pantaleo et al. 2017). This dynamic membrane biogenesis and remodelling during asexual parasite replication likely requires extensive lipid supply.

Being a eukaryote, the parasite also develops membrane bound organelles including a nucleus, Golgi apparatus, endoplasmic reticulum and mitochondria (Figure 1). The lipid



composition of organelles is distinct, partially due to the compartmentalisation of lipid metabolism. For example, fatty acid elongation takes place in the endoplasmic reticulum of the parasite (Ramakrishnan et al. 2013) whereas PG is specific to the inner membrane of the mitochondria. The lipid composition of parasite organelles not only increases parasite lipid requirements, but also contributes to the diversity of parasite lipids.

In addition, *P. falciparum* develops parasite-specific organelles such as the digestive vacuole, apicoplast and invasion machinery (Figure 1). The digestive vacuole is where haemoglobin from the host RBC is digested as a source of amino acids (Rosenthal & Meshnick 1996; Loria et al. 1999), and the toxic haem (Loria et al. 1999; Campanale et al. 2003) is sequestered in the form of haemozoin crystals (Slater & Cerami 1992; Sullivan 2002). Lipid bodies rich in neutral lipids have been observed in the digestive vacuole (Jackson et al. 2004) and are proposed to act as a neutral lipid store and/or contribute to the detoxification of haem (Papalexis et al. 2001; Jackson et al. 2004). The apicoplast is a non-photosynthetic plastid thought to have evolved from endosymbiosis of a eukaryotic alga and its plastid (Foth & McFadden 2003; Lim & McFadden 2010; McFadden 2011; van Dooren & Striepen 2013). The apicoplast is bound by four membranes and is the site of the FASII pathway, as detailed in the general introduction. The parasite also contains secretory organelles including rhoptries and micronemes that make up the parasite's invasion machinery. *Plasmodium* parasites contain two pear-shaped acidic rhoptries that may contribute lipids to the PVM during invasion (Bannister & Mitchell 1989; Dluzewski et al. 1995). Indeed, in closely related *T. gondii*, rhoptries contain large amounts of cholesterol and PC (Foussard et al. 1991; Coppens & Joiner 2003). Phosphoinositide metabolism, particularly phosphatidic acid, is involved in the induction of microneme release (Brochet et al. 2014; Bullen et al. 2016). The lipids are therefore crucial to parasite specific functions during asexual replication in the blood.

In addition to generating intra-parasitic organelles, the parasite creates membranous structures in the host RBC cytoplasm that are thought to have a role in protein trafficking and nutrient acquisition (Figure 1). These include the tubulovesicular membrane network (Behari & Haldar 1994; Elmendorf & Haldar 1994) and Mauer's clefts (Atkinson et al. 1988; Elford et al. 1995; Elford et al. 1997; Lanzer et al. 2006). Given tubulovesicular membrane network assembly is blocked by inhibition of sphingomyelin synthesis (Lauer et al. 1997) and a ceramide lipid dye localises to the organelle (Behari & Haldar 1994), sphingolipids likely

play an important role in tubulovesicular membrane network function. In summary, lipids contribute to host cell remodelling during asexual parasite proliferation.

Lipids clearly have many important functions in the asexual blood stage lifecycle of *P. falciparum*, some of which have been studied in great detail. In an attempt to investigate the overarching lipid dynamics over the asexual blood stage lifecycle, Gulati et al. (2015) measured the lipid composition in saponin-isolated parasites. While this study revealed many aspects of *P. falciparum* lipid biology, the experimental approach limited the scope for interpretation. Firstly, given that saponin targets cholesterol-rich membranes, the recorded lipid composition may have been compromised and cholesterol itself could not be measured. Secondly, by isolating the parasite the authors were unable to detect parasite induced lipid modifications in the host cell. This chapter seeks to decipher lipid dynamics in the whole infected RBC during the asexual lifecycle of *P. falciparum*.

### **Results**

Asexual blood stage parasites mature in the 48 h following merozoite invasion through morphologically defined ring, trophozoite and schizont stages. To capture the lipid dynamics of RBC infected with *P. falciparum*, the lipid composition of infected RBC was measured at three time points corresponding to each asexual lifecycle stage: rings 12-16 hpi, trophozoites 24-28 hpi and schizonts 36-40 hpi. Three biological replicates of  $10^7$  cells were measured for each sample. For the complete list of lipid species measured in this study, refer to Supplementary Table 1.

1. Asexual *P. falciparum* accumulates lipids in the host cell

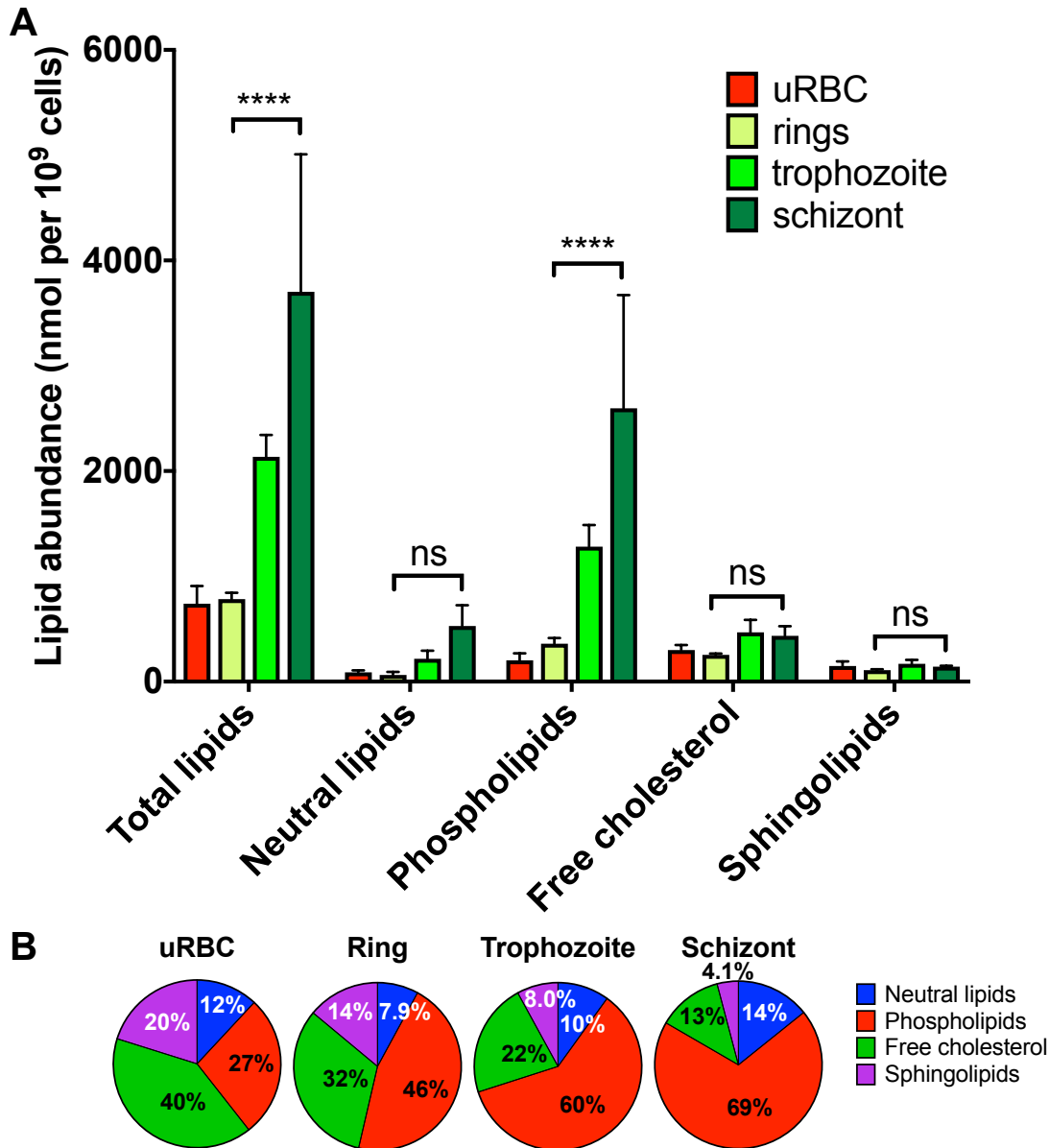


**Figure 2:** Overview of *P. falciparum* lipidome during asexual blood stages. Mean abundance with standard deviation (A) and mean proportions (B) of total lipids and major lipid classes in uninfected red blood cells (uRBC) and red blood cells infected with ring stage *P. falciparum* 12-16 hours post invasion (ring), trophozoite stage *P. falciparum* 24-28 hours post invasion (trophozoite) or schizont stage *P. falciparum* 36-40 hours post invasion (schizont). Statistical significance from two-way ANOVA indicated in A as follows: ns: not significant  $p > 0.1$ , \*\*\*\*:  $p < 0.0001$ .

Overall, parasite invasion and maturation is coupled with an increase in total lipids (Figure 2A). Indeed, trophozoite-infected RBC contain close to five times more lipids than ring-infected RBC. This trend is mirrored in phospholipids but not other major lipid categories (free cholesterol, neutral lipids and sphingolipids), which are relatively stable. Given that

phospholipids are the main component of membranes, this suggests that the increase in lipids in asexual blood stages is mostly due to membrane biogenesis. The predominant lipid proportion in uninfected RBC is cholesterol (Figure 2B). After infection the proportion of free cholesterol decreases from 32 % at 12 hpi to 13 % at schizont stage, as does the proportion of sphingolipids. Meanwhile the proportion of phospholipids and neutral lipids increases over the same period. The latter may indicate that mature blood stage parasites accumulate fatty acid reserves in the form of neutral lipids for rapid membrane lipid synthesis during asexual replication.

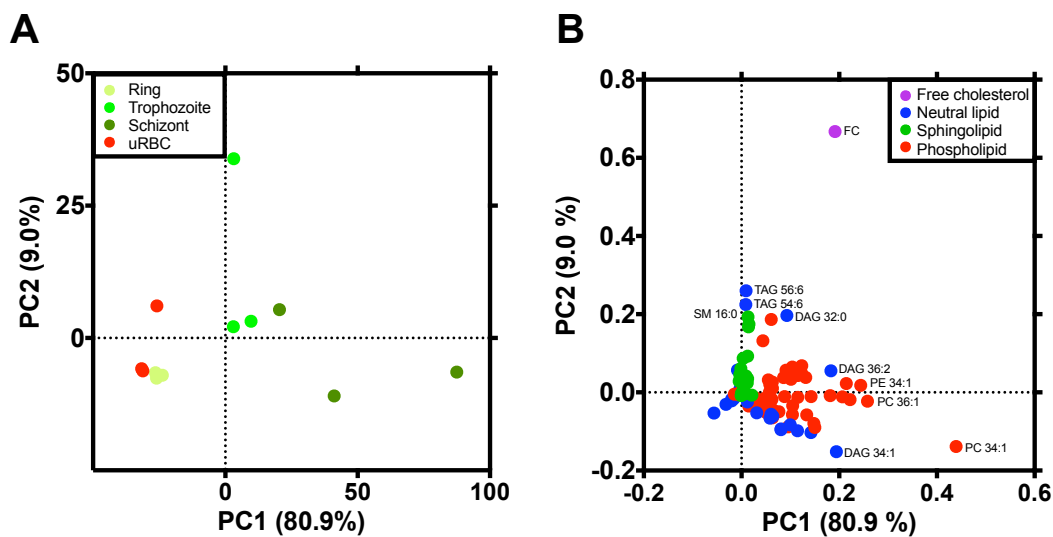


**Figure 3:** A) Principal component analysis plot and B) loading plot of all measured lipids in uninfected red blood cells (uRBC) and red blood cells infected with ring stage *P. falciparum* 12-16 hours post invasion (ring), trophozoite stage *P. falciparum* 24-28 hours post invasion (trophozoite) or schizont stage *P. falciparum* 36-40 hours post invasion (schizont). PC1 and 2: first and second principal component; DAG: diacylglycerol; PC: phosphatidylcholine; PE: phosphatidylethanolamine; SM: sphingomyelin; TAG: triacylglycerol.

Rather than grouping lipid species into broad lipid categories, a principal component analysis determines the contribution of each lipid species to the variation between samples (Figure 3). The first principal component represents the most variation among samples. In the case of Figure 3A, the first principal component accounts for 80.9 % of the variation between samples while the second principal component accounts for only 9.0 % of the total variation. Samples with a similar lipid composition are grouped together in a principal component analysis whereas distant points in the plot have a distinct lipid composition. The corresponding loading plot, such as Figure 3B, indicates the contribution of each lipid species to each of the principal components.

The lipid composition of ring-infected RBC is similar to that of uninfected RBC according to a principal component analysis of all lipids, however trophozoite and schizont-infected RBC lipids are distinctive (Figure 3A). The loading plot indicates that PC 34:1 drives this difference (Figure 3B). In summary, ring-infected RBC lipids are similar to uninfected RBC lipids but by schizont stage, the infected RBC is much richer in phospholipids that are presumably used for membrane biogenesis.

## 2. PE and PC accumulation accounts for most of the lipid increase in schizont-infected RBC

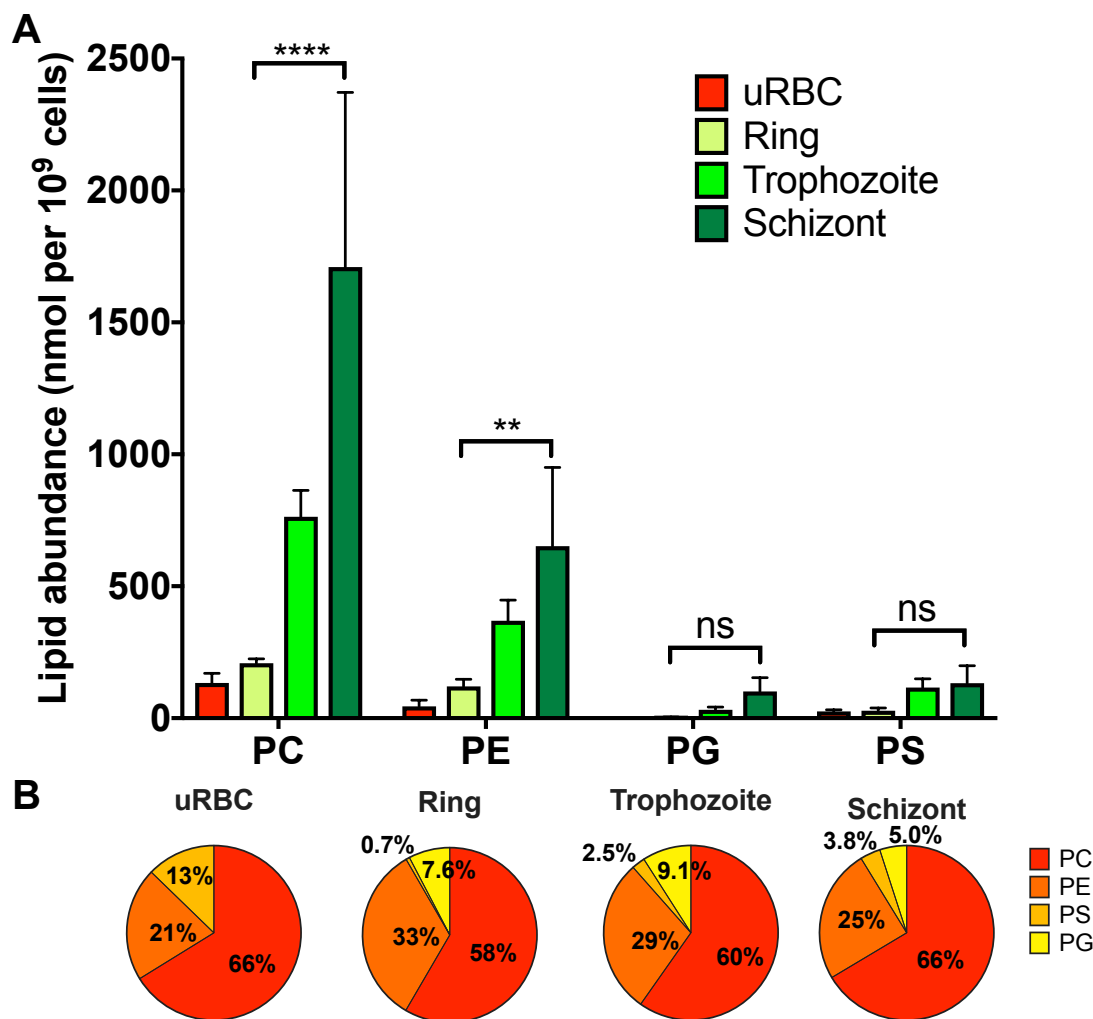


**Figure 4:** Phospholipids in *P. falciparum* during blood stage asexual lifecycle. Mean abundance with standard deviation (A) and mean proportions (B) of phospholipid classes in uninfected red blood cells (uRBC) and red blood cells infected with ring stage *P. falciparum* 12-16 hours post invasion (ring), trophozoite stage *P. falciparum* 24-28 hours post invasion (trophozoite) or schizont stage *P. falciparum* 36-40 hours post invasion (schizont). Statistical significance from two-way ANOVA indicated in A as follows: ns: not significant  $p > 0.1$ , \*\*:  $p < 0.01$ , \*\*\*\*:  $p < 0.0001$ . PC: phosphatidylcholine; PE: phosphatidylethanolamine; PG: phosphatidylglycerol; PS: phosphatidylserine.

Phospholipid abundance increases in the infected RBC between ring and schizont stages, especially that of PC and PE (Figure 4A). PC is the most abundant phospholipid in both uninfected RBC and RBC infected with asexual stage *P. falciparum*, followed by PE (Figure 4B). PC and PE are the main components of cellular membranes and their accumulation in the infected RBC likely correlates with membrane biogenesis. PG appears to be exclusive to infected samples, consistent with the lipid being a marker of mitochondria. Between ring and schizont stage the proportion of PC and PS in the infected RBC increases at the expense of PE and PG.

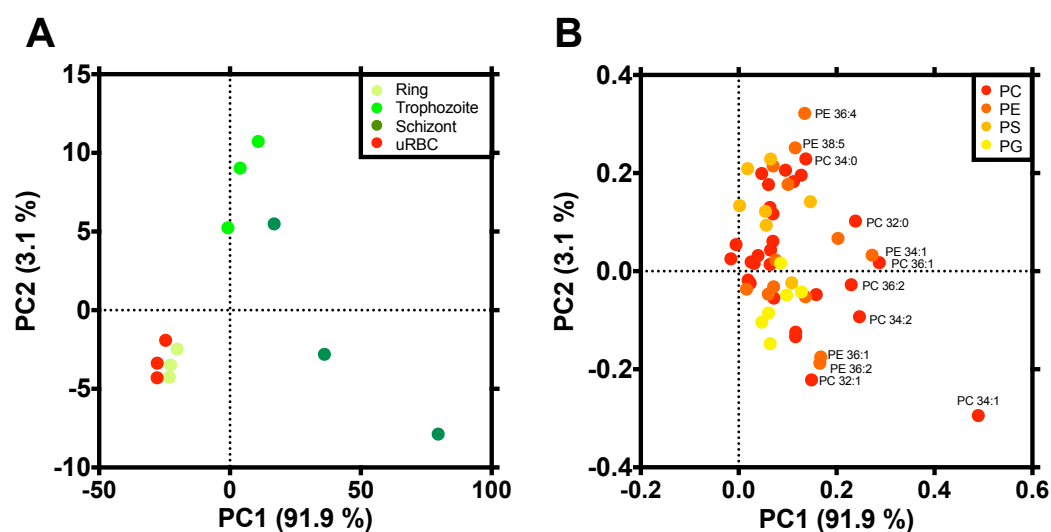


**Figure 5:** Principal component analysis plot (A) and loading plot (B) of phospholipids in uninfected red blood cells (uRBC) and red blood cells infected with ring stage *P. falciparum* 12-16 hours post invasion (ring), trophozoite stage *P. falciparum* 24-28 hours post invasion (trophozoite) or schizont stage *P. falciparum* 36-40 hours post invasion (schizont). PC1 and 2: first and second principal component; PC: phosphatidylcholine; PE: phosphatidylethanolamine; PG: phosphatidylglycerol; PS: phosphatidylserine.

At the individual lipid species level, uninfected RBC and ring-infected RBC have a similar phospholipid composition while trophozoite and schizont-infected RBC have unique compositions of PC and PE species (Figure 5A and B). It appears that the predominant phospholipid classes PC and PE are behind the observed accumulation of lipids during the asexual blood stage lifecycle, suggesting membrane biogenesis is the major lipid function during asexual blood stage parasite replication.

The nature of the most abundant phospholipid species in each sample is consistent between parasite lifecycle stages, but does not always reflect the host cell lipid composition. PC 34:1

and PE 34:1 are the most abundant lipid species in their respective lipid categories in both uninfected RBC and infected RBC at all asexual lifecycle stages. PG 34:1 is the most abundant PG species in all infected RBC samples, although PG is absent in the uninfected RBC. These results are consistent with the *P. falciparum* requirement for exogenous oleic (18:1) and palmitic acid (16:0) (Mi-Ichi et al. 2007). The most abundant PS species in uninfected RBC is PS 38:4, whereas infected RBC equally accumulate PS 36:1. The switch from polyunsaturated fatty acids in PS to monounsaturated fatty acids after infection is consistent with the absence of poly-unsaturated fatty acid synthesis machinery in *Plasmodium* (Ramakrishnan et al. 2013). The preference for PS 36:1 rather than PS 34:1 suggests active fatty acid elongation, potentially mediated by the two fatty acid elongation enzymes expressed in asexual *P. falciparum* blood stages (PF3D7\_0605900 and PF3D7\_0920000) (López-Barragán et al. 2011).

### 3. Subtle sphingolipid modifications distinguish uninfected and asexual parasite infected RBC

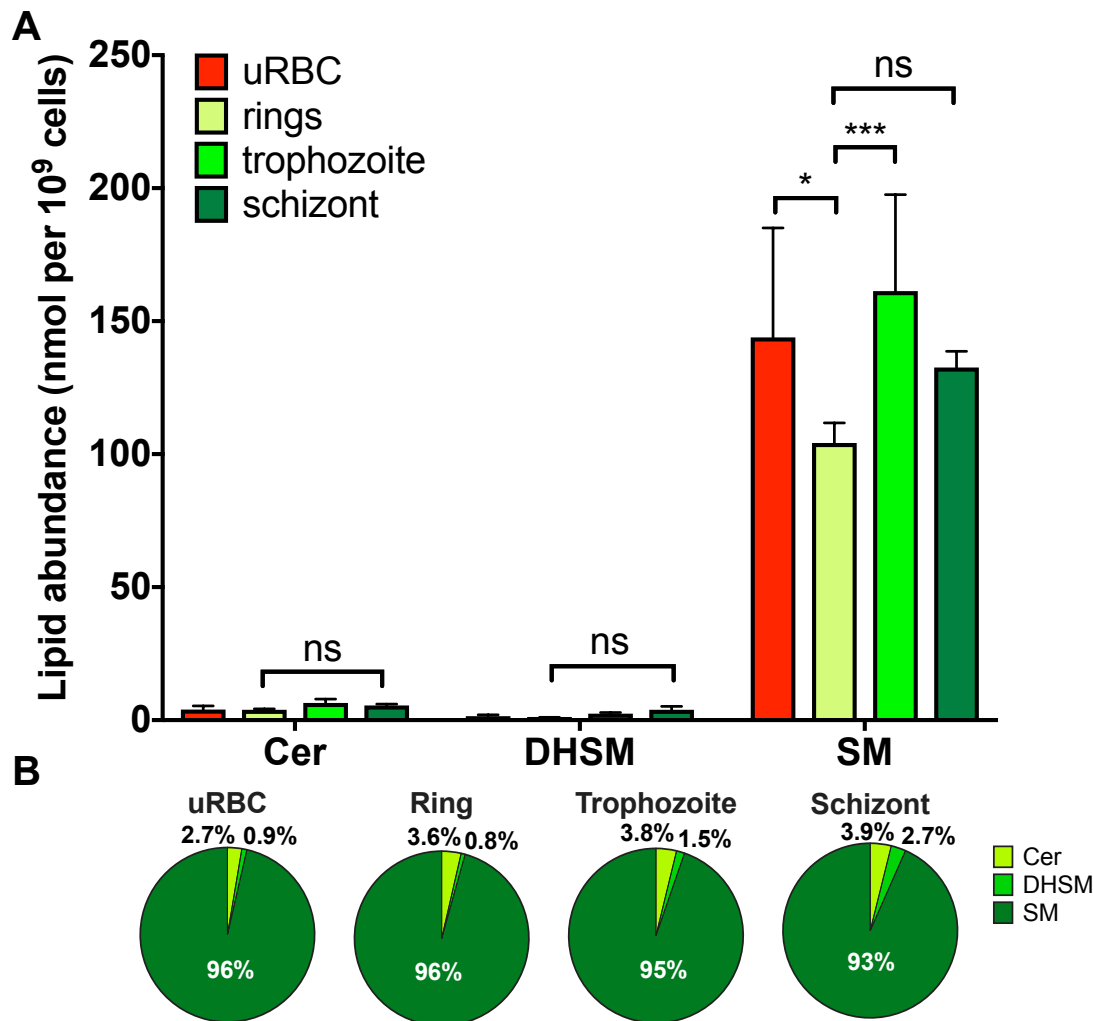


**Figure 6:** Sphingolipids in *P. falciparum* during the asexual blood stages. Mean abundance with standard deviation (A) and mean proportions (B) of sphingolipid classes in uninfected red blood cells (uRBC) and red blood cells infected with ring stage *P. falciparum* 12-16 hours post invasion (ring), trophozoite stage *P. falciparum* 24-28 hours post invasion (trophozoite) or schizont stage *P. falciparum* 36-40 hours post invasion (schizont). Statistical significance from two-way ANOVA indicated in A as follows: ns: not significant  $p > 0.1$ , \*:  $p < 0.1$ , \*\*\*:  $p < 0.001$ . Cer: ceramide; DHSM: dihydrosphingomyelin; SM: sphingomyelin.

The main sphingolipid in all samples is SM (Figure 6A), which may be integrated in lipid rafts of cellular membranes. Ring-infected RBC have less SM than uninfected RBC but the SM level is recovered by trophozoite stage. There were no significant changes in other sphingolipid categories ceramide or DHSM. Ceramide is an important intracellular second messenger, although the relatively subtle local intracellular signalling dynamics are unlikely to be measured at the scale of the present study. In terms of sphingolipid proportions, SM is



the major lipid in all samples but decreases as the parasite matures (Figure 6B). This is coupled with an increase in the proportion of ceramide and DHSM between 12 and 36 hpi.

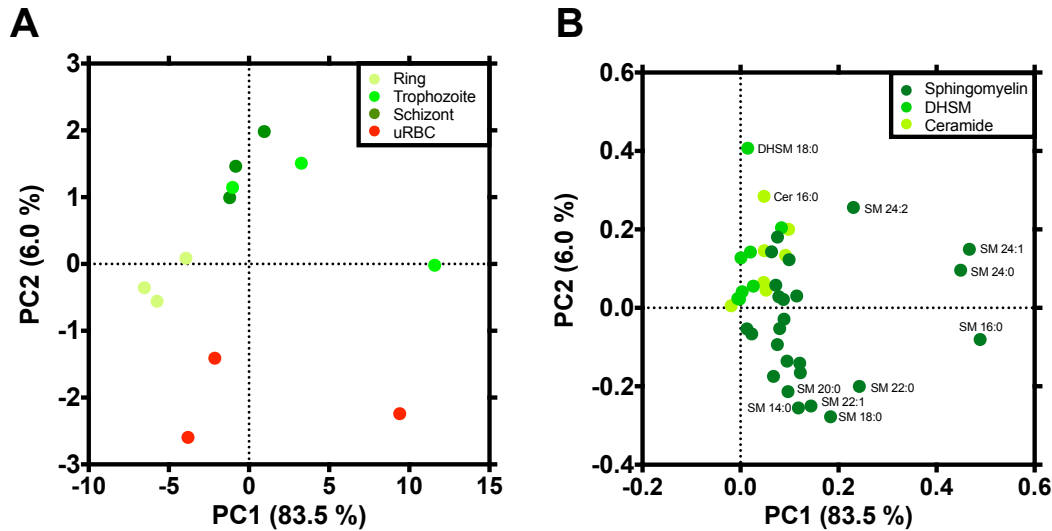


**Figure 7:** Principal component analysis plot (A) and loading plot (B) of sphingolipids in uninfected red blood cells (uRBC) and red blood cells infected with ring stage *P. falciparum* 12-16 hours post invasion (ring), trophozoite stage *P. falciparum* 24-28 hours post invasion (trophozoite) or schizont stage *P. falciparum* 36-40 hours post invasion (schizont). PC1 and 2: first and second principal component; Cer: ceramide; DHSM: dihydrosphingomyelin; SM: sphingomyelin.

Principal component analysis loading only sphingolipids mostly distinguishes ring-infected RBC from RBC infected with mature parasite stages (Figure 7A). Three lipid species, SM 24:1, SM 24:0 and SM 16:0, mostly contribute to this component (Figure 7B). There is much less variation between sphingolipids in infected and uninfected RBC, which mostly differ in DHSM 18:0, Cer 16:0 and SM 24:2 composition (Figure 7A and B).

In terms of the nature of sphingolipid species in each sample, detected DHSM species are all saturated whereas SM and ceramide species contain between 0 and 2 unsaturations. The most abundant ceramide and SM species is similar between uninfected and infected RBC. Cer 24:1 is the most abundant ceramide species while both SM 16:0 and SM 24:1 are the main SM species in all samples. In uninfected RBC, ring and trophozoite-infected RBC DHSM 16:0 is the most abundant DHSM species. In schizont-infected RBC, however, both DHSM 16:0 and 18:0 are the main DHSM species. Apart from DHSM 18:0 that may be synthesised in schizont-infected RBC, the nature of sphingolipids is similar between the host cell and infected RBC, suggesting sphingolipids are mostly scavenged from the host during asexual *P. falciparum* proliferation.

In summary, SM content in infected RBC increases between ring and trophozoite stage, potentially to form lipid rafts alongside cholesterol in the membranes generated during asexual blood stage replication. Various individual sphingolipids subtly distinguish infected and uninfected RBC, perhaps due to intracellular signalling activity.

#### 4. DAG is accumulated during asexual blood stage parasite maturation

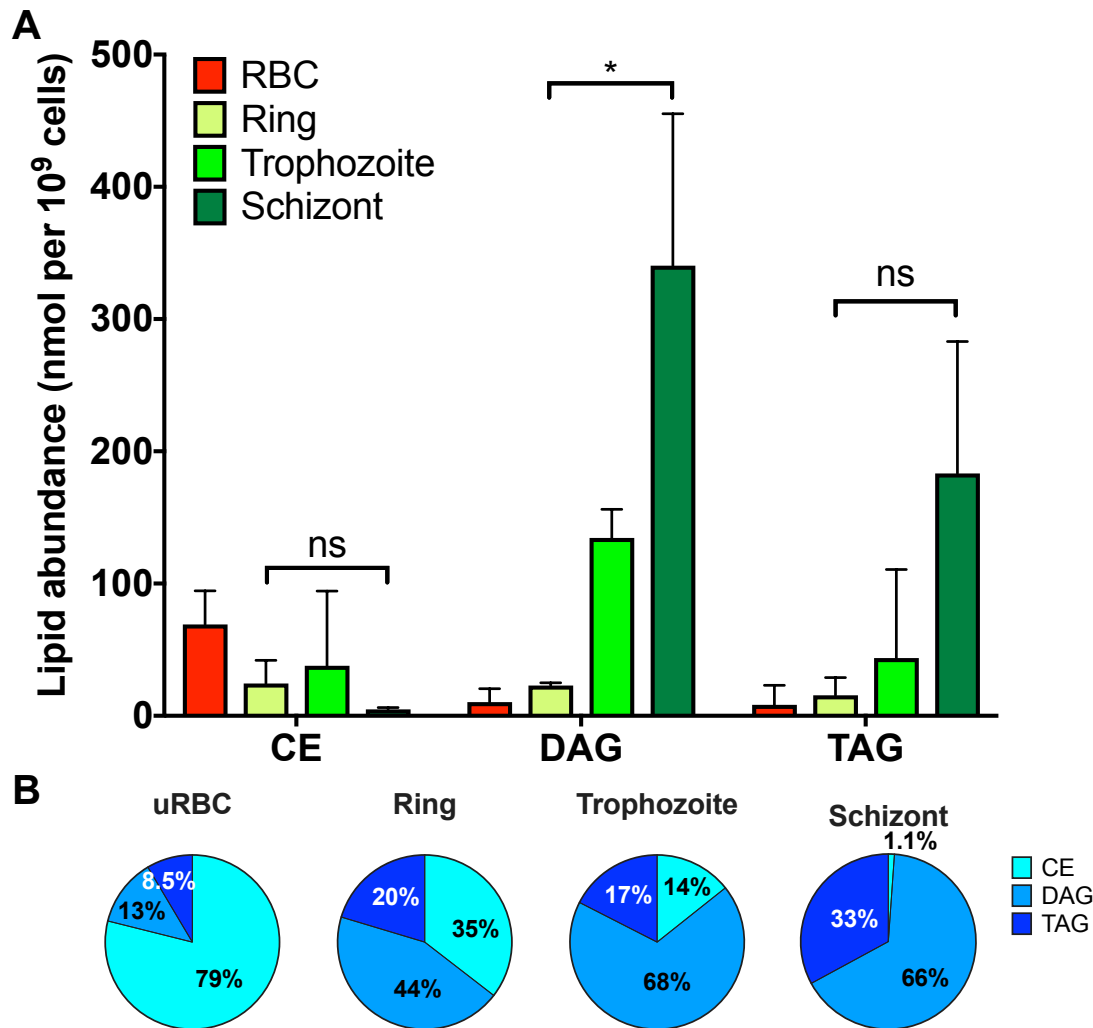


**Figure 8:** Neutral lipids in *P. falciparum* during asexual blood stages. Mean abundance with standard deviation (A) and mean proportions (B) of neutral lipid classes in uninfected red blood cells (uRBC) and red blood cells infected with ring stage *P. falciparum* 12-16 hours post invasion (ring), trophozoite stage *P. falciparum* 24-28 hours post invasion (trophozoite) or schizont stage *P. falciparum* 36-40 hours post invasion (schizont). Statistical significance from two-way ANOVA indicated in A as follows: ns: not significant  $p > 0.1$ , \*:  $p < 0.1$ . CE: cholesteryl ester; DAG: diacylglycerol; TAG: triacylglycerol.

Although overall neutral lipids were not significantly different between ring and schizont-infected RBC (Figure 2A), each class of neutral lipid appears to be dynamic in asexual blood stage parasites (Figure 8). In terms of lipid abundance, DAG increases significantly during

parasite maturation in the infected RBC (Figure 8A). DAG is both an intracellular signalling molecule and a means of storing fatty acids. The proportions of neutral lipid classes are vastly different between infected and uninfected RBC (Figure 8B). CE is the major neutral lipid in uninfected RBC but parasite invasion and maturation switches the dominant neutral lipid to DAG. Whereas DAG contains two fatty acid chains, CE contains only one, making it a less efficient means of fatty acid storage. The proportion of TAG, the most efficient means of fatty acid storage, also increases upon infection and between ring and schizont stages. These results are consistent with active synthesis of DAG and TAG but not CE in asexual blood stage *P. falciparum* from exogenous lipids (Nawabi et al. 2003; Palacpac et al. 2004; Vielemeyer et al. 2004).

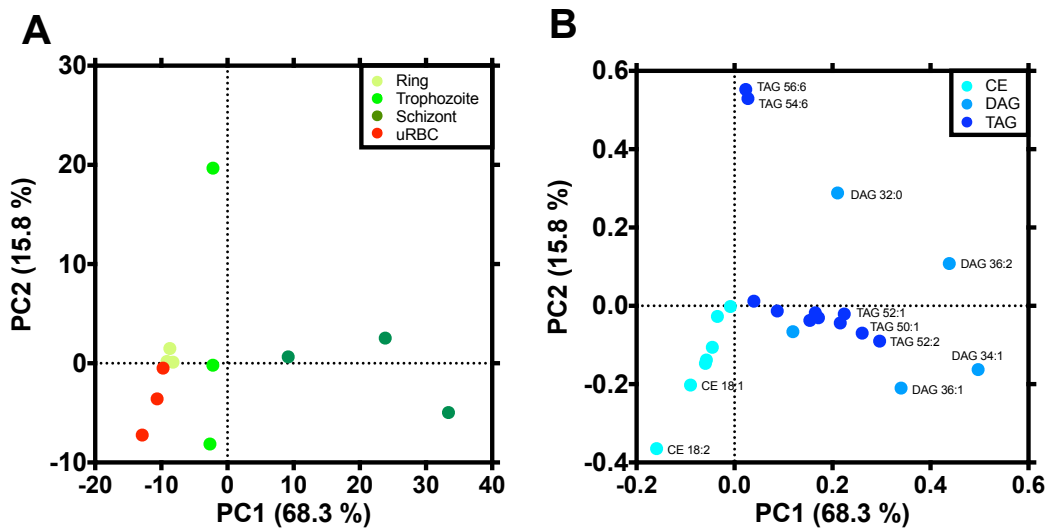


**Figure 9:** Principal component analysis plot (A) and loading plot (B) of neutral lipids in uninfected red blood cells (uRBC) and red blood cells infected with ring stage *P. falciparum* 12-16 hours post invasion (ring), trophozoite stage *P. falciparum* 24-28 hours post invasion (trophozoite) or schizont stage *P. falciparum* 36-40 hours post invasion (schizont). PC1 and 2: first and second principal component; CE: cholesteryl ester; DAG: diacylglycerol; TAG: triacylglycerol.

Neutral lipid composition appears to vary over time from uninfected RBC to ring, trophozoite then schizont-infected RBC samples based on decreasing CE species and increasing DAG and TAG species (Figure 9). Three DAG species (DAG 34:1, DAG 36:1 and DAG 36:2) and three TAG species (TAG 52:1, TAG 50:1 and TAG 52:2) contribute the most to distinguishing schizont-infected RBC from the other samples (Figure 9B). Together with the results in Figure 2, it appears overall neutral lipid abundance remains stable over the asexual lifecycle by balancing CE decrease with TAG and especially DAG increase. This would result in a net increase in cellular fatty acid storage during the asexual blood stage lifecycle.

In addition, the nature of the most abundant TAG and DAG species varies between uninfected RBC and schizont-infected RBC, whereas CE 18:2 is the major CE species in all samples. Indeed, schizont-infected RBC accumulate TAG 52:2 rather than TAG 56:6 and 54:6 that dominates TAG species in all other samples. Similarly, DAG 34:1 is a major DAG species specifically in schizont-infected RBC alongside DAG 36:2 that is the dominant DAG species in other samples. This switch in the nature of DAG and TAG species, but not CE species, suggests active DAG and TAG synthesis in schizont-infected RBC and an absence of CE synthesis, consistent with previous experiments with labelled lipids (Nawabi et al. 2003; Vielemeyer et al. 2004; Palacpac et al. 2004).

### Discussion

This chapter highlighted lipid dynamics during the asexual blood stage *P. falciparum* lifecycle summarised in Figure 10.

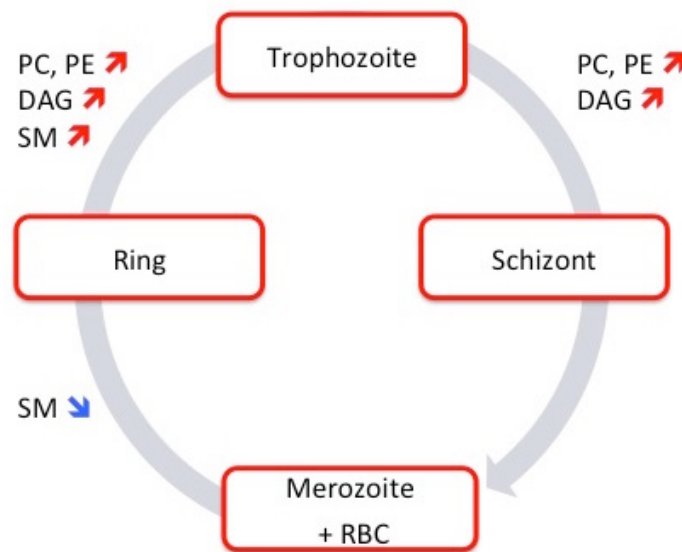


**Figure 10:** Summary of changes in lipid abundance over the asexual *P. falciparum* blood stages. Red and blue arrows indicate differences in lipid categories over 12 hour intervals of the lifecycle between uninfected red blood cells (RBC) prior to merozoite invasion, ring-infected red blood cells 12-16 hours post invasion (ring), trophozoite-infected red blood cells 24-28 hours post invasion (trophozoite) and schizont-infected red blood cells 36-40 hours post invasion (schizont). DAG: diacylglycerol; PC: phosphatidylcholine; PE: phosphatidylethanolamine; SM: sphingomyelin.

Major phospholipids PC and PE drive an overall increase in lipids after parasite invasion of the RBC and during asexual maturation (Figure 10). Given that phospholipids are the main components of the membranes surrounding the parasite and its organelles, it is not surprising

that asexual parasite development is coupled with phospholipid accumulation. Gulati et al. (2015) found little difference between uninfected RBC and saponin-isolated asexual *P. falciparum* phospholipids. This could indicate that the additional phospholipids localise to the infected RBC cytoplasm rather than the parasite itself. Some phospholipids are indeed components of the tubulovesicular membrane network, Mauer's clefts and RBC plasma membrane. It is unlikely, however, that these membranes alone could account for such an increase in phospholipids. Parasite phospholipids were perhaps lost during saponin isolation in the previous study. Another class of phospholipids, phosphatidylinositol, was not measured in this study since the developmental time points are too distant to draw conclusions on intracellular signalling dynamics involving such lipids.

In terms of individual lipid species, phospholipids with saturated or monounsaturated fatty acid chains, in particular PC 34:1, PC 32:0 and PE 34:1, are more abundant in infected RBC, consistent with previous measurements (Gulati et al. 2015) and the parasite's inability to synthesise polyunsaturated fatty acids (Ramakrishnan et al. 2013). This correlates with the parasite's dependence on exogenous oleic (18:1) and palmitic (16:0) acid (Mi-Ichi et al. 2007). The present study also identified minor phospholipid lysophosphatidylcholine that is imported from the serum by an unknown mechanism and used to synthesise PC (Brancucci et al. 2017; Kilian et al. 2018).

SM was less abundant in ring-infected RBC than in uninfected RBC or trophozoite-infected RBC. This suggests that parasite invasion and early maturation is coupled with catabolism of SM. Ceramide production from SM is essential for asexual parasite proliferation (Gulati et al. 2015), however the decrease in SM was not mirrored by an increase in ceramide. Alternatively, membrane lipids such as SM could be shed from the infected RBC in the form of microvesicles. Metabolic labelling experiments are required to ascertain the destiny of the lost SM in ring-infected RBC. In terms of minor sphingolipids, DHSM was detected in infected RBC, consistent with dihydroceramide (DHCer), the precursor of DHSM, being identified previously (Gulati et al. 2015). Unlike other sphingolipids, the nature of the most abundant DHSM species changed between uninfected RBC and schizont-infected RBC, suggesting *de novo* synthesis or import from the extracellular environment of this minor sphingolipid.

Neutral lipid abundance is highly dynamic during asexual blood stage *P. falciparum* proliferation. DAG is accumulated in the infected RBC between ring and schizont stages. DAG and TAG are a means of storing toxic fatty acids (Nolan et al. 2018) but may also play a role in haem detoxification as described in the introduction, or intracellular signalling *via* DAG. DAG and TAG are more abundant in saponin-isolated asexual stage *P. falciparum* (Gulati et al. 2015). This supports the notion that the neutral lipid store of asexual parasites is within the parasite itself. Previously described incorporation of exogenous lipids in DAG and TAG during asexual *P. falciparum* proliferation is consistent the accumulation of neutral lipids observed in the present study (Nawabi et al. 2003; Palacpac et al. 2004; Vielemeyer et al. 2004).

CE switches from being the major lipid of uninfected RBC to a minor neutral lipid post-invasion. CE is a means of storing both cholesterol and fatty acid chains. *Plasmodium* parasites cannot synthesise cholesterol and therefore acquire the sterol from their host (Sherman 1979). Although FASII is active, it is dispensable for asexual *P. falciparum* proliferation (Yu et al. 2008; Vaughan et al. 2009). Instead fatty acid scavenging is essential for blood stage parasites and heavily influences the fatty acid composition of parasite lipids (Mitamura et al. 2000; Asahi et al. 2005; Mi-Ichi et al. 2006; Asahi 2009; Botté et al. 2013). Exogenous fatty acids are indeed incorporated into various lipids (Krishnegowda & Gowda 2003; Mi-Ichi et al. 2006). Potentially host RBC CE stores are a source of parasite cholesterol and fatty acids during asexual blood stage proliferation. Given the absence of CE synthesis in asexual blood stages, the drop in the proportion of CE in asexual blood stages is not surprising (Nawabi et al. 2003; Palacpac et al. 2004; Vielemeyer et al. 2004).

Overall, infection and maturation of the asexual parasite within the host RBC is coupled with an increase in lipids that exceeds the supply of the host RBC. The parasite must therefore scavenge lipids and/or synthesise lipids *de novo* to sustain asexual parasite proliferation. Whether this is also the case during gametocytogenesis and after transition to the radically different mosquito host is the object of part 2 of this chapter.

## Part 2

### Lipid dynamics over the lifecycle of *P. berghei*

#### Introduction

Of the four laboratory-adapted rodent malaria parasites (*P. berghei*, *P. yoelii*, *P. chabaudi* and *P. vinckei*) *P. berghei* is the most widely used model for severe malaria including studies of placental malaria, cerebral malaria and malaria-induced lung pathology (de Oca et al. 2013; de Moraes et al. 2016; Ghazanfari et al. 2018). Indeed, infection with *P. berghei* is lethal within 1-3 weeks in most laboratory rodents. By contrast to the human malaria parasite *P. falciparum*, the whole *P. berghei* lifecycle can be investigated *in vivo* with relative ease. In addition, there are more tools available to manipulate the *P. berghei* genome since it does not share the prohibitively high AT frequency of the *P. falciparum* genome (de Koning-Ward et al. 2015). *P. berghei* is therefore a popular model for the study of *Plasmodium* biology.

*P. berghei* was first discovered by Vincke and Lips in 1948 (van den Berghe 1954; Vincke 1954; Yoeli 1965). In the laboratory *P. berghei* can infect white mice, rats and hamsters, however the natural rodent host is the thicket rat where infection with *P. berghei* is chronic. *Anopheles durenii* is the natural parasite vector but *Anopheles stephensi* is also susceptible and commonly used in lab settings.

The overall lifecycle features are conserved among *Plasmodium* species with a few notable exceptions in the blood stages. The *P. berghei* parasite preferentially invades reticulocytes (Cromer et al. 2006), whereas *P. falciparum* proliferates in mature RBC. In addition, *P. berghei* development is much faster: asexual blood stage replication takes 22 to 23 h and gametocytes develop in 36 h (Mons et al. 1985), whereas *P. falciparum* replicates asexually in the blood over 48 h and gametocytes take 10-12 days to mature. Finally, *P. falciparum* gametocytes are unique in their namesake sickle shape – other *Plasmodium* species including *P. berghei* develop round gametocytes instead.

In a recent genome-wide phenotypic screen of *P. berghei*, lipid metabolism was highlighted as a key metabolic process for parasite survival (Bushell et al. 2017). Synthesis of glycosylphosphatidylinositol (GPI) anchors is an essential metabolic function in the parasite. GPI are complex glycolipids that anchor proteins at the cell membrane and are the main trigger for pro-inflammatory immune response of cerebral malaria (Krishnegowda et al. 2005;

Gowda 2007; Zhu et al. 2009; Zhu et al. 2012; Kumar et al. 2012; Punsawad et al. 2013; Mbengue et al. 2016; Qingyang Liu et al. 2018). PC synthesis was also highlighted as an important process for asexual parasite replication, consistent with previous observations that synthesis of PC and PE through the Kennedy pathway is essential in *P. berghei* (Dechamps et al. 2010). Transporters involved in lipid scavenging and maintenance of the lipid bilayer asymmetry are also important for parasite growth (Bushell et al. 2017). Reticulocytes, which are preferred host cells for blood stage *P. berghei*, show metabolic markers of phospholipid and fatty acid metabolism, which may be scavenged by the intracellular parasite (Srivastava et al. 2015). In addition to sourcing lipids from the host, *Plasmodium* encodes enzymes for the *de novo* synthesis of some lipids. *De novo* sphingolipid synthesis and fatty acid synthesis are dispensable for *P. berghei* asexual blood stage replication (Bushell et al. 2017).

In this chapter *P. berghei* is used as a model organism to extend the investigation of *Plasmodium* lipid metabolism from the asexual blood stage to gametocytogenesis and development in the mosquito vector. A comparison of the lipid dynamics between *Plasmodium* species is explored in the final part of this chapter.

## Results

Lipid abundance was measured in schizont, gametocyte and sporozoite-infected host cells. The abundance of lipids in blood stage samples was measured in three biological replicates of  $10^7$  infected or uninfected mouse RBC. Mosquito stage sample preparation differed slightly for technical reasons. Lipids were measured in two biological replicates of whole mosquito salivary glands infected with a total of  $10^6$  sporozoites. Unlike the RBC, salivary glands are multicellular organs. In order to compare the host cell lipids accessible to the parasite in blood and salivary gland stages, the lipid abundance in the uninfected and infected salivary gland was divided by the average number of cells per salivary gland to obtain lipid abundance “per host cell”. For a complete list of lipid species measured in this study, refer to Supplementary Table 2.

Differences in host cell lipids are also the main difference between mouse and mosquito infected host cells. This could be an artefact of measuring the lipids of the parasite with the lipids of the host cell. To estimate the parasite lipid contribution, the lipid composition of the



host cell is subtracted from the lipidome of the infected cell. This could include actual parasite lipids, but also host cell lipid modifications that result from parasite infection.

### 1. Lipids in *P. berghei*-infected host cells are parasite-stage-specific

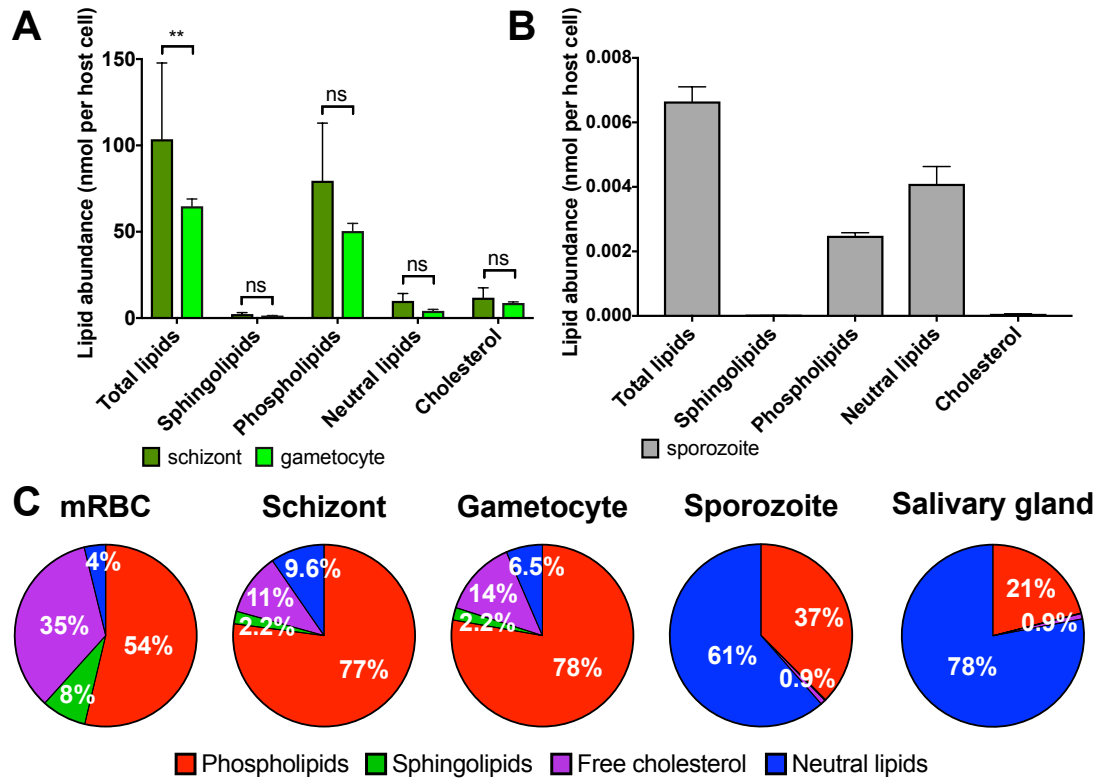


**Figure 1:** Overview of the lipid dynamics during the lifecycle of *P. berghei*. Mean abundance with standard deviation (A and B) and average proportion (C) of total lipids, phospholipids, neutral lipids, sphingolipids and free cholesterol at three time points during the parasite lifecycle: schizont and gametocyte-infected mouse red blood cell (mRBC); and sporozoite-infected mosquito salivary gland. Statistical significance from two-way ANOVA indicated in A as follows: ns: not significant  $p > 0.1$ , \*\*:  $p < 0.01$ .

Phospholipids represent more than three quarters of lipids in *P. berghei*-infected RBC while neutral lipids dominate sporozoite-infected salivary gland lipids (Figure 1A-C). This change in lipid composition is also observed between uninfected mouse RBC and the mosquito salivary gland (Figure 1C). Given that phospholipids are structural membrane components unlike neutral lipids that store fatty acids, the change in lipid composition suggests host-specific parasite biology. Total lipids are less abundant in gametocyte-infected RBC compared to schizont-infected RBC, suggesting parasite-stage-specific lipid metabolism (Figure 1A). By sporozoite stage the lipid abundance per host cell is much smaller, consistent with the overall difference in size between the sporozoite and blood stages, and perhaps indicative of significant differences in host cell lipid abundance. Parasite infection reduces

the proportion of cholesterol and sphingolipids compared to the mouse RBC (Figure 1C). Sphingolipids and cholesterol are barely present in mosquito salivary glands or sporozoites (Figure 1B and C) consistent with the parasite and mosquito's inability to synthesise sterols.

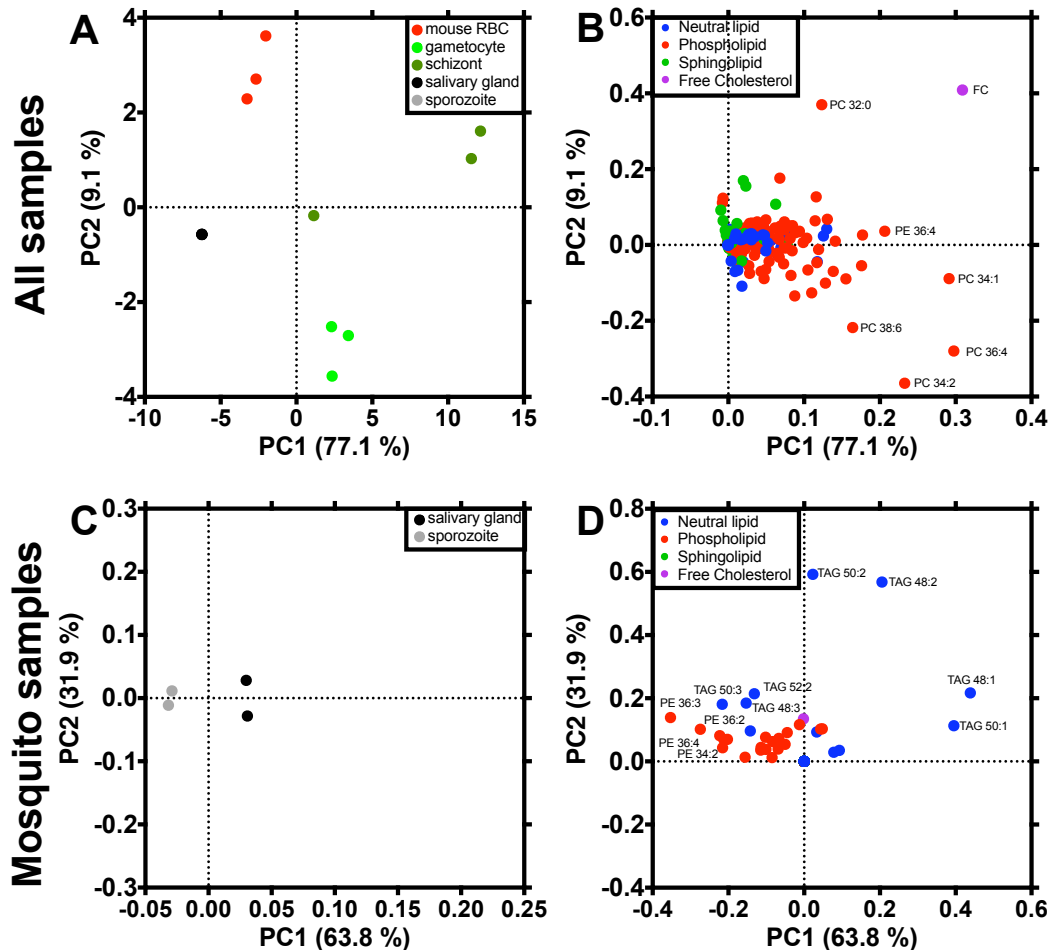


**Figure 2** Principal component analysis plot of all lipids measured in uninfected mouse red blood cells (mouse RBC), gametocyte and schizont-infected mouse red blood cells, uninfected mosquito salivary glands and sporozoite-infected salivary glands (A) or only mosquito stages (C) with corresponding loading plots (B and D). In A sporozoite and salivary gland points are overlapping. PC1 and 2: first and second principal component; FC: free cholesterol; PC: phosphatidylcholine; PE: phosphatidylethanolamine; TAG: triacylglycerol.

Principal component analysis of the lipid composition in all samples does not distinguish between infected and uninfected salivary glands, however mosquito stages are clearly separated from uninfected mouse RBC, and mouse RBC infected with schizonts or gametocytes (Figure 2A). The mosquito and mouse samples are distinguished based on phospholipid species and free cholesterol (Figure 2B). Relative to all other samples, gametocytes contain more PC 38:6, PC 36:4 and PC 34:2. The uninfected mouse RBC is characterised by FC and PC 32:0.

To observe the individual lipid species that characterise sporozoite infection of the salivary gland, a principal component analysis of only the infected and uninfected mosquito salivary gland was performed (Figure 2C). Infection of the salivary gland is mostly characterised by increase of several PE species (PE 36:3, PE 36:4, PE 36:2 and PE 34:2) and a decrease in TAG species (TAG 48:1, TAG 48:2 and TAG 50:1) (Figure 2D). In general, phospholipid accumulation is indicative of membrane biogenesis. Sporozoite depletion of TAG reserves in the mosquito salivary gland suggests that parasite development in the mosquito is accompanied by catabolising TAG from the host.

In summary, differences in the lipid profile of the mouse and mosquito host impact the proportions of major lipid categories in *P. berghei*-infected cells. However, the lipid profile of the host cell is also modified upon infection in a parasite-stage-specific manner.

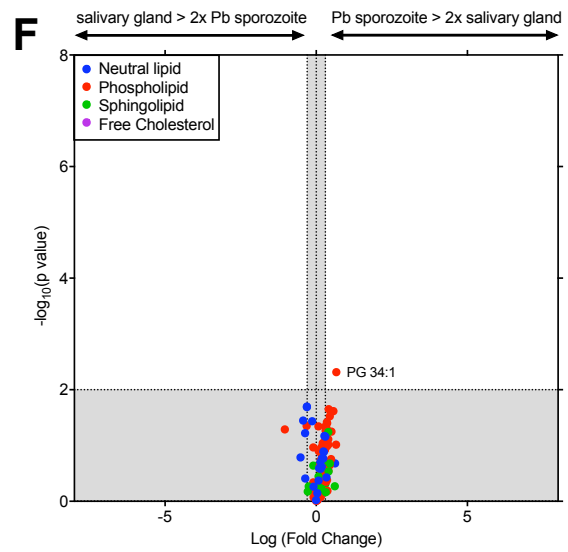
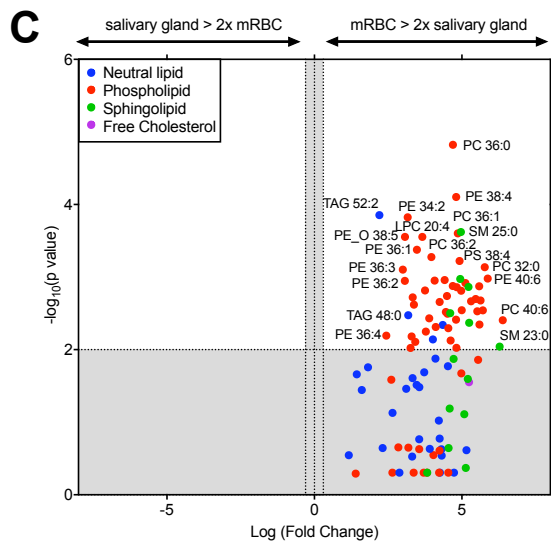
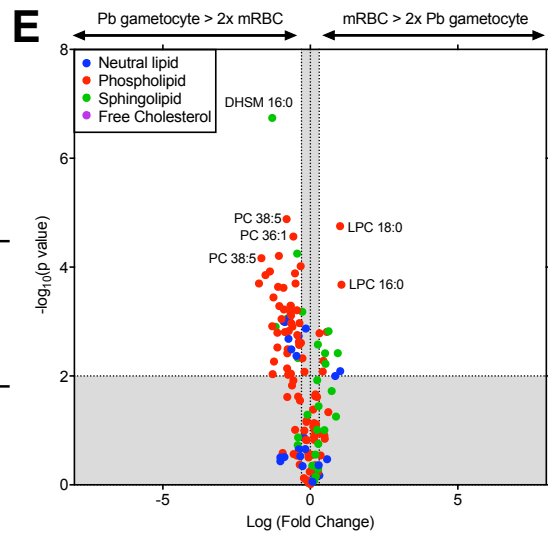
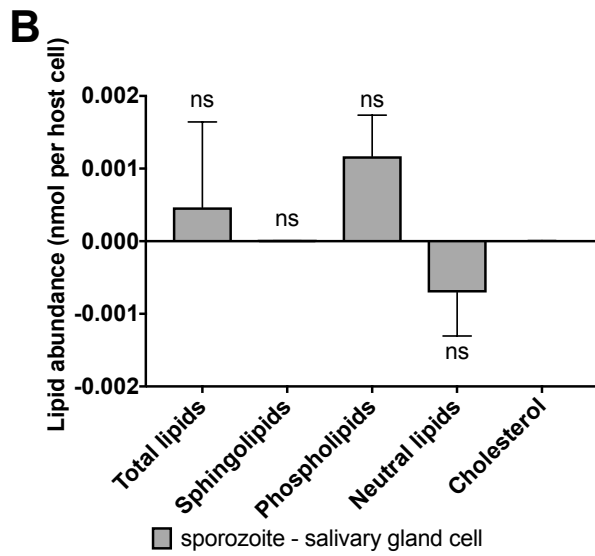
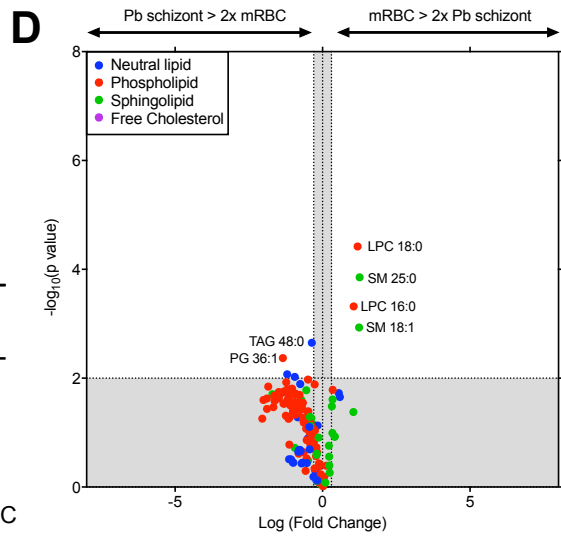
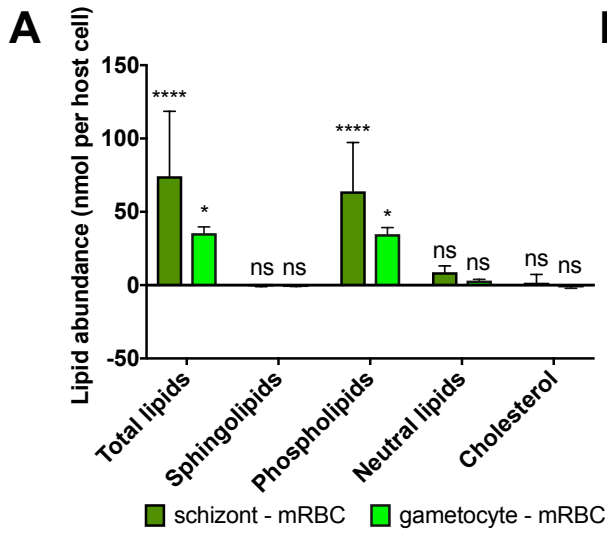


**Figure 3:** Host cell impact on the lipidome of *P. berghei*. A) Mean abundance with standard deviation of total lipids, neutral lipids, sphingolipids, phospholipids and cholesterol in *P. berghei* gametocyte and schizont-infected mouse red blood cells (mRBC) after subtraction of host cell lipid abundance. B) Mean abundance with standard deviation of lipids in *P. berghei* sporozoite-infected mosquito salivary glands after subtraction of host cell lipid abundance. Statistical significance of the change in lipid abundance between uninfected and infected host cells calculated by two-way ANOVA is indicated on top of each bar in A and B as follows: ns: not significant, \*:  $p < 0.1$ , \*\*\*\*:  $p < 0.0001$ . C) Volcano plot comparing the lipid profile of host cells: uninfected mouse red blood cell (mRBC) and uninfected mosquito salivary gland cell (salivary gland). D-F) Volcano plots comparing the lipid profile of *P. berghei*-infected cells (schizonts in D, gametocytes in E and sporozoites in F) with the lipidome of the uninfected host cell (mouse red blood cell in D and E or mosquito salivary gland in F). Statistical significance (p value) in C-F calculated by multiple student t-tests and grey area corresponds to  $p > 0.01$  and/or less than 2 fold change. DHSM: dihydrosphingomyelin; LPC: lysophosphatidylcholine; PC: phosphatidylcholine; PE: phosphatidylethanolamine; PG: phosphatidylglycerol; PS: phosphatidylserine; SM: sphingomyelin; TAG: triacylglycerol.

To highlight the parasite impact on the host cell lipid composition and to assist inter-host comparisons, the lipidome of the host cell was subtracted from that of the infected cell. Infected mouse RBC contain more lipids overall, due to phospholipid accumulation at both schizont and gametocyte stage (Figure 3A). This is consistent with the prolific membrane biogenesis during parasite development. Infection of salivary glands had no significant impact on overall lipid classes (Figure 3B).

Comparison of the lipidome of each host cell in Figure 3C clearly shows that mouse RBC contain significantly more of all individual lipid species found in both host cells. However, the sporozoite only increases PG 34:1 in the salivary gland (Figure 3F), suggesting that lipids in the lipid-rich mouse host are not carried over through to the lipid-poor sporozoite stage. Instead each parasite stage appears to have different lipid requirements that result in stage-specific modifications to the host cell lipidome.

At the individual lipid species level, parasite depletion of host cell lipids indicates parasite mediated lipid catabolism, while accumulation of other lipid species suggests either *de novo* synthesis or lipid scavenging from the extra-cellular environment. Mouse RBC LPC 18:0 and LPC 16:0 is decreased upon infection by both schizonts and gametocytes, while schizonts also deplete RBC SM 25:0 and SM 18:1 (Figure 3D and E). LPC is a major substrate for phospholipid metabolism in *Plasmodium*, and serum depletion of LPC induces gametocytogenesis (Brancucci et al. 2017). Many individual lipids appear more abundant in gametocyte and schizont-infected RBC compared to uninfected RBC, although variation

among schizont-infected RBC samples may have reduced the statistical significance of such changes (Figure 3D and E). DHSM 16:0 is one of the significantly more abundant lipids in gametocyte-infected RBC relative to uninfected mouse RBC. PG 34:1 accumulation is a hallmark of sporozoite infection of the salivary gland (Figure 3F).

## 2. Phospholipids in *P. berghei*-infected cells reflect host cell phospholipid composition

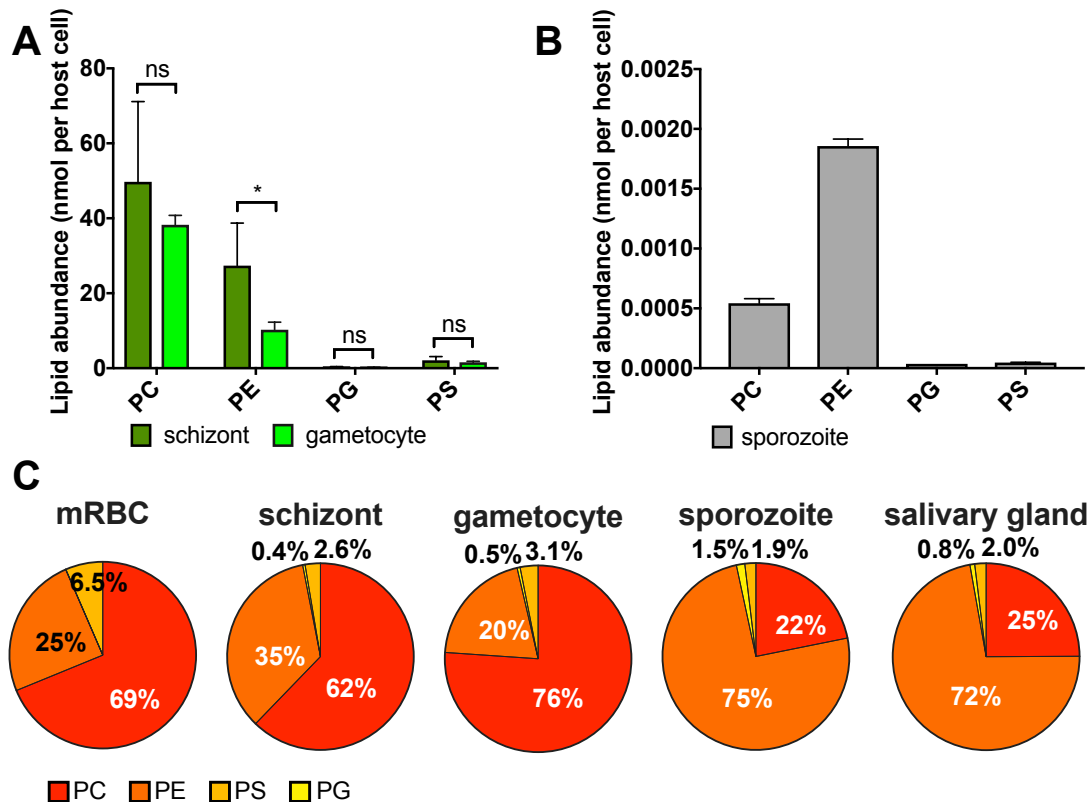


**Figure 4:** Phospholipid dynamics during the lifecycle of *P. berghei*. Average abundance with standard deviation (A) and average proportion (B) of phosphatidylcholine (PC), phosphatidylethanolamine (PE), phosphatidylserine (PS) and phosphatidylglycerol (PG) at three time points during the parasite lifecycle: schizonts and gametocytes in the mouse red blood cell (mRBC); and sporozoites in the mosquito salivary gland. Statistical significance from two-way ANOVA indicated in A as follows: ns: not significant  $p > 0.1$ , \*:  $p < 0.1$ .

Phospholipids are the most abundant lipid in mouse stages unlike in mosquito stages (Figure 1C). The principal phospholipid class also changes from PC in mouse stages to PE in mosquito stages (Figure 4). PG was not detected in uninfected mouse RBC but represented a small proportion of all other samples. This distribution is consistent with the observation in mammalian cells that PG is specific to mitochondrial membranes. Similar to total phospholipids, PE is less abundant in gametocyte-infected RBC compared to schizont-

infected RBC, and sporozoite-infected salivary glands contain much less of all phospholipids compared to infected mouse RBC (Figure 4A and B). Phospholipid accumulation appears to correlate with stage-specific membrane requirements for cell division: schizonts divide into 12-18 daughter merozoites while male gametocytes only yield 8 male gametes and female gametocytes and sporozoites are non-replicative.

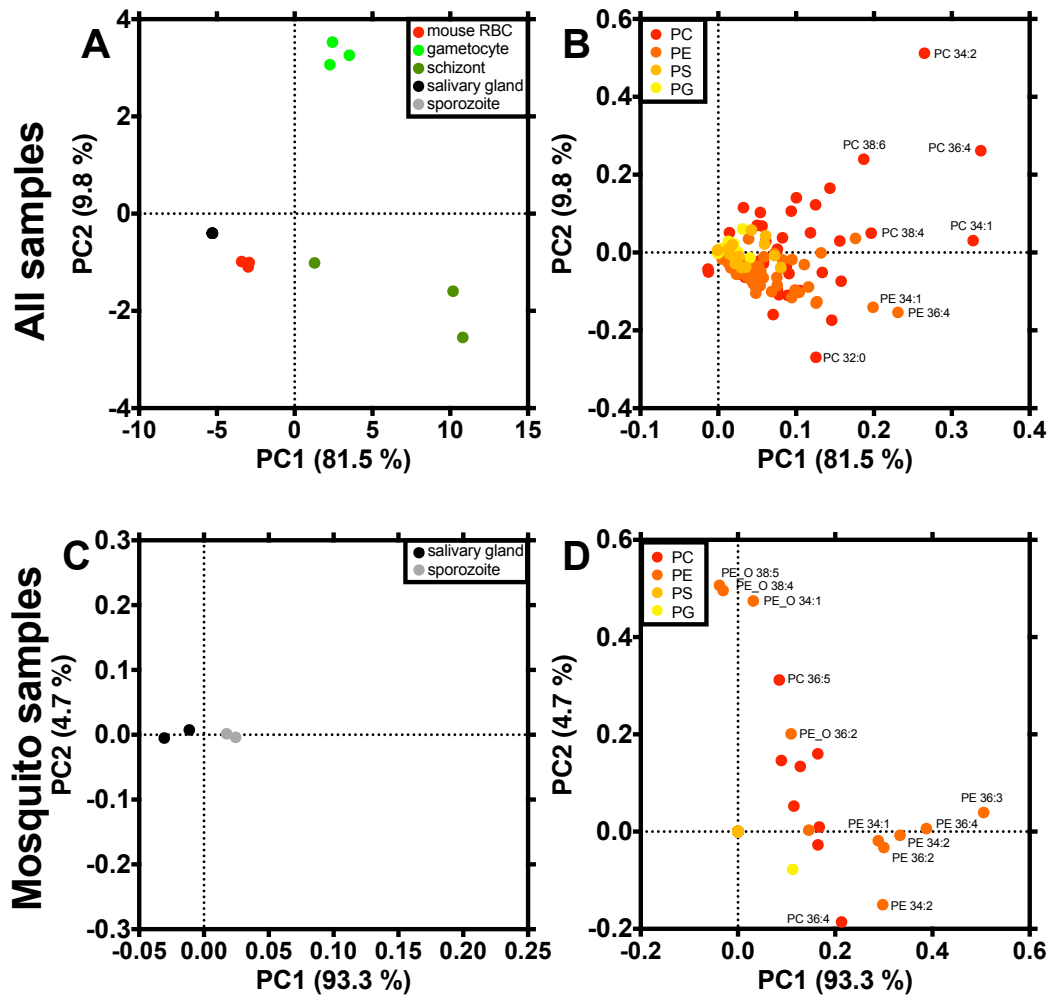


**Figure 5:** Principal component analysis plot (A and C) and loading plot (B and C) of phospholipids measured in uninfected mouse red blood cells (mRBC), *P. berghei* gametocyte and schizont-infected mouse red blood cells, uninfected mosquito salivary glands and *P. berghei* sporozoite-infected salivary glands (A and B) or only mosquito stages (C and D). In A salivary gland and sporozoite points are overlapping. PC1 and 2: first and second principal component; PC: phosphatidylcholine; PE: phosphatidylethanolamine; PS: phosphatidylserine; PG: phosphatidylglycerol.

The principal component analysis of phospholipids in all samples (Figure 5A and B), clusters mosquito samples in proximity to uninfected mouse RBC, suggesting both host cell phospholipids are similar. Infected blood stage samples are characterised by PC 34:1 and PC 36:4. Schizont-infected RBC are further characterised by PE 36:4, PE 34:1 and PC 32:0,

while gametocyte-infected RBC are distinguished by PC 34:2 instead. Principal component analysis of only the mosquito stage samples shows very little difference between infected and uninfected samples (Figure 5C and D). If anything, infection of the salivary gland is characterised by PE species (PE 36:2, PE 36:3, PE 36:4 and PE 34:2).

With the exception of PG, the main lipid species in each phospholipid category varies between samples. PG 34:1 is indeed one of the main PG species in all samples. This is surprising given PG is much more abundant in infected samples, although it may reflect a host source of fatty acid chains for parasite PG synthesis. The main PS species reflects the host cell lipid profile: PS 38:4 is the most abundant species in all mouse samples while PS 36:2 dominates mosquito samples. *P. berghei* may therefore source PS directly from the host cell.

The main PC and PE species are distinct between uninfected mouse RBC and infected RBC but are the same in mosquito salivary glands with or without parasite infection. Whereas PC 32:0 is the main PC species in uninfected mouse RBC, infected mouse RBC mostly contain PC 32:2, PC 34:1 and PC 36:4, all containing a 16:0 fatty acid. Given the lack of polyunsaturated fatty acid synthesis in *Plasmodium* (Ramakrishnan et al. 2013), this suggests blood stage parasites scavenge polyunsaturated fatty acids or PC containing such fatty acids from the extracellular host environment. Infected and uninfected mosquito salivary glands mostly contain PC 34:2. Overall, this suggests PC abundance in blood stage *P. berghei* and perhaps mosquito stages relies on lipid scavenging from the host. Similarly, PE 38:5 is the main PE species in uninfected RBC, but upon infection with either gametocytes or schizonts PE 36:1, PE 34:1 and PE 34:2 become the main PE species. Mosquito salivary glands with or without parasite infection contain mostly PE 36:3. This distribution would be consistent with parasites synthesising PE with *de novo* synthesised saturated or monounsaturated fatty acids in blood stages, but scavenging host PE at sporozoite stage.

Overall, phospholipids distinguish mouse from mosquito stages, and asexual from sexual blood stages. However, sporozoite infection barely modifies the phospholipid composition of the salivary gland, if at all. Phospholipid dynamics appear to be correlated with stage-specific requirements for membrane biogenesis.



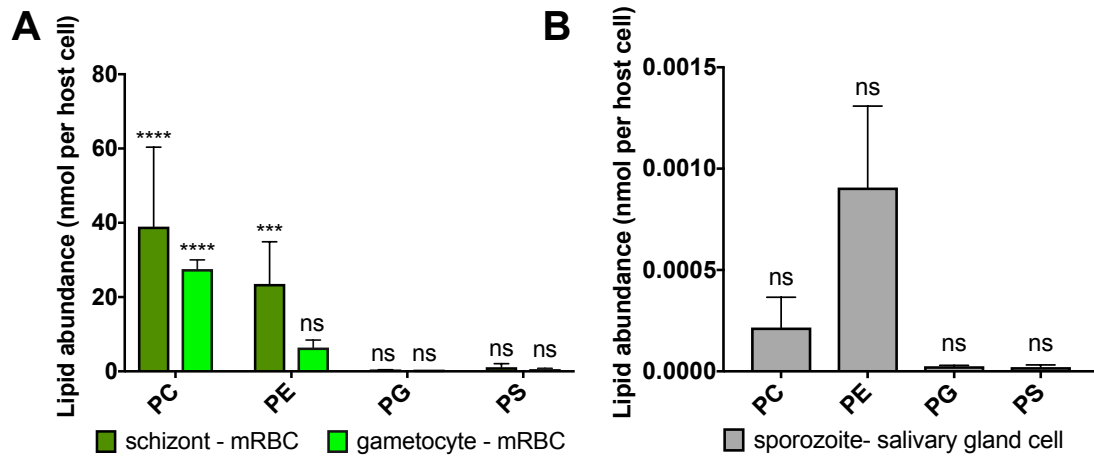


**Figure 6:** Host cell impact on the phospholipids of *P. berghei*. Average abundance and standard deviation of phosphatidylcholine (PC), phosphatidylethanolamine (PE), phosphatidylserine (PS) and phosphatidylglycerol (PG) in *P. berghei* schizont and gametocyte-infected mouse red blood cells (A) or sporozoite-infected mosquito salivary glands (B) after subtraction of host cell lipid abundance (uninfected mouse red blood cell (mRBC) in A or uninfected salivary gland cell in B). Statistical significance of the difference between infected and uninfected host cell lipids calculated by two-way ANOVA indicated as follows: ns: not significant  $p > 0.1$ , \*\*\*:  $p < 0.001$ , \*\*\*\*:  $p < 0.0001$ .

In the mouse host, phospholipids are increased upon infection by *P. berghei*, whereas mosquito stage modifications are insignificant (Figure 6A and B). Schizonts stockpile both PC and PE while gametocytes mostly increase host cell PC abundance. In the mosquito, PE is the most changed upon infection.

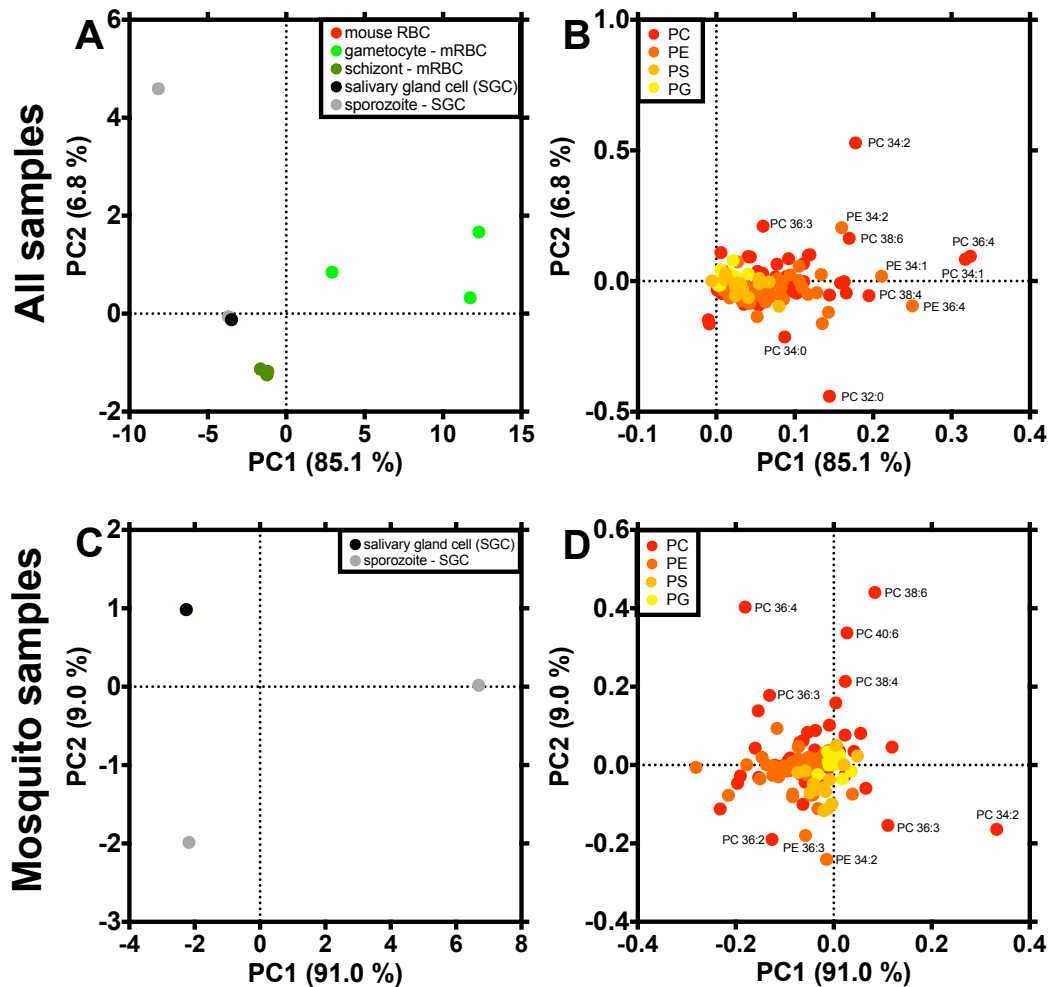


**Figure 7:** Principal component analysis of phospholipids in uninfected host cells (mouse red blood cell (mRBC) or mosquito salivary gland cell (SGC)) and *P. berghei*-infected host cells at schizont, gametocyte and sporozoite stage after subtraction of respective host cell lipid abundance. Analysis plot of all samples (A) or mosquito samples only (C) with corresponding loading plots (B and D). In A and C both salivary gland points are overlapping. In A schizont samples overlap with uninfected mouse red blood cell samples. PC1 and 2: first and second principal component; PC: phosphatidylcholine; PE: phosphatidylethanolamine; PS: phosphatidylserine; PG: phosphatidylglycerol.

After subtraction of the host cell phospholipids, principal component analysis of all samples mostly distinguishes gametocyte-infected RBC from the other samples based on PC and PE species (Figure 7A and B). Phospholipid species that distinguished infected from uninfected RBC in Figure 5A and B are similar to those that characterise gametocyte-infected RBC from other samples, including schizont-infected RBC after subtraction of host cell phospholipids in Figure 7A and B. In the mosquito samples, the main variation in phospholipid composition was between biological replicates rather than between the host and parasite, suggesting that the phospholipid of sporozoites and the salivary gland are overall very similar. Although

overall phospholipids are increased upon infection of the salivary gland, individual lipid species PC 40:6, PC 48:6 and PC 38:6 are depleted (Figure 7C and D) suggesting PC remains an important phospholipid in sporozoite stages even though PE is the main phospholipid class.

In summary, *P. berghei* infection is characterised by an increase in overall PE and PC, especially in the mouse RBC. The impact of sporozoites on the phospholipid composition of the salivary gland is minor. Sporozoites deplete host cell PC species suggesting PC catabolism remains functionally significant in the PE-rich mosquito salivary gland. After subtraction of host cell phospholipids, phospholipids in schizont-infected RBC, but not gametocyte-infected RBC, are similar to those of the host RBC indicating that gametocyte-infected RBC phospholipids may be synthesised *de novo* or sourced from beyond the host cell.

### 3. Sphingomyelin is the main sphingolipid of *P. berghei*-infected and uninfected host cells

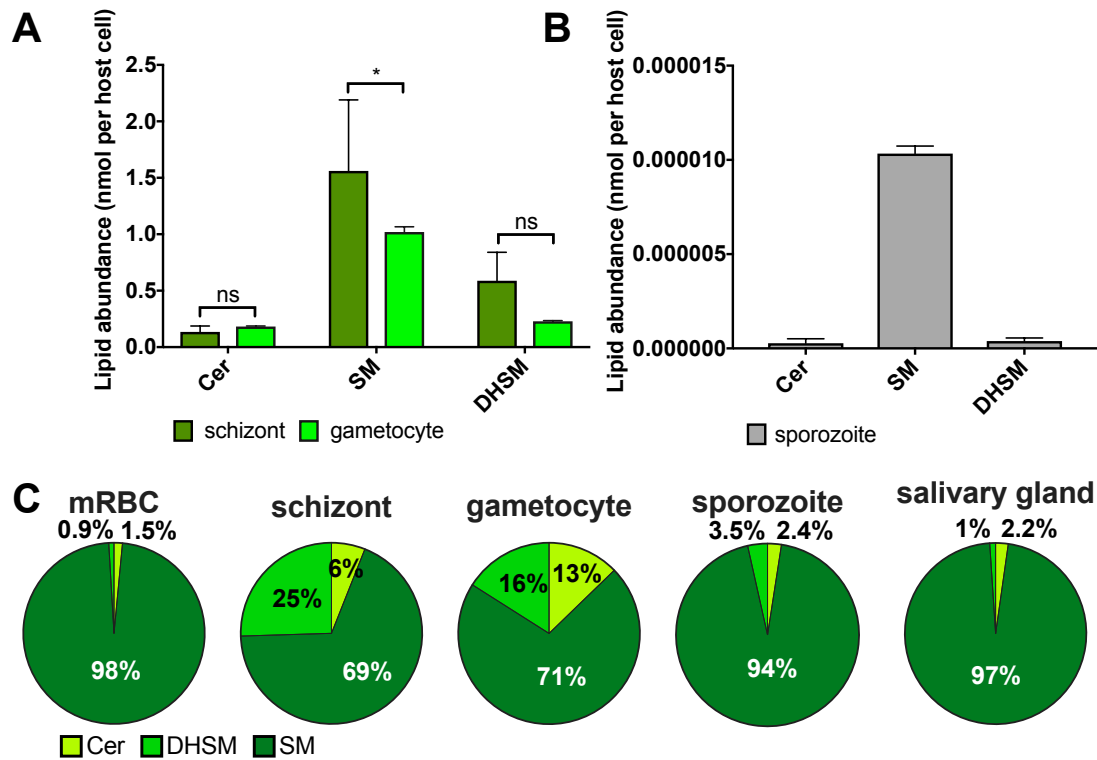


**Figure 8:** Sphingolipid dynamics during the lifecycle of *P. berghei*. Average abundance with standard deviation (A) and average proportion (B) of ceramide (Cer), sphingomyelin (SM) and dihydrosphingomyelin (DHSM) in host cells and at three time points during the parasite lifecycle: schizonts and gametocytes in the mouse red blood cell (mRBC) and sporozoites in the mosquito salivary gland. Statistical significance from two-way ANOVA indicated in A as follows: ns: not significant  $p > 0.1$ , \*:  $p < 0.1$ .

Sphingomyelin is the main sphingolipid in *P. berghei*-infected cells, regardless of the parasite stage or host cell (Figure 8). Schizont-infected mouse RBC contain significantly more sphingomyelin than gametocyte-infected mouse RBC (Figure 8A). Sphingomyelin is a component of membrane lipid rafts that contribute the membrane structure and form intracellular signalling platforms. Parasite infection increases the proportion of other sphingolipid species ceramide and DHSM, especially in blood stages (Figure 8C). This could indicate parasite mediated intracellular signalling or active sphingomyelin metabolism.

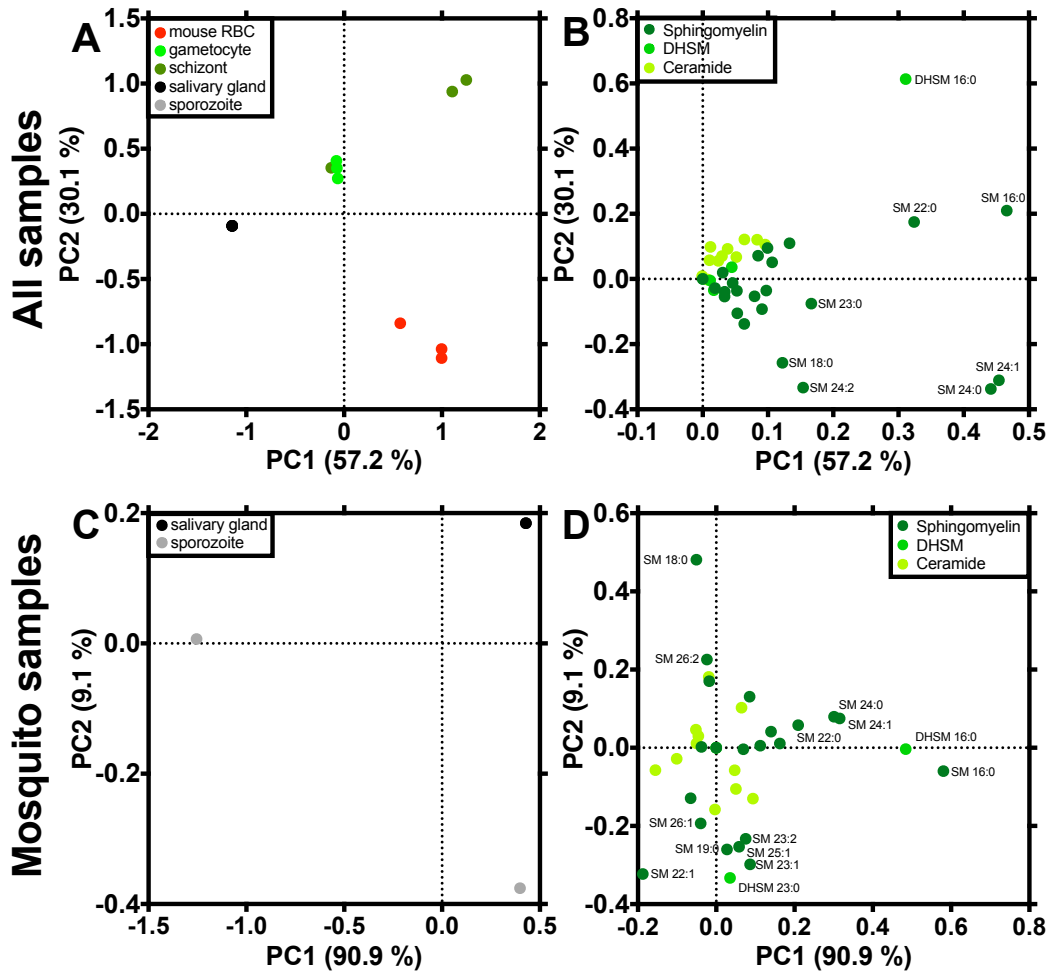


**Figure 9:** Principal component analysis plot (A and C) and loading plot (B and D) of sphingolipids measured in uninfected mouse red blood cells (mouse RBC), *P. berghei* gametocyte and schizont-infected mouse red blood cells, uninfected mosquito salivary glands and *P. berghei* sporozoite-infected salivary glands (A and B) or only mosquito stages (C and D). In A sporozoite and salivary gland points are overlapping. In C both biological repeats of the salivary gland are overlapping. PC1 and 2: first and second principal component; Cer: ceramide; SM: sphingomyelin; DHSM: dihydrosphingomyelin.

Principal component analysis of sphingolipids in all samples identifies three clusters (Figure 9A and B). Firstly, uninfected salivary glands and the sporozoite sample are grouped together. Secondly, uninfected mouse RBC cluster apart based on four SM species (SM 18:0, SM 24:2, SM 24:1 and SM 24:0), which may be metabolised by the parasite. Thirdly, infected mouse RBC samples are grouped together based on the contribution of DHSM 16:0, SM 16:0 and SM 22:0. Overall distinction between mosquito and mouse samples is driven by SM 22:0, SM 16:0, DHSM 16:0, SM 24:1 and SM 24:0.

For better resolution the mosquito samples were subjected to a separate sphingolipid principal component analysis (Figure 9C and D). However, the most variation was in fact observed between biological replicates of the sporozoite sample, rather than between infected and uninfected salivary gland lipids. This suggests that the sphingolipid composition of the infected and uninfected mosquito salivary gland is very similar. SM 18:0 and SM 26:2 drive the small difference in sphingolipids between infected and uninfected salivary glands, and may be metabolised by the parasite.

The nature of sphingolipid species in each sample varied. Cer 22:1 is the main ceramide species in gametocyte-infected RBC, whereas Cer 24:1 is the main species in uninfected and schizont-infected RBC. Cer 16:0 is the main ceramide species in the salivary gland with or without infection. Unlike mouse blood stages, the salivary gland samples only contain saturated ceramide species, suggesting a lack of desaturase activity in sporozoites. SM 24:0 and SM 24:2 are the most abundant SM species in uninfected RBC. SM 16:0 is the most abundant in schizont-infected RBC and SM 22:0 dominates SM species in gametocyte-infected RBC. Mosquito stage samples mostly contain SM 16:0, potentially synthesised from the abundant Cer 16:0, and SM 18:0. DHSM species are all saturated. The most abundant DHSM species in all mouse samples is DHSM 16:0. Very little DHSM is detected in mosquito samples, DHSM 19:0 being the most abundant. Overall, the nature of sphingolipids varies between samples, although mosquito stage sphingolipids are consistently saturated.

In general, sphingolipid differences between samples are subtle, with SM dominating the sphingolipid profile in all samples. SM is a key component of lipid rafts that not only contribute to the structure of the surrounding membrane, but are also intracellular signalling platforms. Specific SM species are more abundant in mouse samples relative to mosquito samples and other sphingolipids DHSM and Cer represent a greater proportion of infected mouse RBC compared to uninfected mouse RBC.

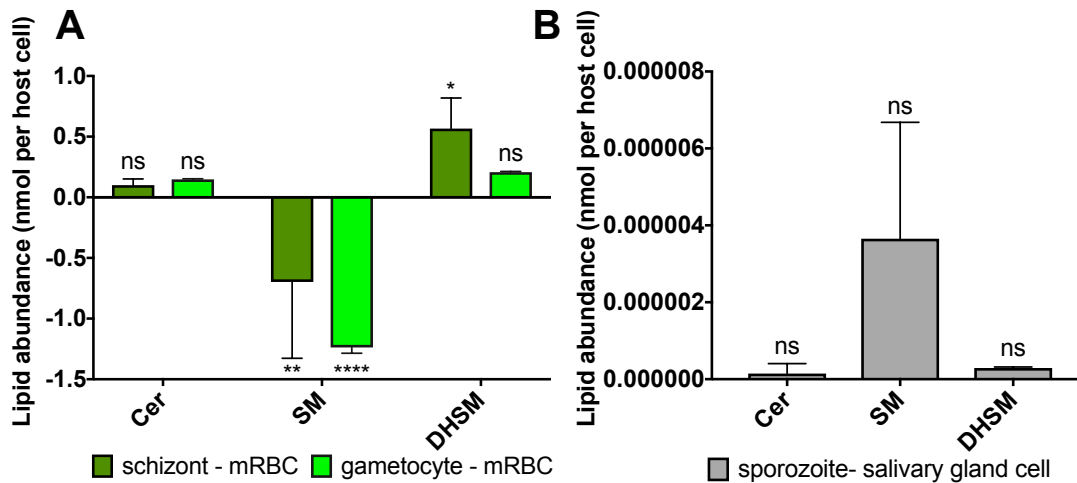


**Figure 10:** Host cell impact on the sphingolipids of *P. berghei*. Average abundance with standard deviation of ceramide (Cer), sphingomyelin (SM) and dihydrosphingomyelin (DHSM) in *P. berghei* gametocyte and schizont-infected mouse red blood cells (A) or *P. berghei* sporozoite-infected salivary glands (B) after subtraction of their respective host cell lipid abundance. Statistical significance of difference between host cell and infected host cell from two-way ANOVA indicated as follows: ns: not significant  $p > 0.1$ , \*:  $p < 0.1$ , \*\*:  $p < 0.01$ , \*\*\*\*:  $p < 0.0001$ .

The sphingolipid profile of the host cell was subtracted from that of the infected cell to highlight the parasite's impact on host cell lipids (Figure 10). Blood stage *P. berghei* depletes the host RBC of SM unlike sporozoites (Figure 10A and B). Other sphingolipids DHSM and ceramide are slightly more abundant upon infection, especially DHSM at schizont stage. The ratio of SM/DHSM impacts membrane rigidity, which may be functionally significant for *P. berghei* blood stages. Fluctuations in ceramide abundance may reflect intracellular signalling.

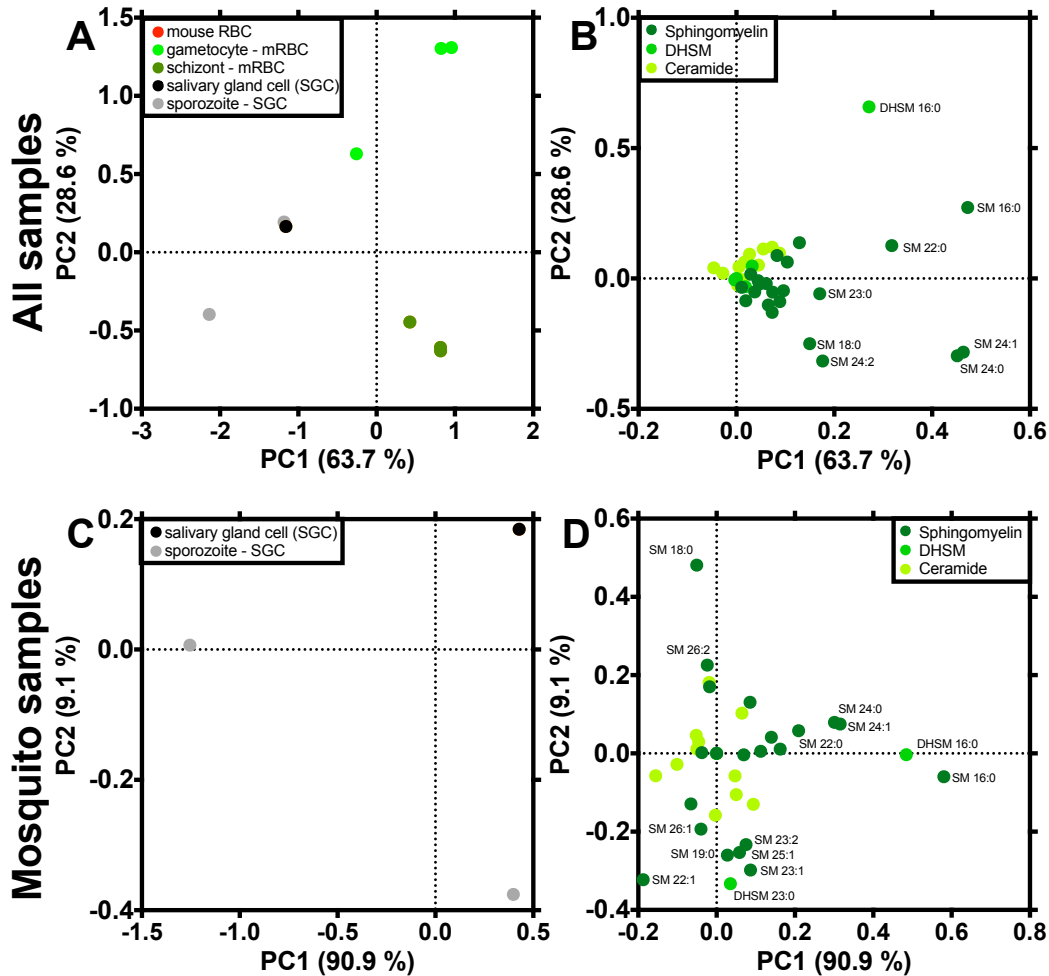


**Figure 11:** Principal component analysis plot of sphingolipids in uninfected host cells and *P. berghei*-infected host cells after subtraction of host cell lipid abundance (mouse red blood cell (mRBC) or mosquito salivary gland cell (SGC)). Analysis of all samples (A) or mosquito samples only (C) with corresponding loading plots (B and D). Both biological replicates of the salivary gland are overlapping in A and C. Schizont samples overlap with uninfected mouse red blood cell samples in A. PC1 and 2: first and second principal component; Cer: ceramide; SM: sphingomyelin; DHSM: dihydrosphingomyelin.

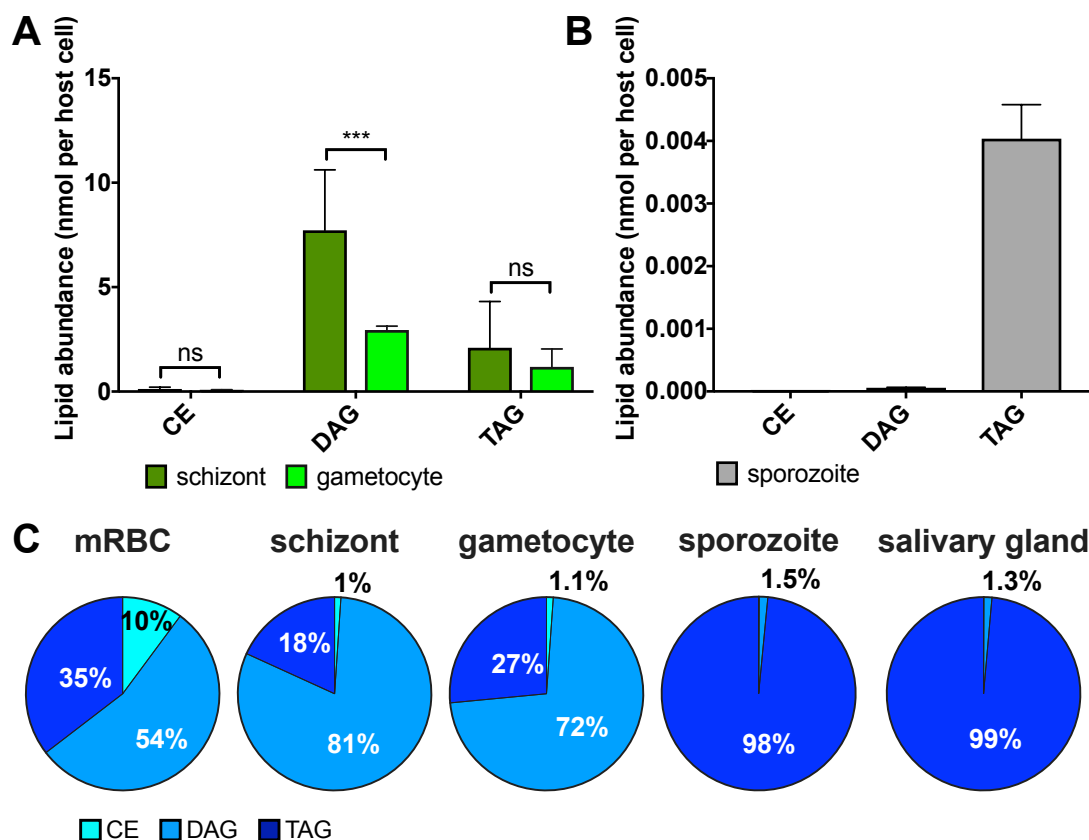
After subtraction of host cell lipids, sphingolipids in schizont-infected mouse RBC are similar to those in uninfected mouse RBC, as illustrated by overlapping points in a principal component analysis (Figure 11A and B). The corresponding loading plot is very similar to Figure 9B, except schizont-infected RBC lipids with host cell lipids subtracted cluster with their host RBC, rather than with gametocyte-infected RBC. This suggests that gametocyte-infected RBC sphingolipids are stage-specific and differ from host cell lipids, whereas schizont-infected RBC accumulate similar lipids to those found in the host cell. Subtraction of host cell sphingolipids from those of sporozoite-infected salivary glands does not impact the distribution of samples in a principal component analysis (Figure 11C and D is similar to



Figure 9C and D), suggesting sporozoite-infected salivary gland lipids are similar to salivary gland lipids.

Overall, parasite induced sphingolipid modifications to the host cell are subtle and host-cell-specific: infection of mouse RBC depletes SM, unlike sporozoite infection of the salivary gland. The distinctive gametocyte-infected RBC sphingolipid composition may represent preparations for transition to the mosquito vector and suggests *de novo* sphingolipid synthesis occurs in gametocyte-infected RBC.

#### 4. Neutral lipid store is switched upon mouse to mosquito host transition



**Figure 12:** Neutral lipid dynamics during the lifecycle of *P. berghei*. Mean and standard deviation of abundance (A) and proportion (B) of cholesteryl ester (CE), diacylglycerol (DAG) and triacylglycerol (TAG) at three time points during the parasite lifecycle: schizonts and gametocytes in the mouse red blood cell (mRBC); and sporozoites in the mosquito salivary gland. Statistical significance from two-way ANOVA indicated in A as follows: ns: not significant  $p > 0.1$ , \*\*\*:  $p < 0.001$ .

Neutral lipid composition switches between mouse and mosquito hosts in both uninfected and infected cells (Figure 12). Half of the neutral lipids in mouse RBC are DAG species, and this proportion increases upon infection (Figure 12C). Gametocyte-infected mouse RBC contain

less DAG than schizont-infected mouse RBC (Figure 12A). The proportion of TAG and CE decreases after infection, with CE representing only 1 % of neutral lipids in schizont-infected RBC and gametocyte-infected RBC, compared to 10 % in uninfected mouse RBC. Mosquito salivary gland neutral lipids are mostly TAG species in the presence or absence of *P. berghei* infection (Figure 12B and C). From a fatty acid storage point of view, TAG is a more efficient storage lipid than DAG, so sporozoite stage parasites appear to stockpile fatty acids. Although not as efficient at fatty acid storage, DAG is also an intracellular second messenger that may be functionally important for blood stage parasite development.

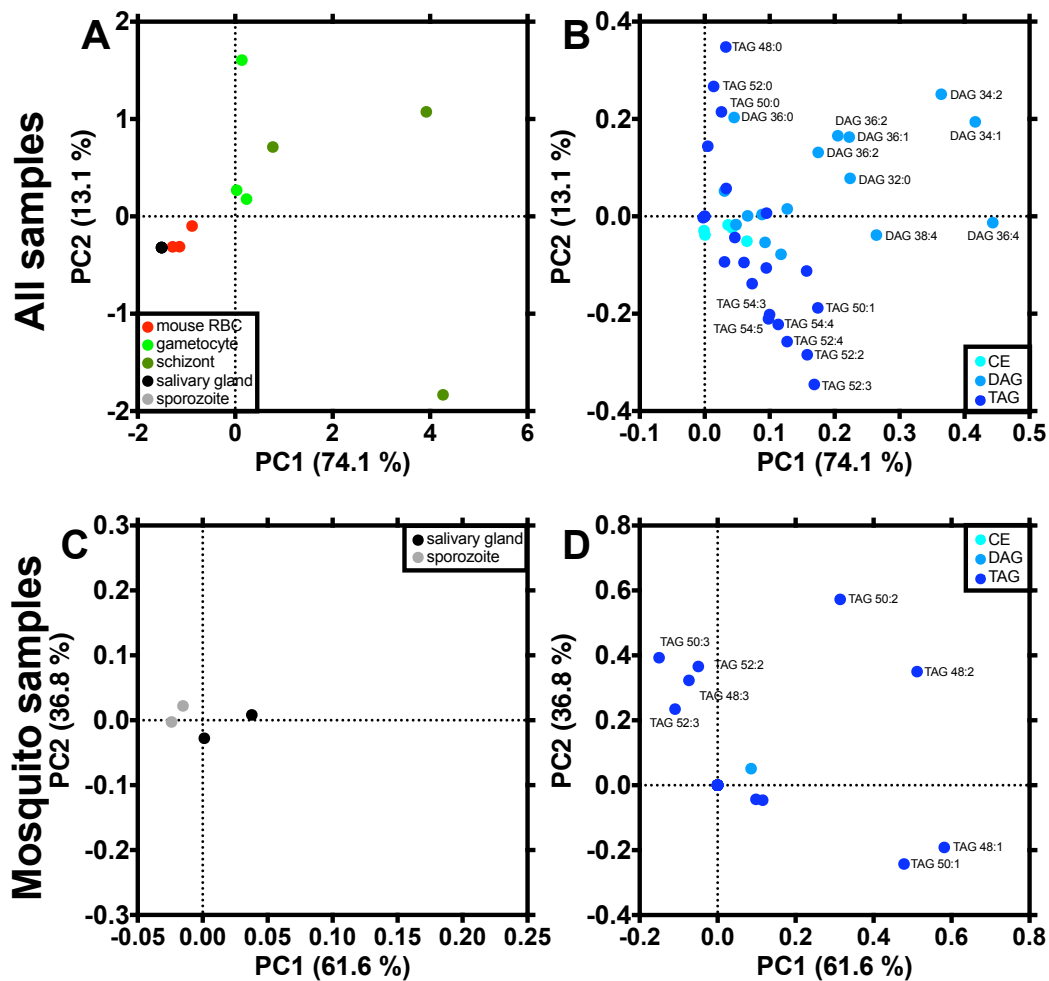


**Figure 13:** Principal component analysis plot (A and C) and loading plot (B and D) of neutral lipids measured in uninfected mouse red blood cells (mouse RBC), *P. berghei*-infected mouse red blood cell at gametocyte and schizont stage, uninfected mosquito salivary gland cells and *P. berghei* sporozoite-infected mosquito salivary gland cell (A and B) or only mosquito stages (C and D). In A salivary gland and sporozoite points are overlapping. PC1 and 2: first and second principal component; CE: cholesteryl ester; DAG: diacylglycerol; TAG: triacylglycerol.

At the individual neutral lipid species level, DAG species distinguish infected mouse RBC from the other samples (Figure 13A and B). TAG species are highly variable between biological replicates of the infected mouse RBC, while mosquito stages and uninfected mouse RBC have similar neutral lipid profiles. Infection of the mosquito salivary gland is marked by a decrease in specific TAG species (TAG 50:1, TAG 50:2, TAG48:1 and TAG 48:2, Figure 13C and D), potentially indicating parasite catabolism of TAG stores in the mosquito. Overall, DAG is the key neutral lipid that distinguishes infected from uninfected mouse RBC stages while TAG dominates the neutral lipid profile of mosquito stages.

The nature of neutral lipid species appears to vary between samples. The most abundant DAG species in infected mouse RBC are DAG 34:1, DAG 34:2 and DAG 36:4. Very little DAG, mostly DAG 34:1, DAG 34:2 and DAG 36:2, are present in uninfected mouse RBC. In mosquito samples DAG 34:1 is the most abundant DAG species. In general, DAG 34:1 appears to dominate DAG species in all samples. TAG 52:2 is one of the main TAG species in uninfected or schizont-infected mouse RBC and uninfected or sporozoite-infected mosquito salivary glands, but not in gametocyte-infected mouse RBC where the major TAG species is TAG 48:0. The switch in TAG species in gametocytes stage may reflect specific lipid requirements for transmission to the mosquito host. The main CE species in all samples were CE 16:0 and CE 18:1. Uninfected RBC also contained a large proportion of CE 18:2, which may be catabolised upon infection. Overall, the dynamic nature of neutral lipids throughout the parasite lifecycle suggests active neutral lipid metabolism.

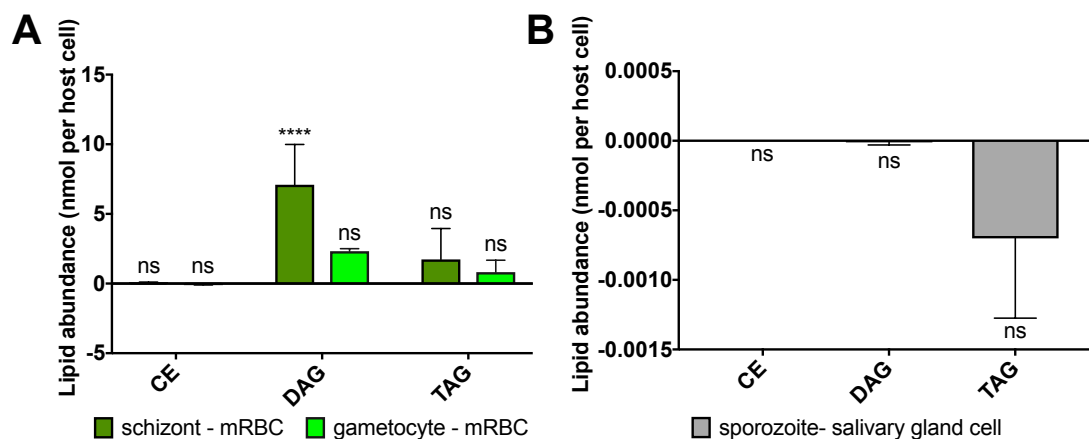


**Figure 14:** Host cell impact on the neutral lipids of *P. berghei*. Average abundance and standard deviation of cholesteryl ester (CE), diacylglycerol (DAG), triacylglycerol (TAG) in *P. berghei*-infected mouse red blood cells at schizont and gametocyte stages (A) or sporozoite-infected mosquito salivary glands (B) after subtraction of host cell lipid abundance (uninfected mouse red blood cell (mRBC) or mosquito salivary gland cell). Statistical significance of the difference between infected and uninfected host cell lipids calculated by two-way ANOVA indicated as follows: ns: not significant  $p > 0.1$ , \*\*\*\*:  $p < 0.0001$ .

Neutral lipid modifications are host cell, and parasite-stage-specific (Figure 14). Mouse RBC infected with schizonts accumulate DAG but there is little change in TAG and CE abundance (Figure 14A). Gametocyte or sporozoite infection has no significant impact on neutral lipid abundance in the host cell (Figure 14A and B). However, subtle gametocyte-infected RBC lipid accumulations are similar to those in the schizont-infected RBC, whereas sporozoite infection subtly depletes TAG in the mosquito salivary gland. Overall, this suggests that sporozoite-stage parasites deplete host cell fatty acid stores, whereas blood stage parasites stockpile fatty acids and/or have more active DAG signalling pathways.

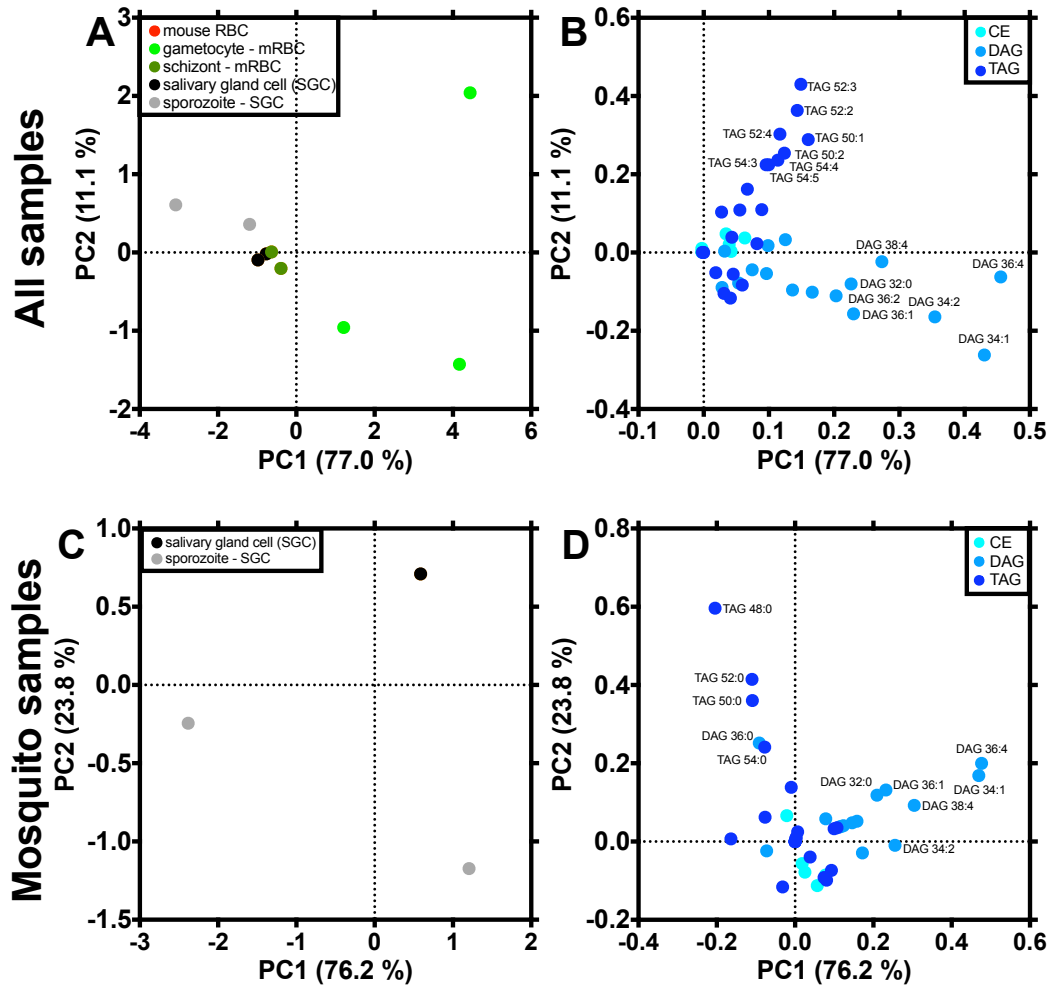


**Figure 15:** Principal component analysis of neutral lipids in uninfected host cells and *P. berghei*-infected host cells at gametocyte, schizont and sporozoite stage after subtraction of host cell lipid abundance (uninfected mouse red blood cell (mouse RBC) or uninfected mosquito salivary gland cell (SGC)). Analysis plot of all samples (A) or mosquito samples only (C) with corresponding loading plots (B and D). After subtraction of host cell neutral lipids, schizont samples overlap with uninfected mouse red blood cells in A. In C both biological repeats of the uninfected salivary gland cell are overlapping. PC1 and 2: first and second principal component; CE: cholesteryl ester; DAG: diacylglycerol; TAG: triacylglycerol.

Principal component analysis comparing neutral lipids in all samples clusters both host cells and schizont-infected RBC with host cell neutral lipids subtracted (Figure 15A). Whereas uninfected mouse RBC are characterised by TAG and DAG accumulation (Figure 13B), gametocyte-infected RBC with host cell neutral lipids subtracted are distinguished by DAG species alone (Figure 15B), highlighting gametocyte-specific neutral lipid metabolism or intracellular signalling. Between mosquito samples, TAG 50:0, TAG 48:0 and TAG 52:0 are the main lipids accumulated in uninfected salivary glands relative to sporozoite-infected RBC

with host cell neutral lipids removed (Figure 15C and D), consistent with the overall TAG dynamic (Figure 14B).

In summary, infection of mouse RBC increases DAG and TAG abundance while sporozoite infection depletes the TAG resource of the mosquito salivary gland. After subtraction of the host cell lipids, schizont-infected RBC neutral lipid composition is similar to that of its host cell but gametocyte-infected RBC accumulate distinctive TAG species, suggesting stage-specific neutral lipid metabolism. These TAG species may be fatty acid reserves for gametocyte activation and further parasite development in the mosquito.

### Discussion

Comparison of the lipid content of uninfected and infected host cells throughout the *P. berghei* lifecycle identified stage-specific lipid modifications (Figure 16).

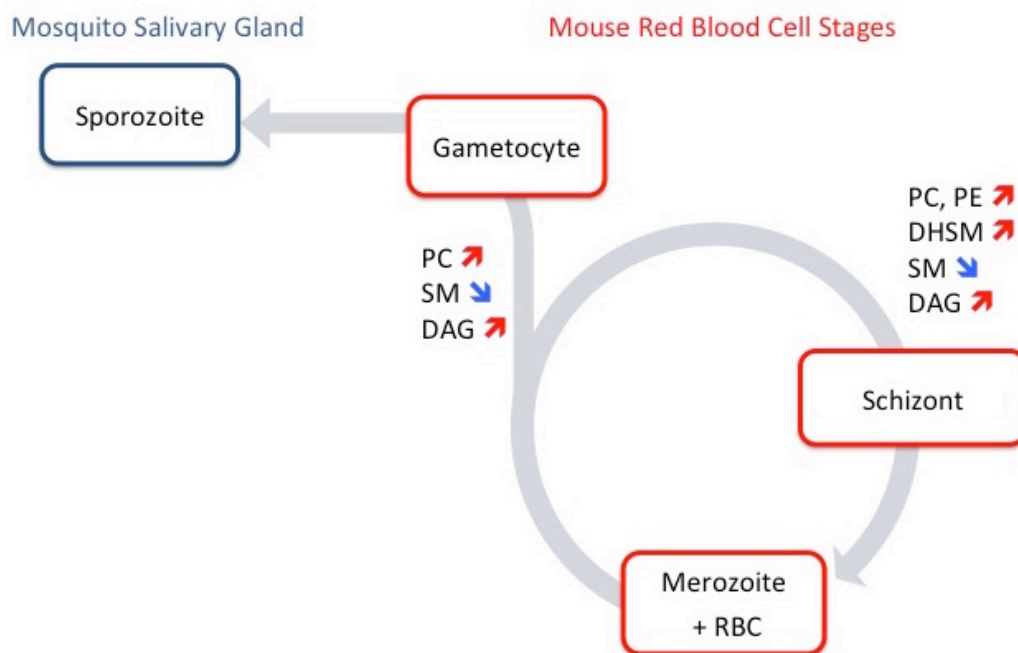


**Figure 16:** Overview of major lipid differences between uninfected mouse red blood cells (RBC) prior to *P. berghei* merozoite invasion and gametocyte or schizont-infected mouse red blood cells. Gametocyte stage *P. berghei* connects the mouse and mosquito stages of the parasite lifecycle. DAG: diacylglycerol; DHSM: dihydrosphingomyelin; PC: phosphatidylcholine; PE: phosphatidylethanolamine; SM: sphingomyelin.

Comparison of *P. berghei*-infected mouse RBC and *P. berghei*-infected salivary glands mostly highlights differences in the host cell lipid composition. The overall lipid abundance of sporozoite-infected salivary glands (when divided by the number of cells per salivary

gland) is much less than blood stage parasite-infected RBC. This is consistent with the smaller size of sporozoites and may also reflect significantly different lipid abundance between the host cells. Phospholipids dominate the lipid profile of mouse RBC samples whereas neutral lipids are the major lipid class in the mosquito salivary gland (Figure 1C). This suggests that *P. berghei* sources lipids from its host cell environment, consistent with the finding that lipid transporters are essential (Bushell et al. 2017). *Plasmodium* parasites are unable to synthesise cholesterol, however Niemann-Pick type C protein 1 (PBANKA\_020590), a lipid/sterol: H<sup>+</sup> symporter, is essential in *P. berghei* and may be specifically required for scavenging cholesterol from the host cell. ATP2 (PBANKA\_143480), a phospholipid flippase, is also essential for *P. berghei* (Pasini et al. 2013; Kenthirapalan et al. 2016) and may mediate phospholipid scavenging from the host cell. ATP8 (PBANKA\_143830), another phospholipid flippase, guanylyl cyclases  $\alpha$  (PBANKA\_091030) and guanylyl cyclase  $\beta$  (PBANKA\_113670), both phospholipases and guanylyl cyclases, are required for normal proliferation, suggesting that they may also have an important function in the parasite (Bushell et al. 2017). Together with the results of the present study, it is likely that lipid scavenging from the host cell contributes to the lipid profile of the *P. berghei*-infected host cell and essential parasite functions.

Comparison of uninfected and infected host cell lipids ensured that this observation was not an artefact of measuring the parasite lipid abundance with its host cell. Indeed, lipid profile differences between parasite stages persisted when the lipidome of the host cell was removed. In the case of phospholipids, the parasite accumulates the same phospholipid classes found in the host cell. This could be the result of stage-specific lipid requirements, but is more likely an indication of lipid scavenging, or perhaps hijacking of the reticulocyte phospholipid metabolic pathway (Srivastava et al. 2015). From an evolutionary perspective, parasitism is generally accompanied by gene loss (Vivarès et al. 2002; Wolf & Koonin 2013; Jackson et al. 2016) since the parasite can make use of host cell functions. Although functionally overlapping genes could provide protection from mutation (Boone et al. 2007; Costanzo et al. 2010), remaining parasite genes are therefore mostly involved in essential but parasite specific functions. Similarities in the host and parasite lipid profiles suggest *P. berghei* lipid metabolism is reduced following host-parasite co-evolution.

Mouse RBC infected with *P. berghei* schizonts or gametocytes have a similar phospholipid and sphingolipid composition until the host cell lipid component is removed. Overall, it

appears that after removing host cell lipids schizont-infected RBC have a similar composition to their host cell, whereas gametocyte-infected RBC lipids are unique. This could indicate that schizonts rely more on lipid scavenging while gametocytes synthesise more lipids *de novo* in preparation for transition to the mosquito. Indeed, the lipid profile of the mouse RBC is very different to that of the mosquito host environment. Gametocyte-specific lipids are perhaps a metabolic adaptation for survival in the mosquito vector. If so, gametocyte lipids may be sex-specific since female gametocytes contribute most of their lipids to the zygote, whereas male gametocytes are relatively short lived in the mosquito.

At the individual lipid species level, LPC in the mouse RBC was depleted upon infection. In *P. falciparum*, LPC from the serum is a source of choline used for PC synthesis (Wein et al. 2018). LPC (and SM) hydrolysis by phospholipase C is essential for asexual *P. falciparum* proliferation (Hanada et al. 2002). Lack of LPC induces stress-triggered gametocytogenesis in *P. falciparum* (Brancucci et al. 2017). In the present study, LPC depletion is coupled with the accumulation of PC in schizont and gametocyte-infected RBC. The *P. berghei* parasite may therefore source LPC from the host RBC for PC synthesis during blood stage development. Membrane biosynthesis is likely the function of the phospholipids accumulated in *P. berghei* parasites.

Neutral lipids are the major lipid category in the mosquito salivary gland and it appears that sporozoites deplete this reserve. TAG is an important cellular store of fatty acids, which may be required for sporozoite development. In the mouse RBC the parasite instead stockpiles DAG and TAG, perhaps to sequester toxic fatty acids as previously observed in *T. gondii* (Nolan et al. 2018). DAG is an intracellular signalling molecule that may mediate blood-stage-specific parasite functions. Blood stage parasites potentially source neutral lipids or fatty acids to form neutral lipids from circulating lipoproteins in the serum.

Sphingolipids are a minor component of the infected or uninfected host cell throughout the parasite lifecycle. As such, changes in sphingolipids are subtle, but nevertheless distinctive of parasite stage. In particular, SM is reduced by catabolism or selective blebbing off of SM-rich domains in blood stage *P. berghei* but accumulated in the sporozoite. SM along with cholesterol is a component of lipid rafts in the membrane, which have previously been implicated in protein trafficking, parasite invasion, organelle biogenesis and membrane remodelling (Samuel et al. 2001; Sanders et al. 2005; Di Girolamo et al. 2008; Yam et al.



2013). SM is also a source of intracellular signalling molecule ceramide that inhibits *Plasmodium* parasite proliferation (Pankova-Kholmyansky et al. 2003). SM in the highly motile sporozoite may be required for migration from the mosquito midgut wall to the salivary gland, through the human skin to the liver or for hepatocyte invasion.

In addition, DHSM 16:0 consistently appears as a marker of gametocytes of *P. berghei*. DHSM has not been described in *Plasmodium* previously, however in mammalian cells high abundance of DHSM rigidifies lipid rafts and prevents human immunodeficiency virus infection (Vieira et al. 2010). Potentially the presence of DHSM modulates the function of lipid rafts in *Plasmodium* during gametocytogenesis.

During the lifecycle of *P. berghei*, changes in lipid metabolism mark the transition from asexual to sexual blood stage. The parasite likely scavenges lipids from both the mammalian and mosquito host, while synthesising other lipids *de novo* in a host-specific manner.

## Part 3

### Lipid scavenging in asexual blood stage *Plasmodium* parasites

#### Introduction

Asexual *Plasmodium* parasite infection of the RBC is coupled with characteristic lipid changes. In the first two sections of this chapter the investigation of parasite lipids lead to several hypotheses that are further developed here by comparing lipid modification in *P. berghei* and *P. falciparum*.

Lipid modifications correlate with parasite lifecycle-stage-specific functions. For example, phospholipid accumulation in *P. falciparum* schizont-infected RBC coincides with membrane biogenesis during asexual replication. Although overall lifecycle stages are conserved among *Plasmodium* species, *P. berghei* and *P. falciparum* asexual blood stages differ in their replication time and number of daughter cells. If lipids are related to function, species-specific functions may result in species-specific lipid profiles. Conversely differences in lipids between *Plasmodium* species may highlight species-specific lipid functions.

The lipid profile of the host cell impacts the lipid composition of the infected host cell. Reductive host-parasite co-evolution may have resulted in parasites adopting host cell lipid traits. Rather than synthesising their own lipids, parasites scavenge lipids found in the host, which results in similar lipid characteristics between the host cell and parasite. *Plasmodium* speciation likely co-evolved with their hosts such that current *Plasmodium* parasites are host-species-specific. Taken together, species-specific lipid traits of *Plasmodium* parasites may reflect host cell species-specific lipid characteristics.

Although lipid similarities exist between parasite and host, other lipids are unique, suggesting *de novo* lipid synthesis. In the second part of this chapter, *P. berghei* gametocytes appear to synthesise lipids *de novo* whereas schizonts rely more on lipid scavenging. This is likely in preparation for gametocyte transition between mammalian and mosquito host environments. Similarly, if the mouse and human RBC lipid environment is different, species-specific lipid traits that are inconsistent with differences between host cells, may instead be indicative of *de novo* lipid synthesis in compensation of host cell lipid disparities. Lipids that fall in this category likely have an essential, conserved function in *Plasmodium* species.

Here the lipid profile of the host RBC in mice and humans is compared to highlight lipid differences between host cells. The schizont stage lipid modifications to the host RBC in *P. falciparum* and *P. berghei* are next compared to identify conserved and species-specific lipid modifications. Together these results distinguish species-specific lipid modifications that are adaptations to different host cell environments, or that drive species-specific metabolic functions.

## Results

The lipid composition of uninfected mouse and human RBC was described in the first two parts of this chapter in comparison to infected RBC. Here the lipid composition of each species of uninfected host RBC is contrasted.

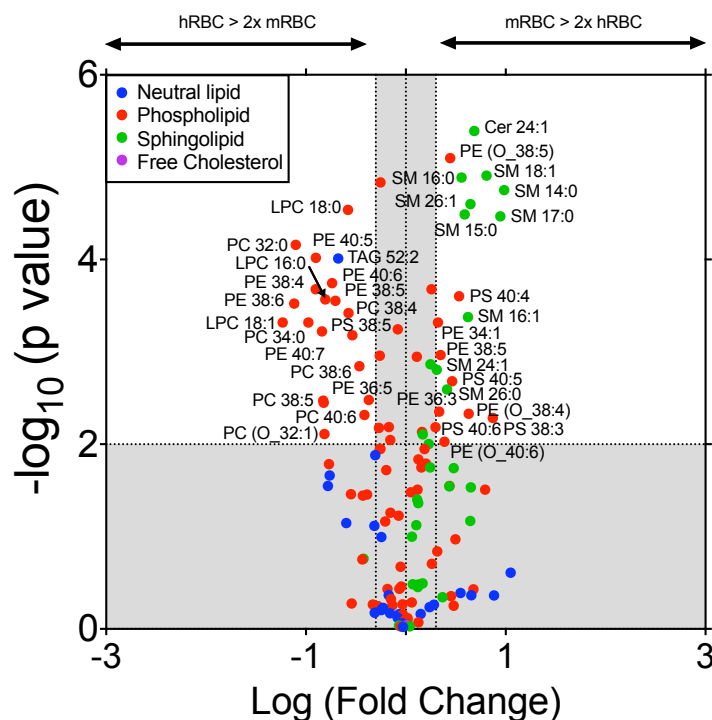


**Figure 1:** Volcano plot of differences in lipid species between mouse red blood cells (mRBC) and human red blood cells (hRBC). Statistical significance (p values) calculated by multiple student t tests. Grey area indicates changes that are less than 2 fold and/or non significant ( $p > 0.01$ ). Cer: ceramide; PE: phosphatidylethanolamine; PC: phosphatidylcholine; PS: phosphatidylserine; LPC: lysophosphatidylcholine; SM: sphingomyelin; TAG: triacylglycerol.

Although mice and humans are both mammalian hosts for *Plasmodium*, mouse and human RBC lipids are not identical (Figure 1). Sphingolipid species are clearly more abundant in

mouse RBC relative to human RBC. With the exception of Cer 24:1, all of the significantly more abundant sphingolipids are SM species. Phospholipids are variable between mouse and human RBC. All phospholipid species accumulated in the mouse RBC are either PE or PS species. Human RBC on the other hand accumulate a variety of phospholipids, including three LPC species. The only significantly different neutral lipid species is TAG 52:2 that is more abundant in human RBC. The lipid environment of the *P. berghei* and *P. falciparum* schizonts is therefore host-specific.

**Table 1:** Comparison of *P. berghei* and *P. falciparum* lipid differences between schizont-infected RBC and uninfected host RBC. Statistical significance of the difference in lipid subclass abundance between the schizont-infected RBC and corresponding uninfected RBC calculated by two-way ANOVA is indicated as follows: ns: not significant  $p > 0.01$ ; \*\*\*\*:  $p < 0.0001$ ; \*\*\*:  $p < 0.001$ , \*\*:  $p < 0.01$ . Individual lipid species were compared with multiple student t-tests, as illustrated in Supplementary Figure 1 volcano plots. Lipid species indicated in the table have a  $p < 0.01$ . The ten PC species that are more abundant in *P. falciparum* schizont-infected RBC compared to uninfected RBC are: PC 38:4, 38:5, 36:5, 36:4, 40:7, 38:3, 40:6, 36:0, 38:6 and O<sub>38</sub>:4. Red indicates an increase upon infection, blue a decrease.

Lipid class	Lipid sub class	<i>P. falciparum</i>	<i>P. berghei</i>
Free cholesterol	-	ns	ns
Phospholipid	PC	**** various PC species	**** LPC 16:0, LPC 18:0
	PE	*** 36:4, 38:4, 38:5	***
	PS	ns	ns
	PG	ns	ns 36:1
Neutral lipid	TAG	ns	ns 48:0
	DAG	ns	**** 34:1, 36:2
	CE	ns	ns
Sphingolipid	Cer	ns 16:0	ns
	SM	ns	** 18:1, 25:0
	DHSM	ns	ns

A cross-species comparison of host cell lipid modifications by schizont stage *Plasmodium* parasites is summarised in Table 1. Some differences between uninfected host RBC and schizont-infected RBC are consistent among species. Overall PC and PE are more abundant

after infection with schizont stage parasites, regardless of parasite species. Cholesterol, PS, PG, TAG, CE, Cer and DHSM in the RBC were not significantly modified upon infection by schizonts in either species. These lipid changes (or lack thereof) likely reflect conserved schizont functions, such as accumulation of phospholipids for membrane biogenesis during asexual replication.

Other modifications to the host RBC are species specific. Notably, only *P. berghei* schizonts deplete SM but accumulate DAG. The SM depletion is also reflected at the individual lipid species level since SM 25:0 and SM 18:1 are significantly less abundant in the *P. berghei* schizont-infected mouse RBC. Similarly, DAG 34:1 and DAG 36:2 are significantly more abundant in *P. berghei* schizont-infected mouse RBC compared to uninfected mouse RBC. None of the significantly different individual lipids are consistent between *Plasmodium* species, suggesting that the parasites may induce similar overall lipid modifications via different lipid species.

### **Discussion**

Although *P. berghei* is commonly used as a model organism for *P. falciparum* infection, species-specific lipid modifications to the host RBC upon schizont infection are highlighted in this chapter. To ascertain whether these differences are adaptations to different host cell environments, the lipid composition of the human and mouse host RBC is also compared.

The lipid profile of human and mouse RBC presented here may differ slightly to the *in vivo* lipid environment of *Plasmodium* parasites. For technical reasons, the mouse and human RBC samples were prepared following different protocols that may result in slightly different sample purities. More importantly, the samples contain both mature RBC and a minority of reticulocytes. As detailed in the general introduction, *P. falciparum* invades mature RBC whereas *P. berghei* prefers reticulocytes. The conclusions drawn in this chapter assume that the lipid profile of reticulocytes and mature RBC of a given host are not significantly different, similar to the proteome (Gautier et al. 2018).

Conserved lipid modifications in *P. berghei* and *P. falciparum* are increased PE and PC. PE species are variable between mouse and human RBC, and *Plasmodium* parasites may have developed mechanisms to overcome this variation ancestrally by parasite-driven PE

accumulation. Despite several PC species being more abundant in human RBC exclusively, the PC requirement of *P. berghei* and *P. falciparum* schizonts appears to surpass the PC resource of either host RBC. This suggests a conserved mechanism of PC synthesis and/or scavenging from beyond the host RBC.

Some species-specific modifications to the host cell may compensate for differences between host cells. Unlike *P. falciparum*, *P. berghei* schizonts deplete the host RBC of SM. Interestingly, mouse RBC contain more of many SM species, including SM 18:1 that was significantly depleted in *P. berghei* schizont-infected RBC. Potentially SM homeostasis is important for *Plasmodium* schizont development, and *P. berghei* infection of the SM-rich mouse RBC is dependant on depleting the SM of the host cell environment by specific metabolism or selective blebbing off of SM-rich domains. SM metabolism by sphingomyelinase is a source of intracellular signalling molecule ceramide that can be cytotoxic in high doses (Pankova-Kholmyansky et al. 2003). SM also contributes to the structure of cellular membranes thus impacting many functions including invasion of the host cell and surface protein trafficking. Similarly, human RBC are relatively deficient in PE 38:5, but *P. falciparum* schizont-infected human RBC stockpile this lipid as if to compensate for its absence in the host cell. The phospholipid content of cellular membranes also impacts membrane structure and associated functions.

Other species-specific host cell modifications exacerbate differences between human and mouse RBC. LPC 16:0 and LPC 18:0 are lacking in the mouse RBC, and are further depleted upon *P. berghei* schizont infection. This suggests that the LPC requirements of the parasite are not adapted to the host cell environment. LPC catabolism may reflect an essential parasite function that is non redundant with host cell function. PE 38:4, PC 38:4, PC 38:5 and PC 40:6 are more abundant in the human RBC relative to the mouse RBC, and are stockpiled in *P. falciparum* schizont-infected human RBC. These lipids may reflect host-parasite co-evolution – the parasite favours abundant host lipids as they can be directly scavenged from the host.

Another set of differences in lipids between host and parasite species hint at potential parasite metabolism of scavenged host cell lipids. PE species 36:5, 40:7 and 40:6 that are more abundant in human RBC may be the source of corresponding PC species 36:5, 40:7 and 40:6 that are more abundant in *P. falciparum* schizont-infected human RBC. Similarly, PC\_O

38:4 may be accumulated in *P. falciparum* schizont-infected human RBC from the relatively abundant host cell PC 38:4. Although it is tempting to speculate that the parasite lipids are directly metabolised to form parasite lipids, these similarities between parasite and host lipids could also be the result of general fatty acid chain composition in the host environment. Either way, these lipids are likely sourced more or less directly from the host environment.

The rest of the species-specific schizont-induced lipid modifications to the host cell are independent of differences between human and mouse RBC lipids. In particular accumulation of DAG by *P. berghei*-infected mouse RBC is not related to any DAG variations between human and mouse host RBC. Such lipids are strong candidates for *de novo* synthesis by the parasite. This suggests that these lipids play an essential, species-specific function that warrants further investigation.

Overall, *Plasmodium* schizonts modify the lipid composition of the host cell in both conserved and species-specific manners. The accumulation of PC and PE in both species likely reflects conserved *Plasmodium* functions. The host RBC lipid composition is host-species-specific. Parasite-host co-evolution may explain some parasite-species-specific lipid traits. Other parasite-species-specific lipid modifications such as DAG accumulation in *P. berghei* schizont-infected mouse RBC are independent of inter-host species differences, highlighting metabolic pathways that are likely essential for schizont stage parasites, but non-redundant with host lipids. This parasite lipid metabolism is a prime target for the rational design of antimalarial drugs.

## Conclusion

The dynamic lipid profile of a *Plasmodium*-infected host cell is impacted by host cell lipid composition and parasite lifecycle stage. Some modifications, such as the accumulation of PC in schizont-infected RBC, are conserved among *P. berghei* and *P. falciparum*, and relate to lifecycle-stage-specific functions (membrane biogenesis during parasite replication). Other lipid changes are *Plasmodium* species-specific and may compensate for differences in the host cell environment. *P. berghei* gametocyte-infected RBC lipids are unique, potentially to prepare for transition between the human and mosquito host. Given that female gametocytes contribute most to the fertilized zygote, whereas male gametocytes are short-lived in the mosquito, the lipid composition of gametocytes may be sex-specific. It would be interesting to investigate whether the unique lipid biology in gametocytes is conserved among *Plasmodium* species, and whether it is consistent between gametocyte sexes.

The following chapters of this thesis focus on *P. falciparum* gametocytes. At the time this research was started, there were limited means of analysing sex-specific *P. falciparum* gametocyte biology so a method for the separation of male and female gametocytes is presented in the next chapter. In the final results chapter this method is applied to investigate the sex-specific lipid profile of *P. falciparum* gametocytes.





# **Result Chapter 2**

**Novel method and applications for  
the separation of male and female  
gametocytes**

## Overview

By definition, sexual blood stage parasites are either male or female so a sex-specific approach to gametocyte research is warranted. In this chapter, a novel method for the separation of male and female *P. falciparum* gametocytes by FACS is described. As a proof of concept the method is applied to validate novel sex-specific gametocyte markers. In the second part of this chapter, a possible mechanism of sex-determination by sex-specific DNA methylation is explored using the established method. Overall, this chapter reinforces the functional importance of investigating *P. falciparum* gametocytes in a sex-specific manner.

## **Part 1**

### **Novel method for the separation of male and female gametocytes**

#### **Introduction**

Transmission of malaria depends on the switch from asexual proliferation to male and female gametocytogenesis in the human host. Unlike asexual blood stage parasites that are responsible for most of the symptoms of malaria, male and female gametocytes persist in the blood for weeks after symptoms cease (Smalley & Sinden 1977; Gebru et al. 2017) – waiting for mosquito ingestion to activate the next lifecycle stage of the parasite. Eliminating gametocytes and monitoring their prevalence in endemic countries is key to eradicating malaria (Alonso et al. 2011; Jenny Liu et al. 2013).

For this reason, there has recently been a concerted effort to develop gametocyte-killing compounds. The only World Health Organisation recommended course of transmission blocking treatment is 0.25 mg/kg of primaquine (World Health Organisation, 2018). However, primaquine causes haemolysis in patients with glucose 6-phosphate dehydrogenase deficiency, a prevalent disorder in malaria endemic regions (Hockwald et al. 1952; Dern et al. 1954; Recht et al. 2018). The Medicines for Malaria Venture's target candidate profile includes transmission blocking activity, preferably by killing gametocytes rather than mosquito stage parasites (Burrows et al. 2017).

One strategy for drug development is through cell-based drug screens. Most gametocyte drug screens are not sex-specific (D'Alessandro et al. 2013; Zenglei Wang et al. 2014; D'Alessandro et al. 2016). These methods are limited by the natural female bias of gametocytes (Robert et al. 1996; Baker 2010; Tadesse et al. 2018), which may mask male-specific hits. Of the sex-specific gametocyte screens, most rely on gametocyte activation markers (Delves et al. 2013; Miguel-Blanco et al. 2015). These do not distinguish between activation blocking and gametocyte killing compounds, however the Medicines for Malaria Venture favours gametocyte-killing compounds since their application is considered more feasible (Burrows et al. 2017). Ruecker et al. (2014) combine a sex-specific activation assay with a non sex-specific gametocyte-killing assay to infer sex-specific gametocyte-killing compounds. However, a more straightforward technique to screen gametocyte-killing compounds in a sex-specific manner is lacking.

A screen of 20 compounds identified more transmission-blocking candidates targeting males rather than females, but no female-specific drugs (Delves et al. 2013). Antifolates and endoperoxides inhibit male gamete exflagellation but not female gamete P25 (ookinete surface protein (PF3D7\_1031000)) expression (Delves et al. 2013). The tested antifolates pyrimethamine and cycloguanil likely inhibit male gamete activation by blocking folate mediated pyrimidine synthesis required for exclusively male DNA replication. The mechanism of action of endoperoxides in male gametocytes is unclear. Male gametocytes are predicted to develop drug resistance mechanisms faster than females given male-specific genes evolve faster (Khan et al. 2013). While killing one sex of gametocyte would be sufficient to sterilise the parasite and block transmission, it would be safer to target both gametocytes, potentially with a combination of compounds to reduce the risk of resistance developing.

An alternative drug development strategy involves the rational design of compounds targeted to essential, parasite-specific functions. This requires a detailed understanding of the molecular traits of the organism of interest. The sex-specific transcriptome and proteome of gametocytes is now established (Tao et al. 2014; Lasonder et al. 2016; Miao et al. 2017; Reid et al. 2018; Walzer et al. 2018), but metabolomics evidence is limited to combined male and female gametocytes (MacRae et al. 2013; Lamour et al. 2014; Gulati et al. 2015; Tran et al. 2016). These studies are an important resource for the development of sex-specific markers and for the design of gametocyte-killing compounds.

The identification of the male and female transcriptome and proteome mostly relied on the ability to separate large numbers of male and female gametocytes. Tao et al. (2014) predicted the sex-specific proteome prior to the advent of sex-specific markers in part by subtracting the proteome of non-gametocyte-producing *P. falciparum* strain Dd2 from that of the gametocyte-producing strain NF54. Lasonder et al. (2016) established the sex-specific proteome from two independent *P. falciparum* cell lines, each with a sex-specific marker (dynein heavy chain PF3D7\_1023100 for males and female marker P47, PF3D7\_1346800). Both of these markers were tagged in the same cell line to determine the sex specific transcriptome (Lasonder et al. 2016). Surprisingly the authors observed parasites expressing both the male and female markers, casting doubt on the validity of these markers. Another sex-specific proteome was published soon afterwards by Miao et al. (2017) using alpha tubulin II expression to distinguish male and female gametocytes. Initially considered a male

specific gametocyte marker (Rawlings et al. 1992), it was later observed at low levels in female gametocytes (Schwank et al. 2010). Most recently single cell transcriptomics further refined our understanding of the sex-specific transcriptome (Reid et al. 2018; Walzer et al. 2018). In the Reid et al. (2018) study, *P. falciparum* and *P. berghei* sex-specific transcriptomes are inferred from existing bulk population sex-specific transcriptomes (Lasonder et al. 2016). In Walzer et al. (2018), the expression of 87 previously annotated gametocyte-specific genes were measured by multiplex qRT-PCR from single gametocytes. This report also found that dynein heavy chain (used as a male marker in Lasonder et al. (2016)) was present in both male and female gametocytes. Overall, multiple strategies have contributed to our understanding of the sex-specific biology of male and female gametocytes, each more or less hinging on tagging a sex-specific gene.

The ability to separate male and female gametocytes has also enriched the available sex-specific molecular markers to monitor gametocyte sex ratio in the field or in the lab by qRT-PCR. Initially *pfs25* was routinely used as a generic gametocyte marker, however it was later found to be highly enriched in female gametocytes (Schneider et al. 2015; Lasonder et al. 2016). Male markers were subsequently included in the sex-specific gametocyte measurements (Stone et al. 2017; Santolamazza et al. 2017; Meerstein-Kessel et al. 2018; Roth et al. 2018; Graumans et al. 2019). Ultimately, a reliable means of measuring male and female gametocyte density and sex ratio may predict the transmissibility of the parasite, currently measured by expensive membrane feeding assays (Tadesse et al. 2018).

In this chapter a novel FACS-based method is established for the separation and collection of male and female *P. falciparum* gametocytes that express an exclusively female GFP tag (Tran et al. 2014). The purity measurements of male and female populations monitored by FACS, Giemsa-stained thin smears and live cell fluorescence microscopy are presented. The sorting strategy is also confirmed by measuring the expression of validated sex-specific markers and asexual transcripts by qRT-PCR in collected populations. The method is finally applied to validate three novel sex-specific gametocyte markers for qRT-PCR.

## **Results**

Asexual *P. falciparum* with GFP tagged gABCG2 (Tran et al. 2014) was cultured as described previously (Maier & Rug 2013) and induced to form gametocytes as per Fivelman et al. (2007) with modifications to reduce asexual parasite proliferation. Briefly, synchronous asexual parasites were stressed over 48 h by increasing culture parasitemia and only partial removal of spent culture medium. Stressed rings, including rings committed to gametocytogenesis, were sorbitol synchronised (Lambros & Vanderberg 1979) and enriched by removing pigment containing mature asexual parasites and mature gametocytes with a magnet. The following day, the culture was treated with sorbitol to eliminate asexual parasites. From this day onwards, the culture medium was replaced daily and supplemented with 50 mM N-acetyl-D-glucosamine to inhibit asexual re-invasion of RBC (Gupta et al. 1985). Two days prior and the day before FACS, the culture was treated with sorbitol to eliminate asexual parasites. Gametocytes were magnet enriched the day before FACS to improve the sorting efficiency (i.e. increase the proportion of collected cells). In this study, gametocytes were collected 9 days after commitment (predominantly at stage IV). However, since the GFP signal is expressed from stage I onwards in a female-specific manner (Tran et al. 2014), gametocytes could also be sorted from 2 days after commitment.

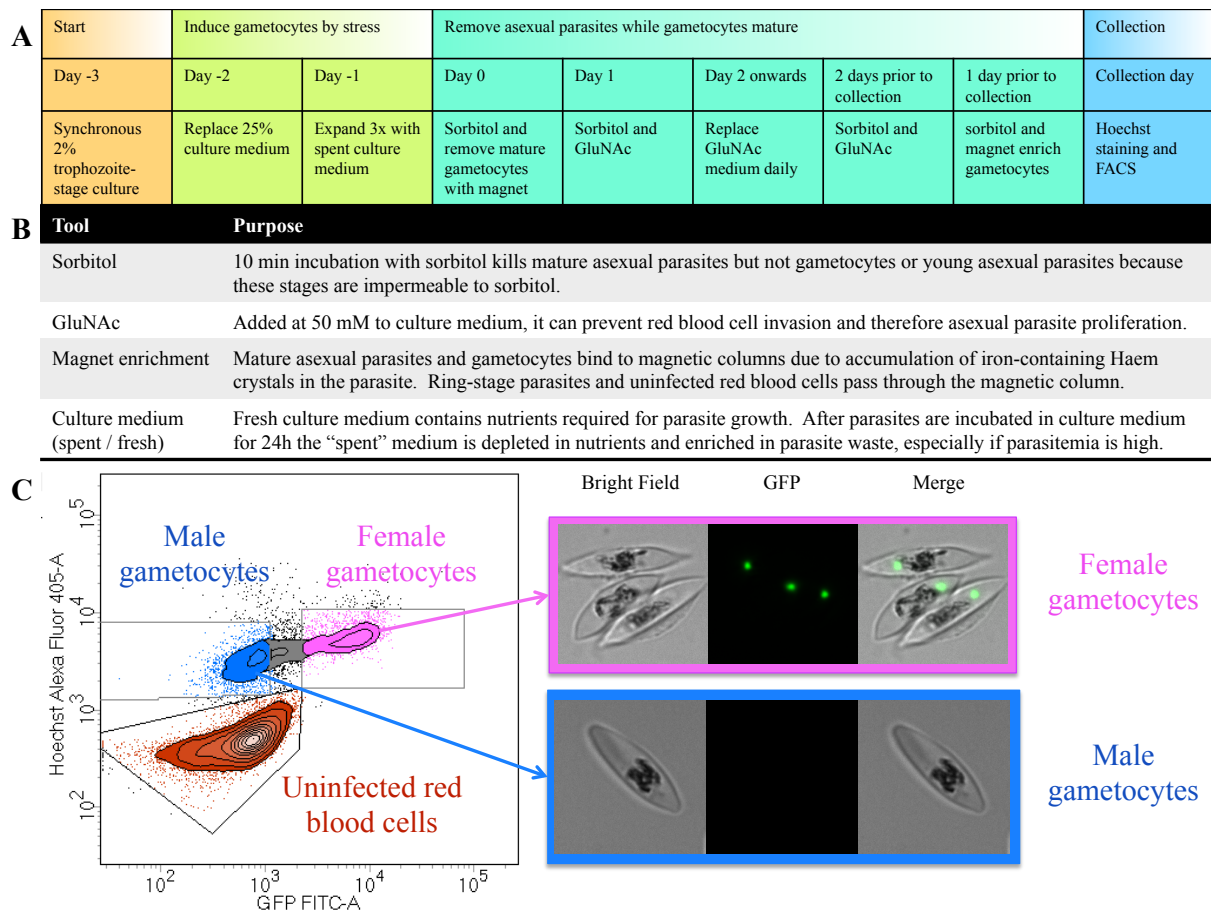


**Figure 1:** Generation and collection of male and female gametocytes. A) Timeline of gametocyte culturing technique with B) explanation of terms. C) Representative FACS gating strategy of male and female gametocytes (left) based on Hoechst 33342 staining detected in Alexa Fluor 405 channel and GFP signal detected in FITC channel. Live collected male and female gametocytes were imaged by restorative widefield deconvolution microscope detecting GFP fluorescence on FITC channel (right).

Gametocytes were stained with DNA stain Hoechst 33342 and sorted live at 37 °C on a BD FACS Aria I. After selecting single, whole cells based on forward and side scatter, gametocytes (Hoechst positive) were distinguished from uninfected RBC (Hoechst negative). Of the Hoechst positive gametocytes, only female gametocytes were GFP positive. Gates were drawn to favour sample purity over yield (Figure 1).



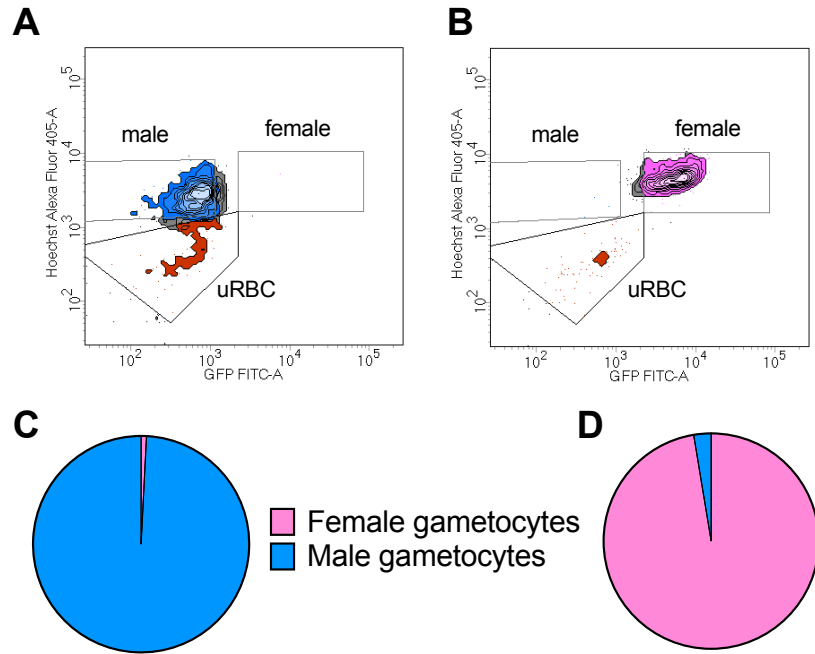


**Figure 2:** Quality controls of male/female sorting strategy. A and B: FACS plot of re-sorted male (A) and female (B) gametocyte populations showing cells re-sorted in female gate (pink), male gate (blue), uninfected red blood cell gate (red) or between gates (grey). C and D: Proportions of male population (C) or female population (D) re-sorted in female gate (pink) or male gate (blue) averaged from 39 independent experiments.

The purity of collected cells was assessed by FACS, Giemsa-stained thin smear and live cell fluorescence microscopy. Immediately after sorting, a fraction of the collected cells was re-sorted using the same gating strategy. In each population, over 80 % of the cells were re-sorted in the same gate with less than 1 % falling in the gate of the opposite sex (Figure 2). The other cells contained in each population were mostly Hoechst negative uninfected RBC. Giemsa-stained thin smear and live cell fluorescence microscopy confirmed the sorting strategy (Figure 1).

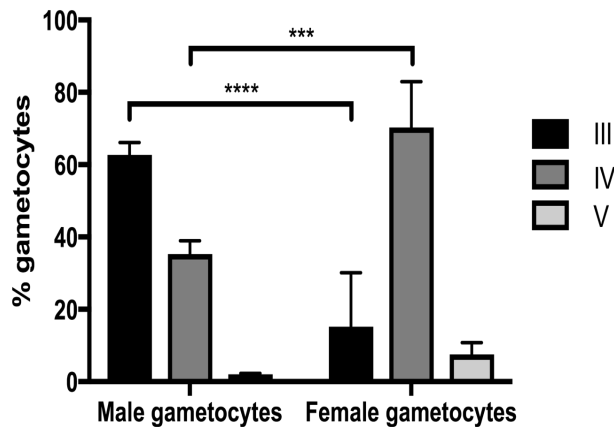


**Figure 3:** Gametocyte stage in sorted male and female populations on day 9 post commitment. Following FACS, the male and female gametocyte stage was determined from a Giemsa-stained thin smear. Mean and standard deviation from three biological repeats with results from two-way ANOVA is indicated as follows: \*\*\*\*:  $p < 0.0001$ ; \*\*\*:  $p = 0.001$ .

The stage of gametocytes in each sorted population was determined by Giemsa-stained thin smear. Gametocytes mature through five morphologically defined stages, stage V being the most mature (Hawking et al. 1971; Sinden 1982; Alano 2007), identified here as follows. Stage V gametocytes have characteristic rounded extremities whereas stage IV and III gametocyte ends are pointed. In addition, stage IV gametocytes are more elongated and thinner than stage III gametocytes. Surprisingly, the average age of gametocytes after FACS on day 9 post commitment to gametocytogenesis was different between male and female populations. Stage-specific counting of Giemsa-stained thin smears suggests gametocytes in the female sample are predominantly at stage IV while the gametocytes in the male sample are split between stage III and IV (Figure 3).

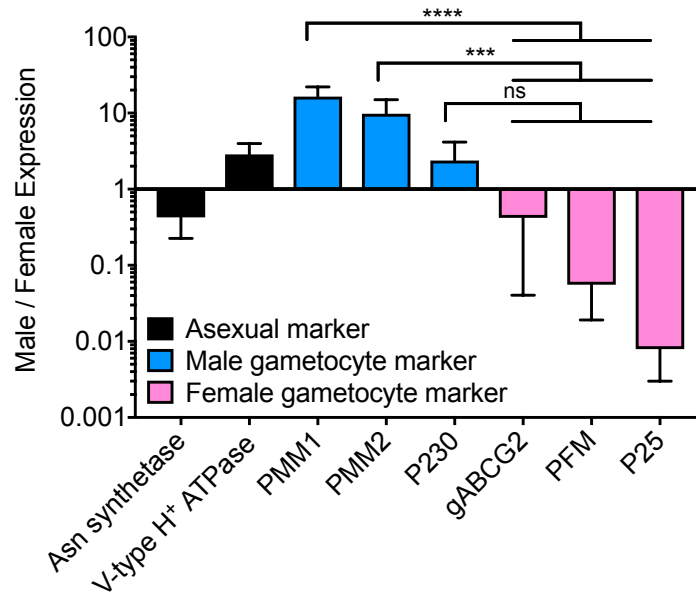


**Figure 4:** Male/female expression of asexual markers (black), male markers (blue) or female markers (pink) relative to reference gene PF3D7\_0317300 measured by qRT-PCR of male and female gametocyte populations collected by FACS. Relative target gene expression is calculated as follows from 4 technical repeats with E being the real-time PCR efficiency and CP being the crossing point, as initially proposed by Pfaffl (2001) and described in Material and Methods:

$$\text{Ratio} = (E_{\text{target}}^{\Delta\text{CP}_{\text{target}}(\text{female-male})}) / (E_{\text{ref}}^{\Delta\text{CP}_{\text{ref}}(\text{female-male})})$$

Asn synthetase: Asparagine synthetase -glutamine hydrolysing (PF3D7\_0309500); V-type H<sup>+</sup> ATPase: V-type proton ATPase catalytic subunit A (PF3D7\_1311900); PMM1 and 2: Putative Male Marker 1 (*Plasmodium* exported protein (PHISTa) PF3D7\_1477700) and 2 (PF3D7\_1438800); P230: 6 cysteine protein (PF3D7\_0208900); gABCG2: gametocyte ABC transporter G family member 2 (PF3D7\_1426500); PFM: Putative Female Marker (PF3D7\_1447600); P25: ookinete surface protein (PF3D7\_1031000).

To further validate the sorting strategy, the expression of known sex-specific gametocyte markers (*pfs230p* for males; *gabcg2* and *pfs25* for females) were measured by qRT-PCR in the collected populations (Figure 4). After normalisation to the reference gene PF3D7\_0317300 selected based on transcriptome data (López-Barragán et al. 2011; Lasonder et al. 2016), there was no significant difference in the male/female gametocyte expression of male marker *pfs230p* and either female marker.

Given that this result contradicts the microscopy observations, the relative expression of asexual, male gametocyte and female gametocyte transcripts was measured by qRT-PCR in the sorted gametocyte populations (Figure 4). These novel markers were selected based on transcriptome data (López-Barragán et al. 2011; Lasonder et al. 2016). Asexual transcript abundance was similar in male and female gametocyte populations, as expected. In addition,

the expression of both male markers was significantly higher than that of established and putative female markers in the male population relative to the female population. Together these results support the sorting strategy.

### **Discussion**

The ability to separate male and female gametocytes paves the way for the investigation of the sex-specific biology of *P. falciparum* gametocytes. In this chapter a method for the separation of male and female gametocytes was established and applied to validate three novel sex-specific markers.

The method to separate male and female gametocytes offers an alternative to published methods. Unlike in the proteomics study by Lasonder et al. (2016), but similar to the Miao et al. (2017) method, male and female gametocytes were sourced from the same culture. This is especially advantageous for the study of highly variable traits such as metabolism, or high throughput drug screens.

The female marker used in this study, gABCG2 originally described by Tran et al. (2014), has been independently validated as highly female enriched (Lasonder et al. 2016; Miao et al. 2017). The sex-specificity of the markers used by Lasonder et al. (2016) by contrast is somewhat dubious (Lasonder et al. 2016; Walzer et al. 2018). In Miao et al. (2017) a differentially expressed, rather than a sex-specific gene is tagged for sex separation by FACS (Schwank et al. 2010) but the purity data presented in the paper is convincing. Ultimately, the use of multiple sex-specific markers to study gametocytes is an excellent means of crosschecking existing sex-specific datasets. In addition, alternative markers could be used as a control for sex-specific studies, especially when the function of the marker and the possible functional impact of tagging the marker are unknown.

One limitation of the technique described in this chapter is the lack of a male specific marker. In this method male gametocytes are defined as Hoechst positive but GFP negative. This would also be the fluorescence profile of any asexual stage parasites, hence the additional sorbitol and magnet purification steps to remove asexual parasites prior to FACS. While the purity counts described in this chapter suggest the proportion of asexual parasites is minimal, the Miao et al. (2017) method of excluding asexual parasites by FACS is much more

straightforward. Ideally the gABCG2 female GFP tag would be used in conjunction with a male specific tag fluorescing at a separate wavelength. For example, the Putative Male Marker 1 (*Plasmodium* exported protein (PHISTa) PF3D7\_1477700) confirmed by qRTPCR in this chapter could be tagged with mCherry in the gABCG2-GFP parasite line.

As described here, the collected male and female gametocytes are appropriate for both large data type analysis or medium throughput screening. The main limitation to using this method for high throughput applications is the laborious culturing of gametocytes and their time-consuming magnet purification. A semi-automated culturing system such as a Wave Bioreactor (Demanga et al. 2017) and an automated magnet purification similar to autoMACS Pro Separator (Miltenyi Biotec) but amenable to processing large volumes of culture would improve the labour cost of this method.

The observation that sorted male gametocytes appear less mature than female gametocytes (Figure 3) was surprising. This result highlights the advantage of collecting male and female gametocytes from the same culture and the power of a sex-specific marker expressed at all gametocyte stages. Sex-specific gametocyte maturation rates have previously been alluded to by Bounkeua et al. (2010) who observed mature male gametocytes from day 12 but female gametocytes only from day 14 post commitment. From an evolutionary point of view, this could be a means of avoiding self-fertilization since only stage V gametocytes are accessible to mosquitos (Aguilar et al. 2014) where fertilization takes place. These observations are indirect however, and the protocol could inadvertently be age biased. For example, mature male gametocytes could have been activated and excluded by FACS due to rapid DNA replication, thus more intense Hoechst 33342 staining. While this would account for the absence of stage V male gametocytes, it does not explain why there are more stage III than stage IV male parasites. Alternatively, since the fluorescence intensity of the gABCG2-GFP expression increases with gametocyte age, immature female gametocytes with low gABCG2-GFP expression may be included in the male population. This is unlikely, however, given the stringent gating strategy that excludes cells with low GFP intensity and the rigorous synchronisation of the culture immediately prior to gametocyte commitment. In general, gametocyte stages are subtle and were not counted blind. Ideally the Giemsa-stained thin smears would be re-counted blind by an independent experimenter. Further experiments are warranted to confirm this observation such as monitoring the expression of stage specific

markers in each sex during gametocytogenesis (Eksi et al. 2008) and confirming the sex of the gametocytes in each population with sex-specific antibodies.

RNA extracted from one biological repeat of collected male and female gametocytes appears to validate three novel sex-specific markers by qRT-PCR. Although alternative sex-specific markers exist, using a selection of sex-specific markers is the most reliable means of determining the sex ratio. The male/female expression of both putative male markers was significantly greater than that of established female markers *gabcg2* and *pfs25*, unlike previously described male marker *pfs230p*. The male markers identified in this study may be more appropriate for qRT-PCR detection of transcripts, whereas *pfs230p* is an established protein marker. The putative female marker also outperformed previously described female marker *gabcg2*, but not *pfs25*. Further biological repeats are required to confirm these observations and the function of these novel sex-specific markers warrants further investigation.

Ultimately a better understanding of the sex-specific biology of gametocytes gleaned from the analysis of gametocytes separated using this method could lead to better malaria transmission blocking strategies in the field.

## Part 2

### Sex-specific DNA methylation in *P. falciparum*

#### Introduction

The mechanism of sex determination in *Plasmodium* is only partially understood. In the asexual cycle preceding the formation of gametocytes, all merozoites from a given schizont form gametocytes of the same sex (Bruce et al. 1990). This observation implies that the decision to commit to gametocytogenesis and sex determination occurs in the asexual cycle preceding formation of gametocytes. Gametocytogenesis requires activation of the transcription factor gene *ap2-g* (activating enhancer binding protein 2 gamma, PF3D7\_1222600) (Kafsack et al. 2014; Sinha et al. 2014) that is silenced epigenetically during asexual blood stage replication (Brancucci et al. 2014; Coleman et al. 2014). Given that *ap2-g* induces transcription of numerous sex-specific markers (Yeoh et al. 2017; Painter et al. 2017) and the sex ratio of induced gametocytes is not impacted by the timing of *ap2-g* overexpression (Kent et al. 2018), sex determination likely occurs concurrently with or upstream of *ap2-g* expression.

Recent studies in *P. berghei* suggest that *ap2-g* overexpression can induce gametocytogenesis in the same developmental cycle up to 12 hpi (Kent et al. 2018). This could be due to significant differences between *P. berghei* and *P. falciparum* gametocytogenesis, or it could indicate that asexual parasites in the cycle prior to gametocytogenesis are predisposed but not irreversibly committed to form gametocytes or schizonts until 12 hpi in the same developmental cycle. The “predisposition” to form gametocytes could result from environmental queues (Brancucci et al. 2017) or epigenetic pre-programming (Brancucci et al. 2014; Filarsky et al. 2018). In this section DNA methylation, an epigenetic marker, is explored as a possible means of predisposing asexual parasites to gametocytogenesis and gametocyte sex determination.

The function of DNA methylation in other organisms is variable and has been reported in genes and regulatory regions. In mammalian cells, methylation of cytosine-guanine (CpG) islands that usually overlap with the gene promoter regions are involved in stable gene repression, notably for X inactivation (Jaenisch & Bird 2003) and genomic imprinting (Li et al. 1993). Otherwise the impact of methylation on gene expression in mammalian cells is variable and likely context-specific (Schübeler 2015). For example, cytosine methylation in

human transcription factor binding sites impacts transcription factor affinity, but not necessarily negatively as previously thought (Yin et al. 2017). The role of intra-genic DNA methylation is also unclear. It has been proposed to play a role in stabilising chromatin by countering RNA polymerase displacement of nucleosomes, suppressing intragenic promoters (Maunakea et al. 2010) or regulating alternative splicing (Maunakea et al. 2013).

In *P. falciparum* evidence of nucleic acid methylation is conflicting. Recently *P. falciparum* transfer ribonucleic acid (tRNA) Aspartic Acid DNA methyltransferase 1, a conserved homologue of DNA methyltransferase 2, was shown to methylate aspartic acid tRNA at cytosine 38, but not the encoding DNA *in vitro* (Govindaraju et al. 2017). Although DNA cytosine methylation was not observed by Choi et al. (2006) in *Plasmodium* or by Gissot et al. (2008) in other apicomplexan parasites, other studies identified cytosine methylation in *P. falciparum* by restriction enzyme digest (Pollack et al. 1991) and by mass spectrometry (Ponts et al. 2013), and at low levels in other apicomplexans by enzyme-linked immunosorbent assay (Gong et al. 2017). Given the genome of *P. falciparum* is one of the most AT rich genomes sequenced to date (Gardner et al. 2002), cytosine methylation is likely rare and only detectable with the most sensitive techniques.

Whole genome bisulfite sequencing of mixed asexual blood stage *P. falciparum* suggests that 0.63 % of sequenced cytosines are methylated, 72 % of which are in exons (Ponts et al. 2013). Most methylation events were observed in less than a third of the reads, which the authors explain as stage-specific methylation (Ponts et al. 2013). Unlike in mammalian cells where methylation marks are mostly stable, it appears that the relatively few methylation events in *P. falciparum* DNA are *de novo*, stage-specific methylations. However, a third of the cytosines in the genome were not sequenced in this study even with a very low minimum coverage threshold: the current standard sequencing depth in the Epigenomics Roadmap is at least five times that of the Ponts et al. (2013) study. Current sequencing technology could increase the genome coverage and sequencing depth to improve the reliability of the existing map of cytosine methylation in *P. falciparum*.

Although epigenetic regulation may play a role in gametocytogenesis and/or sex-determination in *P. falciparum*, the role of DNA methylation in these developmental milestones has not been investigated. Here the FACS method described above is applied to collect male and female stage IV-V gametocytes for whole genome bisulfite sequencing. In



addition, synchronised trophozoite stage parasite DNA is bisulfite sequenced. The preliminary results from two biological repeats presented below focuses on stage-specific intragenic methylation events deduced from the whole genome methylation map of male gametocytes, female gametocytes and mature asexual blood stage *P. falciparum*. Ongoing bisulfite sequencing of additional biological repeats and confirmation of methylation sites by restriction enzyme digest will determine whether these preliminary results are statistically robust.

## Results

To determine the sex and stage-specific DNA methylation pattern in *P. falciparum*, DNA from two biological repeats of trophozoite stage asexual parasites, male gametocytes and female gametocytes was bisulfite sequenced. Unmethylated  $\lambda$  phage DNA was added to each sample to control for sequencing errors misinterpreted as bisulfite conversions.

### 1. Overview of DNA methylation in *Plasmodium*

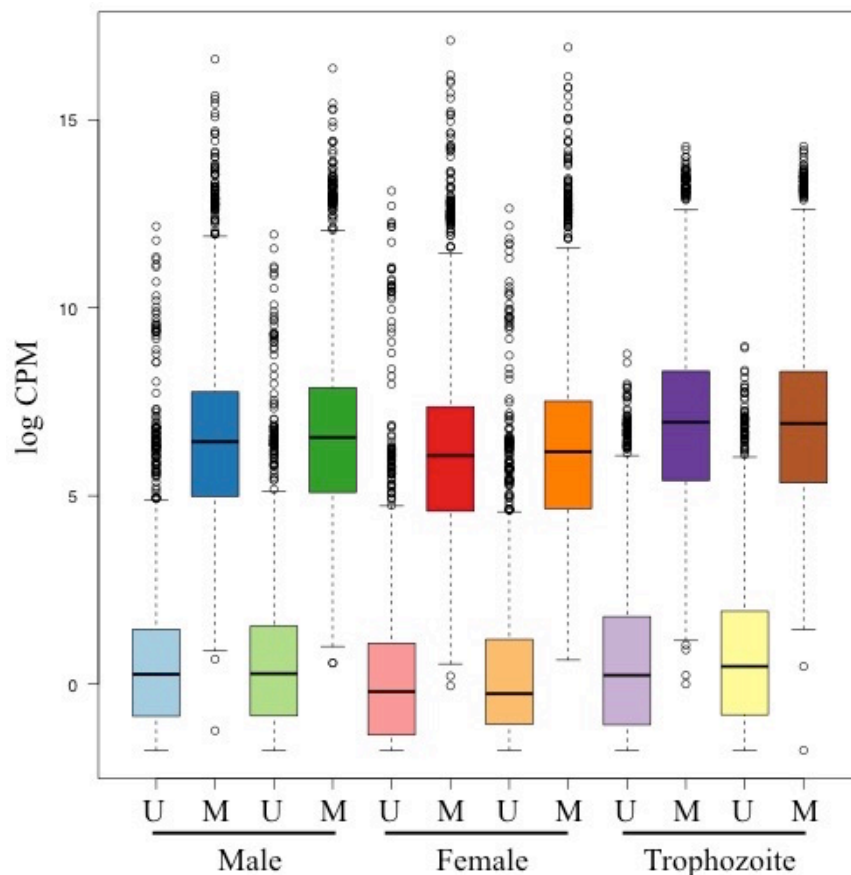


**Figure 1:** Box plot of methylated cytosine counts per million (CPM) in two biological repeats of unsequenced  $\lambda$  phage DNA (U) and bisulfite converted methylated DNA (M) from at least 25 million male gametocytes (Male), female gametocytes (Female) and trophozoites.

DNA methylation was detected at all measured parasite stages in 1-3 % of CpG contexts (Figure 1). Control unmethylated  $\lambda$  phage DNA had less than 0.5 % methylation calls, suggesting the observed methylation events were not sequencing errors. DNA methylation rates are similar in all blood stage parasites measured in this experiment, indicating that gametocytogenesis and sex determination is not the result of a major switch in DNA methylation status.

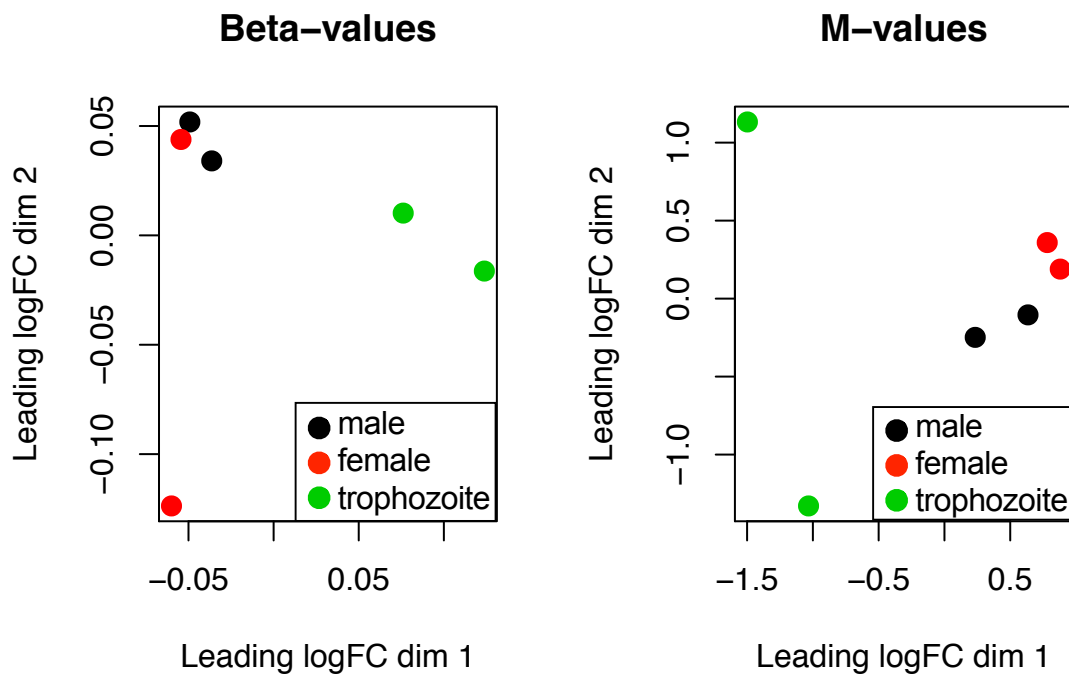


**Figure 2:** Multi-dimensional scaling plot of  $M = \log_2(M/U)$  and  $\beta = M/(M+U)$  values, with  $M$  = methylated cytosines and  $U$  = unmethylated cytosines. The leading log-fold change (FC) is the average log-fold change between the most differentially methylated CpG loci between two samples. Male gametocyte samples are represented in black, female gametocytes in red and trophozoites in green.

While overall methylation counts may not be indicative of parasite stage or sex, specific methylation events may distinguish each sample. The methylation level of a given cytosine is expressed as  $M = \log_2(M/U)$  and  $\beta = M/(M+U)$  values, with  $M$  being the count of methylated cytosines and  $U$  the number of unmethylated cytosines. The leading fold change is the most differentially methylated CpG loci between two samples. In the first dimension of the multi-dimensional scaling plot of the leading  $M$  and  $\beta$ -values, asexual trophozoite samples are clearly distinguished from either gametocyte sex, however male and female gametocytes are grouped together (Figure 2). This suggests that the most differentially methylated CpG loci

among these samples identifies gametocytes from asexual parasites, but not in a sex-specific manner. The second dimension of the multi-dimensional scaling plot of leading M and  $\beta$ -values separates biological replicates of trophozoites and female gametocytes respectively. This suggests that some variation in the leading M and  $\beta$ -values is not related to the parasite lifecycle stage or gametocyte sex.

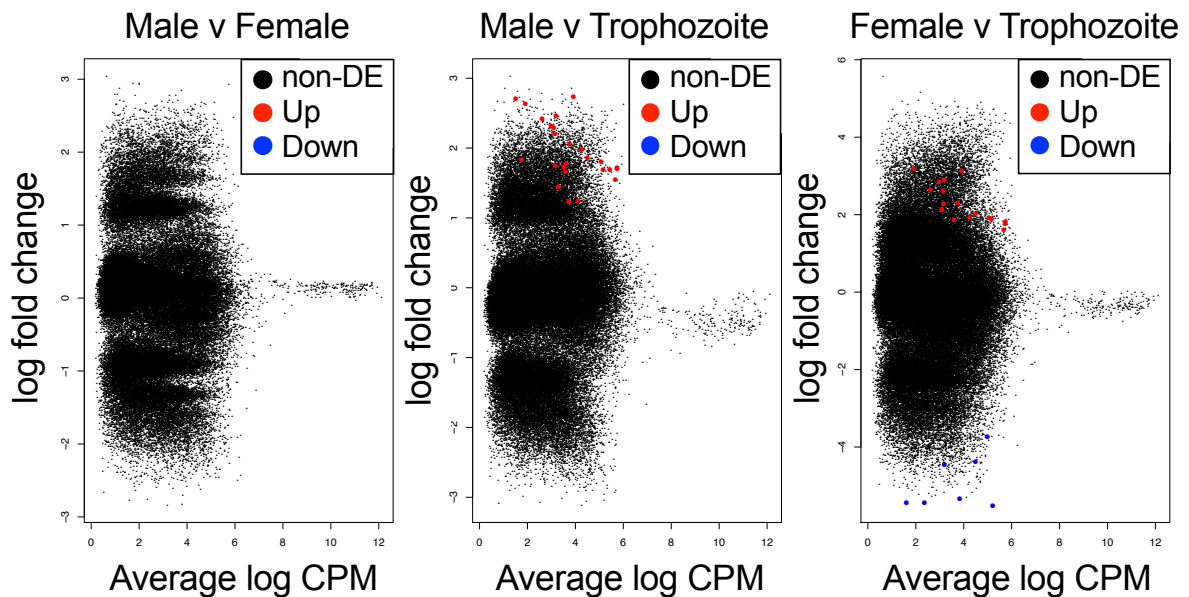


**Figure 3:** Mean – Difference plot of log fold change of the methylation level and average abundance of each CpG loci in log counts per million (CPM). Statistical significance ( $p < 0.001$ ) was calculated using likelihood ratio tests in *edgeR* with Benjamini-Hochberg multiple testing correction to control the false discovery rate (Chen et al. 2017). Blue indicates significantly down methylated sites, red significantly upregulated loci, black indicates non-differentially expressed (non-DE) genes.

Investigation of the individual CpG loci suggests that methylation of most cytosines is infrequent with an average log counts per million below 6, i.e. methylation was observed in less than 1 % of cases (Figure 3). A large proportion of these sites appear to be variably methylated between samples, however only a subset are statistically robust changes between samples. The variation between biological repeats revealed in Figure 2, and the fact that only two biological repeats are analysed here may explain the lack of statistically significant differentially methylated CpG loci. The most frequently methylated sites are stably methylated in trophozoites, male gametocytes and female gametocytes.

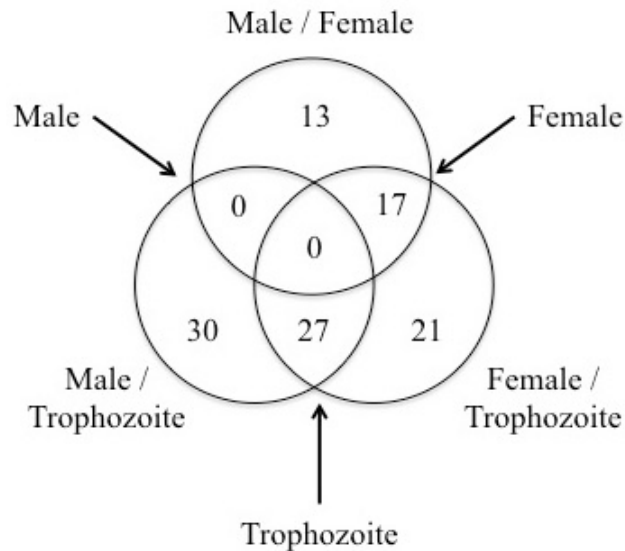


**Figure 4:** Venn diagram of differentially methylated genes between male gametocytes, female gametocytes and trophozoites.

The differentially methylated loci were mapped to the annotated 3D7 strain *P. falciparum* reference genome to identify differentially methylated genes between the samples. Differential methylation ( $p < 0.001$ ) was observed in 30 genes between male and female gametocytes, in 65 genes between female gametocytes and trophozoites and in 57 genes between male gametocytes and trophozoites (Figure 4). Of these, 27 genes distinguished trophozoites from both male and female gametocytes and 17 genes were characteristic of female gametocytes in comparison to both male gametocytes and trophozoites. No genes were consistently differentially methylated in male gametocytes compared to the other samples. Together this suggests that intragenic DNA methylation distinguishes asexual from sexual blood stages, and characterises female gametocytes among the samples of this study.

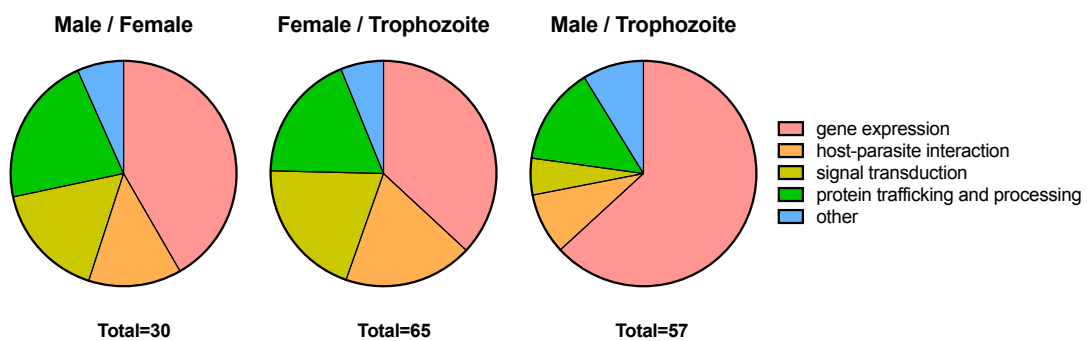


**Figure 5:** Functions of differentially methylated genes in each two-way comparison of male gametocytes, female gametocytes and trophozoites.

Most differentially methylated genes are functionally related, as determined by their gene annotation or homology to characterised genes (Figure 5). In all two-way comparisons

between male gametocytes, female gametocytes and trophozoites, most intragenic differential methylation targets genes involved in gene expression. Genes involved in signal transduction, host-parasite interaction and protein trafficking and processing also appear to be differentially methylated. Three genes differentially methylated between male and female gametocytes have two functional annotations: PF3D7\_1420500 and PF3D7\_0825900 (gene expression and signal transduction), and PD3D7\_1006700 (gene expression and protein trafficking). Overall, it appears that stage and sex-specific DNA methylation targets genes involved in important cellular processes, especially gene expression, that could have important downstream effects on the stage and sex-specific biology of *Plasmodium*. The specific genes differentially methylated between trophozoites and gametocytes, and between gametocyte sexes are presented below.

## **2. Genes targeted by gametocyte-specific DNA methylation**

Between female gametocytes and trophozoites there were 25 differentially methylated genes with  $p < 0.0001$  and 65 genes with  $p < 0.001$  (Table 1). Comparison of male gametocyte DNA methylation with that of trophozoites highlights 23 differentially methylated genes with  $p < 0.0001$  and 57 genes with  $p < 0.001$  (Table 2). Many apicoplast and mitochondrial genome genes were differentially methylated in gametocytes compared to asexual trophozoite stage *P. falciparum*.

**Table 1:** Differentially methylated genes between female gametocytes and asexual trophozoite stage parasites. Genes are listed in order of statistical significance in each functional category. Bold indicates significant differences with  $p < 0.0001$ , otherwise  $p < 0.001$ .

Function	Gene ID	Characterised gene name and description
Gene translation	<b>PF3D7_API00600</b>	tRNA Methionine
	<b>PF3D7_API00900</b>	tRNA Aspartic acid
	<b>PF3D7_API01100</b>	tRNA Glutamic acid
	<b>PF3D7_API02900</b>	elongation factor Tu
	<b>PF3D7_API01000</b>	tRNA Lysine
	<b>PF3D7_API04700</b>	FeS cluster assembly protein SufB
	<b>PF3D7_API05900</b>	small subunit ribosomal RNA
	<b>PF3D7_API00800</b>	tRNA Serine
	<b>PF3D7_1431000</b>	mitochondrial ribosomal protein L17-2 precursor
	<b>PF3D7_1204000</b>	PBLAST homolog of U3 small nucleolar RNA associated protein 11
	PF3D7_0729300	60S ribosomal export protein nonsense-mediated mRNA 3
	PF3D7_1024400	GO term: RNA binding, endonuclease activity
	PF3D7_0509600	asparagine-tRNA ligase
	PF3D7_1359400	CUG triplet repeat RNA-binding protein Elav-like family member 1, GO term: RNA binding
Gene transcription	<b>PF3D7_0404100</b>	AP2 domain transcription factor AP2-SP2
	<b>PF3D7_0509300</b>	GO term: nuclear localisation
	<b>PF3D7_API04300</b>	DNA-directed RNA polymerase subunit $\beta$
	PF3D7_1367400	PBLAST homolog of signal transducer and activator of transcription B and type 2 histone deacetylase
	PF3D7_1413000	PBLAST homolog of putative mediator or RNA polymerase II transcription subunit 24 and GATA zinc finger DNA binding domain-containing protein 14
	PF3D7_0917400	PBLAST homolog of PfSET1 histone lysine N-methyltransferase
	PF3D7_0307900	PBLAST homolog of PfSET1 histone lysine N-methyltransferase
	PF3D7_1325800	PBLAST homolog of PfSETvs, var gene silencing histone lysine N-methyltransferase
	PF3D7_1354100	PBLAST homolog of homeobox protein 2 and putative mediator of RNA polymerase II transcription subunit 24
	PF3D7_0620300	PBLAST homolog of DNA directed RNA polymerase subunit $\beta$
	Host-parasite interaction	<b>PF3D7_1150100</b>
<b>PF3D7_0518900</b>		Predicted adhesin
<b>PF3D7_0402300</b>		reticulocyte binding protein homologue 1
PF3D7_0711900		repetitive interspersed family protein (RIFIN)
PF3D7_1035300		glutamate-rich protein (GLURP), immunogenic
PF3D7_0104000		thrombospondin-related sporozoite protein, required for hepatocyte invasion (Labaied et al. 2007) or not (Costa et al. 2018)
PF3D7_1229400		macrophage migration inhibitory factor
PF3D7_1038400		gametocyte-specific protein, role in rupture of host RBC during gamete egress.
PF3D7_1335400		reticulocyte binding protein 2 homologue a
PF3D7_0307900	PBLAST homolog of reticulocyte binding protein	

Signal transduction	<b>PF3D7_1404600</b>	adenylyl cyclase $\alpha$
	<b>PF3D7_1420500</b>	PBLAST homolog of hybrid signal transduction histidine kinase M
	<b>PF3D7_0628500</b>	4 phosphorylation sites, ATP binding
	PF3D7_1223100	Cyclic adenosine monophosphate-dependent protein kinase regulatory subunit
	PF3D7_0109600	cold-shock protein
	PF3D7_0902200	serine/threonine protein kinase, FIKK family
	PF3D7_1413000	PBLAST homolog of probable cyclin-dependent serine/threonine-protein kinase
	PF3D7_0937200	lysophospholipase
	PF3D7_0501100	heat shock protein 40, type II
	PF3D7_0526700	PBLAST homolog of two serine/threonine kinases
	PF3D7_0919800	TLD domain-containing protein, PBLAST homolog of serine/threonine kinase and signal transduction histidine kinase A
	PF3D7_1201500	Xeroderma Pigmentosum complementation group A binding protein 1, GPN-loop guanosine triphosphatase
	PF3D7_1354100	PBLAST homolog of probable cycline-dependent serine/threonine-protein kinase
Protein trafficking and processing	<b>PF3D7_1337700</b>	GO term: part of myosin complex, ATP binding/ actin binding/motor activity
	<b>PF3D7_1324700</b>	soluble N-ethylmaleimide sensitive fusion protein attachment protein receptor (SNARE) protein
	<b>PF3D7_0316900</b>	E3 ubiquitin-protein ligase
	<b>PF3D7_0919300</b>	thioredoxin-like protein 1, Part of microtubule associated complex in <i>T. gondii</i> (Jun Liu et al. 2013)
	<b>PF3D7_1447600</b>	Contains signal peptide and transmembrane domain
	PF3D7_1468300	leucine-rich repeat protein, protein binding
	PF3D7_0828400	mitochondrial oxidase assembly protein 1
	PF3D7_1126700	autophagy-related protein 23
	PF3D7_1355600	Photosensitised INA Labelled protein 1 interacting protein 1, Role in membrane trafficking in gametocytes (Parkyn Schneider et al. 2017)
	PF3D7_1006700	GO term: vesicle mediated transport
	PF3D7_1344900	Structurally similar to <i>P. falciparum</i> and <i>Staphylococcus aureus</i> peptidases
PF3D7_0528700	peptidyl-prolyl cis-trans isomerase	
Mitochondrial respiration	PF3D7_0915000	type II NADH:ubiquinone oxidoreductase
	PF3D7_1345700	isocitrate dehydrogenase [NADP], mitochondrial
Other	PF3D7_0715900	cation diffusion facilitator family protein, GO term: zinc transmembrane transporter
	PF3D7_0321300	Almost exclusively expressed in female stage V gametocytes.

**Table 2:** Differentially methylated genes between male gametocytes and asexual trophozoite-stage parasites. Genes are listed in order of statistical significance in each functional category. Bold indicates significant differences with  $p < 0.0001$ , otherwise  $p < 0.001$ .

Function	Gene ID	Characterised gene name and description
Gene translation	<b>PF3D7_API00600</b>	tRNA Methionine
	<b>PF3D7_API00900</b>	tRNA Aspartic acid
	<b>PF3D7_API01100</b>	tRNA Glutamic acid
	<b>PF3D7_API02900</b>	elongation factor Tu
	<b>PF3D7_API04700</b>	FeS cluster assembly protein SufB
	<b>PF3D7_API01000</b>	tRNA Lysine
	<b>PF3D7_API06700</b>	large subunit ribosomal RNA
	<b>PF3D7_API00800</b>	tRNA Serine
	<b>PF3D7_API05900</b>	small subunit ribosomal RNA
	<b>malmito_rna_RNA5</b>	ribosomal RNA fragment RNA5
	<b>malmito_rna_24</b>	ribosomal RNA fragment RNA24t
	<b>malmito_rna_RNA6</b>	ribosomal RNA fragment RNA6
	<b>malmito_rna_1</b>	ribosomal RNA fragment RNA1
	<b>malmito_SSUB</b>	small subunit ribosomal RNA fragment B
	<b>malmito_rna_RNA4</b>	ribosomal RNA fragment RNA4
	<b>malmito_rna_RNA18</b>	ribosomal RNA fragment RNA18
	<b>PF3D7_0729300</b>	60S ribosomal export protein nonsense-mediated mRNA 3
	mal_rna_19	ribosomal RNA fragment RNA19
	malmito_rna_SSUF	small subunit ribosomal RNA fragment F
	PF3D7_1431000	mitochondrial ribosomal protein L17-2 precursor
	PF3D7_1359400	CUG triplet repeat RNA-binding protein Elav-like family member 1, GO term: RNA binding
	malmito_rna_26	ribosomal RNA fragment RNA26t
	malmito_rna_10	ribosomal RNA fragment RNA10
	malmito_rna_LSUC	large subunit ribosomal RNA fragment C
	PF3D7_0211900	pseudouridine synthase, putative, GO term: RNA binding and modifying
	PF3D7_0808500	<i>Plasmodium</i> RNA of unknown function 6
	malmito_rna_16	ribosomal RNA fragment RNA16
	mal_rna_14	large subunit ribosomal RNA fragment A
	mal_mito_RNA19	ribosomal RNA fragment RNA8
	malmito_rna_LSUG	large subunit ribosomal RNA fragment G
malmito_rna_RNA22	ribosomal RNA fragment RNA22	
PF3D7_1022000	RNA-binding protein	
Gene transcription	<b>PF3D7_API04300</b>	DNA-directed RNA polymerase subunit $\beta$
	PF3D7_0419000	PBLAST homolog of coiled-coil domain proteins, generally regulators of gene transcription (transcription factors)
	PF3D7_0822800	U5 small nuclear ribonucleoprotein 40 kDa protein
	PF3D7_0620300	PBLAST homolog of DNA-directed RNA polymerase subunit $\beta$
Mitochondrial respiration	<b>mal_mito_3</b>	cytochrome b
	<b>PF3D7_0915000</b>	type II NADH:ubiquinone oxidoreductase
	PF3D7_1345700	isocitrate dehydrogenase [NADP], mitochondrial



Host-parasite interaction	<b>PF3D7_0711900</b>	repetitive interspersed family protein (RIFIN)
	PF3D7_1036300	duffy binding-like merozoite surface protein 2
	PF3D7_0104000	thrombospondin-related sporozoite protein, Required for hepatocyte invasion (Labaied et al. 2007) or not (Costa et al. 2018)
	PF3D7_0620300	PBLAST homolog of reticulocyte binding protein
	PF3D7_1038400	gametocyte-specific protein, Role in rupture of host RBC during gamete egress
Protein trafficking and processing	<b>PF3D7_0316900</b>	E3 ubiquitin-protein ligase, putative
	<b>PF3D7_1337700</b>	GO term: part of myosin complex, ATP binding, actin binding, motor activity
	PF3D7_0919300	thioredoxin-like protein 1, putative, Part of microtubule associated complex in <i>Toxoplasma gondii</i> (Jun Liu et al. 2013)
	PF3D7_1355600	Photosensitised INA Labelled protein 1 interacting protein 1, proposed role in membrane trafficking in gametocytes (Parkyn Schneider et al. 2017)
	PF3D7_0724700	Structurally similar to <i>P. falciparum</i> and <i>Staphylococcus aureus</i> peptidases
	PF3D7_1302000	Erythrocyte membrane protein 1-trafficking protein
	PF3D7_0908800	mitochondrial carrier protein
Signal transduction	PF3D7_1342300	tetratricopeptide repeat protein, GO term: protein binding
	PF3D7_0628500	4 phosphorylation sites, ATP binding
	PF3D7_1223100	Cyclic adenosine monophosphate -dependent protein kinase regulatory subunit
Other	PF3D7_1201600	Never in mitosis gene A related kinase 3
	PF3D7_1148200	Unspecified product
	PF3D7_1208700	Unknown function

In comparing both female and male gametocytes to trophozoite stage asexual parasites (Tables 1 and 2), the most significantly different methylation occurred in tRNA genes (methionine, asparagine, glutamic acid, lysine and serine). Other genes involved in translation were also differentially methylated between trophozoites and either gametocyte sex: small subunit ribosomal RNA PF3D7\_API05900, mitochondria ribosomal protein L17-2 precursor PF3D7\_1431000, 60S ribosomal export protein nonsense-mediated messenger RNA 3 PF3D7\_0729300 and FeS cluster assembly protein SufB PF3D7\_API04700. The latter is required for Fe-S cluster assembly, which are co-factors for many proteins including tRNA methyltransferase (Ralph et al. 2004). Specifically between trophozoites and female gametocytes (Table 1) Asparagine-tRNA ligase PF3D7\_0509600 and translational elongation factor Tu PF3D7\_API02900 were differentially methylated. Male gametocyte DNA methylation differed to that of trophozoites in the large subunit ribosomal RNA gene, an RNA binding protein PF3D7\_1022000 and 13 different genes in the mitochondrial genome encoding ribosomal RNA fragments (Table 2). These results suggest that gametocyte-

specific methylation may impact translation, especially in the parasite's apicoplast and the mitochondria.

Both male and female gametocyte DNA is differentially methylated in genes relating to mitochondrial respiration compared to asexual trophozoite-stage parasites. In particular PF3D7\_0915000, type II NADH:ubiquinone oxidoreductase and mitochondrial isocitrate dehydrogenase [NADP], PF3D7\_1345700, are differentially methylated between gametocytes and trophozoites. In addition, male gametocyte DNA is differentially methylated in mal\_mito\_3 encoding cytochrome b compared to trophozoites. Respiration may therefore differ in asexual and sexual blood stage *P. falciparum*, perhaps in relation to the unique host environment of each parasite stage.

Other gametocyte-specific DNA methylation patterns target genes involved in gene transcription, host-parasite interaction, signal transduction, protein trafficking and processing and ion homeostasis (Tables 1 and 2). PF3D7\_0321300 is an uncharacterised gene expressed almost exclusively in female gametocytes and differentially methylated between female gametocytes and trophozoites. In male gametocytes two genes of unknown function were differentially methylated compared to trophozoites: PF3D7\_1148200 and PF3D7\_1208700. The functional significance of these genes in the asexual to sexual blood stage transition warrants further investigation.

### **3. Genes targeted by sex-specific DNA methylation**

In comparing DNA methylation between male and female gametocytes, differential methylation was observed in 7 genes with  $p < 0.0001$  or 30 genes with  $p < 0.001$  (Table 3). Unlike the gametocyte-specific methylation described above, all of the genes methylated in a sex-specific manner are in the nuclear genome.

**Table 3:** Differentially methylated genes between male and female gametocytes. Genes are listed in order of statistical significance in each functional category. Bold indicates significant differences with  $p < 0.0001$ , otherwise  $p < 0.001$ .

Function	Gene ID	Characterised gene name and description
Signal transduction	<b>PF3D7_1420500</b>	PBLAST homolog of hybrid signal transduction histidine kinase M
	<b>PF3D7_1404600</b>	Adenylyl cyclase $\alpha$
	PF3D7_1104900	Calcium/calmodulin-dependent protein kinase
	PF3D7_1456400	PBLAST homolog of serine/threonine kinase
	PF3D7_1106800	Protein kinase
	PF3D7_0825900	PBLAST homolog of serine/threonine kinase
Gene expression	<b>PF3D7_0509300</b>	Nuclear localisation
	<b>PF3D7_0404100</b>	ApiAP2, transcription factor
	<b>PF3D7_0917400</b>	PBLAST homolog of PfSET1 histone lysine N-methyltransferase
	<b>PF3D7_1420500</b>	PBLAST homolog of Myb-like protein D, family of transcription factors
	<b>PF3D7_0725600</b>	18S ribosomal RNA
	PF3D7_1354100	PBLAST homolog of RNA polymerase II transcription subunit 24
	PF3D7_1235000	protein 1 interacting with heat shock protein 90 domain-containing protein, part of complex involved in RNA polymerase II assembly (Ahmad et al. 2013)
	PF3D7_1006700	PBLAST homolog of zinc finger containing protein, generally involved in DNA binding
	PF3D7_1131000	RNA binding protein s1
	PF3D7_0714500	Transcription elongation factor s-II
	PF3D7_1131400	PBLAST homolog of PfSET1 histone lysine N-methyltransferase
	PF3D7_1350900	AP2 domain transcription factor AP2-O4
	PF3D7_0825900	PBLAST homolog of zinc finger containing protein (DNA binding function)
	PF3D7_0609500	PBLAST homolog of plastid encoded RNA polymerase subunit $\beta$
Protein trafficking and processing	PF3D7_0826000	PBLAST homolog of proteases
	PF3D7_1032500	degradation-in-the-endoplasmic-reticulum-protein-1-like protein, part of the endoplasmic reticulum associated degradation complex that mediates protein transport to the apicoplast (Spork et al. 2009)
	PF3D7_1429800	Coatmer subunit $\beta$
	PF3D7_0828400	mitochondrial oxidase assembly protein 1
	PF3D7_1006700	GO term: vesicle mediated transport
	PF3D7_1324700	soluble N-ethylmaleimide sensitive fusion protein attachment protein receptor (SNARE) protein
	PF3D7_0902200	Serine/threonine protein kinase FIKK family, located in Maurer's cleft, role in GPI anchor biosynthesis
Host-parasite interaction	<b>PF3D7_1150100</b>	repetitive interspersed family protein (RIFIN) Type B (Joannin et al. 2008)
	PF3D7_1229400	Macrophage migration inhibitory factor
	PF3D7_1035300	Glutamate-rich protein (GLURP), immunogenic
	PF3D7_0518900	Predicted function: host-parasite adhesion (Ansari et al. 2008)
Ion homeostasis	PF3D7_0715900	Cation diffusion facilitator family protein, GO term: zinc transmembrane transporter
	PF3D7_1333800	Voldacs domain-containing protein, regulator of volume decrease after cellular swelling

Many differentially methylated genes between male and female gametocytes were associated with intracellular signalling (Table 3). Adenylyl cyclase (AC)  $\alpha$  is expressed in gametocytes (Muhia et al. 2003) and is fused with a potassium channel, potentially making it a voltage

sensitive AC that produces cyclic adenosine monophosphate in response to potassium conductance (Weber et al. 2004). AC $\alpha$  has many verified splice variants that may respond to different stimuli (Baker & Kelly 2004). Although uncharacterised, protein basic local alignment search tool (PBLAST) of PF3D7\_1420500 revealed homology to hybrid signal transduction histidine kinase M involved in phosphorelay signal transduction of osmotic stress response in *Arabidopsis* (Urao et al. 1999). Additional kinases are differentially methylated between male and female gametocytes with a lower statistical significance ( $p < 0.001$ ). These include Calcium/calmodulin-dependent protein kinase PF3D7\_1104900; protein kinase PF3D7\_1106800; PF3D7\_1456400 and PF3D7\_0825900 that are homologous to a serine/threonine kinases by PBLAST. Methylation of these genes may modulate the parasite's ability to respond to environmental signals.

Other differentially methylated genes between male and female gametocytes regulate gene expression *via* transcription modulation (Table 3). ApiAP2 PF3D7\_0404100 is a member of the same family of transcription factors as AP2-G, a key trigger for gametocytogenesis. PBLAST of uncharacterised PF3D7\_1420500 highlighted similarities to Myb-like protein D, a family of transcription factors previously described in *Plasmodium* (Gissot et al. 2005). PBLAST of uncharacterised PF3D7\_0917400 revealed homology to PfSET1, a histone lysine methyltransferase predicted to methylate H3K4 (Cui et al. 2008), a histone marker associated with transcription activation (Alvarez-Venegas & Avramova 2002; Santos-Rosa et al. 2002). PF3D7\_0725600 encodes ribosomal 18S RNA, whose abundance impacts overall transcription capacity. Uncharacterised PF3D7\_0509300 localises to the nucleus (Oehring et al. 2012), and may therefore impact gene expression. Genes differentially methylated between male and female gametocytes with less statistical significance ( $p < 0.001$ ) include another AP2 domain transcription factor, AP2-O4. PF3D7\_0825900 and PF3D7\_1006700 are homologous to zinc finger-containing proteins, generally involved in DNA binding. PF3D7\_1131400 is homologous to PfSET1 histone lysine methyltransferase, involved in epigenetic regulation of gene expression as described above. Sex-specific methylation of these genes may modify their expression, and thus impact the downstream DNA transcription in a sex-specific manner.

Sex-specific DNA methylation also appears to impact the RNA level of gene expression *via* RNA binding protein s1 PF3D7\_1131000, PF3D7\_0714500 that encodes the transcription elongation factor s-II, and uncharacterised PF3D7\_1354100 that has some homology to RNA

polymerase II transcription subunit 5 in *Dictyostelium discoideum*. PF3D7\_0609500 is uncharacterised but is homologous to plastid encoded RNA polymerase subunit  $\beta$ . PF3D7\_1235000 is a PIH1 (protein interacting with heat shock protein 90) domain-containing protein that is part of a protein complex involved in many cellular functions including RNA polymerase II assembly (Ahmad et al. 2013). Should methylation modify the expression of these genes, it would impact the translation of a whole cascade of downstream genes, and would therefore have a major impact of cell physiology.

Additional genes involved in vesicle-mediated protein transport and processing are differentially methylated between male and female gametocytes with less statistical significance ( $p < 0.001$ , Table 3). PF3D7\_1032500 is a degradation-in-the-endoplasmic-reticulum-protein-1-like protein that contributes to the endoplasmic reticulum associated degradation complex, which mediates protein transport to the apicoplast (Spork et al. 2009). PF3D7\_0828400, mitochondrial oxidase assembly protein 1, is a mitochondrial inner membrane insertase. PF3D7\_0902200 may be involved in surface protein trafficking as it is located in Mauer's clefts and contributes to GPI anchor biogenesis. Coatamer subunit  $\beta$  PF3D7\_1429800, and a soluble N-ethylmaleimide sensitive fusion protein attachment protein receptor (SNARE) protein PF3D7\_1324700 are involved with vesicle-mediated transport. In addition, uncharacterised PF3D7\_1006700 is attributed to gene ontology (GO) term "vesicle mediated transport". Finally PF3D7\_0826000 has 32 % homology to *P. falciparum* arginase that could contribute to protein processing. Overall, it appears that differential DNA methylation between male and female gametocytes targets membrane protein trafficking and processing.

Other differentially methylated genes between male and female gametocytes are involved in host-parasite interactions (Table 3). These include immunogenic Glutamate-rich protein (GLURP) PF3D7\_1035300, predicted host-parasite adhesion protein PF3D7\_0518900 (Ansari et al. 2008), and PF3D7\_1150100, a type B repetitive interspersed family (RIFIN) protein (Joannin et al. 2008) that may be involved in immune evasion in the human host. PF3D7\_1229400 is a macrophage migration inhibitory factor that disrupts memory T-cell response to infection (Cordery et al. 2007; Augustijn et al. 2007; Dobson et al. 2009; Zhensheng Wang et al. 2009; Pantouris et al. 2014; Baeza Garcia et al. 2018). Gametocytes need to avoid immune detection for much longer than asexual blood stage parasites and the findings of this study suggest that the parasite-host interactions may also be sex-specific.

The other differentially methylated genes between male and female gametocytes are involved in ion homeostasis (Table 3). PF3D7\_0715900 is a cation diffusion facilitator family protein proposed to transport zinc. PF3D7\_1333800 is a Voldacs domain-containing protein, which is characteristic of nucleotide-sensitive chloride current inducing proteins that are regulators of volume decrease after cell swelling. This protein may be involved in the rounding up of female gametocytes upon ingestion by the mosquito.

In summary, intragenic DNA methylation in *P. falciparum* gametocytes is sex-specific. Differentially methylated genes are involved in signal transduction, gene transcription and translation, protein trafficking and processing, host-parasite interaction and ion homeostasis. Through these important functions DNA methylation may play a key role in the sex-specific biology of gametocytes.

### **Discussion**

Bisulfite DNA sequencing of two biological replicates of asexual trophozoites, female gametocytes and male gametocytes suggests DNA methylation is present in *P. falciparum*. Intra-genic methylation patterns are different between asexual and sexual blood stage parasites, and are sex-specific at the gametocyte stage.

The functional significance of intra-genic DNA methylation remains to be investigated. Different intragenic methylation status between gametocyte sexes does not correlate with sex-specific gene expression. Indeed, the expression of only 57.1 % (four of the seven differentially methylated genes with  $p < 0.0001$ ) was at least two fold different between male and female gametocytes (Lasonder et al. 2016). This is similar to the overall percentage of differentially regulated genes (3095 of 5460 genes, or 56.7 %) suggesting that intragenic methylation does not universally induce or suppress gene expression in gametocytes. The impact of DNA methylation on the intensity of gene expression, if any, appears to be context-specific. This is similar to observations in mammalian and plant species (Schübeler 2015). Some differentially methylated genes such as AC $\alpha$  encode alternative transcripts. Splicing of such genes may be regulated by DNA methylation. Alternative AC $\alpha$  transcripts may mediate different parasite responses to environmental queues (Baker & Kelly 2004) that could be regulated by DNA methylation in a parasite stage and sex-specific manner.

While sex-specific DNA methylation is exclusive to the nuclear genome, many of the differentially methylated genes between trophozoites and gametocytes are in the apicoplast and mitochondrial genomes. The essential function of the apicoplast in gametocytes and asexual blood stages is the biogenesis of isoprenoid precursor isopentenyl diphosphate (Wiley et al. 2015). The apicoplast contains a 35 kb circular genome encoding 30 proteins, 2 ribosomal ribonucleic acid (rRNA) genes and a complete set of tRNA for translation within the organelle (Wilson et al. 1996). The mitochondrial genome in *P. falciparum* is only 6 kb and encodes three electron transport chain proteins (Suplick et al. 1988; Vaidya et al. 1989; Feagin 1992) and highly fragmented mitochondrial rRNA (Suplick et al. 1990; Feagin et al. 1992; Feagin et al. 2012) that assemble by an unknown mechanism to form a functional mitoribosomal complex. The mitochondria does not encode any tRNA so mitochondrial translation relies on the import of tRNA from the cytoplasm (Sharma & Sharma 2015). Both the apicoplast and mitochondrial genome appear to be targeted by DNA methylation, perhaps in response to stage-specific isopentenyl diphosphate and energy requirements.

Alternatively, the high proportion of apicoplast gene hits may reflect different mechanisms of gene expression regulation in the genomic or plastid genome. Apicoplast genes, including those encoding tRNAs, are polycistronic (Wilson et al. 1996). Arrays of genes relating to translation are therefore transcribed in tandem, and then endonucleases cleave the transcript into monocistronic messenger RNA. In this context DNA methylation could be involved with regulating the expression of the methylated gene, but also the expression of downstream genes.

Although the function of DNA methylation is unclear in *P. falciparum*, intragenic methylation appears to target functionally related genes. Both sex-specific and gametocyte-specific DNA methylation occurred in genes relating to gene transcription and translation, consistent with the transcriptome and proteome being stage and sex-specific. Repression of translation of maternal transcripts prior to fertilisation has previously been described in *P. falciparum*, and may also be impacted by sex-specific DNA methylation.

Plastid encoded genes relating to translation were particularly targeted by differential DNA methylation between gametocytes and asexual trophozoites suggesting that DNA methylation may regulate the intensity of plastid gene expression by modulating translation efficiency.

Several mechanisms of translational regulation have recently been highlighted in *P. falciparum*, including codon usage (Chan et al. 2017). Given that there are fewer tRNA than there are codons, translation depends on wobble base pairing (Crick 1966) whereby the third nucleotide of a codon is not subject to strict Watson-Crick base pairing with the first nucleotide of the anticodon. In *P. falciparum* the use of G/U wobble codons is negatively correlated to protein abundance, and may be a mechanism of translational regulation (Chan et al. 2017). Similar to the apicoplast genome in *P. falciparum*, the Trypanosome parasite genome is polycistronic. Recently codon choice was highlighted as the main mechanism of regulating gene expression in *T. brucei* (de Freitas Nascimento et al. 2018). During the asexual blood stage replication cycle of *P. falciparum*, post translational modifications of tRNA are also linked to stage-specific protein expression (Ng et al. 2018). Methylation of the RNA in aspartic acid tRNA (but not the encoding DNA) by tRNA Aspartic Acid DNA methyltransferase 1 homologue was recently demonstrated *in vitro* and *in vivo* (Govindaraju et al. 2017). The results of the present study suggest that methylation of apicoplast encoded tRNA genes may be an additional layer of translational regulation at the developmental switch from asexual blood stage replication to gametocytogenesis.

In summary, although cytosines are few in number in the *P. falciparum* genome, DNA methylation targets genes that regulate cascades of gene expression and intracellular signalling in a parasite stage and sex-specific manner. Few methylation events may therefore regulate the major developmental switch from asexual blood stage replication to gametocytogenesis, and may impact the sex-specific biology of *P. falciparum* gametocytes.



## Conclusion

By establishing a method to separate male and female gametocytes, key sex-specific traits were brought to light. Sex-specific gametocyte markers were validated for more accurate monitoring of gametocyte carriage in the field and the method was applied to investigate DNA methylation as a possible means of sex-determination in the malaria parasite. The preliminary results suggest that intragenic DNA methylation is gametocyte and sex-specific in mature gametocytes, and could impact cascades of functionally diverse downstream genes. Overall, this chapter has highlighted the sex-specific nature of *P. falciparum* gametocyte biology.

# **Result Chapter 3**

## **Sex-specific lipid metabolism in *Plasmodium* gametocytes**

## Overview

Having established a method for the separation and collection of male and female gametocytes, the sex-specific lipid profile of *P. falciparum* gametocytes is explored in the first part of this chapter. After characterising the lipid composition, the functional significance of *de novo* synthesis of sex-specific lipids is explored by chemical inhibition and reverse genetics of key lipid metabolising enzymes. Finally, gametocyte lipid scavenging from beyond the host cell is explored by comparing lipid dynamics *in vivo* and *in vitro*.

## Part 1

### Sex-specific lipid metabolism in *P. falciparum* gametocytes

#### Introduction

Transmission of *P. falciparum* from the human to mosquito host depends on male and female gametocytes. Gametocytogenesis is by far the longest developmental sexual stage in *P. falciparum*. After 10-12 days of maturation in the human RBC, ingestion by a mosquito rapidly activates the gametocytes to form mature gametes capable of sexual reproduction (Bennink et al. 2016). Within 15 minutes of the blood meal, each gametocyte egresses from the host RBC. While male gametocytes multiply into eight flagellated microgametes, female gametocytes form an immobile spherical macrogamete, poised for fertilisation. The zygote develops in the extracellular environment until invasion of the mosquito midgut wall 19-36 h post blood meal (Aikawa et al. 1984; Sinden et al. 1985; Vlachou et al. 2004).

Such a rapid sex-specific metamorphosis is necessarily preceded by sex-specific preparations in the human host during the relatively slow gametocytogenesis. Surprisingly though, gametocyte sex dimorphism is subtle and mostly limited to the ultrastructural level. From stage III onwards development of the mitochondria, ribosomes and dense spherules distinguish female from male gametocytes (Langreth et al. 1978; Jensen 1979; Sinden 1982). By stage IV, osmiophilic bodies are also observed by electron microscopy mostly in female gametocytes (Sinden 1982; Ponnudurai et al. 1986). Under light microscopy, female gametocytes are slightly larger, possess a more concentrated pigment pattern, and appear bluer than male gametocytes after Giemsa staining (Baker 2010).

Recently the tagging of sex-specific molecular markers has revealed sex-specific gene and protein expression profiles (Lasonder et al. 2016; Miao et al. 2017). These studies identified differences in the expression of lipid metabolic pathways including phosphatidylcholine biosynthesis, fatty acid biosynthesis and ether lipid metabolism (Lasonder et al. 2016). Whether this results in differences in the lipid composition between male and female gametocytes remains unknown.

Sphingomyelin synthase 2 is a predominantly female expressed gene identified in the sex-specific transcriptome (Lasonder et al. 2016). *P. falciparum* encodes two sphingomyelin

synthases (SMS, (Gardner et al. 2002)), one of which is expressed throughout blood stages (SMS1, PF3D7\_0625000), the other of which is gametocyte specific and female enriched (SMS2, PF3D7\_0625100) (López-Barragán et al. 2011; Lasonder et al. 2016). Sphingomyelin synthase not only generates sphingomyelin, but also regulates the levels of secondary messenger molecules ceramide and DAG as outlined in the general introduction (Fyrst & Saba 2010).

Given that mature gametocytes persist in the blood for weeks, they were generally thought to be metabolically dormant parasites (Canning & Sinden 1975; Sinden et al. 1978). However, the lipidome of gametocytes changes significantly between young and mature gametocytes (Gulati et al. 2015; Tran et al. 2016), suggesting that lipid metabolism is active during gametocytogenesis. In particular, Gulati et al. (2015) identified intermediate products of sphingolipid metabolism in mature gametocytes, revealing that *de novo* sphingomyelin synthesis occurs during gametocytogenesis. If not metabolically dormant, the longevity of gametocytes in the same host RBC likely requires gametocyte-specific metabolism.

In the first part of this chapter the lipidome of gametocytes resulting from the stage and sex-specific expression of lipid-associated genes is explored. Unlike previous studies, male and female gametocytes are distinguished to identify sex-specific lipid traits. The functional significance of *de novo* sphingomyelin synthesis in gametocytes *via* SMS1 and SMS2 is investigated by pharmacological inhibition and reverse genetics.

## **Results**

The abundance of over 230 lipid species was measured in male and female gametocytes by mass spectrometry and compared to the lipid profile of the host RBC and mature asexual stage parasite infected RBC (26-42 hpi). Gametocyte and asexual blood stage parasites were analysed in their host RBC. For the complete list of lipid species measured in this study, refer to Supplementary Table 1.

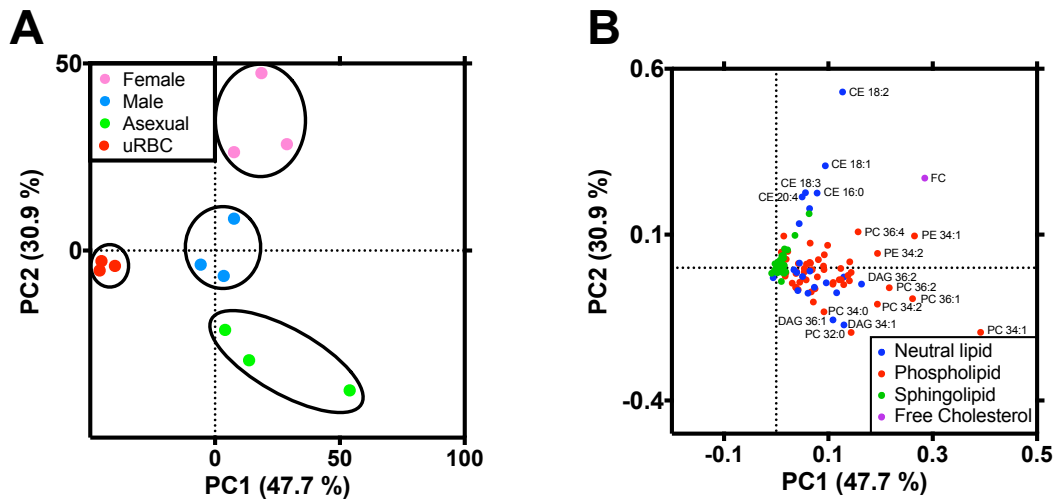


**Figure 1:** Principal component analysis (A) and loading plot (B) of the lipidome of uninfected red blood cells (uRBC) and red blood cells infected with asexual stage parasites (Asexual), female gametocytes (Female) and male gametocytes (Male). Black circles in A indicate sample groups. PC1 and 2: first and second principal component; CE: cholesteryl ester; FC: free cholesterol; PC: phosphatidylcholine; PE: phosphatidylethanolamine; DAG: diacylglycerol.

Principal component analysis of total lipids clearly distinguishes infected from uninfected RBC (Figure 1A). Furthermore, asexual parasite-infected RBC, male gametocyte-infected RBC and female gametocyte-infected RBC are separated by the second principal component (Figure 1A), which is driven by CE species and FC in one direction, and DAG and PC species in the other (Figure 1B). Clearly a switch in lipid profile marks commitment to gametocytogenesis and sex determination in *P. falciparum*.

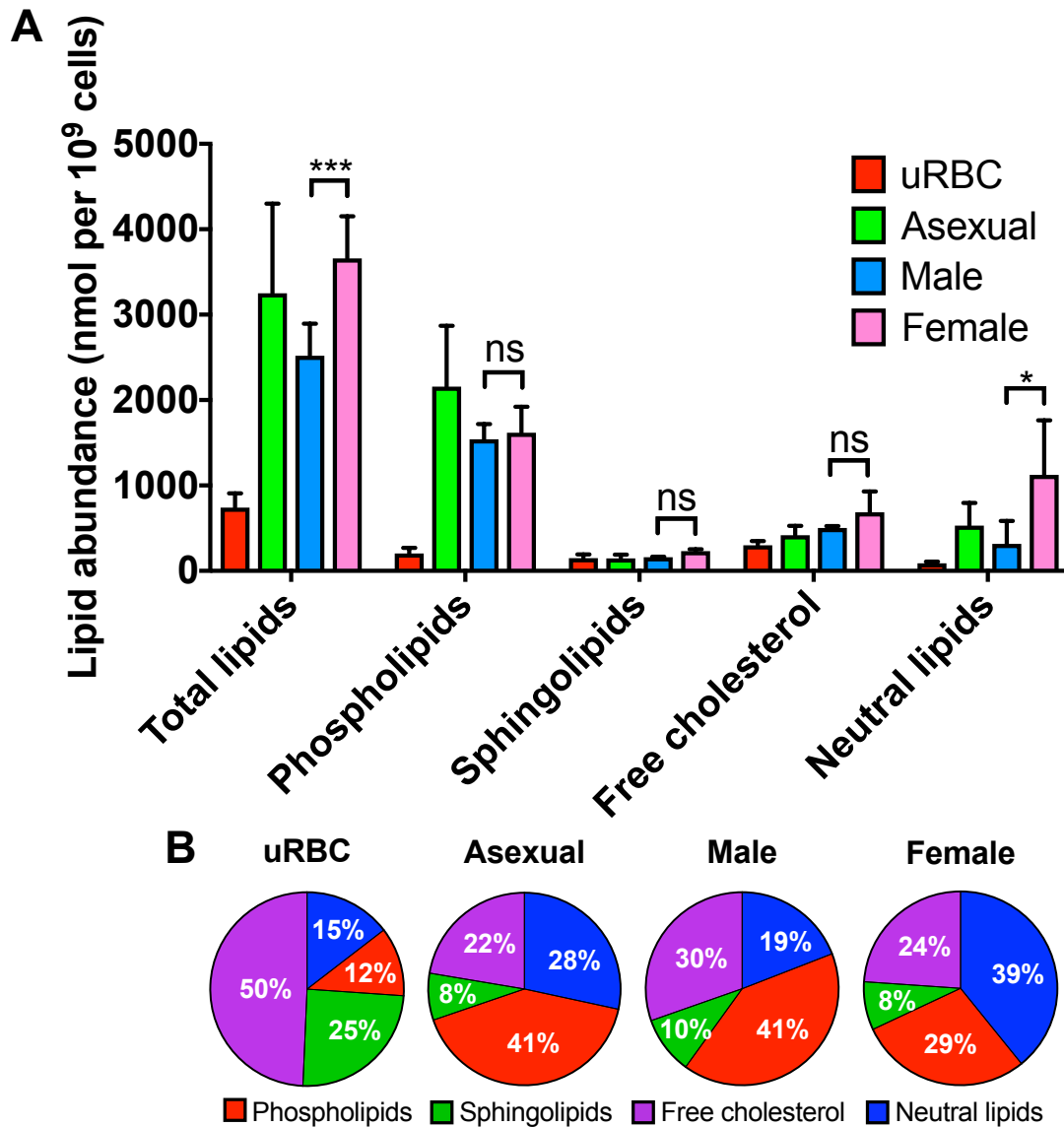


**Figure 2:** Mean lipid abundance with standard deviation (A) and proportions (B) of lipid classes in uninfected red blood cells (uRBC) and red blood cells infected with asexual stage parasites (Asexual), male gametocytes (Male) and female gametocytes (Female). Results averaged from three independent biological replicates of  $10^7$  cells. Significance calculated by ANOVA. \*\*\*:  $p < 0.001$ , \*:  $p < 0.1$ , ns: not significant,  $p > 0.1$

Upon infection, total lipid abundance increases 3-5 fold and in sexual stages, female gametocyte-infected RBC accumulate significantly more lipids than male gametocyte-infected RBC (Figure 2A). Of the four main lipid categories (phospholipids, sphingolipids, free cholesterol and neutral lipids), only neutral lipids are significantly more abundant in female gametocyte-infected RBC compared to male gametocyte-infected RBC (Figure 2A). Neutral lipids account for 39 % of lipids in female gametocyte-infected RBC compared to only 19 % in male gametocyte-infected RBC (Figure 2B). It appears that female gametocytes

stockpile neutral lipids, potentially as a fatty acid reserve for post-fertilisation development of the zygote in the mosquito.

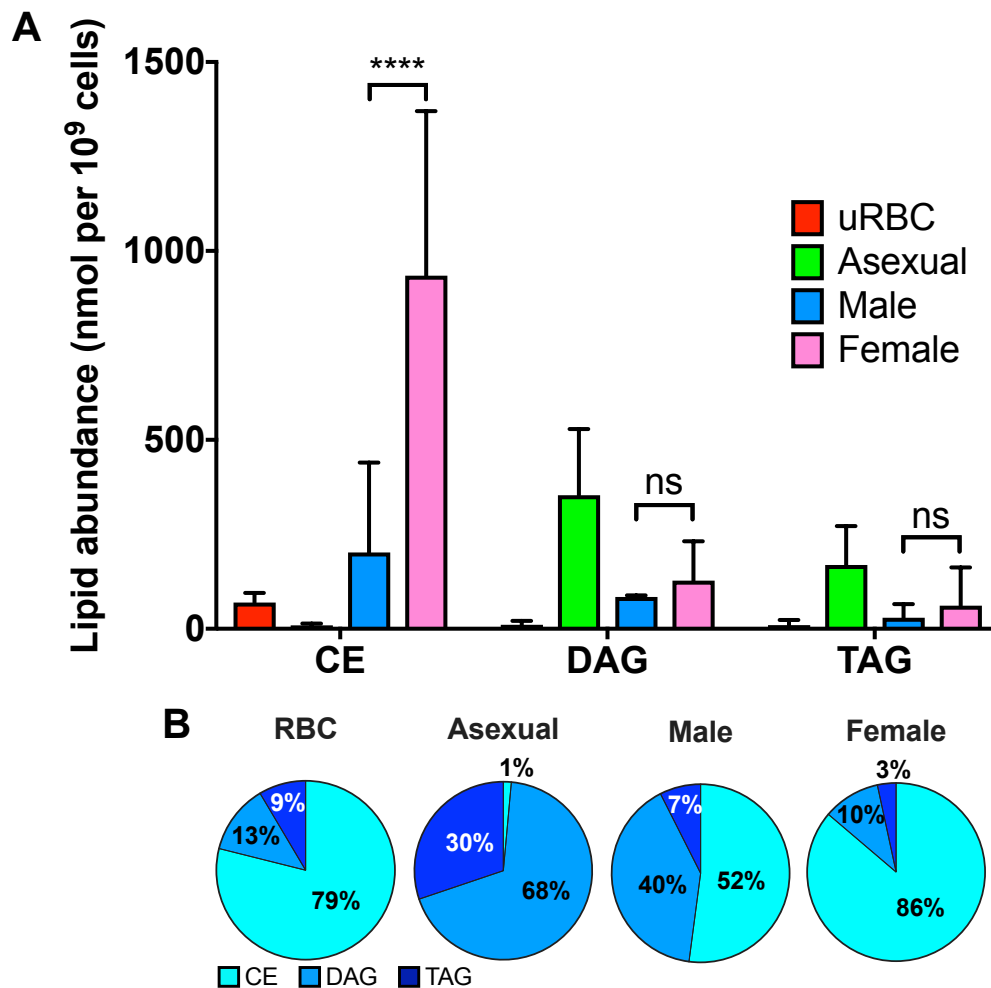


**Figure 3:** Mean neutral lipid abundance with standard deviation (A) and mean proportions (B) of uninfected red blood cells (uRBC) and red blood cells infected with asexual stage parasites (Asexual), male gametocytes (Male) or female gametocytes (Female). Results averaged from three independent biological replicates of 10<sup>7</sup> cells. Significance calculated by ANOVA. \*\*\*\*:  $p < 0.0001$ , ns: not significant,  $p > 0.1$ . CE: cholesteryl ester; DAG: diacylglycerol; TAG: triacylglycerol.

The nature of neutral lipids in asexual parasite-infected RBC contrasts to that of gametocyte-infected RBC (Figure 3). Of the three categories of neutral lipids (CE, DAG and TAG), DAG is the predominant neutral lipid in asexual parasite-infected RBC, whereas CE dominates the neutral lipid profile of gametocyte-infected RBC and uninfected RBC (Figure 3A and B). The proportions of neutral lipid categories are highly dynamic upon infection with asexual or sexual stage *P. falciparum*. In addition, neutral lipids are sex-specific: female gametocyte-



infected RBC accumulate significantly more CE than male gametocyte-infected RBC (Figure 3A).

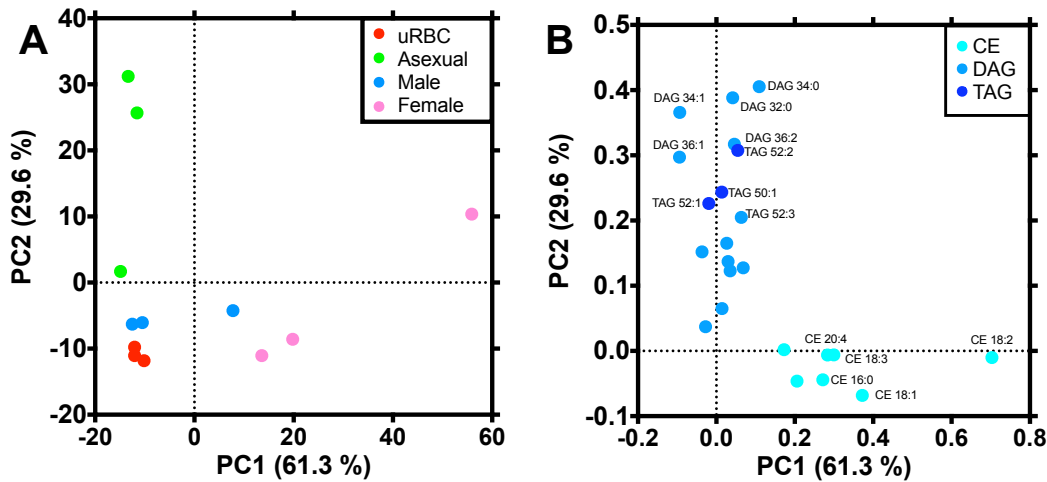


**Figure 4:** Principal component analysis (left) and loading plot (right) of neutral lipid composition of uninfected red blood cells (uRBC) and red blood cells infected with asexual stage parasites (Asexual), male gametocytes (Male) or female gametocytes (Female). PC1 and 2: first and second principal component; CE: cholesteryl ester; DAG: diacylglycerol; TAG: triacylglycerol.

These trends are also observed at the individual lipid species level (Figure 4). Highly abundant CE species characterise female gametocyte-infected RBC while asexual parasite-infected RBC are distinguished by DAG and TAG species (Figure 4A and B). Given that mosquitoes cannot synthesise cholesterol, CE reserves in the female gametocyte-infected RBC may be a means of storing cholesterol for development in the mosquito vector. DAG and TAG on the other hand are efficient fatty acid stores that may be required for male-specific functions such as cell division and exflagellation.

The nature of neutral lipids in asexual parasite and gametocyte-infected RBC is different to that of uninfected RBC. In infected RBC at both asexual and sexual stage, TAG 52:2 is the most abundant TAG species. In uninfected RBC, TAG 56:6 and TAG 54:6 are the most abundant TAG species. This suggests TAG synthesis occurs in asexual and sexual blood stage *P. falciparum*. The most abundant DAG species in all samples is DAG 36:2, although asexual parasite-infected RBC also contain similar levels of DAG 34:1, perhaps as a result of asexual blood stage parasite specific DAG synthesis. No saturated CE species were detected in any samples and CE 18:2 is the most abundant CE species in all samples. The similar nature of CE species in both infected and uninfected RBC is consistent with parasite

scavenging CE from the host or synthesising CE from cholesterol and fatty acids sourced directly from the host.

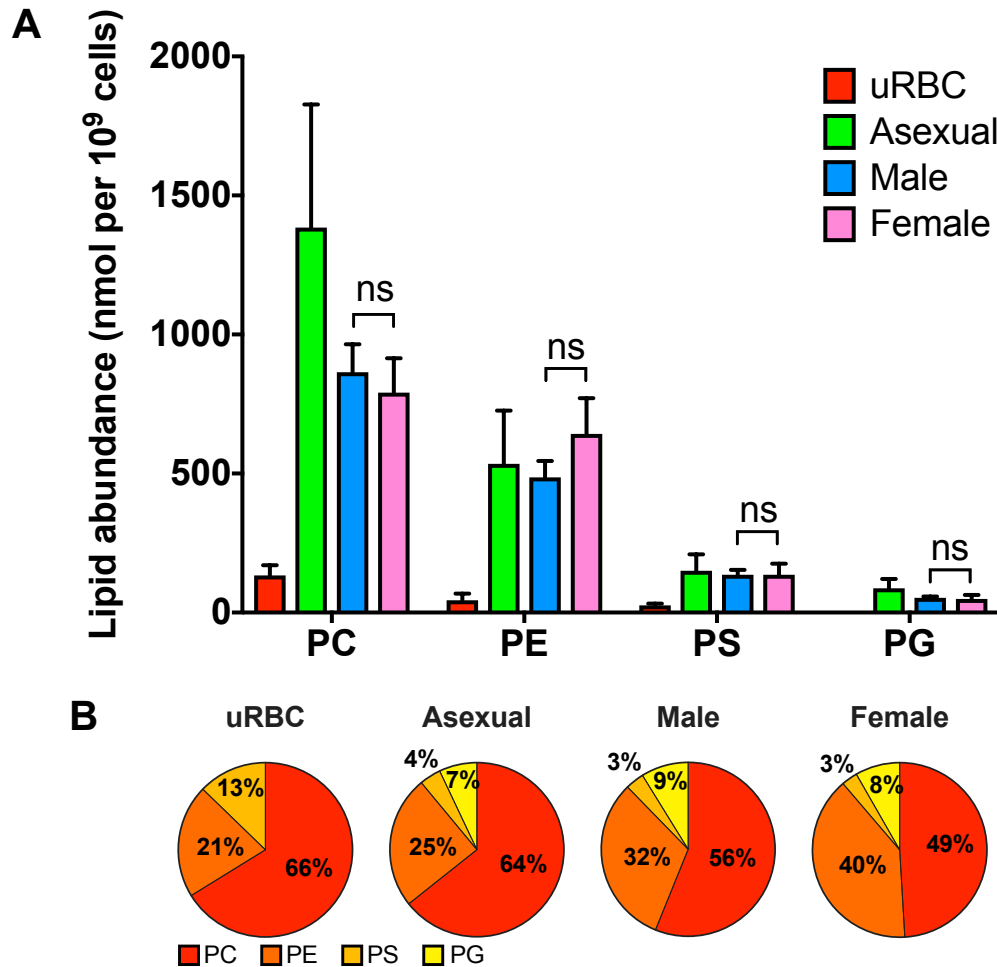


**Figure 5:** Mean phospholipid composition with standard deviation (A) and mean proportions (B) of uninfected red blood cells (uRBC) and red blood cells infected with asexual stage parasites (Asexual), male gametocytes (Male) or female gametocytes (Female). Results averaged from three independent biological replicates of  $10^7$  cells. Significance calculated by two-way ANOVA. ns: not significant,  $p > 0.1$ . PC: phosphatidylcholine; PE: phosphatidylethanolamine; PS: phosphatidylserine; PG phosphatidylglycerol.

Although male gametocyte-infected RBC have a higher proportion of phospholipids (41 % phospholipids in males compared to 29 % in females, Figure 2B), phospholipid abundance is surprisingly similar in male and female gametocyte-infected RBC (Figure 2A). There were no significant differences in major phospholipid groups between sexes (Figure 5A). Male gametocyte-infected RBC contain slightly more PC but slightly less PE than female gametocyte-infected RBC, both in terms of abundance and proportion of phospholipids (Figure 5A and B). Phospholipids are the main component of membranes and are likely required for male-specific cell division, but also organelle biogenesis in both sexes of gametocytes.

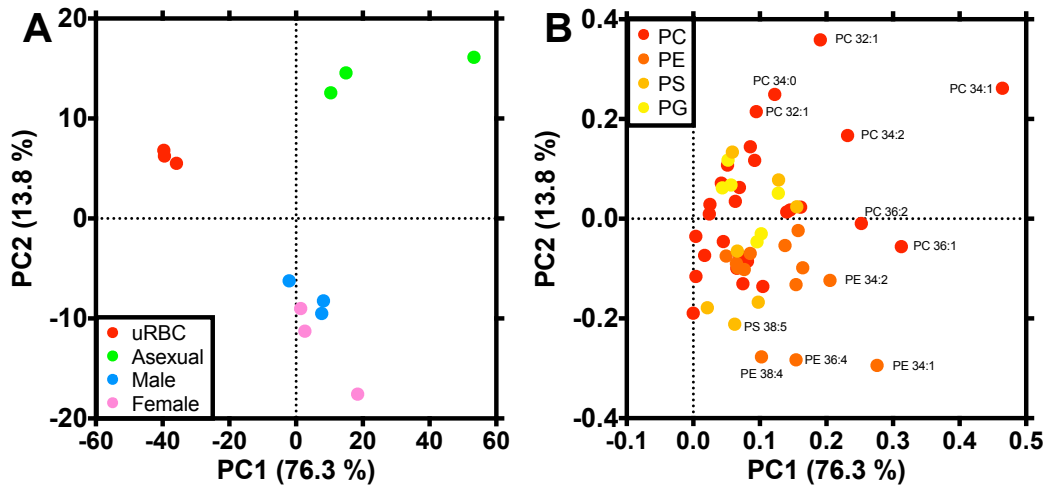


**Figure 6:** Principal component analysis (left) and loading plot (right) of phospholipid composition of uninfected red blood cells (uRBC) and red blood cells infected with asexual stage parasites (Asexual), male gametocytes (Male) or female gametocytes (Female). PC1 and 2: first and second principal component; PC: phosphatidylcholine; PE: phosphatidylethanolamine; PS: phosphatidylserine; PG phosphatidylglycerol.

Principal component analysis based only on phospholipids does not distinguish between male and female gametocyte-infected RBC (Figure 6A). However, gametocyte-infected RBC cluster apart from uninfected RBC and asexual parasite-infected RBC mostly due to PE species (Figure 6B). Overall, male and female gametocyte-infected RBC phospholipids are similar to each other, but distinct from host cell and asexual parasite-infected RBC phospholipids. Gametocyte-infected RBC phospholipids appear to mostly contribute to generic membrane functions such as organelle biogenesis, rather than sex-specific functions such as male-specific cell division.

The most abundant phospholipid species in each phospholipid category contains oleic and palmitic fatty acyl chains. PC 34:1 and PE 34:1 are the most abundant PC and PE species in all samples. PG is specific to infected RBC, although the nature of PG differs between parasite stages. While PG 34:1 is the most abundant in asexual parasite-infected RBC, PG 34:1, PG 36:1 and PG 36:2 are the major PG species in gametocyte-infected RBC. Specific PG synthesis in gametocytes is consistent with the unique mitochondrial structure of sexual stage parasites.

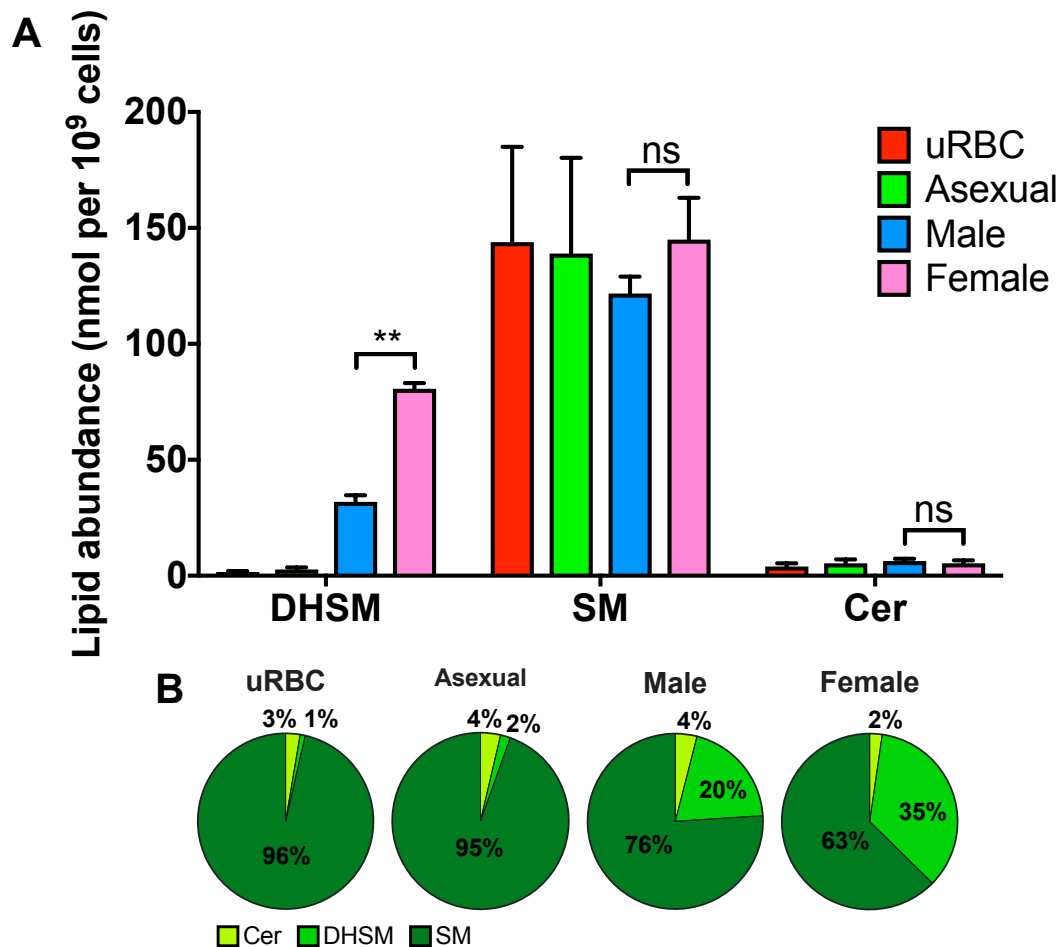


**Figure 7:** Mean sphingolipid abundance with standard deviation (A) and mean proportion (B) in uninfected red blood cells (uRBC) and red blood cells infected with asexual stage parasites (Asexual), male gametocytes (Male) or female gametocytes (Female). Results averaged from three independent biological replicates of  $10^7$  cells. Significance calculated by two-way ANOVA. \*\*:  $p < 0.01$ , ns: not significant,  $p > 0.1$ . DHSM: dihydrosphingomyelin; SM: sphingomyelin; Cer: ceramide.

Like phospholipids, overall sphingolipid abundance is not significantly different between male and female gametocyte-infected RBC (Figure 2A). However, breaking down sphingolipids into its three main categories (SM, DHSM and ceramide) reveals gametocyte and sex-specific sphingolipids (Figure 7). Major sphingolipid SM abundance is similar in all samples and does not appear to be modified upon infection (Figure 7A). Gametocyte-infected RBC (especially females) accumulate DHSM (Figure 7A and B) driving the DHSM/SM ratio from close to 0 in uninfected RBC and asexual parasite-infected RBC to approximately 0.3 in gametocytes. An increase in the DHSM/SM ratio increases the membrane rigidity, and potentially the function of sphingomyelin-rich lipid rafts in parasite membranes.

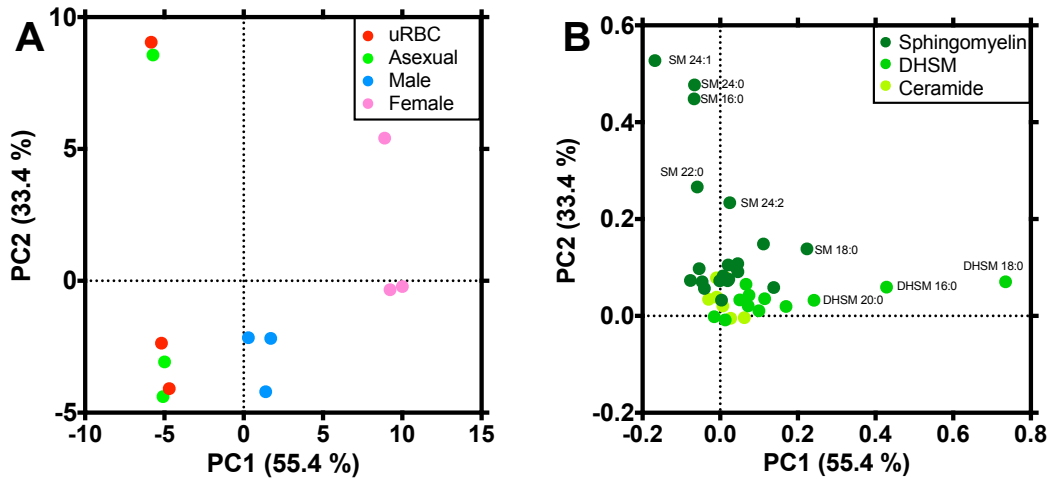


**Figure 8:** Principal component analysis (left) and loading plot (right) of sphingolipid composition of uninfected red blood cells (uRBC) and red blood cells infected with asexual stage parasites (Asexual), male gametocytes (Male) or female gametocytes (Female). PC1 and 2: first and second principal component; DHSM: dihydrosphingomyelin; SM: sphingomyelin; Cer: ceramide.

Principal component analysis loading only sphingolipids does not distinguish uninfected RBC from asexual parasite-infected RBC but male and female gametocyte-infected RBC cluster separately (Figure 8A). DHSM 20:0, 16:0 and 18:0 especially distinguish gametocyte-infected RBC from the other samples (Figure 8B). Overall, accumulation of DHSM marks gametocytogenesis and is predominantly female. Given that DHSM is not present in the host RBC and the parasite encodes enzymes for sphingomyelin synthesis, this parasite stage and sex-specific accumulation of DHSM may reflect active *de novo* sphingolipid synthesis in gametocytes.

The main sphingolipid species in each category is the same in all samples, with the exception of DHSM. Cer 24:1 is the most abundant ceramide species and SM 16:0 and SM 24:1 are the major SM species in all samples. All DHSM species are saturated and DHSM 18:0 is the most abundant species in all samples. Unlike gametocyte-infected RBC, uninfected RBC and asexual parasite-infected RBC equally stockpile DHSM 16:0. The gametocyte-specific nature of DHSM species suggests this parasite stage synthesises DHSM *de novo*.

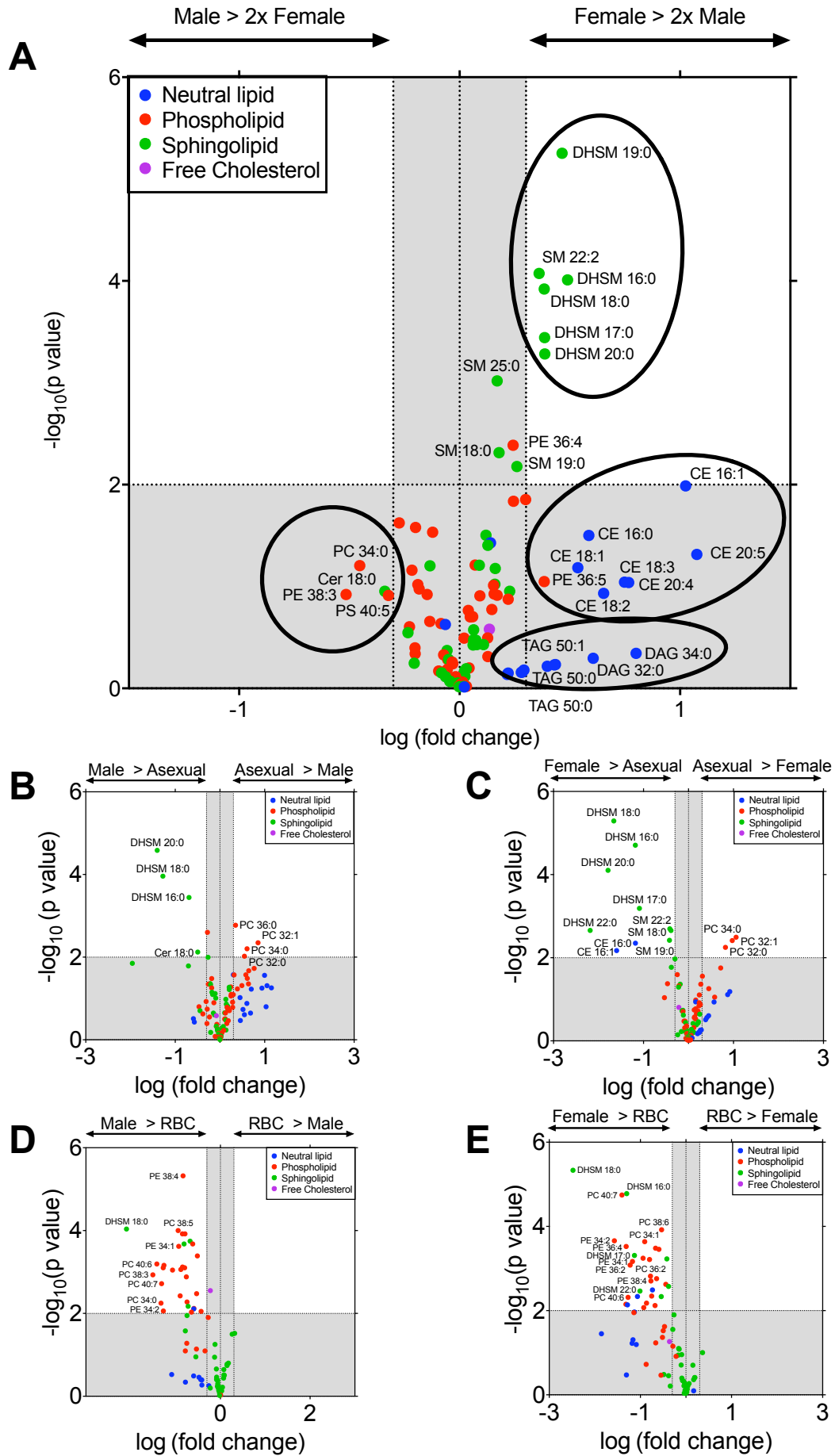


**Figure 9:** Volcano plot of lipid species in male and female gametocyte-infected red blood cells. A, B and D: Comparison of male gametocyte-infected red blood cell lipids to female gametocyte-infected red blood cells (A), asexual-stage infected red blood cells (B) and uninfected red blood cell (RBC) (D). C and E: Comparison of female gametocyte-infected red blood cell lipids to asexual-stage infected red blood cells (C) and uninfected red blood cells (E). Fold change averaged from three biological repeats of  $10^7$  cells each. P values calculated by student t tests. Grey area represents changes that are less than two fold different between samples and/or have a significance of  $p > 0.01$ . Circles in A highlight groups of lipids. DAG: diacylglycerol; DHSM: dihydrosphingomyelin; CE: cholesteryl ester; PC: phosphatidylcholine; PE: phosphatidylethanolamine; PS: phosphatidylserine; SM: sphingomyelin; TAG: triacylglycerol.

Of the lipid species with more than a two fold difference between male and female gametocyte-infected RBC, six are significantly more abundant in female gametocyte-infected RBC (Figure 9A). Five of these are saturated DHSM species, the other is SM 22:2. Neutral lipid species are highly variable and therefore lack statistical significance. No lipid species are significantly more abundant in male gametocyte-infected RBC. Overall, the lipid profile of male and female gametocyte-infected RBC points towards DHSM as a key characteristic of female gametocytes.

Compared to asexual stage parasite-infected RBC both sexes of gametocyte-infected RBC contain more DHSM 20:0, 18:0 and 16:0 (Figure 9B-C), suggesting that DHSM accumulation is in preparation for mosquito stage development. Asexual parasite-infected RBC on the other hand accumulate significantly more of some PC species compared to both sexes of gametocyte-infected RBC. This is consistent with asexual replication requiring phospholipid-rich membrane biogenesis. CE 16:1 and CE 16:0 are the only lipid species that are more abundant in female gametocyte-infected RBC but not in males, when compared to asexual parasite-infected RBC. Potentially CE is a means of storing cholesterol for zygote development in the cholesterol-poor mosquito host. Phospholipid and sphingolipid species are significantly more abundant in each sex of gametocyte-infected RBC compared to uninfected RBC, perhaps due to the presence of numerous parasite membranes in the infected host cell (Figure 9D-E). Overall, gametocytes significantly modify the lipid profile of the host RBC during maturation in a manner that distinguishes them from asexual parasites.

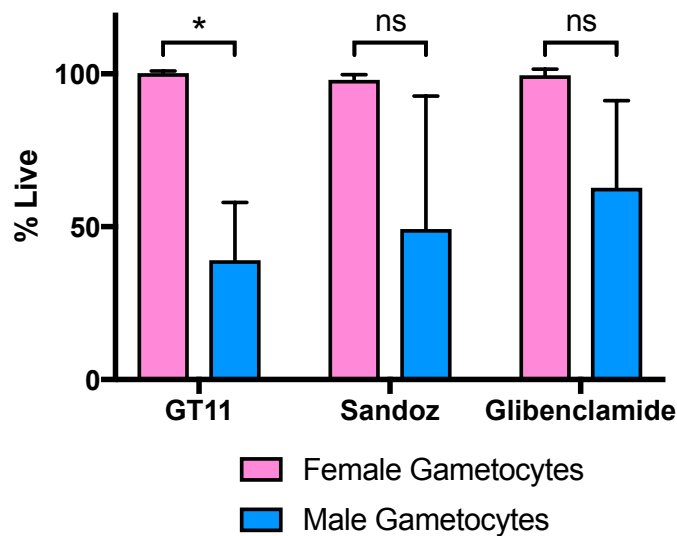


**Figure 10:** Gametocyte viability following chemical inhibition of DHSM or CE synthesis. DHSM synthesis was disrupted with 10  $\mu\text{M}$  GT11 and CE synthesis was inhibited with 10  $\mu\text{M}$  Sandoz 58-035 or 10  $\mu\text{M}$  glibenclamide from day 2 to 6 post-commitment. For each gametocyte sex, results are normalised to viability following exposure to the DMSO solvent control and 100  $\mu\text{M}$  artemisinin. Average result and standard deviation presented from three biological replicates, each performed in technical triplicate. Significance calculated by student t test. \*:  $p < 0.1$ ; ns: not significant,  $p > 0.1$

To investigate the functional significance of the sex-specific lipid composition, gametocytes were exposed to three compounds that block the synthesis of the most sex specific lipids, CE and DHSM from day 2 to 6 post commitment (Figure 10). The sex-specific viability of gametocytes was measured by flow cytometry detecting male and female gametocytes as described in Result Chapter 2 part I and measuring viability with Mitotracker Deep Red stain. At 10  $\mu\text{M}$  only DHSM synthesis inhibitor GT11 impacts gametocyte viability in a male-specific manner. This suggests that the gametocyte sensitivity to lipid synthesis inhibition is inversely correlated to the abundance of the targeted lipid.

Given the apparent sex-specific functional significance of sphingolipid synthesis in gametocytes, the final step in the metabolic pathway mediated by SMS (see general introduction) was next investigated. The high abundance of DHSM in gametocytes, and especially in female gametocytes, correlates to SMS2 rather than SMS1 expression, suggesting distinct roles for each enzyme. A reverse genetics approach was therefore applied to discriminate between the functional role of SMS1 and SMS2 in gametocytes.



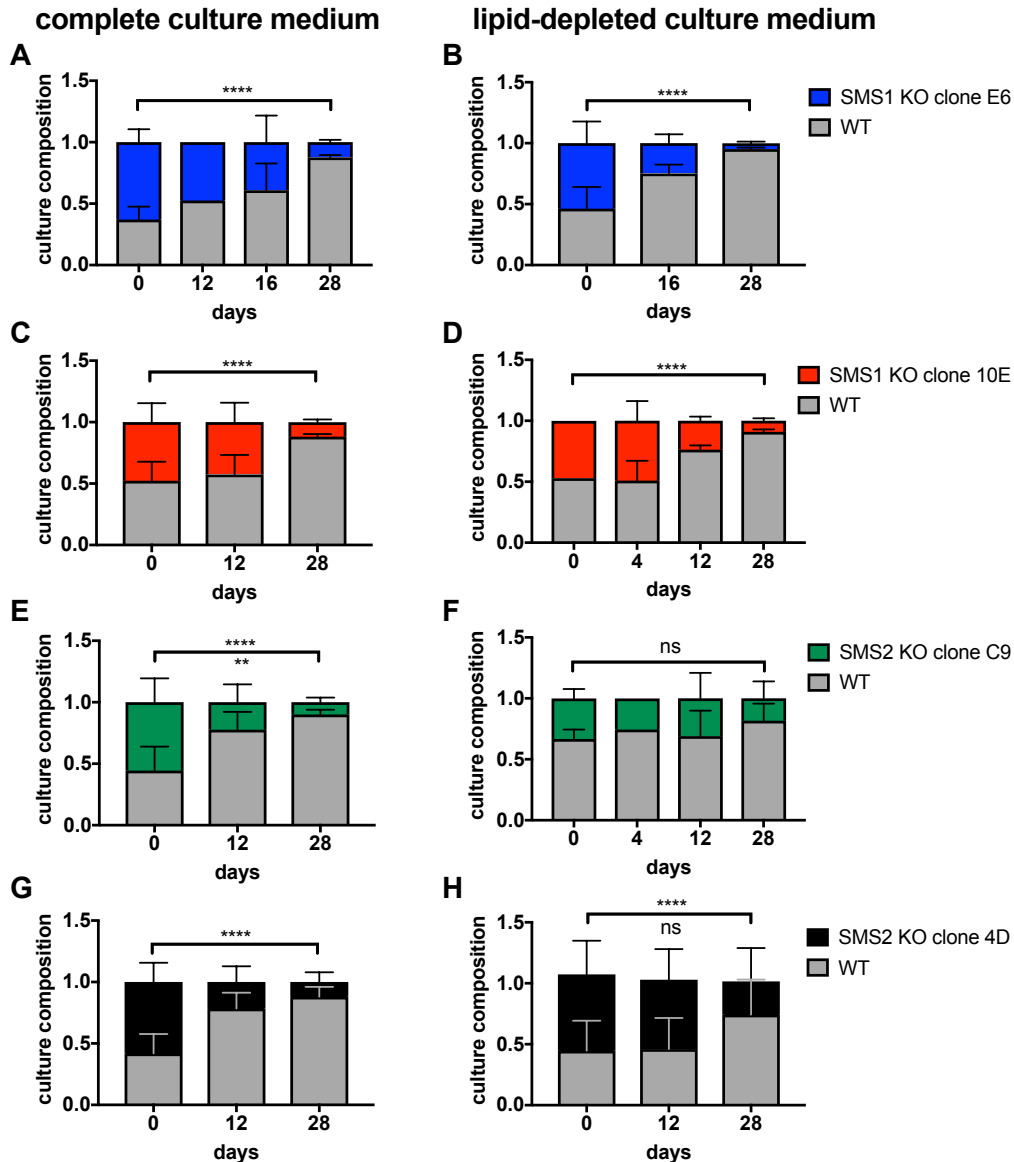


**Figure 11:** Fitness competition between 3D7 WT and SMS1 KO or SMS2 KO clones in complete and lipid-depleted culture medium over 28 days. On day 0 equal amounts of 3D7 WT (grey) and SMS1 KO clone E6 (blue, A and B), SMS1 KO clone E10 (red, C and D), SMS2 KO clone C9 (green, E and F) or SMS2 KO clone 4D (black, G and H) were combined in a co-culture with either complete culture medium (A, C, E and G) or culture medium containing 25 % of the lipids in complete culture medium (B, D, F and H). The proportion of each genotype in the culture was monitored on day 0, 12 and 28 by qPCR of the hDHFR resistance cassette (to detect KO genotype) and the disrupted section of the SMS1 or 2 genes (to detect WT genotype). At some time points technical problems inhibited monitoring the culture so measurements were performed 4 days afterwards instead. Results from 2-4 independent biological repeats are shown as mean and standard deviation, while results from one biological repeat are presented as mean of three technical repeats without error bar. The proportion of WT and KO genotypes is expressed as a ratio stacked in one column (see Materials and Methods for calculations). Statistical significance was calculated by two-way ANOVA comparing the mean ratios on day 0 and day 28. In E and H, the statistical significance of the proportion of KO genotype is shown on top and that of the proportion of WT genotype is shown below, otherwise both WT and KO genotype have the same statistical significance. \*\*\*\*:  $p < 0.0001$ ; \*\*:  $p < 0.01$ ; ns: not significant.

Each SMS gene was disrupted by homologous recombination and integration was confirmed by Southern blot (Supplementary Figures 2 and 3). Three independent attempts to disrupt both SMS1 and SMS2 genes together did not yield any parasites after transfection. This suggests that the SMS genes are redundant in asexual blood stages and that function of at least one SMS is essential for asexual parasite proliferation in the blood. In 28 day co-cultures WT parasites quickly outgrew each of the KO parasites (Figure 11A, C, E and G), suggesting that SMS1 and SMS2 are each required for optimal asexual parasite proliferation. Depleting the culture medium lipids by 75 % did not exacerbate the growth defect observed in each KO cell line (Figure 11B, D, F and H). In fact the apparent fitness cost of SMS2 KO clone C9 was lost in lipid depleted culturing conditions (Figure 11F). Overall, it appears that *de novo* sphingomyelin synthesis contributes to asexual blood stage parasite proliferation regardless of exogenous sphingomyelin availability.

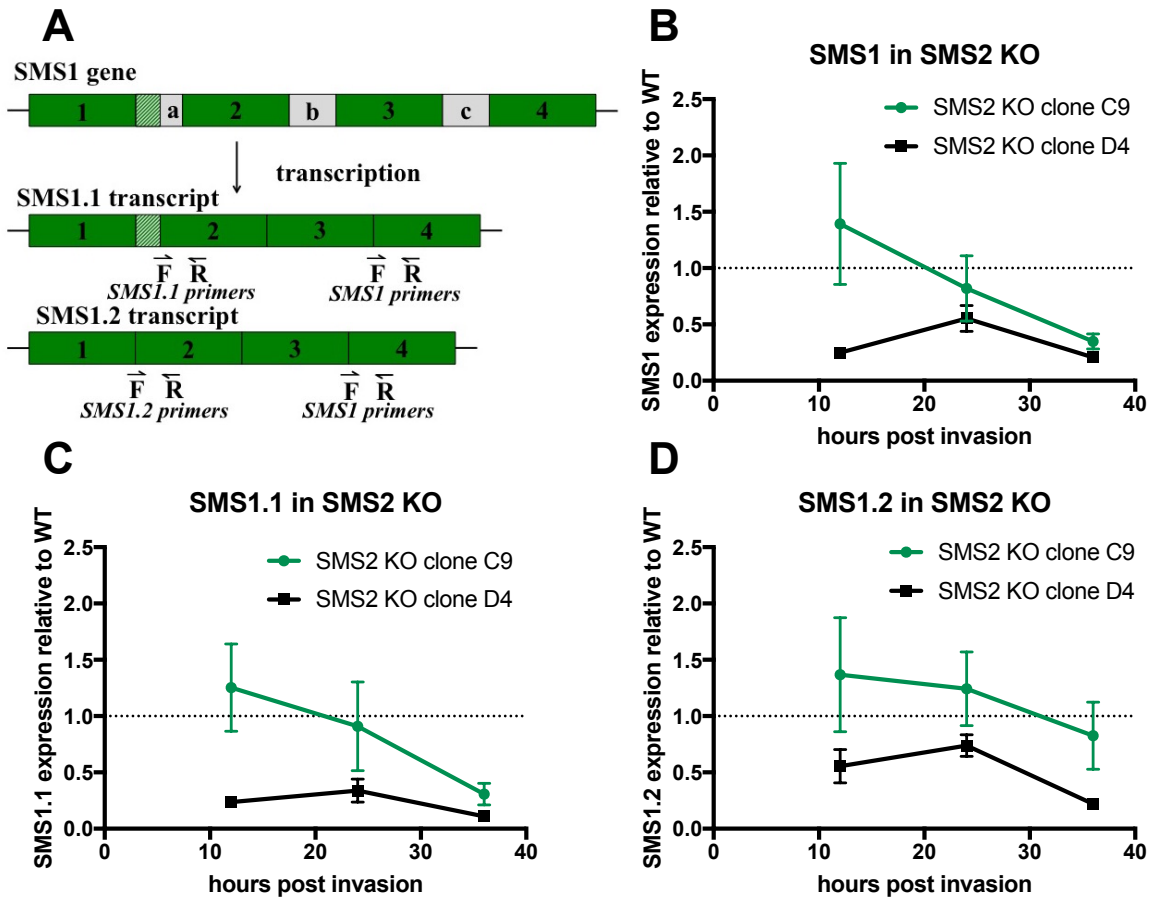


**Figure 12:** Expression of SMS1 gene after disruption of SMS2 gene in asexual stage parasites at 12-16, 24-28 and 36-40 hours post invasion. A) Diagram of SMS1 gene with four introns (green boxes 1-4) and three exons (grey boxes a-c) alternatively spliced as SMS1.1 or SMS1.2 transcripts with different intron 1-2 junctions (hashed box). SMS1 primers (F: forward; R: reverse) detect both SMS1 transcripts whereas SMS1.1 and SMS1.2 primers are specific to each transcript. B-D) Overall expression of SMS1 (B) or of each alternative SMS1 transcript, SMS1.1 (C) or SMS1.2 (D) in SMS2 KO clones C9 (green) and D4 (black). Mean gene expression with standard deviation is relative to the transcript abundance measured in 3D7 WT parasites at the same lifecycle stage, and normalised to a reference gene as described in Materials and Methods.

Given SMS KO parasites have a growth defect but are not hyper sensitive to culture medium lipid depletion, the possibility of partial compensation through the reciprocal SMS gene was explored next. If SMS1 and SMS2 are redundant, perhaps the overexpression of one of the SMS genes is sufficient to maintain some asexual parasite proliferation in the absence of the other. The relative expression of SMS1 in SMS2 KO parasites compared to WT parasites was measured by qRT-PCR at three time points during the asexual lifecycle (12, 24 and 36 hpi, Figure 12). Given that SMS1 has two predicted transcripts, three primer pairs were designed to quantify total SMS1 expression, SMS1.1 expression only or SMS1.2 expression only (Figure 12A). Total SMS1 expression was lower in SMS2 KO parasites compared to

WT parasites at 36 hpi, similar to WT parasites at 24 hpi and variable between SMS2 KO clones at 12 hpi (Figure 12B). A similar expression profile was observed for each SMS1 transcript, although SMS1.2 expression in KO parasites was similar to that of WT parasites at 36 hpi (Figure 12 C-D). The similar expression profile of SMS1, SMS1.1 and SMS1.2 suggests that the transcript specific primers may not be as specific as predicted. Overall this suggests that SMS2 disruption is not compensated for by up regulation of SMS1.

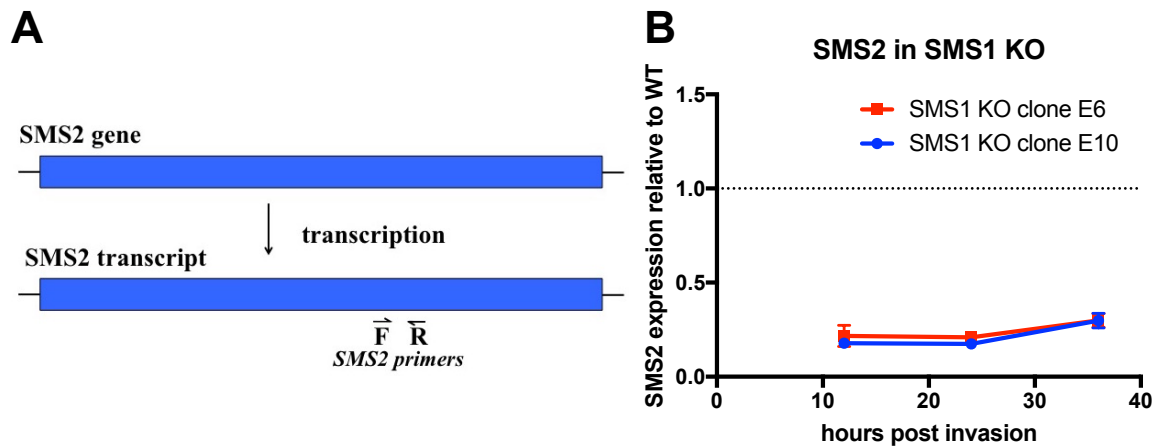


**Figure 13:** Expression of SMS2 gene after disruption of SMS1 gene in asexual blood stage parasites at 12-16, 24-28 and 36-40 hours post invasion. A) Diagram of SMS2 gene and transcript with one intron (blue box). SMS2 primers (F: forward; R: reverse) detect both SMS2 gene and transcript given that there are no exons in the gene. B) Expression of SMS2 in SMS1 KO clones E6 (red) and E10 (blue). Mean gene expression with standard deviation is relative to the transcript abundance measured in 3D7 WT parasites at the same lifecycle stage, and normalised to a reference gene as described in Materials and Methods.

The same experiment was performed on SMS1 KO parasites. Unlike SMS1, SMS2 does not contain exons, and as such the primers for qRTPCR are not specific to the transcript (Figure 13A). SMS2 was not over-expressed during the asexual lifecycle after disruption of SMS1 (Figure 13B). In fact, SMS2 transcripts appear less abundant compared to 3D7 WT. The function of this down regulation is unclear, but this result definitively shows that disruption of SMS1 was not compensated for by up regulation of the reciprocal SMS.

Both SMS1 KO and SMS2 KO parasites could commit to gametocytogenesis (Supplementary Figure 4A and B). The rate of gametocyte commitment is variable in WT cultures, as illustrated by the differing WT gametocytemia over time between Supplementary Figure 4A and B. Preliminary experiments suggest that any difference between gametocytogenesis in WT and each SMS KO parasites is subtle, and further experiments are required to ascertain

whether the differences are beyond the normal variation between gametocyte commitment events.

Gametocyte commitment varied between clones of SMS1 KO (Supplementary Figure 4A). The apparent increase in gametocytemia in SMS1 KO clone E10 is surprising given that gametocytes do not proliferate after commitment. It is likely that residual asexual parasite proliferation in this culture is responsible for the apparent increase in gametocytemia, and as such this experiment needs to be repeated. SMS1 KO clone E6 gametocytemia was similar to WT, suggesting SMS1 activity does not impact gametocytogenesis.

SMS2 KO gametocytogenesis may differ from that of WT parasites (Supplementary Figure 4B). In the absence of SMS2, more gametocytes were formed and gametocytemia dropped more rapidly than in WT cultures over 8 days. It appears that while SMS1 is dispensable for gametocytogenesis, SMS2 may play a role in gametocyte commitment rate and gametocyte maturation and/or viability. Further experiments are required to confirm this apparent subtle phenotype.

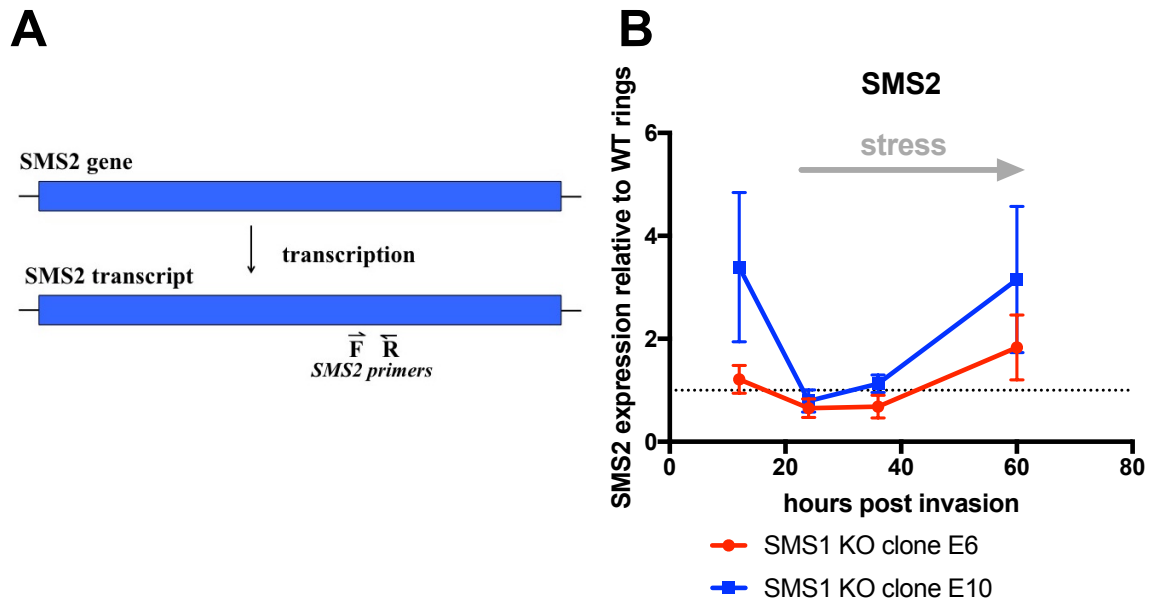


**Figure 14:** Expression of SMS2 gene after disruption of SMS1 gene in stressed asexual stage parasites. A) Diagram of primers for qRT-PCR of SMS2 transcripts (F: forward, R: reverse). B) SMS2 expression at 12-18 hours post invasion (unstressed ring), 24-28 hours post invasion (stressed trophozoite), 36-40 hours post invasion (stressed schizont) and 60-64 hours post initial invasion, 12-16 hours post second invasion (stressed ring) in SMS1 KO clones E6 (red) and E10 (blue) relative to SMS2 expression in unstressed WT rings and normalised to a reference gene as described in Materials and Methods. Data presented as means and standard deviation from three independent biological repeats. Culture stress (grey arrow) consisted of overpopulation without adequate medium supplementation as per gametocyte commitment protocol from day -3 to 0.

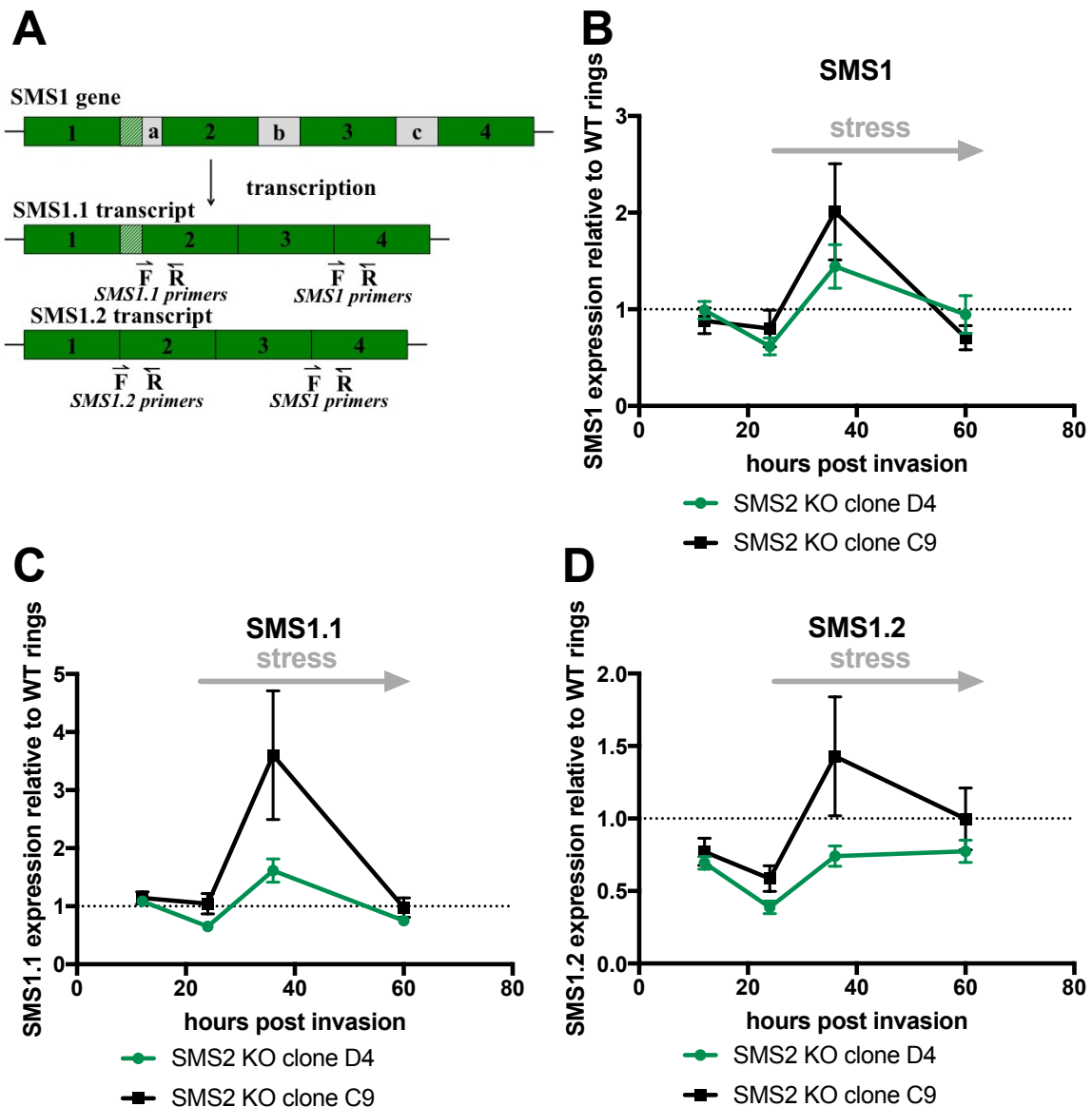


**Figure 15:** Expression of SMS1 gene after disruption of SMS2 gene in stressed asexual stage parasites. A) Diagram of primers for qRT-PCR of SMS1, SMS1.1 and SMS1.2 transcripts (F: forward, R: reverse). B) SMS1 expression at 12-16 hours post invasion (unstressed ring), 24-28 hours post invasion (stressed trophozoite), 36-40 hours post invasion (stressed schizont) and 60-64 hours post initial invasion or 12-16 hours post second invasion (stressed ring) in SMS2 KO clones D4 (green) and C9 (black) relative to SMS1 expression in unstressed WT rings 12-16 hours post invasion and normalised to a reference gene as described in Materials and Methods. C) SMS1.1 expression in the same samples relative to SMS1.1 expression in unstressed WT rings 12-16 hours post invasion. D) SMS1.2 expression in the same samples relative to SMS1.2 expression in unstressed WT rings 12-16 hours post invasion. Data presented as means and standard deviation from three independent biological repeats. Culture stress (grey arrow) consisted of overpopulation without adequate medium supplementation as per gametocyte commitment protocol from day -3 to 0.

The impact of SMS2 disruption on gametocyte commitment rate is surprising given SMS2 is barely expressed in asexual stages (López-Barragán et al. 2011). Potentially SMS expression

is induced in asexual stages in response to stress prior to gametocytogenesis. SMS1 and 2 expression was therefore measured by qRT-PCR during stress-mediated gametocyte commitment (Figures 14 and 15). SMS2 and both alternative transcripts of SMS1 were expressed during stressed asexual stages in both WT and KO parasites (Figures 14 and 15). The altered gametocyte commitment rate observed in SMS2 KO parasites (Supplementary Figure 4B) is therefore plausible. Disruption of neither SMS1 nor SMS2 gene loci was compensated by up regulation of the reciprocal SMS gene during stress (Figures 14 and 15). In SMS1 KO parasites, the normal gametocytogenesis observed in Supplementary Figure 4A is therefore not the result of stress-induced compensation *via* SMS2 overexpression.

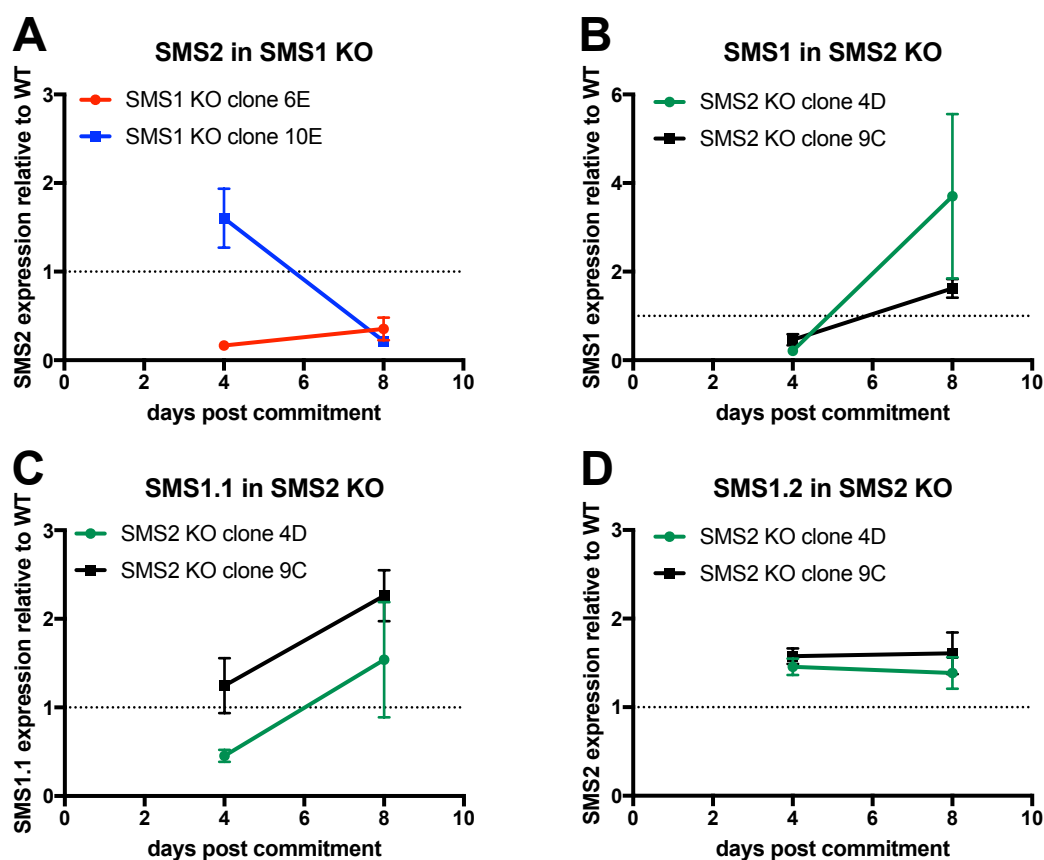


**Figure 16:** Expression of alternative SMS gene after disruption of the other SMS gene in gametocytes on day 4 and 8 post commitment. A) SMS2 expression in SMS1 KO clones E10 (blue) or E6 (red). B-D) Overall expression of SMS1 (B) or of each alternative SMS1 transcript, SMS1.1 (C) or SMS1.2 (D) in SMS2 KO clones C9 (black) and D4 (green). Gene expression from three biological repeats each measured in triplicate and represented as mean with standard deviation is relative to the expression level measured in 3D7 WT parasites at the same lifecycle stage, and normalised to a reference gene as described in Materials and Methods.



In gametocytes, expression of the non-disrupted SMS gene in SMS1 and SMS2 KO parasites was either similar to that of WT parasites (Figure 16B-D), or inconsistent between clones (Figure 16A). Overall, this suggests that disruption of one SMS gene is not compensated for by overexpression of the other in gametocytes.

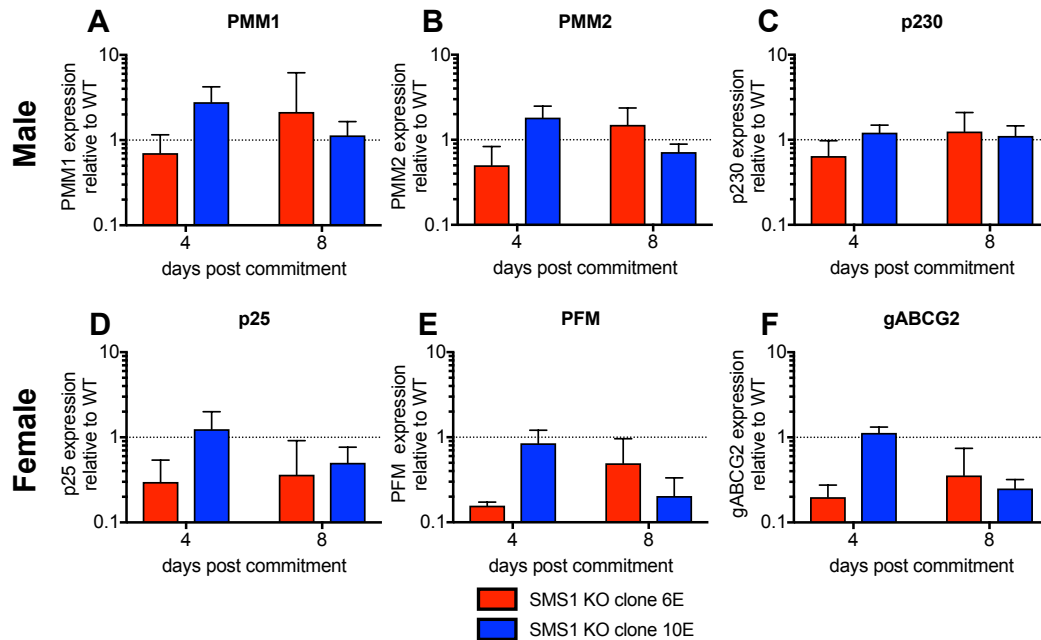


**Figure 17:** Expression of sex-specific markers in SMS1 KO clones 6E (red) and 10E (blue) relative to WT gametocytes on day 4 and 8 post commitment. A-C) Relative expression of male markers: putative male markers 1 (PMM1, *Plasmodium* exported protein (PHISTa) PF3D7\_1477700) and 2 (PMM2, PF3D7\_1438800) and p230 (6 cystein protein, PF3D7\_0208900). D-F) Relative expression of female markers: p25 (ookinete surface protein, PF3D7\_1031000), putative female marker (PFM, PF3D7\_1447600) and gABCG2 (gametocyte ABC transporter G family member 2, PF3D7\_1426500).

Given that the sex-specific transcriptome indicates that SMS2 expression in gametocytes is sex-biased (Lasonder et al. 2016), the impact of disrupting each SMS gene on the gametocyte sex ratio was next investigated. The sex ratio of SMS1 KO gametocytes was measured by qRTPCR of three male and three female markers validated in the previous chapter (Figure 17). WT and SMS1 KO gametocytes express all male-specific markers at a similar level (Figure 17 A-C). Female markers are expressed less in SMS1 KO clone 6E but not in SMS1 KO clone 10E relative to WT (Figure 17 D-F). Taken together, it appears that SMS1 KO gametocytes have a similar sex ratio to WT gametocytes at day 4 and 8 post commitment.

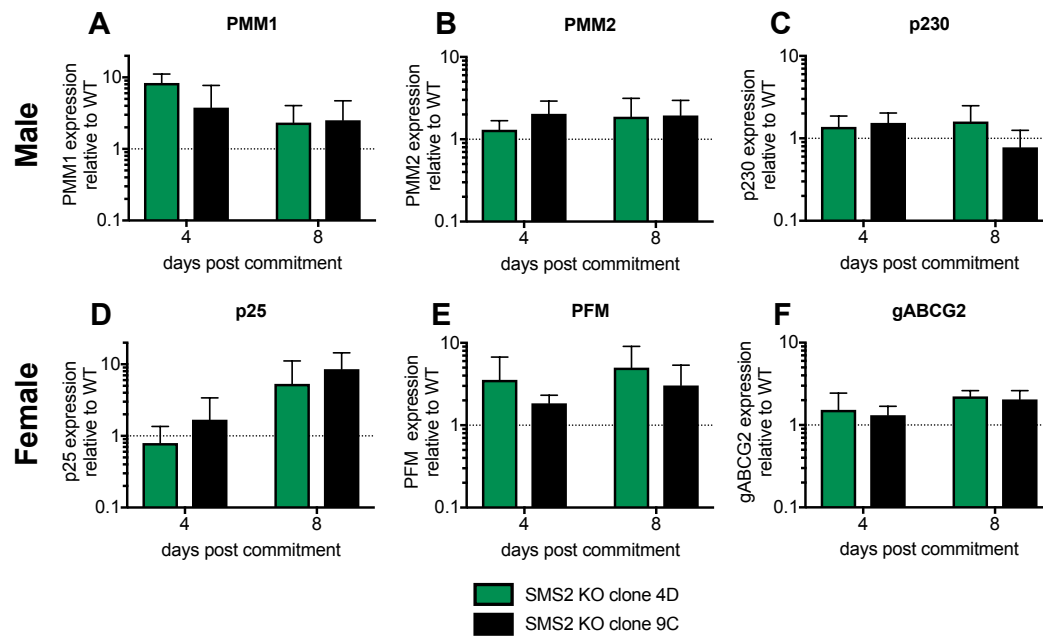


**Figure 18:** Expression of sex-specific markers in SMS2 KO clones 4D (green) and 9C (black) relative to WT gametocytes on day 4 and 8 post commitment. A-C) Relative expression of male markers: putative male markers 1 (PMM1, *Plasmodium* exported protein (PHISTa) PF3D7\_1477700) and 2 (PMM2, PF3D7\_1438800) and p230 (6 cystein protein, PF3D7\_0208900). D-F) Relative expression of female markers: p25 (ookinete surface protein, PF3D7\_1031000), putative female marker (PFM, PF3D7\_1447600) and gABCG2 (gametocyte ABC transporter G family member 2, PF3D7\_1426500).

Based on the same measurements, SMS2 KO gametocyte expression of sex-specific markers is more consistent between clones (Figure 18). The expression of male markers is similar in SMS2 KO and WT gametocytes, except on day 4 post commitment when putative male marker 1 is much more expressed in SMS2 KO gametocytes (Figure 18A-C). Female markers, especially *pfs25* and the putative female marker are expressed much more in mature SMS2 KO gametocytes compared to WT gametocytes (Figure 18D-F). The sex ratio of mature SMS2 KO gametocytes may be more female biased than WT gametocytes, suggesting SMS2 plays a sex-specific function in gametocytogenesis. SMS2 may suppress female gametocytogenesis and/or promote male gametocytogenesis.

### Discussion

In summary the function and abundance of lipids in *P. falciparum* gametocytes is sex-specific. Male/female gametocyte lipid dimorphism precedes gametocyte activation in *P. falciparum* (Figure 19).

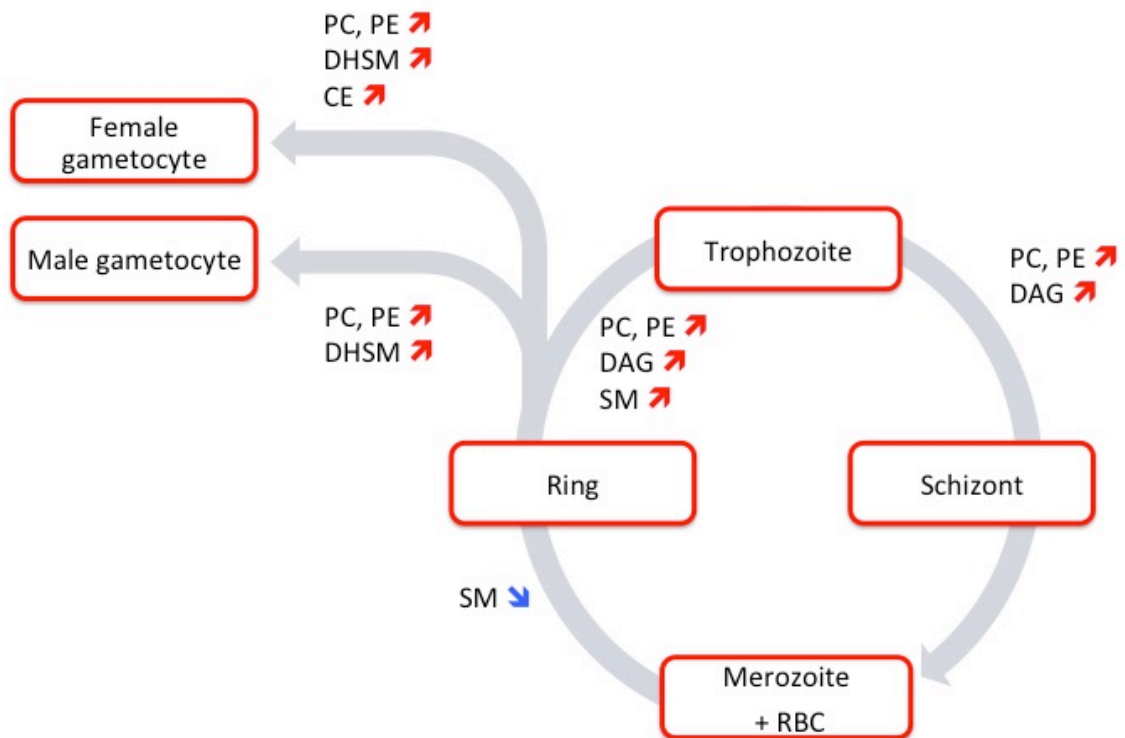


**Figure 19:** Overview of lipid changes in *P. falciparum* during asexual and sexual blood stages. Red and blue arrows indicate significant differences in lipid categories over 12 hour intervals of the asexual lifecycle between uninfected red blood cells (RBC) prior to merozoite invasion, ring stage infected red blood cells 12-16 hours post invasion (ring), trophozoite stage infected red blood cells 24-28 hours post invasion (trophozoite) and schizont infected red blood cells 36-40 hours post invasion (schizont); and between uninfected red blood cells and male or female gametocyte-infected red blood cells. DAG: diacylglycerol; DHSM: dihydrosphingomyelin; PC: phosphatidylcholine; PE: phosphatidylethanolamine; SM: sphingomyelin.

Female gametocyte-infected RBC stockpile the neutral lipid CE. The lipids in the fertilised zygote are contributed by the female gametocyte. While the zygote develops in the midgut lumen, neutral lipids are diverted from the blood meal to the eggs of the mosquito *via* lipophorin (Costa et al. 2018). The zygote is therefore vulnerable to lipid depletion in the mosquito midgut lumen, and may depend on maternal CE reserves at this lifecycle stage. Neutral lipid staining of the female gametocyte previously highlighted a large neutral lipid body (the G-spot) in the cytoplasm (Tran et al. 2014). Potentially the female specific CE store is amassed at the G-spot by the putative lipid transporter gABCG2.

Phospholipid composition was similar in male and female gametocyte-infected RBC, however it distinguished both male and female gametocyte-infected RBC from asexual parasite-infected RBC and uninfected RBC. Less phospholipids were present in gametocyte-infected RBC compared to asexual parasite-infected RBC consistent with Gulati et al. (2015) but not Tran et al. (2016). However, the increase in PS reported by Gulati et al. (2015) was not observed in this study, perhaps due to the fact that the lipid composition of each sex of gametocytes was investigated separately, or because PS is found beyond the parasite and therefore discarded in the saponin isolation of parasites. Surprisingly male gametocyte-infected RBC do not contain more phospholipids than female gametocyte-infected RBC. Phospholipids are the main component of membranes and are likely required for the rapid cell divisions during male gametocyte activation. While additional plasma membranes may not be required in females, female gametocytes contain an elaborate mitochondrial network bound by a double membrane rich in phospholipids, as well as abundant membrane bound osmiophilic bodies (Langreth et al. 1978; Jensen 1979; Sinden 1982; Ponnudurai et al. 1986). Although the phospholipid content of male and female gametocyte-infected RBC is similar, the allocation of phospholipids between organelles, and therefore the function of phospholipids may be sex-specific.

The most distinctive feature of gametocyte-infected RBC, particularly female gametocyte-infected RBC, is the presence of DHSM species. The present study provides greater resolution compared to previous lipidome studies that allude to greater sphingolipids in gametocytes compared to asexual stage parasites (Gulati et al. 2015; Tran et al. 2016). The presence of DHSM is consistent with descriptions of DHCer in gametocytes suggestive of active *de novo* sphingomyelin synthesis (Gulati et al. 2015).

The mechanism of DHSM accumulation in gametocytes is unclear. In mammalian cells supplied with DHCer rather than Cer, DHSM and other saturated sphingolipids were synthesised in addition to their desaturated counterparts (Kok et al. 1997). The same lipid profile was observed in mice lacking DHCer desaturase Des 1 (Siddique et al. 2012). By analogy, accumulation of DHSM in gametocytes may be a downstream effect of more DHCer in the sphingolipid synthesis pathway or a down regulation of DHCer desaturase in gametocytes.

The function of DHSM in gametocytes remains to be investigated. DHSM accumulation in mice resulting from the absence of DHCer desaturase Des 1 increased the expression of cell survival pathways and promoted resistance to apoptosis, presumably by limiting ceramide accumulation (Siddique et al. 2012). In *Plasmodium*, chemical inhibition of sphingomyelin synthase increased intracellular ceramide concentrations and reduced asexual growth (Pankova-Kholmyansky & Flescher 2006). Treatment of asexual stage parasites with tamoxifen had a different impact on lipids synthesised from DHCer or ceramide suggesting that ceramide and DHCer are not interchangeable (Piñero et al. 2018). Potentially the shunt towards saturated sphingolipid species in gametocytes is a means of reducing toxic ceramide build up.

Interestingly the higher abundance of DHSM and CE in female gametocyte-infected RBC appears to selectively protect them from compounds that target their synthesis. Potentially high lipid abundance regulates lipid synthesis with a negative feedback loop. In this case chemical inhibition of lipid synthesis would be redundant with the endogenous mechanism of regulating lipid synthesis, and therefore would not have an effect of cell viability.

Glibenclamide had no effect on female gametocyte viability at 10  $\mu\text{M}$ . Glibenclamide is an inhibitor of cholesterol esterification by ACAT in mammalian cells. In *P. falciparum*, glibenclamide has been identified as a new permeability pathway inhibitor, however it was not lethal to asexual stage parasites unless the serum content of the culture medium was reduced from 10 to 2 % (Kirk et al. 1993). In minimal serum conditions the asexual parasite proliferation half maximal growth inhibition concentration is 39  $\mu\text{M}$  (Kirk et al. 1993). Potentially the serum in the culture medium acts as a sink for glibenclamide as proposed by Kirk et al. (1993) and the effect of the drug on gametocytes would be amplified in serum depleted conditions. If this were the case, glibenclamide would not be a suitable antimalarial treatment in patients. Alternatively, if the mechanism of action of glibenclamide were through inhibition of the new permeability pathways rather than through inhibition of CE synthesis, gametocytes would be insensitive to glibenclamide since they lack these transporters (Lambros & Vanderberg 1979).

In the present study Sandoz 58-035 had a similar effect to glibenclamide i.e. no significant effect on gametocyte viability. In the closely related apicomplexan parasite *T. gondii*, 40  $\mu\text{M}$  Sandoz 58-035 slowed intracellular tachizoite replication, whether added to host cells before

infection or 2 h afterwards (Sonda et al. 2001). However, asexual *P. falciparum* is not sensitive to 2 h exposure to 10 µg/mL Sandoz 58-035 (Nawabi et al. 2003). The compound prevents CE synthesis by mammalian ACAT inhibition (Ross et al. 1984) but has not been investigated in the context of the new permeability pathways. The same possible mechanisms of action discussed for glibenclamide apply to Sandoz 58-035.

Perhaps the lack of significant effect of ACAT inhibitors on gametocyte viability is due to the gametocyte preference for Lecithin–cholesterol acyltransferase (LCAT) rather than ACAT mediated CE synthesis. Both compounds used to investigate CE synthesis (glibenclamide and Sandoz 58-035) target ACAT in mammalian cells. However, in mammalian cells CE is synthesised by both ACAT and LCAT, which differ in their source of acyl chains to esterify cholesterol. LCAT transfers an acyl chain from phospholipids onto cholesterol to form cholesteryl ester and lysophospholipids. ACAT on the other hand uses the acyl chain from Acyl CoA. *P. falciparum* encodes a homologue of the human LCAT (PF3D7\_0629300) which is inactive during asexual blood stages (Nawabi et al. 2003). This enzyme is involved in parasite egress from hepatocytes (Burda et al. 2015) and sporozoite migration through cells (Bhanot et al. 2005). It may also be interesting to study LCAT activity in *P. falciparum* gametocytes.

Alternatively gametocytes may be insensitive to inhibitors of CE synthesis because CE is scavenged from the host rather than synthesised *de novo*. This is consistent with the lack of incorporation of exogenously supplied labelled cholesterol or oleic acid in CE in asexual blood stage *P. falciparum* (Nawabi et al. 2003; Vielemeyer et al. 2004). Similar experiments with gametocyte stage *P. falciparum* are required to test this hypothesis.

In the present study 10 µM of GT11 had no effect on female gametocytes but a significant effect on male gametocyte viability. GT11 is an analogue of DHCer that cannot be metabolised by DHCer desaturase, thereby blocking the enzyme responsible for ceramide synthesis (Bedia et al. 2005). Rat DHCer desaturase mostly converts DHCer to ceramide, but 20 % of its activity *in vitro* converts DHSM to SM (Michel et al. 1997). If the same applies in *Plasmodium*, blocking DHCer desaturase with GT11 may therefore inhibit *de novo* synthesis of both SM and DHSM. The predominantly female accumulation of DHSM in gametocytes could theoretically result from more DHSM synthesis from DHCer and/or less DHSM desaturation to form SM. In the latter case the activity of DHSM desaturase would be

inversely proportional to the abundance of DHSM. Assuming that DHSM accumulation is important for parasite viability, parasites with less DHSM would therefore be more sensitive to inhibition of DHSM desaturase. This is consistent with the male gametocyte-specific effect of GT11 since male gametocytes contain less DHSM than female gametocytes. However, GT11 has no effect on asexual stage *P. falciparum* that lack DHSM at 8  $\mu$ M (Bedia et al. 2005). Together this suggests that *de novo* sphingolipid synthesis occurs in gametocytes but not asexual blood stage parasites; and that the female biased DHSM accumulation results at least in part from less DHSM desaturase activity in female gametocytes.

The other possible mechanism of DHSM accumulation is a sex-specific regulation of DHSM synthesis in *P. falciparum* gametocytes. DHSM and SM are synthesised *de novo* by two putative parasite encoded SMS. The function of each of these enzymes was investigated by reverse genetics.

Inhibition of sphingolipid metabolism by disruption of either SMS loci was not lethal, but incurred an asexual proliferation defect. This suggests that *de novo* sphingomyelin synthesis is active in asexual parasite proliferation. Surprisingly this defect was not exacerbated by depleting the culture medium lipids by 75 %. If *de novo* sphingomyelin synthesis were compensating for lack of SM availability in the host, the growth defect in SMS KO parasites would have been more pronounced in lipid depleted medium. SMS activity may be required for intracellular signalling rather than sphingomyelin itself being vital. Indeed, an important role of SMS in mammalian cells is reducing intracellular build up of toxic ceramide. Sphingomyelinase, which metabolises SM and produces ceramide, is expressed in asexual stages (Hanada et al. 2002). SMS may be required to balance sphingomyelinase activity in these stages.

Unlike in the published transcriptome that suggests that SMS2 is gametocyte specific (López-Barragán et al. 2011), this study shows that both genes are expressed in asexual blood stages and that at least one SMS gene is required for asexual parasite replication. Although the role of each alternative transcript of SMS1 was not investigated, transcript specific qRT-PCR showed that both transcripts are present in asexual parasites. This suggests that *de novo* SM synthesis contributes to asexual proliferation in the human RBC. If not temporally separated, it is plausible that the two SMS are spatially separated. Indeed, a quarter of the asexual parasite SMS activity is exported to the tubulovesicular network in host RBC cytoplasm

(Elmendorf & Haldar 1994). It would be interesting to investigate the localisation of each SMS during the lifecycle of the parasite.

Overall, qRTPCR of the alternative SMS transcript suggested that disruption of one SMS locus was not compensated by overexpression of the other SMS gene. This result is in favour of each SMS gene playing distinct roles in the biology of the malaria parasite, and excludes the possibility that *P. falciparum* encodes two tandem SMS genes as a means of quickly up regulating SMS expression. The expression of SMS2 in SMS1 KO, as measured by qRTPCR, unexpectedly appears to be down regulated during the asexual cycle (Figure 13B). This measurement was observed in mature gametocytes but was not replicated in the stressed asexual experiment, which suggests that this is either an experimental error, or that the expression of SMS2 is highly variable independently of lifecycle stage.

The interpretation of the qRTPCR results was generally limited by variation between clones. In particular, SMS2 expression in SMS1 KO clones at early gametocyte stage was inconsistent between clones (Figure 16A). This could be explained by low expression of the gene, meaning that small changes result in large fold changes. As it stands, only broad trends in the qRTPCR results could be interpreted.

The sex ratio of the KO gametocytes was gleaned from the expression of three markers for male and female gametocytes. In SMS1 KO gametocytes, the expression of both male and female markers was similar to WT gametocyte expression. SMS1 KO gametocytes therefore appear to have a normal sex ratio. However, female gametocyte markers were consistently more abundant in SMS2 KO clones than in WT gametocytes of the same age (Figure 18D-F) suggesting that SMS2 disruption increases the female bias of the gametocyte population. This is consistent with SMS2 playing a role in inhibiting female gametocytogenesis and/or promoting male gametocyte development. However, the predominantly female expression profile of SMS2 is inconsistent with this finding. In addition, male markers were either similar or more abundant in SMS2 KO gametocytes, which is inconsistent with the female gametocyte marker expression profile. In summary, estimates of the sex ratio in the SMS1 and SMS2 KO gametocyte populations need to be followed up with microscopic observations but may indicate that SMS2 expression impacts the sex ratio of gametocytes.



Overall, this study has shown that lipid metabolism is not only variable between parasite lifecycle stages, but is also sex-specific. These differences have implications for the effectiveness of drugs targeting metabolic pathways, and should be considered in the design of future transmission blocking antimalarial treatments. In terms of the fundamental biology of the parasite, the lipid profile of gametocytes is a testament to the parasite's ability to thrive in two radically different host environments. The lipidome presented here provides a reference for unravelling the complex sex-specific function of lipids in the *P. falciparum*.

## Part 2

### Lipid scavenging in *Plasmodium* gametocytes

#### Introduction

The lipid composition in the parasite is the result of both parasite lipid metabolism and lipid scavenging from the host environment. In the first part of Result Chapter 3 the contribution of *de novo* lipid synthesis was investigated. Here potential lipid scavenging from the host by *P. falciparum* gametocytes is investigated. Both schizonts and gametocytes have access to the same lipid resources in the host RBC. However, cultured gametocytes have different culture medium requirements than asexual blood stages, suggesting that gametocytes may source gametocyte-specific lipids from beyond the host cell. Given that the lipid scavenging in question is specific to *P. falciparum* gametocytes, the lipidome of *P. falciparum* and *P. berghei* gametocyte-infected RBC are firstly compared to identify *P. falciparum*-specific lipid dynamics.

Human serum and/or lipid rich bovine serum albumin AlbuMAX II are lipid supplements used in *P. falciparum* culture. The former is the parasite's natural lipid supply in the human host, but is more expensive than AlbuMAX II. Although asexual *P. falciparum* can be continuously cultured with only AlbuMAX II and no human serum (Cranmer et al. 1997), asexual parasites have defective erythrocyte membrane protein 1 trafficking to the host cell membrane (Franklin 2004). Similarly, gametocyte transmissibility and sex ratio is modified in the absence of human serum (Ponnudurai et al. 1989; Churcher et al. 2015; Duffy et al. 2016). For economical reasons, gametocytes are therefore cultured with a mixture of human serum and AlbuMAX II (Duffy et al. 2016). Here the lipid composition of three media that more or less support gametocyte transmissibility is analysed. For the complete list of lipids measured in this study, refer to Supplementary Table 3.

**Table 1:** Description of media compositions with lipid sources in bold.

Sample	Description
Asexual medium	RPMI 1640-HEPES with Glutamax, 10 mM glucose, 20 µg/mL gentamicin, 480 µM hypoxanthine, <b>0.5 % (w/v) AlbuMAX II</b>
Gametocyte medium 1	RPMI 1640-HEPES with Glutamax, 10 mM glucose, 20 µg/mL gentamicin, 480 µM hypoxanthine, <b>0.375 % (w/v) AlbuMAX II, 2.5 % (v/v) human serum</b>
Gametocyte medium 2	RPMI 1640 (from Gibco powder), 25 mM HEPES, 50 mg/mL hypoxanthine, 42 mL/L 5 % NaHCO <sub>3</sub> , <b>10 % (v/v) human serum</b>

The lipid profile of asexual medium (AlbuMAX II only, without human serum) and two types of gametocyte media (Table 1) are compared to identify possible lipid candidates that are essential for *P. falciparum* gametocytogenesis *in vitro*. Gametocyte medium 2 is known to support the development of viable gametocytes through to mosquito stage development, while the other very similar gametocyte medium 1 is the medium used in this study. Gametocyte media lipid characteristics are finally compared to the gametocyte-specific lipid modifications in *P. falciparum* gametocytes to infer whether these lipids are directly sourced from the human serum.

### **Results**

Table 2 summarises the gametocyte-specific lipid modifications induced by *P. falciparum* and *P. berghei* by comparing the lipid composition of the schizont-infected RBC to that of the gametocyte-infected RBC. Gametocyte sexes were only separated for the *P. falciparum* dataset.

**Table 2:** Comparison of *P. falciparum* and *P. berghei* lipid differences between schizont and gametocyte-infected RBC. Statistical significance of the difference in lipid sub-class abundance between the gametocyte-infected and schizont-infected RBC calculated by two-way ANOVA is indicated as follows: \*\*\*\*:  $p < 0.0001$ ; ns: not significant  $p > 0.01$ . Individual lipid species were compared with multiple student t-tests, as illustrated in Supplementary Figure 5 volcano plots. Lipid species indicated in the table have a  $p < 0.01$ . Red indicates a significant increase upon infection, blue a decrease.

Lipid class	Lipid sub class	<i>P. falciparum</i> female	<i>P. falciparum</i> male	<i>P. berghei</i> both sexes
Free cholesterol	-	ns	ns	ns
Phospholipid	PC	**** 36:5	**** 36:0, 36:5	ns 36:4
	PE	ns	ns	ns
	PS	ns	ns	ns
	PG	ns	ns	ns
Neutral lipid	TAG	ns	ns 50:1	ns
	DAG	ns 34:1	ns 34:1	****
	CE	**** 16:0	ns	ns
Sphingolipid	Cer	ns	ns 18:0	ns 22:1, 22:2
	SM	ns 18:0, 19:0, 21:0, 22:0	ns 26:1, 26:2	ns 18:1
	DHSM	**** 17:0, 18:0, 19:0, 20:0, 22:0	ns 16:0, 17:0, 18:0, 19:0, 20:0,	ns

Unlike schizont-induced lipid modifications in the RBC, overall gametocyte-infected RBC lipid modifications are consistently species-specific. *P. berghei* gametocyte-infected RBC accumulate less DAG relative to schizont-infected RBC. *P. falciparum* gametocyte-infected RBC modify the lipid composition in a sex specific manner, with the exception of PC being less abundant in both sexes of gametocyte-infected RBC relative to schizont-infected RBC. Only female *P. falciparum* gametocyte-infected RBC accumulate CE and DHSM significantly more than schizont-infected RBC.

Some individual lipid species are significantly different between gametocyte and schizont-infected RBC even though the overall lipid sub-class is not changed. Numerous individual

DHSM species are more abundant in *P. falciparum* male gametocyte-infected RBC relative to schizont-infected RBC, suggesting that DHSM accumulation is *P. falciparum* gametocyte specific but not sex-specific. DAG 34:1 is significantly less abundant in both male and female *P. falciparum* gametocyte-infected RBC relative to schizont-infected RBC, which is consistent with *P. berghei* gametocyte-infected RBC containing less overall DAG than schizont-infected RBC.

Other differences in lipid modifications are apparent at the individual lipid species level. SM species are more abundant in *P. falciparum* female gametocyte-infected RBC but less abundant in *P. falciparum* male gametocyte-infected RBC and in *P. berghei* gametocyte-infected RBC. Potentially SM modifications are sex-specific (increased species in females but decrease in males) and the lack of sex separation in the *P. berghei* gametocyte experiment has masked the sex-specific modifications.

Given the female bias of gametocytes, it is not surprising that other male-specific lipid modifications are not reflected in the *P. berghei* dataset. The observed male-specific increase in Cer 18:0 and decrease in TAG 50:1 may be masked by the female biased population of *P. berghei* samples.

A corollary of this last observation is that female specific lipid modifications that are not observed in the *P. berghei* dataset are likely to be species-specific. In particular, CE accumulation in *P. falciparum* female gametocytes may not only be a sex-specific phenotype, but also a *P. falciparum* species-specific phenotype.

In summary, gametocyte-infected RBC lipid modifications are not conserved between *P. berghei* and *P. falciparum*. Given the female-bias of the gametocyte population, a sex-specific lipidomics analysis of *P. berghei* gametocytes may reveal additional male-specific changes. However, *P. falciparum*-specific lipid modifications observed in both sexes of gametocytes or in female gametocytes alone are likely species-specific.

Having identified gametocyte-specific lipid modifications to the infected host RBC, the next section of this chapter explores the *P. falciparum* gametocyte extracellular lipid requirements. Unlike asexual blood stage parasites, *P. falciparum* gametocytes are known to require human serum culture medium supplementation to be transmissible to mosquitos. Asexual parasite

culture medium is supplemented with AlbuMAX II (lipid rich bovine serum albumin) whereas gametocytes are cultured in medium containing both AlbuMAX II and human serum. The gametocyte medium 2 is known to support the development of viable gametocytes through to mosquito stage development, while the other gametocyte medium 1 is the medium used in this study. Note that throughout this thesis, both asexual and sexual *P. falciparum* cultures were maintained in “gametocyte medium 1” containing both AlbuMAX II and human serum.

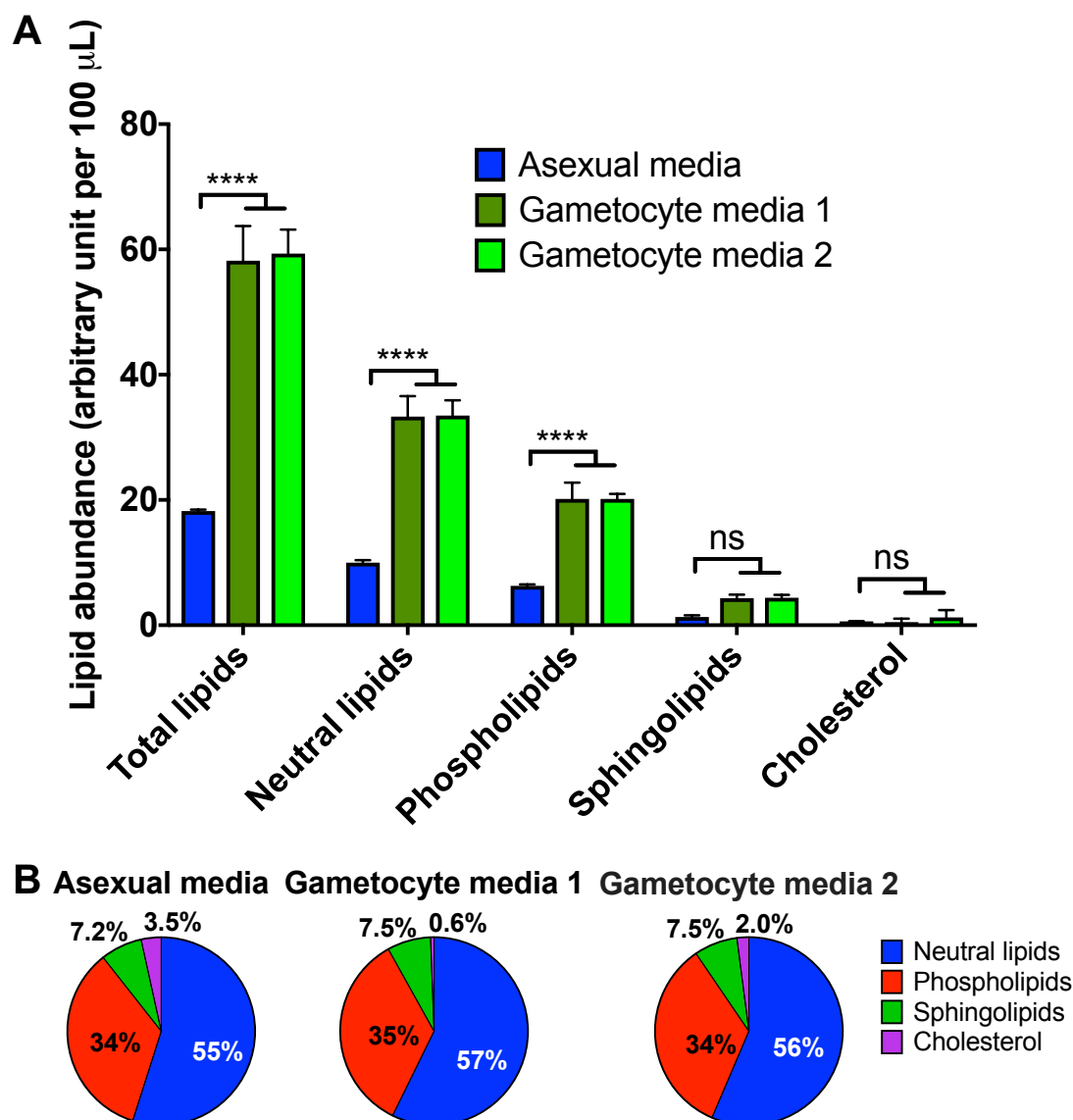


**Figure 1:** Media options lipidome overview. Mean abundance with standard deviation (A) and mean proportions (B) of lipids in 100 µL asexual culture medium, gametocyte culture medium 1 or 2 as defined in Materials and Methods. Statistical significance from two-way ANOVA indicated as follows: \*\*\*\*:  $p < 0.0001$ , ns: not significant  $p > 0.1$ . CE: cholesteryl ester; PC: phosphatidylcholine; FC: free cholesterol.

The lipid composition of 100  $\mu\text{L}$  of each media was measured by direct infusion MSMS. Rather than calibrating the lipid abundance to standard units as done in previous experiments, the lipid quantities are expressed in an arbitrary unit for relative quantification between samples. All media formulas contain the four main classes of lipids: neutral lipids, phospholipids, sphingolipids and cholesterol (Figure 1). Both gametocyte media are more lipid-rich than asexual medium and contain significantly more phospholipids and neutral lipids (Figure 1A). The gametocyte medium 1 is similar to gametocyte medium 2, although it has the lowest proportion of cholesterol of all three media (Figure 1B).

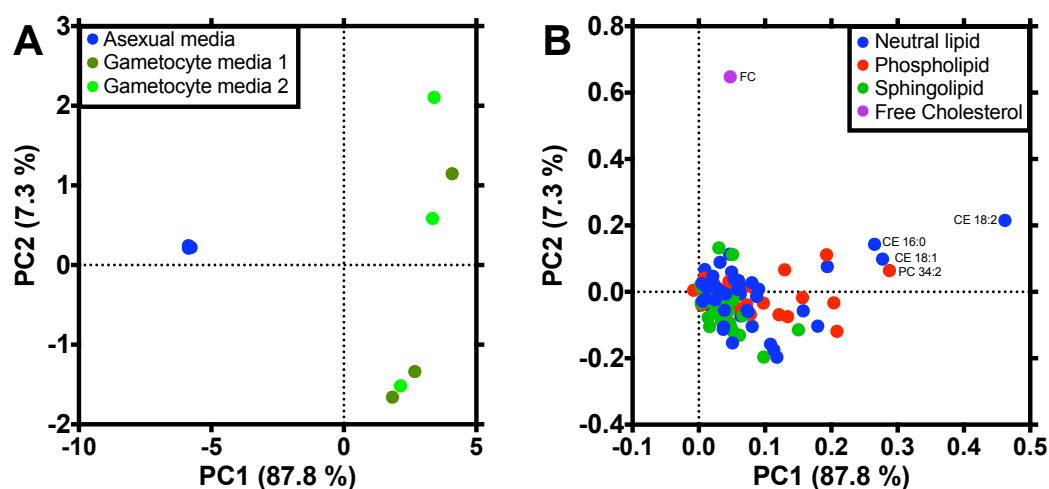


**Figure 2:** Principal component analysis plot (left) and corresponding loading plot (right) of total lipids in 100  $\mu\text{L}$  asexual culture medium and gametocyte culture medium 1 and 2 as defined in Materials and Methods. PC1 and 2: first and second principal component; CE: cholesteryl ester; PC: phosphatidylcholine; FC: free cholesterol.

At the individual lipid species level, both gametocyte media are distinguished from asexual medium in a principal component analysis of all lipids (Figure 2A). CE 16:0, CE 18:1, CE 18:2 and PC 34:2 are distinctively more abundant in the gametocyte media relative to asexual medium (Figure 2B). However, the principal component analysis of total lipids does not clearly distinguish the two gametocyte media (Figure 2A).

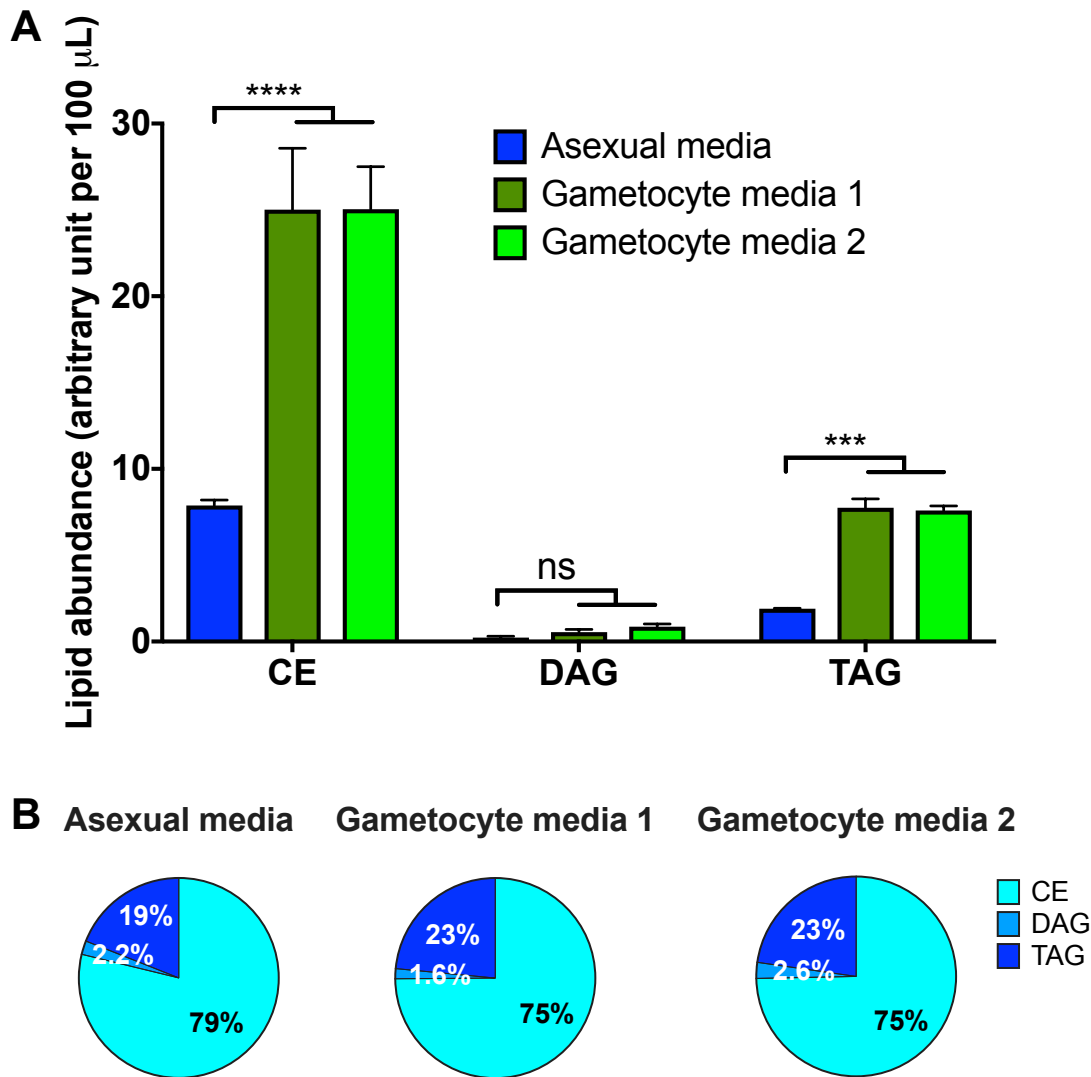


**Figure 3:** Media options neutral lipidome overview. Mean abundance with standard deviation (A) and mean proportions (B) of neutral lipids in 100  $\mu\text{L}$  asexual culture medium and gametocyte culture media 1 and 2 as defined in Materials and Methods. Statistical significance from two-way ANOVA indicated as follows: \*\*\*\*:  $p < 0.0001$ , \*\*\*:  $p < 0.01$ , ns: not significant  $p > 0.1$ . CE: cholesteryl ester; DAG: diacylglycerol; TAG: triacylglycerol.

Neutral lipids are also more abundant in gametocyte media samples compared to asexual medium neutral lipids (Figure 1A). Both TAG and CE are more abundant in gametocyte media options relative to asexual medium (Figure 3A). The main neutral lipid in all samples is CE, while DAG is the least abundant neutral lipid (Figure 3B). TAG represents almost a quarter of gametocyte media neutral lipids, but only 19 % of asexual medium neutral lipids.



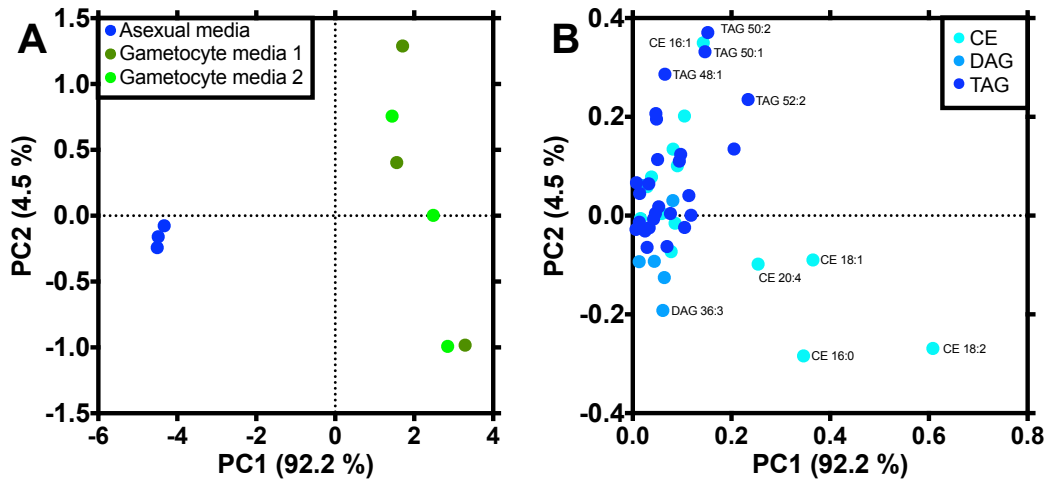


**Figure 4:** Principal component analysis plot (left) and corresponding loading plot (right) of neutral lipids in 100  $\mu$ L asexual culture medium and gametocyte culture media 1 and 2 as defined in Materials and Methods. PC1 and 2: first and second principal component; CE: cholesteryl ester; DAG: diacylglycerol; TAG: triacylglycerol.

At the individual lipid species level, mostly four CE species are characteristically more abundant in both gametocyte media samples relative to asexual medium: CE 16:0, CE 18:1, CE 18:2 and CE 20:4 (Figure 4A and B). Overall, neutral lipids are similar between gametocyte media options but distinct from asexual medium neutral lipids.

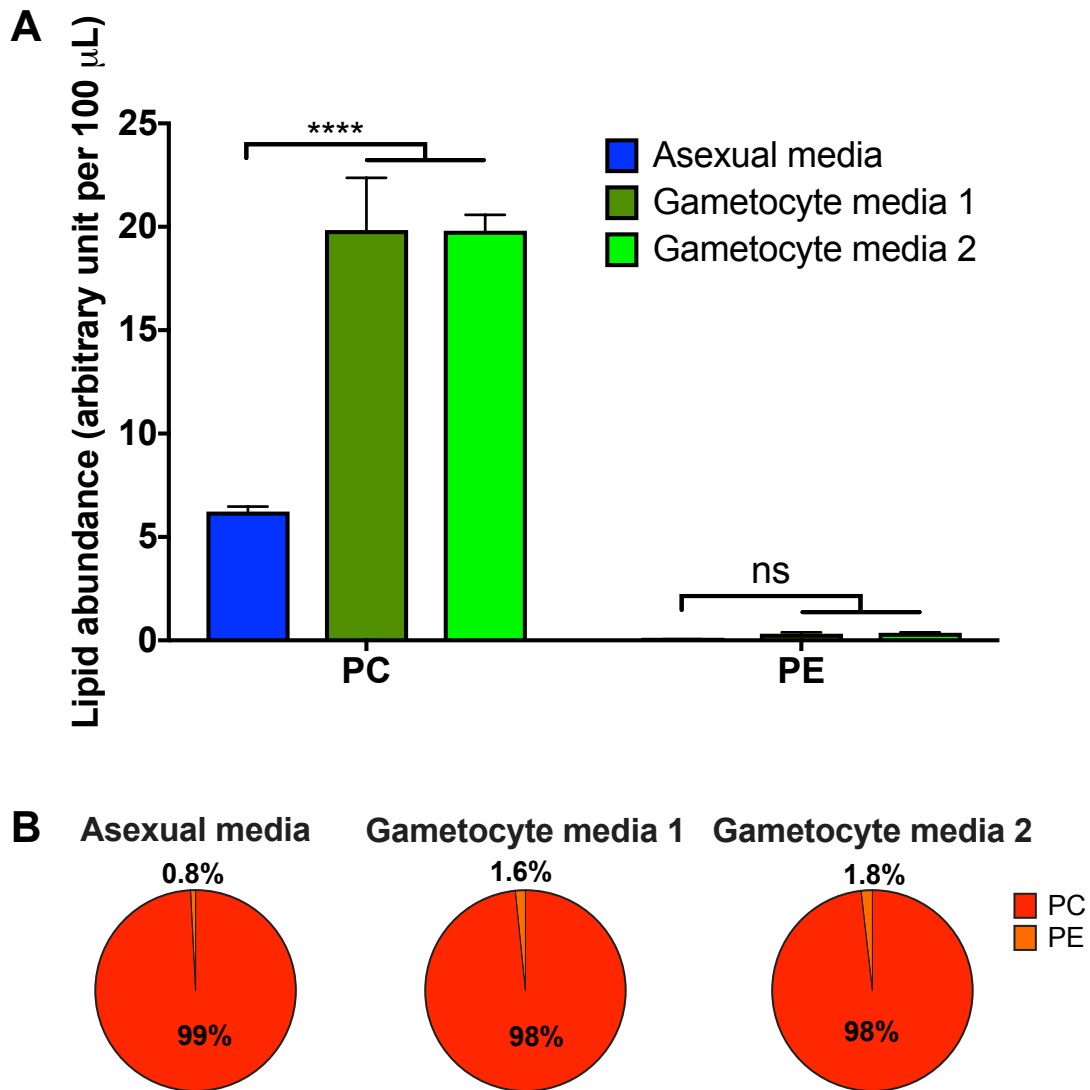


**Figure 5:** Media options phospholipidome overview. Mean abundance with standard deviation (A) and mean proportions (B) of phospholipids in 100  $\mu$ L asexual culture medium and gametocyte culture media 1 and 2 as defined in Materials and Methods. Statistical significance from two-way ANOVA indicated as follows: \*\*\*\*:  $p < 0.0001$ ; ns: not significant  $p > 0.1$ . PC: phosphatidylcholine; PE: phosphatidylethanolamine.

The only phospholipids identified in either media type were PC and trace amounts of PE (Figure 5). PC is more abundant in gametocyte media than in asexual medium (Figure 5A), however in all media samples PC dominates the phospholipid composition (Figure 5B).

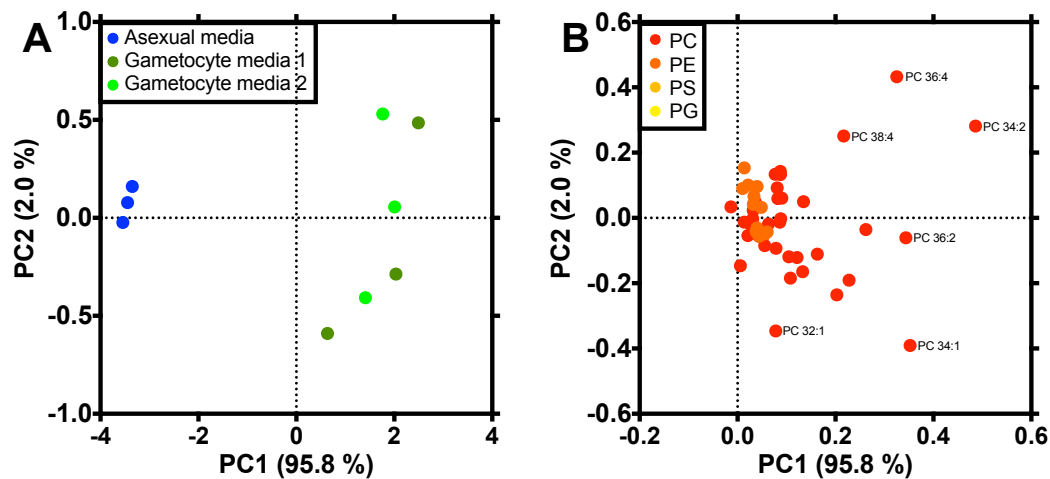


**Figure 6:** Principal component analysis plot (left) and corresponding loading plot (right) of phospholipids in 100  $\mu$ L asexual culture medium and gametocyte culture media 1 and 2 as defined in Materials and Methods. PC1 and 2: first and second principal component; PC: phosphatidylcholine; PE: phosphatidylethanolamine.

At the individual lipid species level, four PC species mostly distinguish asexual from gametocyte media options: PC 34:2, PC 34:1, PC 36:4, PC 36:2 (Figure 6A and B). Overall, both gametocyte media phospholipids are similar but a handful of PC species distinguish gametocyte from asexual medium phospholipid composition.

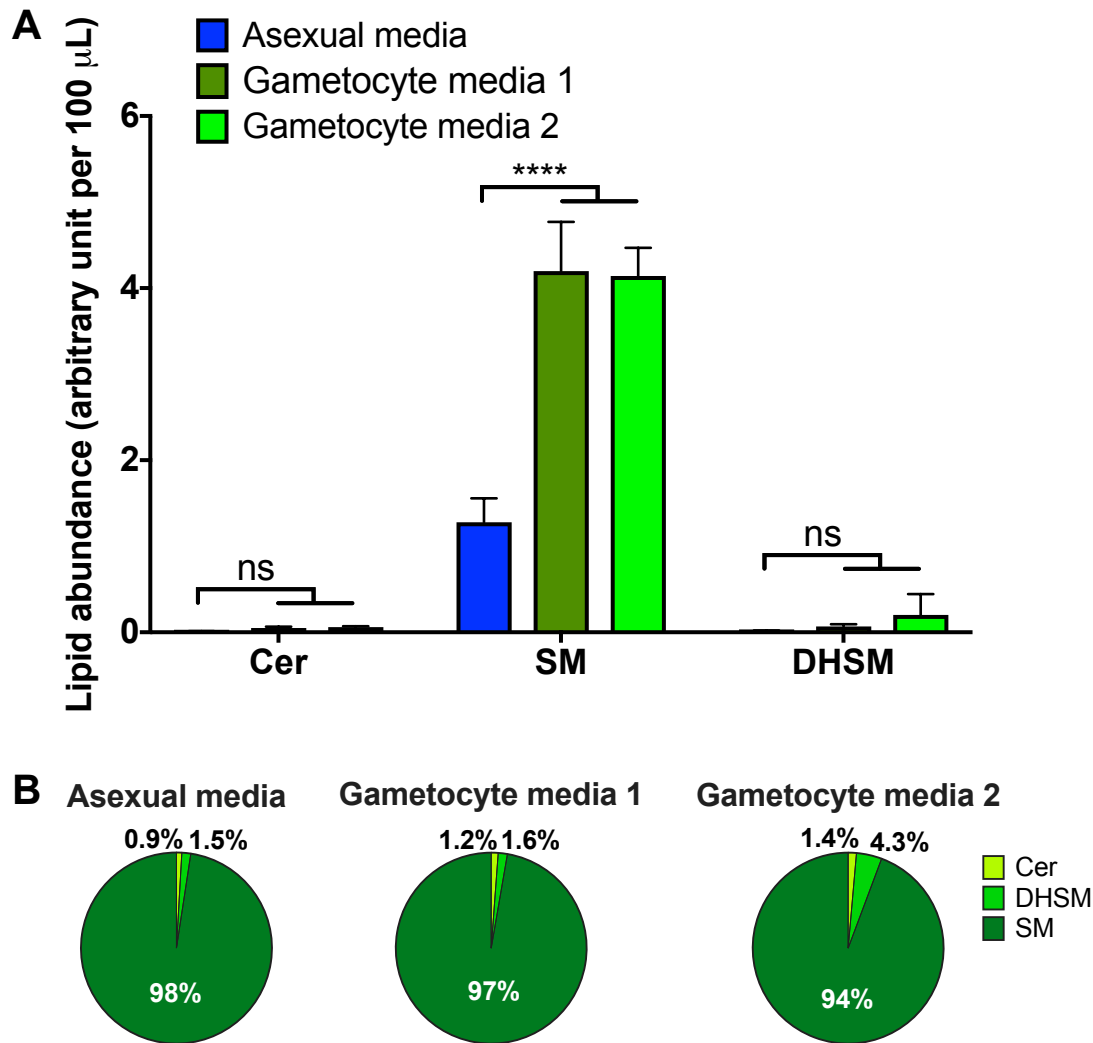


**Figure 7:** Media options sphingolipidome overview. Mean abundance with standard deviation (A) and mean proportions (B) of sphingolipids in 100  $\mu\text{L}$  asexual culture medium and gametocyte culture media 1 and 2 as defined in Materials and Methods. Statistical significance from two-way ANOVA indicated as follows: \*\*\*\*:  $p < 0.0001$ ; ns: not significant  $p > 0.1$ . Cer: ceramide; DHSM: dihydrosphingomyelin; SM: sphingomyelin.

Sphingolipids in all media types are mostly SM species (Figure 7). SM is more abundant in gametocyte media but other sphingolipids are not significantly different between media types (Figure 7A). The gametocyte medium 2 contains a slightly higher proportion of DHSM compared to asexual medium (Figure 7B).

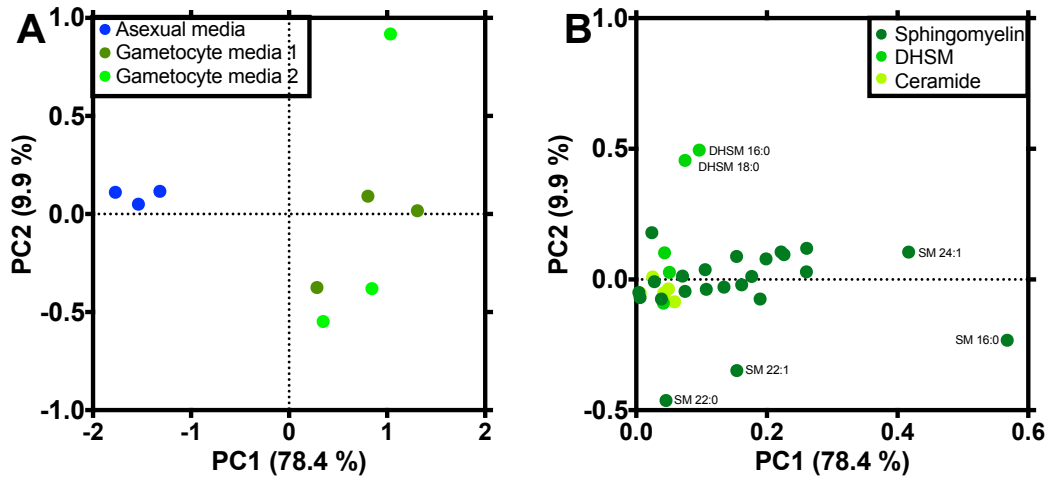


**Figure 8:** Principal component analysis plot (left) and corresponding loading plot (right) of sphingolipids in 100  $\mu$ L asexual culture medium and gametocyte culture media 1 and 2 as defined in Materials and Methods. PC1 and 2: first and second principal component; Cer: ceramide; DHSM: dihydrosphingomyelin; SM: sphingomyelin.

Principal component analysis of sphingolipids clearly separates asexual medium lipids from gametocyte media lipids, but does not distinguish between the two gametocyte media types (Figure 8A). SM 24:1 and SM 16:0 are particularly more abundant in gametocyte media compared to asexual medium (Figure 8B). DHSM 16:0, DHSM 18:0, SM 22:1 and SM 22:0 abundance is variable among biological replicates of both types of gametocyte media.

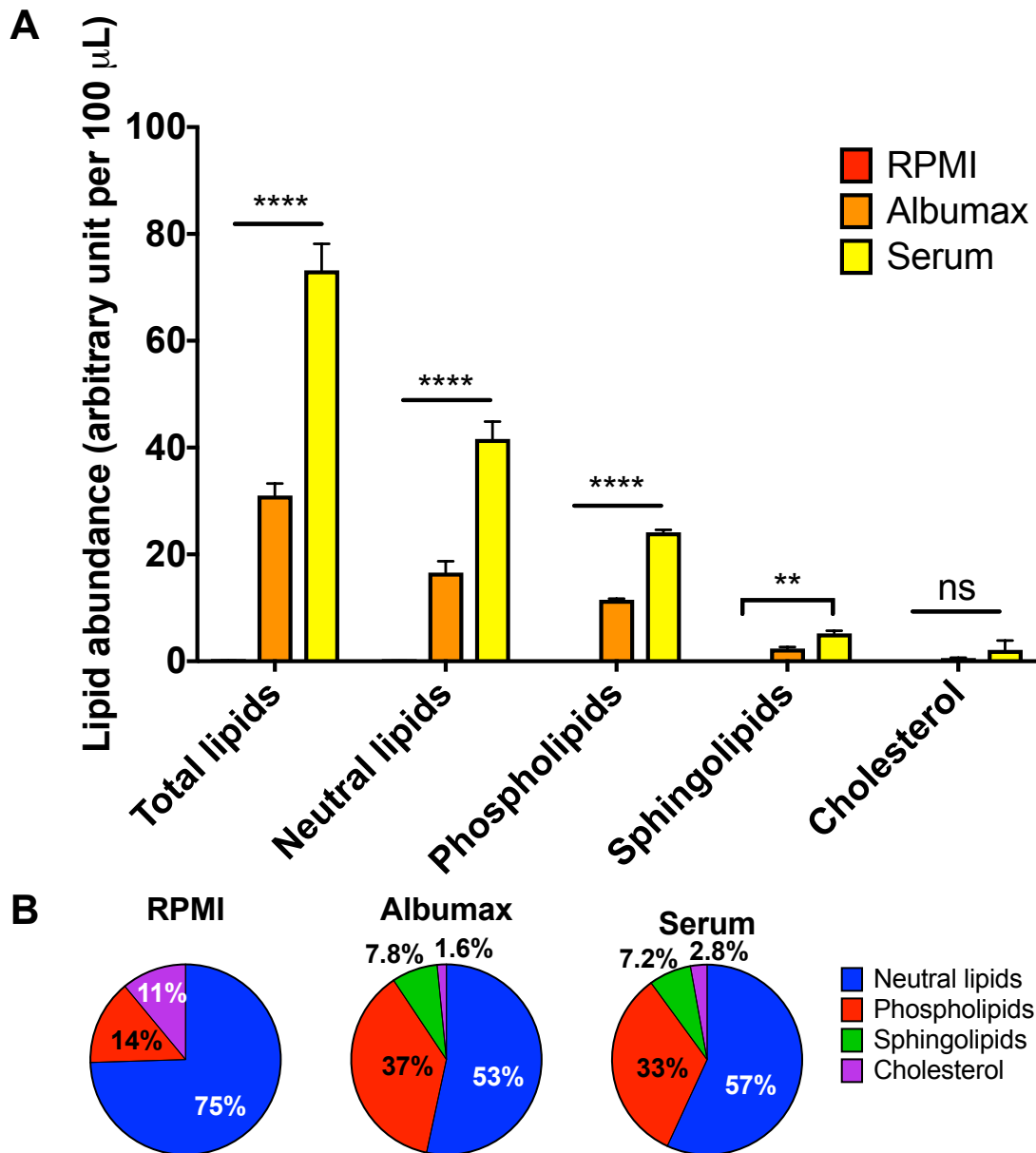


**Figure 9:** Media supplements lipidome overview. Mean abundance with standard deviation (A) and mean proportions (B) of lipids in RPMI, AlbuMAX II and human serum as defined in Material and Methods. Statistical significance from two way ANOVA indicated as follows: \*\*\*\*:  $p < 0.0001$ ; \*\*:  $p < 0.01$ ; ns: not significant  $p > 0.1$ . Straight line indicates statistical significance between all three samples. Sphingolipids in AlbuMAX II are not significantly different to sphingolipids in RPMI or serum.

The main difference between asexual medium and gametocyte media is that gametocyte media is supplemented with human serum (Table 1). In asexual medium human serum is replaced with commercial AlbuMAX II. The RPMI medium contains only traces of lipids so the main lipid supply to the culture (apart from the host cells) is either AlbuMAX II or serum. Given that mass spectrometry is a highly sensitive measurement of lipid abundance, the lipids detected in the RPMI sample likely represent trace amounts of lipids in the background of all

measurements. Serum contains more total lipids, neutral lipids and phospholipids than AlbuMAX II (Figure 9A), but both lipid supplements mostly contain neutral lipids (Figure 9B).

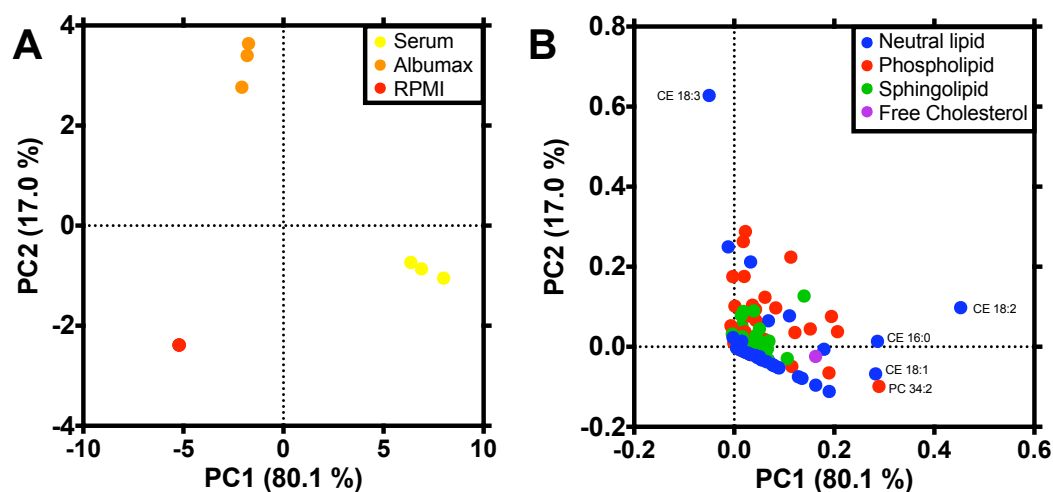


**Figure 10:** Principal component analysis plot (left) and corresponding loading plot (right) of lipids in RPMI, AlbuMAX II and human serum as defined in Material and Methods. PC1 and 2: first and second principal component; CE: cholesteryl ester; PC: phosphatidylcholine.

Despite the proportions of phospholipids, neutral lipids, sphingolipids and cholesterol being similar between AlbuMAX II and serum (Figure 9B), principal component analysis of the individual lipid species clearly separates AlbuMAX II, serum and RPMI (Figure 10A). All three biological repeats of each sample are very similar, as indicated by their tight grouping in the principal component analysis plot. The lipid composition of serum can be variable *in vivo*, so serum from at least five independent human donors was pooled together in each sample. Similarly commercial AlbuMAX II is pooled from many individuals so each biological repeat is an average composition. CE 18:3 is characteristically abundant in AlbuMAX II, whereas CE 18:2, CE 18:1, CE 16:0 and PC 34:2 are particularly abundant in human serum (Figure 10B). In summary, replacing AlbuMAX II with serum for gametocyte culturing not only increases total lipid abundance in the culture medium, but also specifically decreases CE 18:3 abundance and increases the abundance of three CE species and PC 34:2.

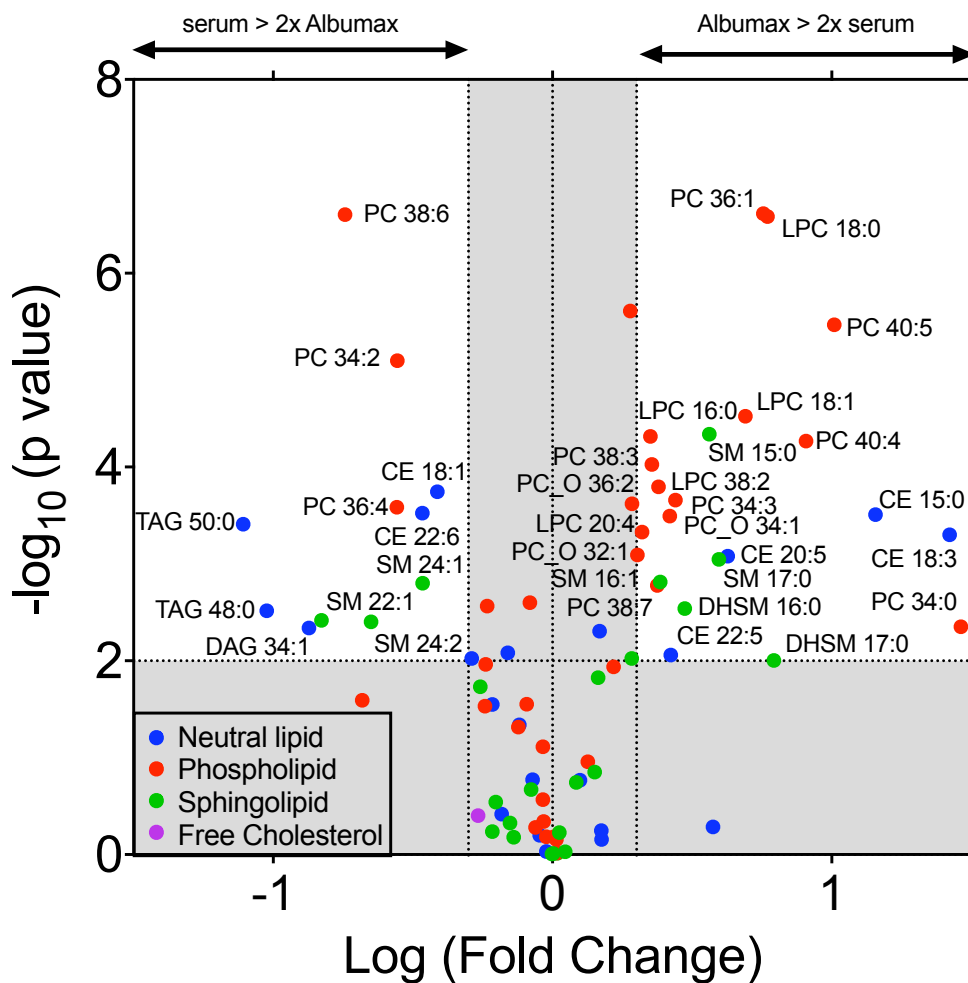


**Figure 11:** Volcano plot of lipids in AlbuMAX II and serum after normalisation to total lipid abundance. Grey area indicates changes that are less than 2 fold and/or with  $p > 0.01$ . CE: cholesteryl ester; DAG: diacylglycerol; DHSM: dihydrosphingomyelin; PC: phosphatidylcholine; LPC: lysophosphatidylcholine; TAG: triacylglycerol.

After normalisation of total lipids in human serum and AlbuMAX II, more individual lipids are differentially distributed between AlbuMAX II and serum (Figure 11). Phospholipids, neutral lipids and sphingolipid species are distributed differently between AlbuMAX II and serum. AlbuMAX II contains a variety of more abundant phospholipid species and sphingolipid species, whereas CE species are the only more abundant neutral lipids. Of note is the higher abundance of minor sphingolipid DHSM and minor phospholipid LPC. Serum on the other hand contains the greatest variety of neutral lipids that are more abundant relative to AlbuMAX II. Indeed, CE, DAG and TAG species are significantly more abundant in serum compared to AlbuMAX II. Overall, after normalisation of total lipid abundance, AlbuMAX II contains more individual lipid species that are more abundant than human serum, including minor lipid species such as DHSM and LPC, which may have functional significance for *Plasmodium* parasite proliferation.



## **Discussion**

The gametocyte lipid profile of *Plasmodium* parasites is parasite species and sex-specific. By comparing the sex-specific lipid modifications in *P. falciparum* gametocytes to the differences in lipid composition between asexual and gametocyte media, and between AlbuMAX II and human serum, the source of some of these lipids can be inferred.

Many lipid modification in the gametocyte-infected RBC are different to the gametocyte-infected RBC lipid composition. As discussed previously, parasite stage-specific lipid modifications in the host RBC reflect differences in the biology of asexual and sexual blood stage parasites such as parasite proliferation in asexual blood stages versus preparing for inter-host transmission in gametocytes. Each parasite stage clearly has specific lipid demands that may be met by stage-specific lipid supply. This likely includes stage-specific regulation of lipid metabolic pathways and lipid scavenging mechanisms. In comparing asexual and sexual blood stage lipid supply, it is important to note that *in vivo* lipid supply involves two different host environments: blood and bone marrow. The bone marrow is a lipid rich environment that may be better replicated in culture by the lipid rich gametocyte media.

All of the lipid differences between gametocyte and schizont-infected RBC are parasite-species-specific. This is consistent with the very different gametocytogenesis between *P. falciparum* and *P. berghei*. The parasite-species-specific lipid modifications may contribute to differences in gametocyte morphology between parasite species: *P. falciparum* gametocytes are characteristically sickle shaped. In addition, gametocytogenesis is much longer in *P. falciparum* compared to *P. berghei*, and this may impact the gametocyte's lipid requirements during gametocytogenesis. Finally, some of the lipid differences between parasite species may reflect differences in the host RBC composition, as discussed in Result Chapter 1. Overall, differences in lipid composition between *P. berghei* and *P. falciparum* reflect the parasite-species-specific gametocytogenesis in *Plasmodium*.

Overall CE, and CE 16:0, are significantly more abundant in female *P. falciparum* gametocyte infected RBC compared to schizont-infected RBC. As discussed in the first section of this chapter, CE is also more abundant in female gametocyte-infected RBC compared to males. Overall CE and CE 16:0 are also more abundant in human serum compared to AlbuMAX II, and in gametocyte media compared to asexual medium. Potentially gametocytes (particularly female gametocytes) have a greater CE requirement and

directly source CE from the media. Supplementation of asexual medium with CE 16:0 may be sufficient to culture transmissible *P. falciparum* gametocytes. To determine whether this is a female-specific lipid requirement, it would be interesting to investigate whether female gametocytes cultured in asexual media with CE 16:0 could be crossed with male gametocytes cultured in asexual media without added CE 16:0.

Overall PC abundance is greater in gametocyte media compared to asexual media, despite PC being less abundant in both male and female *P. falciparum* gametocyte-infected RBC compared to schizont-infected RBC. Four PC species are particularly more abundant in gametocyte media compared to asexual medium (Figure 6). These lipid species may be particularly important for gametocyte development and transmissibility. Neither of the significantly less abundant PC species in *P. falciparum* is different between media options. Together these results suggest that PC differences between asexual and gametocyte media do not impact the lipidome of gametocytes. Consistent with this observation, previous studies have implicated PC synthesis from host serine via phosphoethanolamine methyltransferase to be essential for gametocytogenesis (Bobenchik et al. 2013).

Interestingly LPC species are more abundant in AlbuMAX II compared to human serum. LPC depletion has previously been implicated in commitment to gametocytogenesis (Brancucci et al. 2017). This raises the possibility that AlbuMAX II may not be deficient in an essential lipid, but rather contains excessive inhibitory lipid(s).

Although both male and female *P. falciparum* gametocytes accumulate DHSM species, two of these species were more abundant in AlbuMAX II compared to human serum. DHSM could be present in excess in both human serum and AlbuMAX II, or this could indicate that DHSM is synthesised *de novo* by the parasite, regardless of the lipids in the host environment. Indeed, most significantly different sphingolipid species between *P. falciparum* gametocyte-infected RBC and schizont-infected RBC are not different between asexual and gametocyte media. This suggests that gametocyte and sex-specific *de novo* sphingolipid metabolism occurs in *P. falciparum*.

Similarly, neutral lipid depletion in *P. falciparum* gametocyte-infected RBC relative to schizont-infected RBC (TAG 50:1 and DAG 34:1) is independent of differences in media composition. This suggests that *P. falciparum* gametocytes catabolise neutral lipids.

In summary, *P. falciparum* gametocyte lipid metabolism is sex-specific and species-specific. *P. falciparum* gametocytes accumulate lipids by *de novo* sphingolipid synthesis and by scavenging CE species from human serum. Human serum may be favourable to gametocyte development because it provides CE species accumulated in female gametocytes and because it lacks LPC, which reduces gametocyte commitment. Although *P. berghei* remains the most amenable species of *Plasmodium* for *in vivo* studies, the clear inter-species disparities between gametocytes demands direct analysis of the human pathogen *P. falciparum* for clinical applications.

## Conclusion

The sex-specific biology of *P. falciparum* gametocytes is reflected in their lipid metabolism. Female gametocyte-infected RBC especially accumulate DHSM and CE, which may contribute to post-fertilisation development of the zygote in the mosquito. Male gametocyte-infected RBC that have less DHSM and CE than female gametocyte-infected RBC are more susceptible to compounds that target their synthesis, or genetic disruption of sphingolipid synthesis. The gametocyte lipidome also suggests that scavenging of CE species from human serum may be essential for *in vitro* culture of *P. falciparum* gametocytes. These findings have implications for the suitability of lipid-targeting compounds as transmission blocking anti-malarials, and for *P. falciparum* gametocyte culturing *in vitro*.

# Discussion

## 1. Summary of results

Gametocytes are the parasite lifecycle stage responsible for transmission of malaria from humans to the mosquito vector and are key to parasite sexual reproduction. Compared to asexual blood stage parasites that cause the symptoms of malaria, the fundamental biology of gametocytes is relatively unexplored. This thesis investigates the sex specific biology of *Plasmodium* by comparing asexual to sexual blood stage parasites and by contrasting male and female gametocytes.

Given the key functional role of lipids, the biology of *Plasmodium* parasites is investigated through lipidomics. In the asexual blood stages preceding gametocytogenesis, *P. falciparum* and *P. berghei* schizont-infected RBC accumulate PC, potentially for membrane biogenesis for parasite replication. Parasite-species-specific lipid changes may compensate for differences in the lipids available in mouse and human RBC, reflecting parasite-host co-evolution. The switch from asexual replication to gametocytogenesis is accompanied by a change in the lipid composition of the infected RBC. *P. berghei* gametocyte-infected RBC lipids are distinct to those of the host cell, suggesting *de novo* lipid synthesis occurs in preparation for transition from the human to mosquito host.

A FACS-based method for separating male and female gametocytes was developed in order to investigate gametocytes in a sex-specific manner. As a proof of concept this method was applied to identify novel sex-specific markers for monitoring the sex ratio of gametocytes in the field. In addition, putative identification of sex-specific DNA methylation in functionally related genes reinforced the concept that gametocyte biology is distinct to that of asexual blood stage parasites and is sex-specific.

*P. falciparum* sex-specific lipidomics revealed female gametocytes accumulate significantly more DHSM and CE than males. The function of *de novo* SM (and DHSM) synthesis in gametocytes appears to be sex-specific based on chemical and genetic inhibition of the metabolic pathway. CE on the other hand may be directly imported from the host serum by female gametocytes.

Overall, this thesis confirmed that gametocyte biology is significantly distinct to that of asexual parasite stages in two species of *Plasmodium* and highlighted disparities between

male and female *P. falciparum* gametocytes. Given the importance of gametocytes in both parasite transmission and sexual reproduction, the findings of this thesis contribute to our understanding of this parasite's sexual reproduction that could be applied to develop malaria transmission-blocking interventions in the field.

## **2. Lipidomics as a tool to study parasite biology**

In this thesis the biology of two species of malaria parasites was investigated through the lens of lipidomics. The main advantage of lipidomics is the detailed information on a large set of variables (lipid species). Here the abundance and proportion of over 230 individual lipid species was quantified. This enabled the identification of parasite stage and sex-specific lipid species as well as changes in the overall lipid categories during the parasite lifecycle.

However, the lack of spatial resolution to the lipidome limits the scope for interpretation. Previous reports suggest that the lipidome of the parasite is not homogenous: apicoplast lipids are distinctive (Botté et al. 2013) and there is an inner cholesterol gradient through the membranes of the parasite (Tokumasu et al. 2014). In gametocytes it would be interesting to determine whether the female-specific accumulation of CE localises to the same neutral lipid body as gABCG2, the so-called “G-spot” (Tran et al. 2014). Given the structural differences between the mitochondria of asexual and sexual blood stage *P. falciparum* (Langreth et al. 1978), the mitochondrial specific lipidome may also be stage specific. Indeed, by measuring the lipidome in the whole infected host cell, local changes in the lipidome may be hidden.

Similarly, the temporal resolution of the lipidome in this thesis is insufficient for monitoring highly dynamic events such as intracellular signalling pathways. Many complex intracellular signalling networks likely mediate progression through the parasite lifecycle. More detailed analysis of a whole pathway over a shorter time period would be more appropriate for measuring intracellular signalling events, such as those involving phosphatidylinositol derivatives.

Assuming that the lipid content of a cell is indicative of general cellular processes involving lipids (storage, structure and intracellular signalling), some functional significance could be inferred from the types of lipids present in each sample. For example, accumulation of PC in schizont-infected RBC reflects the membrane biogenesis requirement of schizonts. The present study provides a foundation for more targeted investigations of lipids in *Plasmodium*.

As a proof of concept, the functional significance of sex-specific sphingolipid abundance was investigated by disrupting parasite SMS genes. This specifically dissected the role of *de novo* SM synthesis. Similar approaches could add functional significance to other the lipid differences between parasite stages and sex identified in this thesis.

In comparing the lipids of infected and uninfected host cells, and lipids in the culture medium, potential sources for parasite lipids could be identified, whether scavenged from the host cell, imported from the serum or synthesised *de novo*. These observations could be complemented by investigating the uptake and metabolism of labelled exogenous lipids as previously investigated in the context of exogenous oleic acid (18:1) incorporation into TAG in asexual blood stage parasites (Gulati et al. 2015). In addition, the biological relevance of imported lipids in cultured gametocytes should be tested *in vivo* given that sequestration in the lipid-rich bone marrow is not replicated in culture. Organ on a chip technology of human bone marrow (Torisawa et al. 2014) could be a means of modelling parasite-host interactions during gametocytogenesis.

In summary, detailed characterisation of the nature and abundance of lipids in the parasite and host cell highlighted stage-specific lipid metabolism; lipid scavenging from the host and the state of cellular processes involving lipids. The lipidome established in this thesis provides a holistic map that may direct more targeted studies of lipids in the context of *Plasmodium* biology.

### **3. Lipid scavenging and synthesis by *Plasmodium* parasites**

Parasites scavenge some lipids from the host but also synthesise others *de novo*. In general parasitism is accompanied by loss of parasite genes that are functionally redundant with those of the host. In the context of lipid metabolism, this theory suggests that parasite synthesised lipids are unavailable or unreliably available in the host environment.

Parasites may require a specific lipid species that is not present in the host or the host may not be a reliable source of the lipid that must therefore be synthesised *de novo*. This could be the case of PG synthesis in blood stage parasites. PG is a phospholipid specific to the mitochondria and therefore absent in the host RBC and human serum. Although the parasite encodes enzymes for *de novo* synthesis of PG, the essentiality of this metabolic pathway has not been investigated in *Plasmodium*.



Alternatively, parasites could require more of the lipid than is available for scavenging in the host. Either the lipid is a limited resource, or the parasite is unable to scavenge the lipid from the host. Scavenging lipids from the host could be detrimental for the host cell - requiring parasites to moderate lipid scavenging to maintain host cell viability. Despite fatty acids being abundant in the human host, parasite FASII is essential for liver stage parasite development (Vaughan et al. 2009). This may be an example parasite *de novo* synthesis supplementing lipid scavenging to preserve the host cell integrity. If so, the mechanism by which the parasite regulates FASII in response to host cell fatty acid requirements warrants further investigation.

Another possibility is that parasites require *de novo* synthesis activity, rather than the synthesised lipid itself. Lipid metabolism is not only a source of lipids, but also generates intracellular signalling molecules required for many parasite functions. In the absence of SMS activity, asexual blood stage *P. falciparum* proliferation was slowed in both normal and lipid depleted culturing conditions. Given that SMS regulates ceramide and DAG abundance in the process of synthesising SM, it is plausible that *de novo* SM synthesis is required for generating intracellular signalling molecules regardless of the availability of SM in the host. Similarly, neutral lipid synthesis may be a means of sequestering toxic fatty acids, as previously observed in *T. gondii* (Nolan et al. 2018), rather than neutral lipids themselves being functionally significant.

The results of this thesis suggest that *de novo* synthesis occurs in gametocytes, perhaps in preparation for transmission to the mosquito vector. Unlike the scenarios outlined above where *de novo* synthesis addresses parasite lipid requirements in real time, gametocyte lipid synthesis could anticipate future lipid needs. This suggests that gametocyte lipid metabolism is pre-programmed rather than responsive to environmental queues and implies that the parasite has a means of storing lipids for future use.

Despite the parasite's ability to synthesise some lipids *de novo*, it is dependent on the availability of other lipids in the host. This parasite dependence could potentially be exploited to treat malaria and may be a naturally occurring form of resistance to malaria. Female gametocytes appear to stockpile CE, potentially by importing it directly from the serum. If CE is important for transmission of malaria, it would be interesting to compare

transmission rates with local serum CE concentration. Previously human CE transfer protein deficiency was shown to reduce the pathogenesis of *Schistosoma japonicum* parasites, which may explain the geographical overlap between the parasite distribution and CE transfer protein deficiency occurrence in East Asia (Okumura-Noji et al. 2001; Yokoyama 2014). CE transfer protein inhibitors have been developed in the context of treating hypercholesterolemia and associated atherosclerosis and cardiovascular disease. The most promising candidate, anacetrapib, was effective and showed no side effects in phase III clinical trials but development was later discontinued by Merck (Page et al. 2016; Cicero et al. 2018). Potentially this drug could be repurposed for blocking malaria transmission.

Overall, the investigation of lipids in *Plasmodium* parasites and their host cells suggests that lipid sources vary depending on the lipid species, host lipid availability and parasite lifecycle stage. Essential lipid sources for the parasite are potential antimalarial drug targets.

#### **4. The cost of sex for *Plasmodium* parasites**

In organisms where sexual reproduction contrasts to asexual reproduction, the cost of sex is at least two fold: committing to sexual reproduction is at the expense of more efficient asexual proliferation. In *P. falciparum*, one sexually committed merozoite at best forms either 32 female macrogametes or  $32 \times 8 = 256$  male microgametes in 12 days. On the other hand each asexually committed merozoite could form  $32^6$  daughter merozoites over the same period, making the cost of female gametocytogenesis up to  $32^5$  (~ 33.5 million) fold in *P. falciparum*. How could such a costly mechanism have been maintained? The answer is likely in the long-term benefits of sexual reproduction.

Firstly, the cost may be a parasite means of responding to host stress induced by asexual blood stage proliferation. Each sexually committed gametocyte slightly reduces the overall parasite burden, potentially reducing malaria symptoms and increasing the lifespan of the host. In addition, gametocytes sequester in the host bone marrow that may provide shelter from the increasingly inhospitable environment of a dying host. Interestingly the most virulent parasite, *P. falciparum*, produces gametocytes the slowest and therefore at the greatest cost of asexual parasite proliferation. Perhaps this is because *P. falciparum* asexual blood stage proliferation is more harmful for the human host and triggers a greater parasite stress response.

Secondly, in the broader context of the parasite lifecycle, gametocytes are the only parasite stage that can complete the lifecycle, ultimately resulting in transmission of the parasite to a new human host. Without gametocytogenesis, all parasites would be doomed to die with the human host. Gametocytogenesis is indeed triggered by stress (Carter et al. 2013), and represents the parasite's escape route.

Finally, like any sexual reproduction, gametocytogenesis is a means of genetic recombination that accelerates adaptation (McDonald et al. 2016). In the context of *Plasmodium* parasites, the need to acquire drug resistance mechanisms is a strong selective pressure for acquiring and maintaining drug resistance genes.

The apparently high cost of sexual reproduction on *Plasmodium* parasites is therefore justified and naturally selected for in the context of the parasite lifecycle.

## **5. Confirmation of anisogamy in a unicellular organism**

While anisogamy is common in multicellular organisms, isogamy is the norm in unicellular organisms (Lehtonen et al. 2016). Apicomplexans including *Plasmodium* gametocytes are an interesting exception to this rule.

The results of this thesis show that female gametocytes stockpile neutral lipids, presumably in preparation for development in the relatively nutrient poor mosquito. In anisogamy, parental investment is unequal between females that provide most of the resources for zygote development, and males that contribute only their gene pool. In general, anisogamy increases the size of the adult but decreases the period of fertilisation competency (since male gametes contain limited resources). In the case of *Plasmodium*, reserves may be required to sustain the parasites prior to encystation through gamete activation, fertilisation and zygote development. Gamete activation is sex-specific, but extremely rapid and likely relies mostly on immediate energy sources such as pools of ATP rather than tapping into lipid reserves. Lipid reserves may be destined for zygote development rather than gamete activation and fertilisation. While *Plasmodium* sex dimorphism is evident at the time of fertilisation, this thesis shows that resources are accumulated in a sex-specific manner prior to gamete activation.

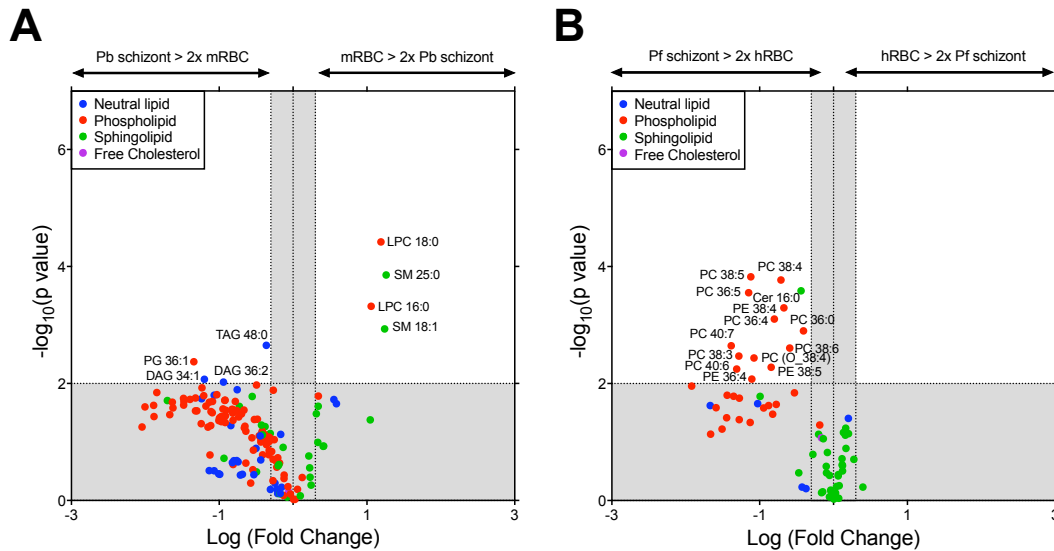
Mature male and female gametocytes also appear to differ in their intragenic DNA methylation. Preliminary results in this thesis support the existence of DNA methylation in *P. falciparum*, and identify parasite stage and sex-specific patterns. Given that many differentially methylated genes are involved in gene transcription and translation, it is tempting to speculate that parasite stage and sex-specific gene expression is regulated by these epigenetic markers. However, the impact of DNA methylation on gene expression, if any, still needs to be experimentally proven in *Plasmodium*. In addition, the timing of the sex-specific DNA methylation warrants further investigation as it may not only distinguish *Plasmodium* sexes, but also determine gametocyte sex. DNA methylation appears to be relatively rare in *P. falciparum*. This highlights the need for a sensitive detection method such as bisulfite sequencing to identify DNA methylation patterns with confidence. The presence of only a few DNA methylation events suggests that the epigenetic marker is highly targeted in *Plasmodium*, and potentially functionally significant. The sex-specific DNA methylation patterns identified in this thesis indicate that sex dimorphism in *Plasmodium* is reflected in epigenetic markers, although the functional significance of such markers is unclear.

Recently measuring the gametocyte sex ratio was proposed as a means of predicting malaria transmissibility (Tadesse et al. 2018). The sex-specific traits identified in this thesis support the notion that gametocyte biology is sex-specific and present novel markers for measuring the gametocyte sex ratio. By enriching our understanding of the fundamental sex-specific biology of *Plasmodium* gametocytes, this thesis opens new avenues for monitoring and blocking malaria transmission.

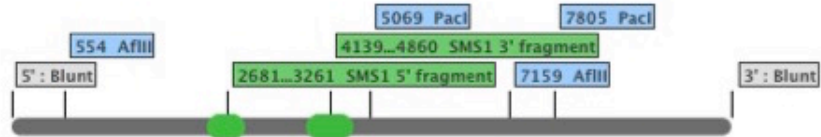
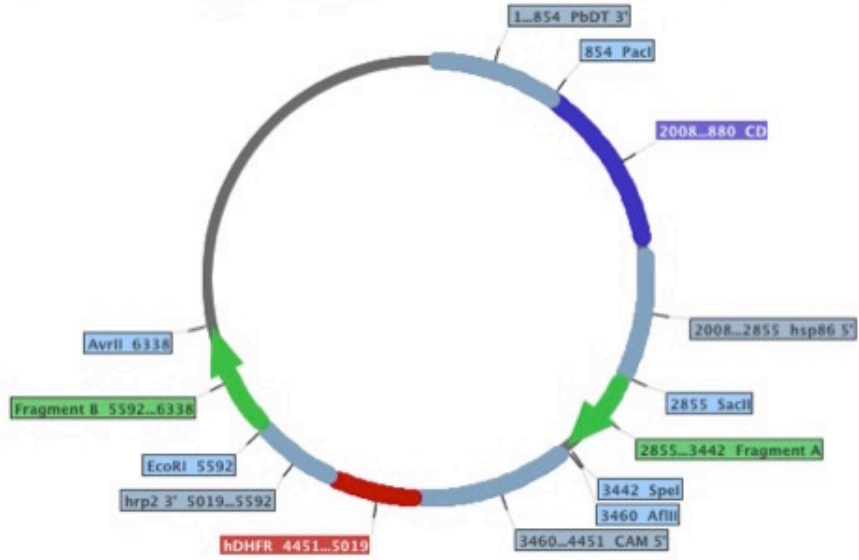
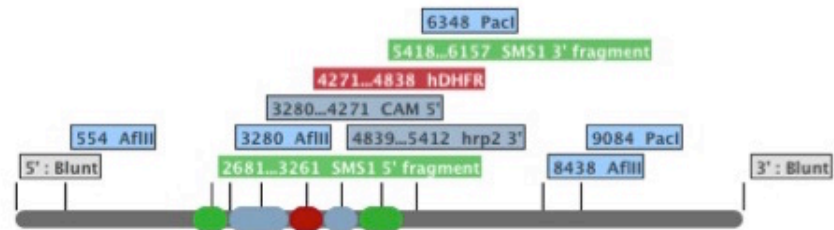
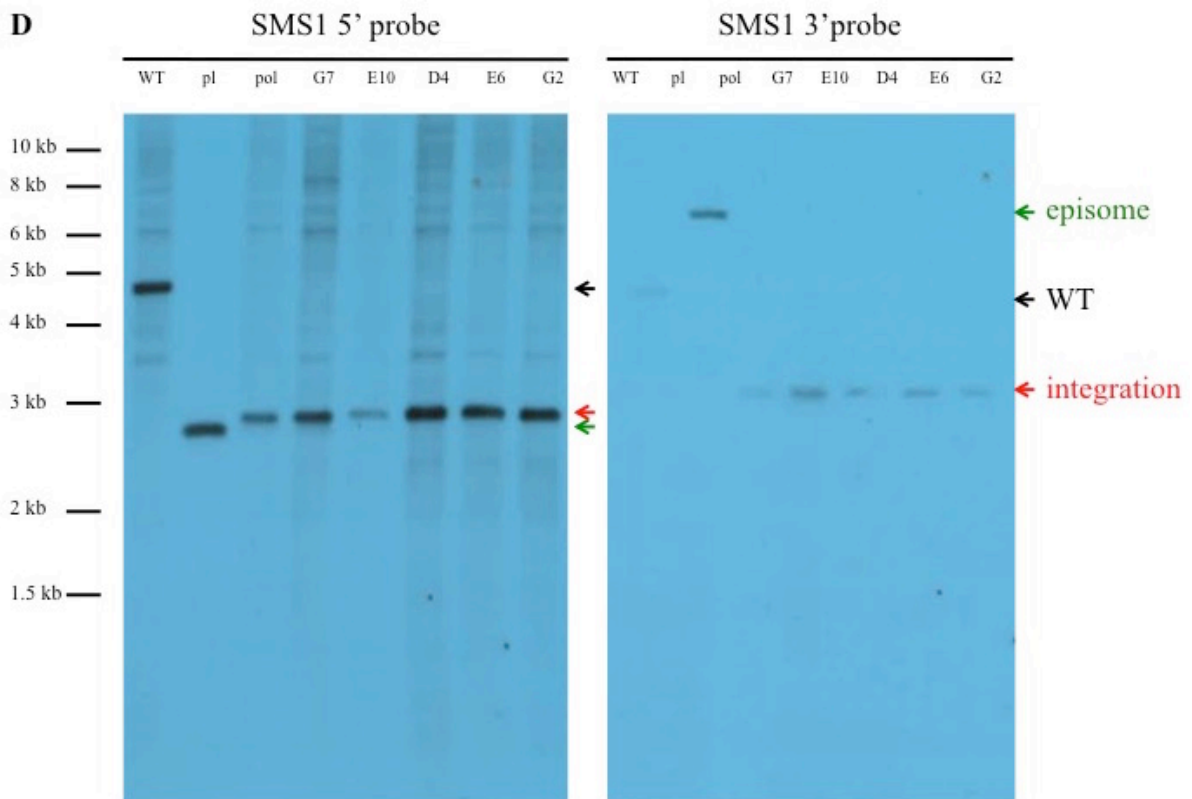
## **6. Conclusion**

Sexual reproduction in *Plasmodium* parasites is preceded by male and female gametocytogenesis and transmission from the human host to mosquito vector. This lifecycle transition not only delineates a parasite stage switch, but also distinguishes male and female sexes. The sex-specific functions of gametocytes result in sex-specific epigenetic markers, gene expression and lipid metabolism that may have implications for effectively monitoring and blocking malaria transmission.

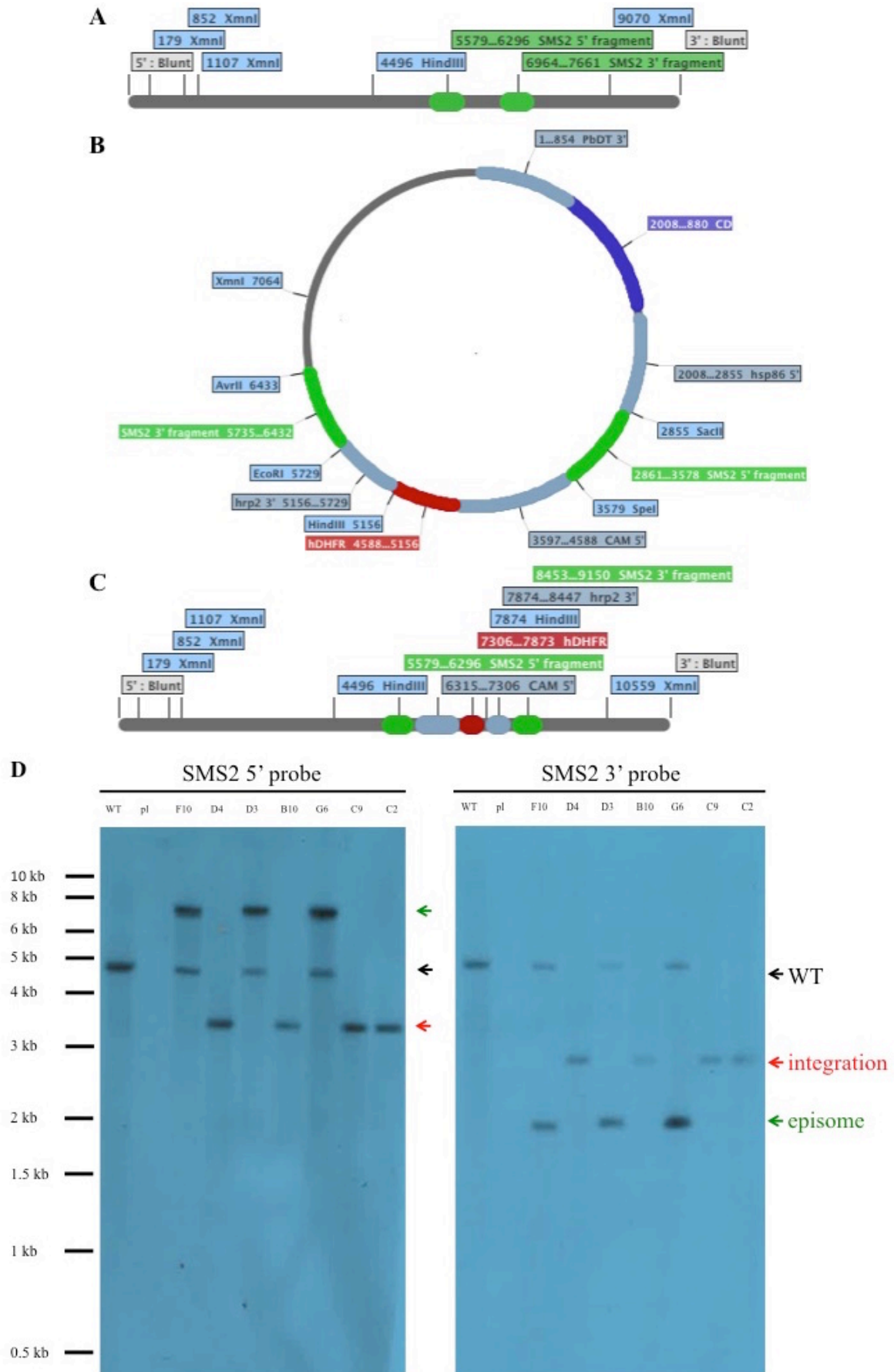
## Supplementary figures



**Supplementary Figure 1:** Volcano plot of total lipids in gametocyte and schizont infected RBC with statistical significance from student t tests. A) *P. berghei* schizont infected mouse RBC (Pb schizont) compared to uninfected mouse red blood cell (mRBC). B) *P. falciparum* schizont infected human RBC (Pf schizont) compared to uninfected human RBC (hRBC). Grey area indicates changes that are less than two fold and/or not significant ( $p > 0.01$ ). P values were calculated by multiple student t-tests. DAG: diacylglycerol, LPC: lysophosphatidylcholine, PC: phosphatidylcholine, PE: phosphatidylethanolamine, PG: phosphatidylglycerol, SM: sphingomyelin, TAG: triacylglycerol.

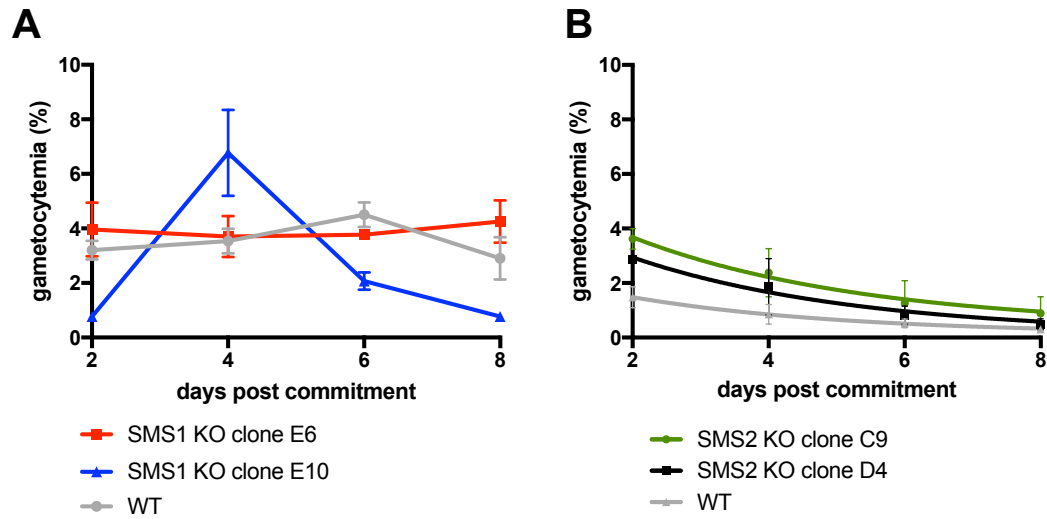
**A****B****C****D**

**Supplementary Figure 2:** Disruption of SMS1 by homologous recombination. A-C) Schematic of WT SMS1 locus with surrounding fragment of genomic DNA (A), pCC-1/SMS1 plasmid (B) and disrupted SMS1 locus with surrounding fragment of genomic DNA (C). SMS1 gene is disrupted by double homologous recombination at the 5' and 3' extremities of the gene in green (SMS1 5' fragment between SacII and SpeI restriction sites and SMS1 3' fragment between EcoRI and AvrII restriction sites), which inserts positive selection marker human dihydrofolate reductase (hDHFR, red) under the control of the calmodulin promoter (CAM 5') and histidine rich protein 2 3' untranslated region (hrp2 3'). The plasmid also contains negative selection marker cytosine deaminase (CD, purple) under the control of heat shock protein 86 promoter (hsp86 5') and *P. berghei* dihydrofolate reductase 3' untranslated region (PbDT 3') that are lost by double recombination. AflIII and PacI restriction digest sites used for Southern blot are also indicated. D) Southern blot showing disruption of SMS1 locus. DNA from 3D7 wild type (WT), SMS1 KO plasmid (pl), polyclonal 3D7 transfected with SMS1 KO plasmid (pol) or clonal 3D7 transfected with SMS1 KO plasmid (G7, E10, D4, E6, G2) digested with AflIII and PacI restriction enzymes and probed with 5' homologous flank probe (SMS1 5' probe, left) or 3' homologous flank probe (SMS1 3' probe, right). Expected SMS1 5' probe band lengths: WT locus: 4,515 bp (black arrow), episomal locus: 2,606 bp (green arrow), integrated locus: 2,726 bp (red arrow). Expected SMS1 3' probe band lengths: WT locus: 4,515 bp (black arrow), episomal locus: 6,243 bp (green arrow), integrated locus: 3,068 bp (red arrow).

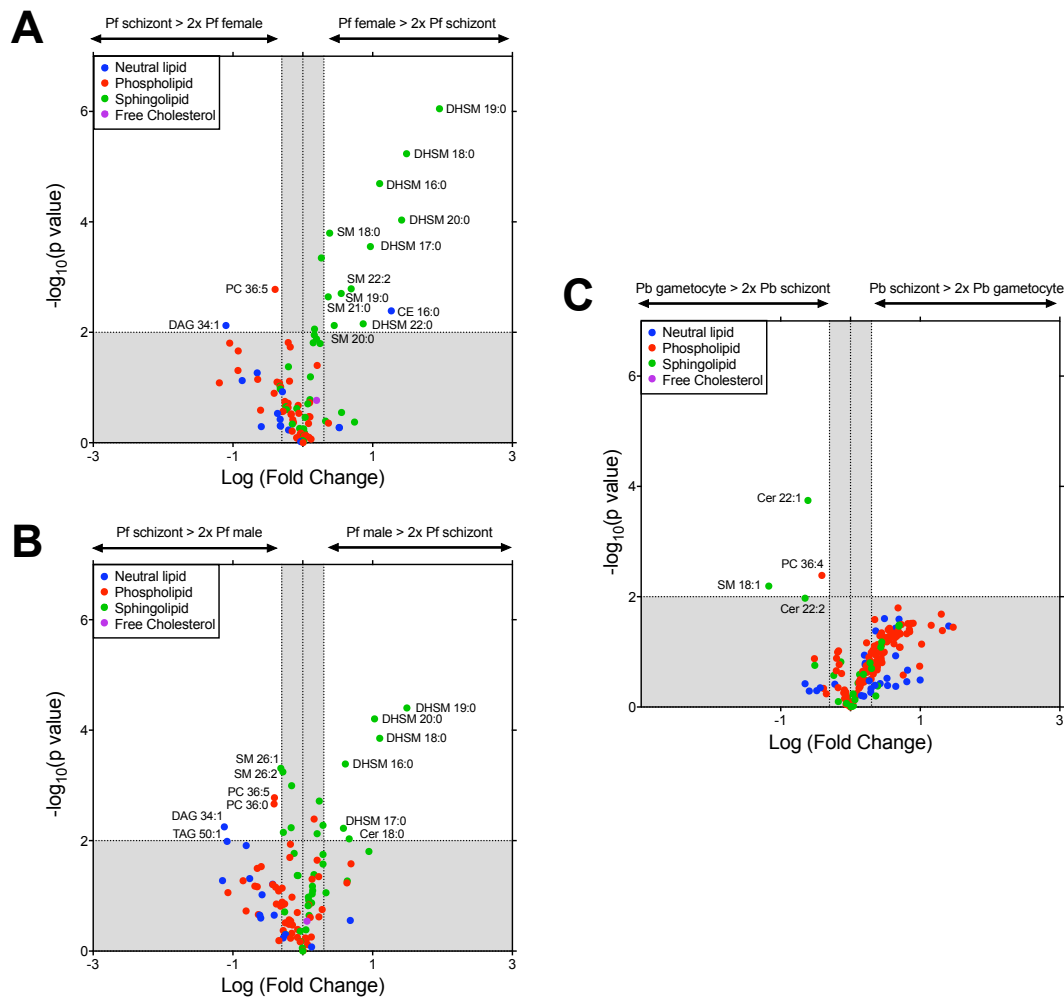




**Supplementary Figure 3:** Disruption of SMS2 by homologous recombination. A-C) Schematic of WT SMS2 locus with surrounding fragment of genomic DNA (A), pCC-1/SMS2 plasmid (B) and disrupted SMS2 locus with surrounding fragment of genomic DNA (C). SMS2 gene is disrupted by double homologous recombination at the 5' and 3' extremities of the gene in green (SMS2 5' fragment between SacII and SpeI restriction sites and SMS2 3' fragment between EcoRI and AvrII restriction sites), which inserts positive selection marker human dihydrofolate reductase (hDHFR, red) under the control of the calmodulin promoter (CAM 5') and histidine rich protein 2 3' untranslated region (hrp2 3'). The plasmid also contains negative selection marker cytosine deaminase (CD, purple) under the control of heat shock protein 86 promoter (hsp86 5') and *P. berghei* dihydrofolate reductase 3' untranslated region (PbDT 3') that are lost by double recombination. XmnI and HindIII restriction digest sites used for Southern blot are also indicated. D) Southern blot showing disruption of SMS2 locus. DNA from 3D7 wild type (WT), SMS2 KO plasmid (pl), or clonal 3D7 transfected with SMS2 KO plasmid (G7, E10, D4, E6 and G2) digested with XmnI and Hind III restriction enzymes probed with 5' homologous flank probe (SMS2 5' probe, left) or 3' homologous flank probe (SMS2 3' probe, right). Expected SMS2 5' probe band lengths: WT locus: 4,574 bp (black arrow), episomal locus: 7,036 bp (green arrow), integrated locus: 3,378 bp (red arrow). Expected SMS2 3' probe band lengths: WT locus: 4,574 bp (black arrow), episomal locus: 1,908 bp (green arrow), integrated locus: 2,685 bp (red arrow).



**Supplementary Figure 4:** Gametocyte commitment rate and survival in A) 3D7 WT (grey), SMS1 KO clones E6 (red) and E10 (blue) and B) 3D7 WT (grey), SMS 2 KO clones C9 (green) and D4 (black). Gametocytemia counted by flow cytometry every two days from day 2 post commitment in 3 or 4 independent cultures for 8 days. Mean and standard deviation in B were fitted with a one phase decay curve while in A lines join the data points.



**Supplementary Figure 5:** Volcano plot of total lipids in gametocyte and schizont-infected red blood cells with statistical significance from student t tests. A) *P. falciparum* female gametocyte-infected human red blood cell (Pf female) compared to *P. falciparum* schizont-infected human red blood cell (Pf schizont). B) *P. falciparum* male gametocyte-infected human red blood cell (Pf male) compared to *P. falciparum* schizont-infected human red blood cell (Pf schizont). C) *P. berghei* combined male and female gametocyte-infected mouse red blood cell (Pb gametocyte) compared to *P. berghei* schizont-infected mouse red blood cell (Pb schizont). CE: cholesteryl ester, Cer: ceramide, DAG: diacylglycerol, DHSM: dihydrosphingomyelin, PC: phosphatidylcholine, SM: sphingomyelin, TAG: triacylglycerol.

**Supplementary Table 1:** list of detected lipid species other than free cholesterol in *P. falciparum*. CE: cholesteryl ester; DAG: diacylglycerol; TAG: triacylglycerol; LPC: lysophosphatidylcholine; PC: phosphatidylcholine; PE: phosphatidylethanolamine; PG: phosphatidylglycerol; PS: phosphatidylserine; Cer: ceramide; DHSM: dihydrosphingomyelin; SM: sphingomyelin.

Neutral Lipids		
CE 16:0	DAG (34:0) 16:0_18:0	TAG 52:1
CE 16:1	DAG (34:1) 16:0_18:1	TAG 52:2
CE 18:1	DAG (36:1) 18:0_18:1	TAG 52:3
CE 18:2	DAG (36:2) 18:1_18:1	TAG 54:2
CE 18:3	TAG 48:0	TAG 54:3
CE 20:4	TAG 50:0	TAG 54:6
CE 20:5	TAG 50:1	TAG 56:6
DAG (32:0) 16:0_16:0	TAG 50:2	

Phospholipids		
LPC 16:0	PC 38:7	PE 38:4
LPC 18:0	PC 40:4	PE 38:5
PC 32:0	PC 40:5	PE 38:6
PC 32:1	PC 40:6	PE 40:5
PC 34:0	PC 40:7	PE 40:6
PC 34:1	PC O-32:0	PG (34:1) 16:0_18:1
PC 34:2	PC O-34:1	PG (34:2) 16:0_18:2
PC 34:3	PC O-36:2	PG (36:1) 18:0_18:1
PC 36:0	PC O-38:4	PG (36:2) 18:0_18:2
PC 36:1	PC O-38:5	PG (36:2) 18:1_18:1
PC 36:2	PE 34:1	PG (36:3) 18:1_18:2
PC 36:3	PE 34:2	PS 34:1
PC 36:4	PE 36:1	PS 36:1
PC 36:5	PE 36:2	PS 36:2
PC 38:3	PE 36:3	PS 38:4
PC 38:4	PE 36:4	PS 38:5
PC 38:5	PE 36:5	PS 40:5
PC 38:6	PE 38:3	PS 40:6

<b>Sphingolipids</b>		
Cer 16:0	DHSM 25:0	SM 22:2
Cer 18:0	SM 14:0	SM 23:0
Cer 19:0	SM 15:0	SM 23:1
Cer 22:0	SM 16:0	SM 24:0
Cer 24:0	SM 16:1	SM 24:1
Cer 24:1	SM 17:0	SM 24:2
Cer 24:2	SM 18:0	SM 24:3
DHSM 16:0	SM 18:1	SM 25:0
DHSM 17:0	SM 19:0	SM 25:1
DHSM 18:0	SM 20:0	SM 26:0
DHSM 19:0	SM 20:1	SM 26:1
DHSM 20:0	SM 21:0	SM 26:2
DHSM 22:0	SM 22:0	
DHSM 24:0	SM 22:1	

**Supplementary Table 2:** list of detected lipid species other than free cholesterol in *P. berghei*. CE: cholesteryl ester; DAG: diacylglycerol; TAG: triacylglycerol; LPC: lysophosphatidylcholine; PC: phosphatidylcholine; PE: phosphatidylethanolamine; PG: phosphatidylglycerol; PS: phosphatidylserine; Cer: ceramide; DHSM: dihydrosphingomyelin; SM: sphingomyelin.

Neutral Lipids		
CE 15:0	DAG (36:2) 18:1_18:1	TAG 50:4
CE 16:0	DAG (36:4) 16:0_20:4	TAG 52:0
CE 18:1	DAG (36:4) 18:2_18:2	TAG 52:1
CE 18:2	DAG (36:5) 16:0_20:5	TAG 52:2
CE 20:4	DAG (38:3) 18:0_20:3	TAG 52:3
CE 20:5	DAG (38:4) 18:0_20:4	TAG 52:4
DAG (32:0) 16:0_16:0	DAG (40:5) 18:0_22:5	TAG 52:5
DAG (32:1) 16:0_16:1	TAG 48:0	TAG 54:0
DAG (34:1) 16:0_18:1	TAG 48:1	TAG 54:1
DAG (34:1) 16:1_18:0	TAG 48:2	TAG 54:2
DAG (34:2) 16:0_18:2	TAG 48:3	TAG 54:3
DAG (34:3) 16:1_18:2	TAG 50:0	TAG 54:4
DAG (36:0) 18:0_18:0	TAG 50:1	TAG 54:5
DAG (36:1) 18:0_18:1	TAG 50:2	TAG 54:6
DAG (36:2) 18:0_18:2	TAG 50:3	TAG 56:8

Phospholipids		
LPC 16:0	PC (O 34:1) O 18:1_16:0	PE (O 36:3) O 18:1_18:2
LPC 18:0	PC (O 36:2) O 18:0_18:2	PE (O 36:4) O 16:1_20:3
LPC 18:1	PC (O 36:4) O 16:0_20:4	PE (O 36:5) O 16:1_20:4
LPC 18:2	PC (O 36:5) O 16:1_20:4	PE (O 36:6) O 16:1_20:5
LPC 20:4	PC (O 38:4) O 18:0_20:4	PE (O 38:4) O 18:0_20:4
LPC 22:5	PC (O 38:5) O 18:1_20:4	PE (O 38:4) O 18:1_20:3
LPC 22:6	PE (34:1) 16:0_18:1	PE (O 38:5) O 16:1_22:4
PC (32:0) 16:0_16:0	PE (34:1) 16:1_18:0	PE (O 38:5) O 18:1_20:4
PC (32:1) 16:0_16:1	PE (34:2) 16:0_18:2	PE (O 38:6) O 16:1_22:5
PC (34:0) 16:0_18:0	PE (34:2) 16:1_18:1	PE (O 38:6) O 18:1_20:5
PC (34:1) 16:0_18:1	PE (36:0) 18:0_18:0	PE (O 38:6) O 18:2_20:4
PC (34:1) 16:1_18:0	PE (36:1) 18:0_18:1	PE (O 38:7) O 16:1_22:6
PC (34:2) 16:0_18:2	PE (36:2) 18:0_18:2	PE (O 40:5) O 18:1_22:4
PC (34:2) 16:1_18:1	PE (36:2) 18:1_18:1	PE (O 40:6) O 18:0_22:6
PC (34:3) 16:0_18:3	PE (36:3) 16:0_20:3	PE (O 40:6) O 18:1_22:5
PC (34:3) 16:1_18:2	PE (36:3) 18:1_18:2	PE (O 40:6) O 18:2_22:4
PC (36:0) 18:0_18:0	PE (36:4) 16:0_20:4	PE (O 40:7) O 18:1_22:6
PC (36:1) 18:0_18:1	PE (36:4) 18:2_18:2	PE (O 40:7) O 18:2_22:5
PC (36:2) 18:0_18:2	PE (36:5) 16:0_20:5	PE (O 40:8) O 18:2_22:6
PC (36:2) 18:1_18:1	PE (36:5) 16:1_20:4	PG (32:0) 16:0_16:0
PC (36:3) 16:0_20:3	PE (38:3) 18:0_20:3	PG (34:0) 16:0_18:0
PC (36:3) 18:1_18:2	PE (38:4) 16:0_22:4	PG (34:1) 16:0_18:1

PC (36:4) 16:0 20:4	PE (38:4) 18:0 20:4	PG (34:2) 16:0 18:2
PC (36:4) 18:2 18:2	PE (38:4) 18:1 20:3	PG (36:0) 18:0 18:0
PC (36:5) 16:0 20:5	PE (38:5) 16:0 22:5	PG (36:1) 18:0 18:1
PC (36:5) 16:1 20:4	PE (38:5) 18:0 20:5	PG (36:2) 18:0 18:2
PC (38:3) 18:0 20:3	PE (38:5) 18:1 20:4	PG (36:2) 18:1 18:1
PC (38:4) 16:0 22:4	PE (38:5) 18:2 20:3	PG (36:3) 18:1 18:2
PC (38:4) 18:0 20:4	PE (38:6) 16:0 22:6	PG (36:4) 18:2 18:2
PC (38:4) 18:1 20:3	PE (38:6) 16:1 22:5	PS (34:1) 16:0 18:1
PC (38:5) 16:0 22:5	PE (38:6) 18:1 20:5	PS (34:2) 16:0 18:2
PC (38:5) 18:0 20:5	PE (38:6) 18:2 20:4	PS (36:1) 18:0 18:1
PC (38:5) 18:1 20:4	PE (38:7) 16:1 22:6	PS (36:2) 18:0 18:2
PC (38:5) 18:2 20:3	PE (40:4) 18:0 22:4	PS (36:2) 18:1 18:1
PC (38:6) 16:0 22:6	PE (40:5) 18:0 22:5	PS (36:3) 16:0 20:3
PC (38:6) 18:1 20:5	PE (40:5) 18:1 22:4	PS (36:4) 16:0 20:4
PC (38:6) 18:2 20:4	PE (40:6) 18:0 22:6	PS (38:3) 18:0 20:3
PC (38:7) 16:1 22:6	PE (40:6) 18:1 22:5	PS (38:4) 18:0 20:4
PC (40:4) 18:0 22:4	PE (40:7) 18:1 22:6	PS (38:5) 18:1 20:4
PC (40:5) 18:0 22:5	PE (40:8) 18:2 22:6	PS (38:6) 16:0 22:6
PC (40:6) 18:0 22:6	PE (42:10) 20:4 22:6	PS (40:4) 18:0 22:4
PC (40:6) 18:1 22:5	PE (42:9) 20:3 22:6	PS (40:5) 18:0 22:5
PC (40:7) 18:1 22:6	PE (O 34:1) O 18:1 16:0	PS (40:6) 18:0 22:6
PC (40:8) 18:2 22:6	PE (O 34:2) O 16:1 18:1	
PC (O 32:0) O 16:0 16:0	PE (O 34:2) O 18:2 16:0	
PC (O 32:1) O 16:1 16:0	PE (O 36:2) O 18:1 18:1	

Sphingolipids		
Cer 16:0	DHSM 19:0	SM 22:0
Cer 18:0	DHSM 23:0	SM 22:1
Cer 19:0	DHSM 25:0	SM 23:0
Cer 20:0	SM 14:0	SM 23:1
Cer 21:0	SM 15:0	SM 23:2
Cer 22:1	SM 16:0	SM 24:0
Cer 22:2	SM 16:1	SM 24:1
Cer 23:0	SM 17:0	SM 24:2
Cer 24:0	SM 18:0	SM 25:0
Cer 24:1	SM 18:1	SM 25:1
Cer 24:2	SM 19:0	SM 26:0
DHSM 16:0	SM 21:0	SM 26:1
DHSM 17:0	SM 21:1	SM 26:2

**Supplementary table 3:** list of detected lipid species other than free cholesterol in culturing media and supplements. CE: cholesteryl ester; DAG: diacylglycerol; TAG: triacylglycerol; LPC: lysophosphatidylcholine; PC: phosphatidylcholine; PE: phosphatidylethanolamine; PG: phosphatidylglycerol; PS: phosphatidylserine; Cer: ceramide; DHSM: dihydrosphingomyelin; SM: sphingomyelin.

Neutral Lipids		
CE 14:0	DAG (36:1) 18:0-18:1	TAG 52:3
CE 15:0	DAG (36:2) 18:1-18:1	TAG 52:4
CE 16:0	DAG (36:3) 18:1-18:2	TAG 52:5
CE 16:1	DAG (38:5) 18:1-20:4	TAG 54:0
CE 18:0	TAG 48:0	TAG 54:1
CE 18:1	TAG 48:1	TAG 54:2
CE 18:2	TAG 48:2	TAG 54:3
CE 18:3	TAG 48:3	TAG 54:4
CE 20:3	TAG 50:0	TAG 54:5
CE 20:4	TAG 50:1	TAG 54:6
CE 20:5	TAG 50:2	TAG 56:4
CE 22:4	TAG 50:3	TAG 56:5
CE 22:5	TAG 50:4	TAG 56:6
CE 22:6	TAG 52:0	TAG 56:7
DAG (34:1) 16:0-18:1	TAG 52:1	
DAG (34:2) 16:0-18:2	TAG 52:2	

Phospholipids		
LPC 16:0	PC 36:4	PC O-36:5
LPC 18:0	PC 36:5	PC O-38:4
LPC 18:1	PC 38:3	PC O-38:5
LPC 18:2	PC 38:4	PE 34:1
LPC 20:4	PC 38:5	PE 34:2
LPC 22:4	PC 38:6	PE 36:1
LPC 22:5	PC 38:7	PE 36:2
LPC 22:6	PC 40:4	PE 36:3
PC 32:0	PC 40:5	PE 36:4
PC 32:1	PC 40:6	PE 38:3
PC 34:0	PC 40:7	PE 38:4
PC 34:1	PC 40:8	PE 38:5
PC 34:2	PC O-32:0	PE 38:6
PC 34:3	PC O-32:1	PE 40:6
PC 36:1	PC O-34:1	PE O-38:5
PC 36:2	PC O-36:2	PE O-38:6
PC 36:3	PC O-36:4	



<b>Sphingolipids</b>		
Cer 16:0	SM 13:0	SM 22:1
Cer 22:0	SM 14:0	SM 23:0
Cer 22:2	SM 15:0	SM 23:1
Cer 23:0	SM 16:0	SM 23:2
Cer 24:0	SM 16:1	SM 24:0
Cer 24:1	SM 17:0	SM 24:1
Cer 25:0	SM 18:0	SM 24:2
DHSM 16:0	SM 18:1	SM 24:3
DHSM 17:0	SM 19:0	SM 25:0
DHSM 18:0	SM 21:0	SM 25:1
DHSM 23:0	SM 21:1	SM 26:2
DHSM 25:0	SM 22:0	

## References

- Abbott, S.K. et al., 2013. An improved high-throughput lipid extraction method for the analysis of human brain lipids. *Lipids*, 48(3), pp.307–318.
- Agop-Nersesian, C. et al., 2010. Biogenesis of the inner membrane complex is dependent on vesicular transport by the alveolate specific GTPase Rab11B. *PLoS Pathogens*, 6(7), p.e1001029.
- Aguilar, R. et al., 2014. Molecular evidence for the localization of *Plasmodium falciparum* immature gametocytes in bone marrow. *Blood*, 123(7), pp.959–966.
- Ahmad, M., Afrin, F. & Tuteja, R., 2013. Identification of R2TP complex of *Leishmania donovani* and *Plasmodium falciparum* using genome wide *in-silico* analysis. *Communicative & Integrative Biology*, 6(6), p.e26005.
- Aikawa, M. et al., 1984. New observations on gametogenesis, fertilization, and zygote transformation in *Plasmodium gallinaceum*. *The Journal of Protozoology*, 31(3), pp.403–413.
- Alano, P., 2007. *Plasmodium falciparum* gametocytes: still many secrets of a hidden life. *Molecular Microbiology*, 66(2), pp.291–302.
- Alonso, P.L. et al., 2011. A research agenda to underpin malaria eradication. *PLoS Medicine*, 8(1), p.e1000406.
- Alvarez-Venegas, R. & Avramova, Z., 2002. SET-domain proteins of the Su(var)3-9, E(z) and trithorax families. *Gene*, 285(1-2), pp.25–37.
- Anderson-White, B. et al., 2012. Cytoskeleton assembly in *Toxoplasma gondii* cell division. *International Review of Cell and Molecular Biology*, 298, pp.1–31.
- Ansari, F.A. et al., 2008. MAAP: malarial adhesins and adhesin-like proteins predictor. *Proteins*, 70(3), pp.659–666.
- Asahi, H., 2009. *Plasmodium falciparum*: Chemically defined medium for continuous intraerythrocytic growth using lipids and recombinant albumin. *Experimental Parasitology*, 121(1), pp.22–28.
- Asahi, H. et al., 2005. Investigating serum factors promoting erythrocytic growth of *Plasmodium falciparum*. *Experimental Parasitology*, 109(1), pp.7–15.
- Ashley, E.A., Pyae Phyo, A. & Woodrow, C.J., 2018. Malaria. *Lancet*, 391(10130), pp.1608–1621.
- Atella, G.C. et al., 2009. The major insect lipoprotein is a lipid source to mosquito stages of malaria parasite. *Acta Tropica*, 109(2), pp.159–162.
- Atkinson, C.T. et al., 1988. Ultrastructural localization of erythrocyte cytoskeletal and integral membrane proteins in *Plasmodium falciparum*-infected erythrocytes. *European Journal of Cell Biology*, 45(2), pp.192–199.

- Augustijn, K.D. et al., 2007. Functional characterization of the *Plasmodium falciparum* and *P. berghei* homologues of macrophage migration inhibitory factor. *Infection and Immunity*, 75(3), pp.1116–1128.
- Baeza Garcia, A. et al., 2018. Neutralization of the *Plasmodium*-encoded MIF ortholog confers protective immunity against malaria infection. *Nature Communications*, 9(1), p.2714.
- Baker, D.A., 2010. Malaria gametocytogenesis. *Molecular and Biochemical Parasitology*, 172(2), pp.57–65.
- Baker, D.A. & Kelly, J.M., 2004. Purine nucleotide cyclases in the malaria parasite. *Trends in Parasitology*, 20(5), pp.227–232.
- Bannister, L.H. & Mitchell, G.H., 1989. The fine structure of secretion by *Plasmodium knowlesi* merozoites during red cell invasion. *The Journal of Protozoology*, 36(4), pp.362–367.
- Bartelt, A. et al., 2017. Quantification of bone fatty acid metabolism and its regulation by adipocyte lipoprotein lipase. *International Journal of Molecular Sciences*, 18(6), p.1264.
- Baruch, D.I. et al., 1995. Cloning the *P. falciparum* gene encoding PfEMP1, a malarial variant antigen and adherence receptor on the surface of parasitized human erythrocytes. *Cell*, 82(1), pp.77–87.
- Beaumelle, B.D., Vial, H.J. & Philippot, J.R., 1987. Reevaluation, using marker enzymes, of the ability of saponin and ammonium chloride to free *Plasmodium* from infected erythrocytes. *The Journal of Parasitology*, 73(4), pp.743–748.
- Beck, J.R. et al., 2010. A novel family of *Toxoplasma* IMC proteins displays a hierarchical organization and functions in coordinating parasite division. *PLoS Pathogens*, 6(9), p.e1001094.
- Bedia, C. et al., 2005. Analogs of the dihydroceramide desaturase inhibitor GT11 modified at the amide function: synthesis and biological activities. *Organic & Biomolecular Chemistry*, 3(20), pp.3707–3712.
- Beetsma, A.L. et al., 1998. *Plasmodium berghei* ANKA: purification of large numbers of infectious gametocytes. *Experimental Parasitology*, 88(1), pp.69–72.
- Behari, R. & Haldar, K., 1994. *Plasmodium falciparum*: protein localization along a novel, lipid-rich tubovesicular membrane network in infected erythrocytes. *Experimental Parasitology*, 79(3), pp.250–259.
- Bennink, S., Kiesow, M.J. & Pradel, G., 2016. The development of malaria parasites in the mosquito midgut. *Cellular Microbiology*, 18(7), pp.905–918.
- Berman, A. et al., 1994. Photoaffinity labelling of *Plasmodium falciparum* proteins involved in phospholipid transport. *Molecular and Biochemical Parasitology*, 67(2), pp.235–243.
- Bhanot, P. et al., 2005. A surface phospholipase is involved in the migration of *Plasmodium* sporozoites through cells. *The Journal of Biological Chemistry*, 280(8), pp.6752–6760.

- Billker, O. et al., 1998. Identification of xanthurenic acid as the putative inducer of malaria development in the mosquito. *Nature*, 392(6673), pp.289–292.
- Bobenchik, A.M. et al., 2013. *Plasmodium falciparum* phosphoethanolamine methyltransferase is essential for malaria transmission. *Proceedings of the National Academy of Sciences of the United States of America*, 110(45), pp.18262–18267.
- Boone, C., Bussey, H. & Andrews, B.J., 2007. Exploring genetic interactions and networks with yeast. *Nature Reviews. Genetics*, 8(6), pp.437–449.
- Botté, C.Y. et al., 2013. Atypical lipid composition in the purified relict plastid (apicoplast) of malaria parasites. *Proceedings of the National Academy of Sciences of the United States of America*, 110(18), pp.7506–7511.
- Bounkeua, V., Li, F. & Vinetz, J.M., 2010. *In vitro* generation of *Plasmodium falciparum* ookinetes. *The American Journal of Tropical Medicine and Hygiene*, 83(6), pp.1187–1194.
- Brancucci, N.M.B. et al., 2014. Heterochromatin protein 1 secures survival and transmission of malaria parasites. *Cell Host & Microbe*, 16(2), pp.165–176.
- Brancucci, N.M.B. et al., 2017. Lysophosphatidylcholine regulates sexual stage differentiation in the human malaria parasite *Plasmodium falciparum*. *Cell*, 171(7), pp.1532–1544.e15.
- Brinster, S. et al., 2009. Type II fatty acid synthesis is not a suitable antibiotic target for Gram-positive pathogens. *Nature*, 458(7234), pp.83–86.
- Brochet, M. et al., 2014. Phosphoinositide metabolism links cGMP-dependent protein kinase G to essential Ca<sup>2+</sup> signals at key decision points in the life cycle of malaria parasites. *PLoS Biology*, 12(3), p.e1001806.
- Bruce, M.C. et al., 1990. Commitment of the malaria parasite *Plasmodium falciparum* to sexual and asexual development. *Parasitology*, 100 Pt 2, pp.191–200.
- Bullen, H.E. et al., 2016. Phosphatidic acid-mediated signaling regulates microneme secretion in *Toxoplasma*. *Cell Host & Microbe*, 19(3), pp.349–360.
- Burda, P.-C. et al., 2015. A *Plasmodium* phospholipase is involved in disruption of the liver stage parasitophorous vacuole membrane. *PLoS Pathogens*, 11(3), p.e1004760.
- Burrows, J.N. et al., 2017. New developments in anti-malarial target candidate and product profiles. *Malaria Journal*, 16(1), p.26.
- Bushell, E. et al., 2017. Functional profiling of a *Plasmodium* genome reveals an abundance of essential genes. *Cell*, 170(2), pp.260–272.e8.
- Campanale, N. et al., 2003. Identification and characterization of heme-interacting proteins in the malaria parasite, *Plasmodium falciparum*. *The Journal of Biological Chemistry*, 278(30), pp.27354–27361.

- Canning, E.U. & Sinden, R.E., 1975. Nuclear organisation in gametocytes of *Plasmodium* and *Hepatozoon*: a cytochemical study. *Zeitschrift für Parasitenkunde*, 46(4), pp.297–299.
- Capel, B., 2017. Vertebrate sex determination: evolutionary plasticity of a fundamental switch. *Nature Reviews. Genetics*, 18(11), pp.675–689.
- Carter, L.M. et al., 2013. Stress and sex in malaria parasites: Why does commitment vary? *Evolution, Medicine, and Public Health*, 2013(1), pp.135–147.
- Carter, L.M., Schneider, P. & Reece, S.E., 2014. Information use and plasticity in the reproductive decisions of malaria parasites. *Malaria Journal*, 13(1), p.115.
- Chan, S. et al., 2017. Frequent GU wobble pairings reduce translation efficiency in *Plasmodium falciparum*. *Scientific Reports*, 7(1), p.723.
- Chen, Y. et al., 2017. Differential methylation analysis of reduced representation bisulfite sequencing experiments using edgeR. *F1000Research*, 6, p.2055.
- Choi, J.-Y. et al., 2016. Characterization of *Plasmodium* phosphatidylserine decarboxylase expressed in yeast and application for inhibitor screening. *Molecular Microbiology*, 99(6), pp.999–1014.
- Choi, S.-W., Keyes, M.K. & Horrocks, P., 2006. LC/ESI-MS demonstrates the absence of 5-methyl-2'-deoxycytosine in *Plasmodium falciparum* genomic DNA. *Molecular and Biochemical Parasitology*, 150(2), pp.350–352.
- Churcher, T.S., Trape, J.-F. & Cohuet, A., 2015. Human-to-mosquito transmission efficiency increases as malaria is controlled. *Nature Communications*, 6, p.6054.
- Cibulskis, R.E. et al., 2016. Malaria: Global progress 2000 - 2015 and future challenges. *Infectious Diseases of Poverty*, 5(1), p.61.
- Cicero, A.F.G., Bove, M. & Borghi, C., 2018. Pharmacokinetics, pharmacodynamics and clinical efficacy of non-statin treatments for hypercholesterolemia. *Expert Opinion on Drug Metabolism & Toxicology*, 14(1), pp.9–15.
- Cirimotich, C.M. et al., 2011. Natural microbe-mediated refractoriness to *Plasmodium* infection in *Anopheles gambiae*. *Science*, 332(6031), pp.855–858.
- Coleman, B.I. et al., 2014. A *Plasmodium falciparum* histone deacetylase regulates antigenic variation and gametocyte conversion. *Cell Host & Microbe*, 16(2), pp.177–186.
- Coppens, I. & Joiner, K.A., 2003. Host but not parasite cholesterol controls *Toxoplasma* cell entry by modulating organelle discharge. *Molecular Biology of the Cell*, 14(9), pp.3804–3820.
- Cordery, D.V. et al., 2007. Characterization of a *Plasmodium falciparum* macrophage-migration inhibitory factor homologue. *The Journal of Infectious Diseases*, 195(6), pp.905–912.
- Costa, D.M. et al., 2018. TRSP is dispensable for the *Plasmodium* pre-erythrocytic phase. *Scientific Reports*, 8(1), p.15101.

- Costa, G. et al., 2018. Non-competitive resource exploitation within mosquito shapes within-host malaria infectivity and virulence. *Nature Communications*, 9(1), p.3474.
- Costanzo, M. et al., 2010. The genetic landscape of a cell. *Science*, 327(5964), pp.425–431.
- Cox-Singh, J. et al., 2008. *Plasmodium knowlesi* malaria in humans is widely distributed and potentially life threatening. *Clinical Infectious Diseases : an official publication of the Infectious Diseases Society of America*, 46(2), pp.165–171.
- Cranmer, S.L. et al., 1997. An alternative to serum for cultivation of *Plasmodium falciparum* *in vitro*. *Transactions of the Royal Society of Tropical Medicine and Hygiene*, 91(3), pp.363–365.
- Crick, F.H., 1966. Codon-anticodon pairing: the wobble hypothesis. *Journal of Molecular Biology*, 19(2), pp.548–555.
- Cromer, D. et al., 2006. Preferential invasion of reticulocytes during late-stage *Plasmodium berghei* infection accounts for reduced circulating reticulocyte levels. *International Journal for Parasitology*, 36(13), pp.1389–1397.
- Cui, L. et al., 2008. Histone lysine methyltransferases and demethylases in *Plasmodium falciparum*. *International Journal for Parasitology*, 38(10), pp.1083–1097.
- Cullis, P.R. & de Kruijff, B., 1979. Lipid polymorphism and the functional roles of lipids in biological membranes. *Biochimica et Biophysica Acta*, 559(4), pp.399–420.
- D'Alessandro, S. et al., 2016. A chemical susceptibility profile of the *Plasmodium falciparum* transmission stages by complementary cell-based gametocyte assays. *The Journal of Antimicrobial Chemotherapy*, 71(5), pp.1148–1158.
- D'Alessandro, S. et al., 2013. A *Plasmodium falciparum* screening assay for anti-gametocyte drugs based on parasite lactate dehydrogenase detection. *The Journal of Antimicrobial Chemotherapy*, 68(9), pp.2048–2058.
- Daum, G., 1985. Lipids of mitochondria. *Biochimica et Biophysica Acta*, 822(1), pp.1–42.
- de Freitas Nascimento, J. et al., 2018. Codon choice directs constitutive mRNA levels in trypanosomes. *eLife*, 7, p.2087.
- de Koning-Ward, T.F., Gilson, P.R. & Crabb, B.S., 2015. Advances in molecular genetic systems in malaria., 13(6), pp.373–387.
- de Kroon, A.I. et al., 1999. Isolation and characterization of highly purified mitochondrial outer membranes of the yeast *Saccharomyces cerevisiae* (method). *Molecular Membrane Biology*, 16(2), pp.205–211.
- de Kroon, A.I.P.M., Rijken, P.J. & De Smet, C.H., 2013. Checks and balances in membrane phospholipid class and acyl chain homeostasis, the yeast perspective. *Progress in Lipid Research*, 52(4), pp.374–394.

- de Moraes, L.V. et al., 2016. Murine model for preclinical studies of var2CSA-mediated pathology associated with malaria in pregnancy. *Infection and Immunity*, 84(6), pp.1761–1774.
- De Napoli, M.G. et al., 2013. N-terminal palmitoylation is required for *Toxoplasma gondii* HSP20 inner membrane complex localization. *Biochimica et Biophysica Acta*, 1833(6), pp.1329–1337.
- De Niz, M. et al., 2018. *Plasmodium* gametocytes display homing and vascular transmigration in the host bone marrow. *Science Advances*, 4(5), p.eaat3775.
- de Oca, M.M., Engwerda, C. & Haque, A., 2013. *Plasmodium berghei* ANKA (PbA) infection of C57BL/6J mice: a model of severe malaria. *Methods in Molecular Biology*, 1031(Chapter 23), pp.203–213.
- Dechamps, S. et al., 2010. The Kennedy phospholipid biosynthesis pathways are refractory to genetic disruption in *Plasmodium berghei* and therefore appear essential in blood stages. *Molecular and Biochemical Parasitology*, 173(2), pp.69–80.
- Delves, M.J. et al., 2013. Male and female *Plasmodium falciparum* mature gametocytes show different responses to antimalarial drugs. *Antimicrobial Agents and Chemotherapy*, 57(7), pp.3268–3274.
- Demanga, C.G. et al., 2017. The development of sexual stage malaria gametocytes in a Wave Bioreactor. *Parasites & Vectors*, 10(1), p.216.
- Dern, R.J., Beutler, E. & Alving, A.S., 1954. The hemolytic effect of primaquine. II. The natural course of the hemolytic anemia and the mechanism of its self-limited character. *The Journal of Laboratory and Clinical Medicine*, 44(2), pp.171–176.
- DeVay, R.M. et al., 2009. Coassembly of Mgm1 isoforms requires cardiolipin and mediates mitochondrial inner membrane fusion. *The Journal of Cell Biology*, 186(6), pp.793–803.
- Di Girolamo, F. et al., 2008. *Plasmodium* lipid rafts contain proteins implicated in vesicular trafficking and signalling as well as members of the PIR superfamily, potentially implicated in host immune system interactions. *Proteomics*, 8(12), pp.2500–2513.
- Dicko, A. et al., 2018. Efficacy and safety of primaquine and methylene blue for prevention of *Plasmodium falciparum* transmission in Mali: a phase 2, single-blind, randomised controlled trial. *The Lancet. Infectious Diseases*, 18(6), pp.627–639.
- Dickson, R.C., 2008. Thematic review series: sphingolipids. New insights into sphingolipid metabolism and function in budding yeast. *Journal of Lipid Research*, 49(5), pp.909–921.
- Divo, A.A. et al., 1985. Nutritional requirements of *Plasmodium falciparum* in culture. I. Exogenously supplied dialyzable components necessary for continuous growth. *The Journal of Protozoology*, 32(1), pp.59–64.
- Dluzewski, A.R. et al., 1992. Origins of the parasitophorous vacuole membrane of the malaria parasite, *Plasmodium falciparum*, in human red blood cells. *Journal of Cell Science*, 102 (Pt 3), pp.527–532.

- Dluzewski, A.R. et al., 1995. Origins of the parasitophorous vacuole membrane of the malaria parasite: surface area of the parasitized red cell. *European Journal of Cell Biology*, 68(4), pp.446–449.
- Dobson, S.E. et al., 2009. The crystal structures of macrophage migration inhibitory factor from *Plasmodium falciparum* and *Plasmodium berghei*. *Protein Science : a publication of the Protein Society*, 18(12), pp.2578–2591.
- Dourmashkin, R.R., Dougherty, R.M. & Harris, R.J., 1962. Electron microscopic observations on Rous sarcoma virus and cell membranes. *Nature*, 194, pp.1116–1119.
- Duffy, S. et al., 2016. Large-scale production of *Plasmodium falciparum* gametocytes for malaria drug discovery. *Nature Protocols*, 11(5), pp.976–992.
- Eksi, S., Suri, A. & Williamson, K.C., 2008. Sex- and stage-specific reporter gene expression in *Plasmodium falciparum*. *Molecular and Biochemical Parasitology*, 160(2), pp.148–151.
- Elabbadi, N., Ancelin, M.L. & Vial, H.J., 1997. Phospholipid metabolism of serine in *Plasmodium*-infected erythrocytes involves phosphatidylserine and direct serine decarboxylation. *The Biochemical Journal*, 324 ( Pt 2)(Pt 2), pp.435–445.
- Elford, B.C., Cowan, G.M. & Ferguson, D.J., 1995. Parasite-regulated membrane transport processes and metabolic control in malaria-infected erythrocytes. *The Biochemical Journal*, 308 ( Pt 2)(Pt 2), pp.361–374.
- Elford, B.C., Cowan, G.M. & Ferguson, D.J., 1997. Transport and trafficking in malaria-infected erythrocytes. *Trends in Microbiology*, 5(12), pp.463–5– discussion 465–6.
- Elmendorf, H.G. & Haldar, K., 1994. *Plasmodium falciparum* exports the Golgi marker sphingomyelin synthase into a tubovesicular network in the cytoplasm of mature erythrocytes. *The Journal of Cell Biology*, 124(4), pp.449–462.
- Essaka, D.C. et al., 2010. Monitoring the uptake of glycosphingolipids in *Plasmodium falciparum*-infected erythrocytes using both fluorescence microscopy and capillary electrophoresis with laser-induced fluorescence detection. *Analytical Chemistry*, 82(23), pp.9955–9958.
- Exton, J.H., 1994. Phosphatidylcholine breakdown and signal transduction. *Biochimica et Biophysica Acta*, 1212(1), pp.26–42.
- Fahy, E. et al., 2011. Lipid classification, structures and tools. *Biochimica et Biophysica Acta*, 1811(11), pp.637–647.
- Feagin, J.E., 1992. The 6-kb element of *Plasmodium falciparum* encodes mitochondrial cytochrome genes. *Molecular and Biochemical Parasitology*, 52(1), pp.145–148.
- Feagin, J.E. et al., 1992. Homologies between the contiguous and fragmented rRNAs of the two *Plasmodium falciparum* extrachromosomal DNAs are limited to core sequences. *Nucleic Acids Research*, 20(4), pp.879–887.



- Feagin, J.E. et al., 2012. The fragmented mitochondrial ribosomal RNAs of *Plasmodium falciparum*. *PloS One*, 7(6), p.e38320.
- Filarsky, M. et al., 2018. GDV1 induces sexual commitment of malaria parasites by antagonizing HP1-dependent gene silencing. *Science*, 359(6381), pp.1259–1263.
- Fisher 1930. *The Genetical Theory of Natural Selection*
- Fivelman, Q.L. et al., 2007. Improved synchronous production of *Plasmodium falciparum* gametocytes *in vitro*. *Molecular and Biochemical Parasitology*, 154(1), pp.119–123.
- Flammersfeld, A. et al., 2018. Phospholipases during membrane dynamics in malaria parasites. *International Journal of Medical Microbiology : IJMM*, 308(1), pp.129–141.
- Foth, B.J. & McFadden, G.I., 2003. The apicoplast: a plastid in *Plasmodium falciparum* and other Apicomplexan parasites. *International Review of Cytology*, 224, pp.57–110.
- Foussard, F., Leriche, M.A. & Dubremetz, J.F., 1991. Characterization of the lipid content of *Toxoplasma gondii* rhoptries. *Parasitology*, 102 Pt 3, pp.367–370.
- Francia, M.E. & Striepen, B., 2014. Cell division in apicomplexan parasites., 12(2), pp.125–136.
- Fréchal, K. et al., 2013. Global analysis of apicomplexan protein S-acyl transferases reveals an enzyme essential for invasion. *Traffic*, 14(8), pp.895–911.
- Fung, C. et al., 2012. *Toxoplasma* ISP4 is a central IMC sub-compartment protein whose localization depends on palmitoylation but not myristoylation. *Molecular and Biochemical Parasitology*, 184(2), pp.99–108.
- Fyrst, H. & Saba, J.D., 2010. An update on sphingosine-1-phosphate and other sphingolipid mediators. *Nature Chemical Biology*, 6(7), pp.489–497.
- Gautier, E.F. et al., 2018. Absolute proteome quantification of highly purified populations of circulating reticulocytes and mature erythrocytes. *Blood Advances*, 2(20), pp.2646–2657.
- Gamble, T. et al., 2015. Restriction site-associated DNA sequencing (RAD-seq) reveals an extraordinary number of transitions among gecko sex-determining systems. *Molecular Biology and Evolution*, 32(5), pp.1296–1309.
- Gardner, M.J. et al., 2002. Genome sequence of the human malaria parasite *Plasmodium falciparum*. *Nature*, 419(6906), pp.498–511.
- Gbotosho, G.O. et al., 2011. *Plasmodium falciparum* gametocyte carriage, emergence, clearance and population sex ratios in anaemic and non-anaemic malarious children. *Memorias do Instituto Oswaldo Cruz*, 106(5), pp.562–569.
- Gebert, N. et al., 2009. Mitochondrial cardiolipin involved in outer-membrane protein biogenesis: implications for Barth syndrome. *Current Biology : CB*, 19(24), pp.2133–2139.

- Gebru, T. et al., 2017. Life-span of *in vitro* differentiated *Plasmodium falciparum* gametocytes. *Malaria journal*, 16(1), p.330.
- Gerold, P. & Schwarz, R.T., 2001. Biosynthesis of glycosphingolipids *de-novo* by the human malaria parasite *Plasmodium falciparum*. *Molecular and Biochemical Parasitology*, 112(1), pp.29–37.
- Ghazanfari, N., Mueller, S.N. & Heath, W.R., 2018. Cerebral Malaria in Mouse and Man. *Frontiers in Immunology*, 9, p.2016.
- Gibellini, F. & Smith, T.K., 2010. The Kennedy pathway-*De novo* synthesis of phosphatidylethanolamine and phosphatidylcholine. *IUBMB life*, 62(6), pp.414–428.
- Gillon, A.D., Latham, C.F. & Miller, E.A., 2012. Vesicle-mediated ER export of proteins and lipids. *Biochimica et Biophysica Acta*, 1821(8), pp.1040–1049.
- Ginsburg, H. et al., 1983. New permeability pathways induced in membranes of *Plasmodium falciparum* infected erythrocytes. *Molecular and Biochemical Parasitology*, 8(2), pp.177–190.
- Gissot, M. et al., 2005. PfMyb1, a *Plasmodium falciparum* transcription factor, is required for intra-erythrocytic growth and controls key genes for cell cycle regulation. *Journal of Molecular Biology*, 346(1), pp.29–42.
- Gissot, M. et al., 2008. *Toxoplasma gondii* and *Cryptosporidium parvum* lack detectable DNA cytosine methylation. *Eukaryotic Cell*, 7(3), pp.537–540.
- Gong, Z. et al., 2017. Widespread 5-methylcytosine in the genomes of avian *Coccidia* and other apicomplexan parasites detected by an ELISA-based method. *Parasitology Research*, 116(5), pp.1573–1579.
- Govindaraju, G. et al., 2017. DNA methyltransferase homologue TRDMT1 in *Plasmodium falciparum* specifically methylates endogenous aspartic acid tRNA. *Biochimica et Biophysica Acta. Gene Regulatory Mechanisms*, 1860(10), pp.1047–1057.
- Gowda, D.C., 2007. TLR-mediated cell signaling by malaria GPIs. *Trends in Parasitology*, 23(12), pp.596–604.
- Gratraud, P. et al., 2009. Oleic acid biosynthesis in *Plasmodium falciparum*: characterization of the stearyl-CoA desaturase and investigation as a potential therapeutic target. *PLoS One*, 4(9), p.e6889.
- Graumans, W. et al., 2019. *Plasmodium falciparum* gametocyte enrichment in peripheral blood samples by magnetic fractionation: gametocyte yields and possibilities to reuse columns. *The American Journal of Tropical Medicine and Hygiene*, p.tpmd180773.
- Grellier, P. et al., 1991. Lipid traffic between high density lipoproteins and *Plasmodium falciparum*-infected red blood cells. *The Journal of Cell Biology*, 112(2), pp.267–277.
- Gulati, S. et al., 2015. Profiling the essential nature of lipid metabolism in asexual blood and gametocyte stages of *Plasmodium falciparum*. *Cell Host & Microbe*, 18(3), pp.371–381.

- Gupta, C.M. & Mishra, G.C., 1981. Transbilayer phospholipid asymmetry in *Plasmodium knowlesi*-infected host cell membrane. *Science*, 212(4498), pp.1047–1049.
- Gupta, S.K., Schulman, S. & Vanderberg, J.P., 1985. Stage-dependent toxicity of N-acetylglucosamine to *Plasmodium falciparum*. *The Journal of Protozoology*, 32(1), pp.91–95.
- Haines, T.H. & Dencher, N.A., 2002. Cardiolipin: a proton trap for oxidative phosphorylation. *FEBS letters*, 528(1-3), pp.35–39.
- Haldar, K. & Uyetake, L., 1992. The movement of fluorescent endocytic tracers in *Plasmodium falciparum* infected erythrocytes. *Molecular and Biochemical Parasitology*, 50(1), pp.161–177.
- Haldar, K., de Amorim, A.F. & Cross, G.A., 1989. Transport of fluorescent phospholipid analogues from the erythrocyte membrane to the parasite in *Plasmodium falciparum*-infected cells. *The Journal of Cell Biology*, 108(6), pp.2183–2192.
- Hamilton, W.D., 1967. Extraordinary sex ratios. A sex-ratio theory for sex linkage and inbreeding has new implications in cytogenetics and entomology. *Science*, 156(3774), pp.477–488.
- Hanada, K. et al., 2002. *Plasmodium falciparum* phospholipase C hydrolyzing sphingomyelin and lysocholinephospholipids is a possible target for malaria chemotherapy. *The Journal of Experimental Medicine*, 195(1), pp.23–34.
- Hannun, Y.A. & Obeid, L.M., 2008. Principles of bioactive lipid signalling: lessons from sphingolipids. *Nature Reviews. Molecular Cell Biology*, 9(2), pp.139–150.
- Hawking, F., Wilson, M.E. & Gammage, K., 1971. Evidence for cyclic development and short-lived maturity in the gametocytes of *Plasmodium falciparum*. *Transactions of the Royal Society of Tropical Medicine and Hygiene*, 65(5), pp.549–559.
- Hockwald, R.S. et al., 1952. Toxicity of primaquine in Negroes. *Journal of the American Medical Association*, 149(17), pp.1568–1570.
- Hofmann, N. et al., 2015. Ultra-sensitive detection of *Plasmodium falciparum* by amplification of multi-copy subtelomeric targets. *PLoS Medicine*, 12(3), p.e1001788.
- Holleley, C.E. et al., 2015. Sex reversal triggers the rapid transition from genetic to temperature-dependent sex. *Nature*, 523(7558), pp.79–82.
- Hsiao, L.L. et al., 1991. Modification of host cell membrane lipid composition by the intraerythrocytic human malaria parasite *Plasmodium falciparum*. *The Biochemical Journal*, 274 ( Pt 1)(1), pp.121–132.
- Imwong, M. et al., 2017. Spread of a single multidrug resistant malaria parasite lineage (PfPailin) to Vietnam. *The Lancet. Infectious Diseases*, 17(10), pp.1022–1023.
- Istvan, E.S. et al., 2019. *Plasmodium* Niemann-Pick type C1-related protein is a druggable target required for parasite membrane homeostasis. *eLife*, 8, p.87.

- Jackson, A.P. et al., 2016. Kinetoplastid phylogenomics reveals the evolutionary innovations associated with the origins of parasitism. *Current Biology*, 26(2), pp.161–172.
- Jackson, K.E. et al., 2004. Food vacuole-associated lipid bodies and heterogeneous lipid environments in the malaria parasite, *Plasmodium falciparum*. *Molecular Microbiology*, 54(1), pp.109–122.
- Jaenisch, R. & Bird, A., 2003. Epigenetic regulation of gene expression: how the genome integrates intrinsic and environmental signals. *Nature Genetics*, 33 Suppl(3s), pp.245–254.
- Janse, C.J. et al., 2006. High efficiency transfection of *Plasmodium berghei* facilitates novel selection procedures. *Molecular and Biochemical Parasitology*, 145(1), pp.60–70.
- Jensen, J.B., 1979. Observations on gametogenesis in *Plasmodium falciparum* from continuous culture. *The Journal of Protozoology*, 26(1), pp.129–132.
- Joannin, N. et al., 2008. Sub-grouping and sub-functionalization of the RIFIN multi-copy protein family. *BMC Genomics*, 9(1).
- Joice, R. et al., 2014. *Plasmodium falciparum* transmission stages accumulate in the human bone marrow. *Science Translational Medicine*, 6(244), pp.244re5–244re5.
- Joshi, A.S. et al., 2012. Cardiolipin and mitochondrial phosphatidylethanolamine have overlapping functions in mitochondrial fusion in *Saccharomyces cerevisiae*. *The Journal of Biological Chemistry*, 287(21), pp.17589–17597.
- Kafsack, B.F.C. et al., 2014. A transcriptional switch underlies commitment to sexual development in malaria parasites. *Nature*, 507(7491), pp.248–252.
- Ke, H. et al., 2015. Genetic investigation of tricarboxylic acid metabolism during the *Plasmodium falciparum* life cycle. *Cell Reports*, 11(1), pp.164–174.
- Kent, R.S. et al., 2018. Inducible developmental reprogramming redefines commitment to sexual development in the malaria parasite *Plasmodium berghei*. *Nature Microbiology*, 3(11), pp.1206–1213.
- Kenthirapalan, S. et al., 2016. Functional profiles of orphan membrane transporters in the life cycle of the malaria parasite. *Nature Communications*, 7(1), p.10519.
- Khan, S.M. et al., 2013. Why are male malaria parasites in such a rush?: Sex-specific evolution and host-parasite interactions. *Evolution, Medicine, and Public Health*, 2013(1), pp.3–13.
- Kilian, N. et al., 2018. Role of phospholipid synthesis in the development and differentiation of malaria parasites in the blood. *The Journal of Biological Chemistry*, 293(45), pp.17308–17316.
- Kirk, K. et al., 1993. Glibenclamide and meglitinide block the transport of low molecular weight solutes into malaria-infected erythrocytes. *FEBS Letters*, 323(1-2), pp.123–128.

- Klemm, R.W. et al., 2009. Segregation of sphingolipids and sterols during formation of secretory vesicles at the trans-Golgi network. *The Journal of Cell Biology*, 185(4), pp.601–612.
- Knowles, S.C.L. & Sheldon, B.C., 2008. Evolutionary biology: parasite, know thyself. *Current Biology*, 18(15), pp.R655–R657.
- Kok, J.W. et al., 1997. Dihydroceramide biology. Structure-specific metabolism and intracellular localization. *The Journal of Biological Chemistry*, 272(34), pp.21128–21136.
- Krishnegowda, G. & Gowda, D.C., 2003. Intraerythrocytic *Plasmodium falciparum* incorporates extraneous fatty acids to its lipids without any structural modification. *Molecular and Biochemical Parasitology*, 132(1), pp.55–58.
- Krishnegowda, G. et al., 2005. Induction of proinflammatory responses in macrophages by the glycosylphosphatidylinositols of *Plasmodium falciparum*: cell signaling receptors, glycosylphosphatidylinositol (GPI) structural requirement, and regulation of GPI activity. *The Journal of Biological Chemistry*, 280(9), pp.8606–8616.
- Krotoski, W.A. et al., 1982. Demonstration of hypnozoites in sporozoite-transmitted *Plasmodium vivax* infection. *The American Journal of Tropical Medicine and Hygiene*, 31(6), pp.1291–1293.
- Kumar, S. et al., 2012. CD36 modulates proinflammatory cytokine responses to *Plasmodium falciparum* glycosylphosphatidylinositols and merozoites by dendritic cells. *Parasite Immunology*, 34(7), pp.372–382.
- Kwiatkowski, D.P., 2005. How malaria has affected the human genome and what human genetics can teach us about malaria. *American Journal of Human Genetics*, 77(2), pp.171–192.
- Labaied, M. et al., 2011. *Plasmodium* salvages cholesterol internalized by LDL and synthesized de novo in the liver. *Cellular Microbiology*, 13(4), pp.569–586.
- Labaied, M., Camargo, N. & Kappe, S.H.I., 2007. Depletion of the *Plasmodium berghei* thrombospondin-related sporozoite protein reveals a role in host cell entry by sporozoites. *Molecular and Biochemical Parasitology*, 153(2), pp.158–166.
- Lambros, C. & Vanderberg, J.P., 1979. Synchronization of *Plasmodium falciparum* erythrocytic stages in culture. *The Journal of Parasitology*, 65(3), pp.418–420.
- Lamour, S.D. et al., 2014. Changes in metabolic phenotypes of *Plasmodium falciparum* *in vitro* cultures during gametocyte development. *Malaria Journal*, 13(1), p.468.
- Langreth, S.G. et al., 1978. Fine structure of human malaria *in vitro*. *The Journal of Protozoology*, 25(4), pp.443–452.
- Lanzer, M. et al., 2006. Maurer's clefts: a novel multi-functional organelle in the cytoplasm of *Plasmodium falciparum*-infected erythrocytes. *International Journal for Parasitology*, 36(1), pp.23–36.

- Lasonder, E. et al., 2016. Integrated transcriptomic and proteomic analyses of *P. falciparum* gametocytes: molecular insight into sex-specific processes and translational repression. *Nucleic Acids Research*, 44(13), pp.6087–6101.
- Lauer, S. et al., 2000. Vacuolar uptake of host components, and a role for cholesterol and sphingomyelin in malarial infection. *The EMBO Journal*, 19(14), pp.3556–3564.
- Lauer, S.A. et al., 1997. A membrane network for nutrient import in red cells infected with the malaria parasite. *Science*, 276(5315), pp.1122–1125.
- Lauer, S.A., Chatterjee, S. & Haldar, K., 2001. Uptake and hydrolysis of sphingomyelin analogues in *Plasmodium falciparum*-infected red cells. *Molecular and Biochemical parasitology*, 115(2), pp.275–281.
- Laveran A. Un nouveau parasite trouvé dans le sang de malades atteints de fièvre palustre. Origine parasitaire des accidents de l'impaludisme. *Bull Mém Soc Méd Hôpitaux Paris*. 1881;17:158–164.
- Lehtonen, J., Kokko, H. & Parker, G.A., 2016. What do isogamous organisms teach us about sex and the two sexes? *Philosophical Transactions of the Royal Society of London. Series B, Biological Sciences*, 371(1706), p.20150532.
- Li, E., Beard, C. & Jaenisch, R., 1993. Role for DNA methylation in genomic imprinting. *Nature*, 366(6453), pp.362–365.
- Liebisch, G. et al., 2013. Shorthand notation for lipid structures derived from mass spectrometry. *Journal of Lipid Research*, 54(6), pp.1523–1530.
- Lim, L. & McFadden, G.I., 2010. The evolution, metabolism and functions of the apicoplast. *Philosophical Transactions of the Royal Society of London. Series B, Biological Sciences*, 365(1541), pp.749–763.
- Lingwood, D. & Simons, K., 2010. Lipid rafts as a membrane-organizing principle. *Science*, 327(5961), pp.46–50.
- Liu, Jenny et al., 2013. Malaria eradication: is it possible? Is it worth it? Should we do it? *The Lancet. Global Health*, 1(1), pp.e2–3.
- Liu, Jun et al., 2013. Novel thioredoxin-like proteins are components of a protein complex coating the cortical microtubules of *Toxoplasma gondii*. *Eukaryotic Cell*, 12(12), pp.1588–1599.
- Liu, Jun et al., 2006. *Plasmodium falciparum* ensures its amino acid supply with multiple acquisition pathways and redundant proteolytic enzyme systems. *Proceedings of the National Academy of Sciences of the United States of America*, 103(23), pp.8840–8845.
- Liu, Qingyang et al., 2018. The glycosylphosphatidylinositol transamidase complex subunit PbGPI16 of *Plasmodium berghei* is important for inducing experimental cerebral malaria. J. H. Adams, ed. *Infection and Immunity*, 86(8), p.58.

- Liu, Yangjian et al., 2007. Aquaporin 9 is the major pathway for glycerol uptake by mouse erythrocytes, with implications for malarial virulence. *Proceedings of the National Academy of Sciences of the United States of America*, 104(30), pp.12560–12564.
- Loria, P. et al., 1999. Inhibition of the peroxidative degradation of haem as the basis of action of chloroquine and other quinoline antimalarials. *The Biochemical Journal*, 339 ( Pt 2)(Pt 2), pp.363–370.
- Los, D.A. & Murata, N., 2004. Membrane fluidity and its roles in the perception of environmental signals. *Biochimica et Biophysica Acta*, 1666(1-2), pp.142–157.
- Loukin, S.H., Kung, C. & Saimi, Y., 2007. Lipid perturbations sensitize osmotic down-shock activated Ca<sup>2+</sup> influx, a yeast “deletome” analysis. *FASEB Journal : official publication of the Federation of American Societies for Experimental Biology*, 21(8), pp.1813–1820.
- Loy, D.E. et al., 2017. Out of Africa: origins and evolution of the human malaria parasites *Plasmodium falciparum* and *Plasmodium vivax*. *International Journal for Parasitology*, 47(2-3), pp.87–97.
- López-Barragán, M.J. et al., 2011. Directional gene expression and antisense transcripts in sexual and asexual stages of *Plasmodium falciparum*. *BMC Genomics*, 12(1), p.587.
- MacRae, J.I. et al., 2013. Mitochondrial metabolism of sexual and asexual blood stages of the malaria parasite *Plasmodium falciparum*. *BMC Biology*, 11(1), p.67.
- Maguire, P.A., Prudhomme, J. & Sherman, I.W., 1991. Alterations in erythrocyte membrane phospholipid organization due to the intracellular growth of the human malaria parasite, *Plasmodium falciparum*. *Parasitology*, 102 Pt 2, pp.179–186.
- Maier, A.G. & Rug, M., 2013. *In vitro* culturing *Plasmodium falciparum* erythrocytic stages. *Methods in Molecular Biology*, 923(Chapter 1), pp.3–15.
- Maier, A.G. et al., 2008. Exported proteins required for virulence and rigidity of *Plasmodium falciparum*-infected human erythrocytes. *Cell*, 134(1), pp.48–61.
- Maier, A.G. et al., 2018. *Plasmodium falciparum*. *Trends in Parasitology*.
- Mancio-Silva, L. et al., 2017. Nutrient sensing modulates malaria parasite virulence. *Nature*, 547(7662), pp.213–216.
- Mann, T. & Beckers, C., 2001. Characterization of the subpellicular network, a filamentous membrane skeletal component in the parasite *Toxoplasma gondii*. *Molecular and Biochemical Parasitology*, 115(2), pp.257–268.
- Martínez, P. & Morros, A., 1996. Membrane lipid dynamics during human sperm capacitation. *Frontiers in Bioscience : a Journal and Virtual Library*, 1, pp.d103–17.
- Matuschewski, K., 2017. Vaccines against malaria-still a long way to go. *The FEBS Journal*, 284(16), pp.2560–2568.
- Matyash, V. et al., 2008. Lipid extraction by methyl-tert-butyl ether for high-throughput lipidomics. *Journal of Lipid Research*, 49(5), pp.1137–1146.

- Maunakea, A.K. et al., 2010. Conserved role of intragenic DNA methylation in regulating alternative promoters. *Nature*, 466(7303), pp.253–257.
- Maunakea, A.K. et al., 2013. Intragenic DNA methylation modulates alternative splicing by recruiting MeCP2 to promote exon recognition. *Cell Research*, 23(11), pp.1256–1269.
- Mbengue, B. et al., 2016. Inflammatory cytokine and humoral responses to *Plasmodium falciparum* glycosylphosphatidylinositols correlates with malaria immunity and pathogenesis. *Immunity, Inflammation and Disease*, 4(1), pp.24–34.
- McDonald, M.J., Rice, D.P. & Desai, M.M., 2016. Sex speeds adaptation by altering the dynamics of molecular evolution. *Nature*, 531(7593), pp.233–236.
- McFadden, G.I., 2011. The apicoplast. *Protoplasma*, 248(4), pp.641–650.
- Meerstein-Kessel, L. et al., 2018. A multiplex assay for the sensitive detection and quantification of male and female *Plasmodium falciparum* gametocytes. *Malaria Journal*, 17(1), p.441.
- Mi-Ichi, F., Kano, S. & Mitamura, T., 2007. Oleic acid is indispensable for intraerythrocytic proliferation of *Plasmodium falciparum*. *Parasitology*, 134(Pt 12), pp.1671–1677.
- Mi-Ichi, F., Kita, K. & Mitamura, T., 2006. Intraerythrocytic *Plasmodium falciparum* utilize a broad range of serum-derived fatty acids with limited modification for their growth. *Parasitology*, 133(Pt 4), pp.399–410.
- Miao, J. et al., 2017. Sex-specific biology of the human malaria parasite revealed from the proteomes of mature male and female gametocytes. *Molecular & Cellular Proteomics*, p.mcp.M116.061804.
- Michel, C. et al., 1997. Characterization of ceramide synthesis. A dihydroceramide desaturase introduces the 4,5-trans-double bond of sphingosine at the level of dihydroceramide. *The Journal of Biological Chemistry*, 272(36), pp.22432–22437.
- Mignerot, L. & Coelho, S.M., 2016. The origin and evolution of the sexes: novel insights from a distant eukaryotic lineage. *Comptes Rendus Biologies*, 339(7-8), pp.252–257.
- Miguel-Blanco, C. et al., 2015. Imaging-based high-throughput screening assay to identify new molecules with transmission-blocking potential against *Plasmodium falciparum* female gamete formation. *Antimicrobial Agents and Chemotherapy*, 59(6), pp.3298–3305.
- Mitamura, T. et al., 2000. Serum factors governing intraerythrocytic development and cell cycle progression of *Plasmodium falciparum*. *Parasitology International*, 49(3), pp.219–229.
- Mitchell, T.W., Buffenstein, R. & Hulbert, A.J., 2007. Membrane phospholipid composition may contribute to exceptional longevity of the naked mole-rat (*Heterocephalus glaber*): a comparative study using shotgun lipidomics. *Experimental Gerontology*, 42(11), pp.1053–1062.



- Moll, G.N. et al., 1990. Phospholipid asymmetry in the plasma membrane of malaria infected erythrocytes. *Biochemistry and Cell Biology*, 68(2), pp.579–585.
- Moll, G.N. et al., 1988. Phospholipid uptake by *Plasmodium knowlesi* infected erythrocytes. *FEBS Letters*, 232(2), pp.341–346.
- Mons, B. et al., 1985. Synchronized erythrocytic schizogony and gametocytogenesis of *Plasmodium berghei* *in vivo* and *in vitro*. *Parasitology*, 91 ( Pt 3), pp.423–430.
- Moore, K.A. et al., 2017. Quantification of the association between malaria in pregnancy and stillbirth: a systematic review and meta-analysis. *The Lancet. Global Health*, 5(11), pp.e1101–e1112.
- Mordue, D.G. et al., 1999. Invasion by *Toxoplasma gondii* establishes a moving junction that selectively excludes host cell plasma membrane proteins on the basis of their membrane anchoring. *The Journal of Experimental Medicine*, 190(12), pp.1783–1792.
- Mork, L., Czerwinski, M. & Capel, B., 2014. Predetermination of sexual fate in a turtle with temperature-dependent sex determination. *Developmental Biology*, 386(1), pp.264–271.
- Morrisette, N.S., Murray, J.M. & Roos, D.S., 1997. Subpellicular microtubules associate with an intramembranous particle lattice in the protozoan parasite *Toxoplasma gondii*. *Journal of Cell Science*, 110 ( Pt 1), pp.35–42.
- Muhia, D.K. et al., 2003. Multiple splice variants encode a novel adenylyl cyclase of possible plastid origin expressed in the sexual stage of the malaria parasite *Plasmodium falciparum*. *The Journal of Biological Chemistry*, 278(24), pp.22014–22022.
- Mullen, T.D., Hannun, Y.A. & Obeid, L.M., 2012. Ceramide synthases at the centre of sphingolipid metabolism and biology. *The Biochemical Journal*, 441(3), pp.789–802.
- Nawabi, P. et al., 2003. Neutral-lipid analysis reveals elevation of acylglycerols and lack of cholesterol esters in *Plasmodium falciparum*-infected erythrocytes. *Eukaryotic Cell*, 2(5), pp.1128–1131.
- Nee, S., West, S.A. & Read, A.F., 2002. Inbreeding and parasite sex ratios. *Proceedings. Biological Sciences / The Royal Society*, 269(1492), pp.755–760.
- Ng, C.S. et al., 2018. tRNA epitranscriptomics and biased codon are linked to proteome expression in *Plasmodium falciparum*. *Molecular Systems Biology*, 14(10), p.e8009.
- Nolan, S.J. et al., 2018. Novel approaches to kill *Toxoplasma gondii* by exploiting the uncontrolled uptake of unsaturated fatty acids and vulnerability to lipid storage inhibition of the parasite. *Antimicrobial Agents and Chemotherapy*, 62(10), p.823.
- Obaldia, N. et al., 2018. Bone marrow is a major parasite reservoir in *Plasmodium vivax* infection. *mBio*, 9(3), pp.e00625–18.
- Oehring, S.C. et al., 2012. Organellar proteomics reveals hundreds of novel nuclear proteins in the malaria parasite *Plasmodium falciparum*. *Genome Biology*, 13(11), p.R108.

- Okumura-Noji, K. et al., 2001. Cholesteryl ester transfer protein deficiency causes slow egg embryonation of *Schistosoma japonicum*. *Biochemical and Biophysical Research Communications*, 286(2), pp.305–310.
- Page, M.M., Hooper, A.J. & Burnett, J.R., 2016. Anacetrapib for the treatment of dyslipidaemia: the last bastion of the cholesteryl ester transfer protein inhibitors? *Expert Opinion on Pharmacotherapy*, 17(2), pp.275–281.
- Painter, H.J., Carrasquilla, M. & Llinás, M., 2017. Capturing *in vivo* RNA transcriptional dynamics from the malaria parasite *Plasmodium falciparum*. *Genome Research*, 27(6), pp.1074–1086.
- Palacpac, N.M.Q. et al., 2004. Developmental-stage-specific triacylglycerol biosynthesis, degradation and trafficking as lipid bodies in *Plasmodium falciparum*-infected erythrocytes. *Journal of Cell Science*, 117(Pt 8), pp.1469–1480.
- Pankova-Kholmyansky, I. & Flescher, E., 2006. Potential new antimalarial chemotherapeutics based on sphingolipid metabolism. *Chemotherapy*, 52(4), pp.205–209.
- Pankova-Kholmyansky, I. et al., 2003. Ceramide mediates growth inhibition of the *Plasmodium falciparum* parasite. *Cellular and Molecular Life Sciences*, 60(3), pp.577–587.
- Pantaleo, A. et al., 2017. Syk inhibitors interfere with erythrocyte membrane modification during *P. falciparum* growth and suppress parasite egress. *Blood*, 130(8), pp.1031–1040.
- Pantouris, G. et al., 2014. Crystallographic and receptor binding characterization of *Plasmodium falciparum* macrophage migration inhibitory factor complexed to two potent inhibitors. *Journal of Medicinal Chemistry*, 57(20), pp.8652–8656.
- Papalexis, V. et al., 2001. Histidine-rich protein 2 of the malaria parasite, *Plasmodium falciparum*, is involved in detoxification of the by-products of haemoglobin degradation. *Molecular and Biochemical Parasitology*, 115(1), pp.77–86.
- Parkyn Schneider, M. et al., 2017. Disrupting assembly of the inner membrane complex blocks *Plasmodium falciparum* sexual stage development. *PLoS Pathogens*, 13(10), p.e1006659.
- Parsons, J.B. et al., 2011. Metabolic basis for the differential susceptibility of Gram-positive pathogens to fatty acid synthesis inhibitors. *Proceedings of the National Academy of Sciences of the United States of America*, 108(37), pp.15378–15383.
- Pasini, E.M. et al., 2013. Proteomic and genetic analyses demonstrate that *Plasmodium berghei* blood stages export a large and diverse repertoire of proteins. *Molecular & Cellular Proteomics : MCP*, 12(2), pp.426–448.
- Paul, R.E., Coulson, T.N., et al., 2000. Sex determination in malaria parasites. *Science*, 287(5450), pp.128–131.
- Paul, R.E., Doerig, C. & Brey, P.T., 2000. Erythropoiesis and molecular mechanisms for sexual determination in malaria parasites. *IUBMB Life*, 49(4), pp.245–248.

- Paul, R.E.L., Brey, P.T. & Robert, V., 2002. *Plasmodium* sex determination and transmission to mosquitoes. *Trends in Parasitology*, 18(1), pp.32–38.
- Pessi, G., Kociubinski, G. & Mamoun, C.B., 2004. A pathway for phosphatidylcholine biosynthesis in *Plasmodium falciparum* involving phosphoethanolamine methylation. *Proceedings of the National Academy of Sciences of the United States of America*, 101(16), pp.6206–6211.
- Pfaffl, M.W., 2001. A new mathematical model for relative quantification in real-time RT-PCR. *Nucleic Acids Research*, 29(9), p.e45.
- Pham, N.M. et al., 2018. Malaria and the “last” parasite: how can technology help? *Malaria Journal*, 17(1), p.260.
- Phyo, A.P. et al., 2016. Declining efficacy of artemisinin combination therapy against *P. falciparum* malaria on the Thai-Myanmar border (2003-2013): The role of parasite genetic factors. *Clinical Infectious Diseases : an official publication of the Infectious Diseases Society of America*, 63(6), pp.784–791.
- Piel, F.B. et al., 2010. Global distribution of the sickle cell gene and geographical confirmation of the malaria hypothesis. *Nature Communications*, 1(8), p.104.
- Piñero, T.A. et al., 2018. Effect of tamoxifen on the sphingolipid biosynthetic pathway in the different intraerythrocytic stages of the apicomplexa *Plasmodium falciparum*. *Biochemical and Biophysical Research Communications*, 497(4), pp.1082–1088.
- Pollack, Y., Kogan, N. & Golenser, J., 1991. *Plasmodium falciparum*: evidence for a DNA methylation pattern. *Experimental Parasitology*, 72(4), pp.339–344.
- Ponnudurai, T. et al., 1989. Infectivity of cultured *Plasmodium falciparum* gametocytes to mosquitoes. *Parasitology*, 98 Pt 2, pp.165–173.
- Ponnudurai, T. et al., 1986. Synchronization of *Plasmodium falciparum* gametocytes using an automated suspension culture system. *Parasitology*, 93 ( Pt 2), pp.263–274.
- Ponnudurai, T., Leeuwenberg, A.D. & Meuwissen, J.H., 1981. Chloroquine sensitivity of isolates of *Plasmodium falciparum* adapted to *in vitro* culture. *Tropical and Geographical Medicine*, 33(1), pp.50–54.
- Ponts, N. et al., 2013. Genome-wide mapping of DNA methylation in the human malaria parasite *Plasmodium falciparum*. *Cell Host & Microbe*, 14(6), pp.696–706.
- Promeneur, D. et al., 2007. Aquaglyceroporin PbAQP during intraerythrocytic development of the malaria parasite *Plasmodium berghei*. *Proceedings of the National Academy of Sciences of the United States of America*, 104(7), pp.2211–2216.
- Punsawad, C. et al., 2013. Nuclear factor kappa B modulates apoptosis in the brain endothelial cells and intravascular leukocytes of fatal cerebral malaria. *Malaria Journal*, 12(1), p.260.

- Quinn, A.E. et al., 2009. Isolation and development of a molecular sex marker for *Bassiana duperreyi*, a lizard with XX/XY sex chromosomes and temperature-induced sex reversal. *Molecular Genetics and Genomics* : MGG, 281(6), pp.665–672.
- Ralph, S.A. et al., 2004. Tropical infectious diseases: metabolic maps and functions of the *Plasmodium falciparum* apicoplast, 2(3), pp.203–216.
- Ramakrishnan, S. et al., 2012. Apicoplast and endoplasmic reticulum cooperate in fatty acid biosynthesis in apicomplexan parasite *Toxoplasma gondii*. *The Journal of Biological Chemistry*, 287(7), pp.4957–4971.
- Ramakrishnan, S. et al., 2013. Lipid synthesis in protozoan parasites: a comparison between kinetoplastids and apicomplexans. *Progress in Lipid Research*, 52(4), pp.488–512.
- Rawlings, D.J. et al., 1992. Alpha-tubulin II is a male-specific protein in *Plasmodium falciparum*. *Molecular and Biochemical Parasitology*, 56(2), pp.239–250.
- Read, M. et al., 1993. Microtubular organization visualized by immunofluorescence microscopy during erythrocytic schizogony in *Plasmodium falciparum* and investigation of post-translational modifications of parasite tubulin. *Parasitology*, 106 ( Pt 3), pp.223–232.
- Recht, J., Ashley, E.A. & White, N.J., 2018. Use of primaquine and glucose-6-phosphate dehydrogenase deficiency testing: Divergent policies and practices in malaria endemic countries. *PLoS Neglected Tropical Diseases*, 12(4), p.e0006230.
- Reece, S.E., Drew, D.R. & Gardner, A., 2008. Sex ratio adjustment and kin discrimination in malaria parasites. *Nature*, 453(7195), pp.609–614.
- Reid, A.J. et al., 2018. Single-cell RNA-seq reveals hidden transcriptional variation in malaria parasites. *eLife*, 7, p.1600.
- Reynolds, J.M. et al., 2008. Biochemical and genetic analysis of the phosphoethanolamine methyltransferase of the human malaria parasite *Plasmodium falciparum*. *The Journal of Biological Chemistry*, 283(12), pp.7894–7900.
- Rietveld, A. & Simons, K., 1998. The differential miscibility of lipids as the basis for the formation of functional membrane rafts. *Biochimica et Biophysica Acta*, 1376(3), pp.467–479.
- Robert, V. et al., 1996. Effect of gametocyte sex ratio on infectivity of *Plasmodium falciparum* to *Anopheles gambiae*. *Transactions of the Royal Society of Tropical Medicine and Hygiene*, 90(6), pp.621–624.
- Robert, V. et al., 2003. Sex ratio of *Plasmodium falciparum* gametocytes in inhabitants of Dielmo, Senegal. *Parasitology*, 127(Pt 1), pp.1–8.
- Roncalés, M. et al., 2012. Comparison and optimization of different methods for the *in vitro* production of *Plasmodium falciparum* gametocytes. *Journal of Parasitology Research*, 2012(5), pp.927148–7.

- Rosenthal, P.J. & Meshnick, S.R., 1996. Hemoglobin catabolism and iron utilization by malaria parasites. *Molecular and Biochemical Parasitology*, 83(2), pp.131–139.
- Ross, A.C. et al., 1984. Selective inhibition of acyl coenzyme A:cholesterol acyltransferase by compound 58-035. *The Journal of Biological Chemistry*, 259(2), pp.815–819.
- Roth, J.M. et al., 2018. *Plasmodium falciparum* gametocyte dynamics after pyronaridine-artesunate or artemether-lumefantrine treatment. *Malaria Journal*, 17(1), p.223.
- Rougeron, V. et al., 2013. Epistatic interactions between apolipoprotein E and hemoglobin S genes in regulation of malaria parasitemia. *PloS One*, 8(10), p.e76924.
- Ruecker, A. et al., 2014. A male and female gametocyte functional viability assay to identify biologically relevant malaria transmission-blocking drugs. *Antimicrobial Agents and Chemotherapy*, 58(12), pp.7292–7302.
- Rug, M. & Maier, A.G., 2013. Transfection of *Plasmodium falciparum*. *Methods in Molecular Biology*, 923(Chapter 6), pp.75–98.
- Rutledge, G.G. et al., 2017. *Plasmodium malariae* and *P. ovale* genomes provide insights into malaria parasite evolution. *Nature*, 542(7639), pp.101–104.
- Samuel, B.U. et al., 2001. The role of cholesterol and glycosylphosphatidylinositol-anchored proteins of erythrocyte rafts in regulating raft protein content and malarial infection. *The Journal of Biological Chemistry*, 276(31), pp.29319–29329.
- Sanders, P.R. et al., 2005. Distinct protein classes including novel merozoite surface antigens in Raft-like membranes of *Plasmodium falciparum*. *The Journal of Biological Chemistry*, 280(48), pp.40169–40176.
- Santolamazza, F. et al., 2017. Detection of *Plasmodium falciparum* male and female gametocytes and determination of parasite sex ratio in human endemic populations by novel, cheap and robust RTqPCR assays. *Malaria Journal*, 16(1), p.468.
- Santos-Rosa, H. et al., 2002. Active genes are tri-methylated at K4 of histone H3. *Nature*, 419(6905), pp.407–411.
- Schneider, P. et al., 2015. Quantification of female and male *Plasmodium falciparum* gametocytes by reverse transcriptase quantitative PCR. *Molecular and Biochemical Parasitology*, 199(1-2), pp.29–33.
- Schrevel, J., Asfaux-Foucher, G. & Bafort, J.M., 1977. Ultrastructural study of multiple mitoses during sporogony of *Plasmodium b. berghei*. *Journal of Ultrastructure Research*, 59(3), pp.332–350.
- Schroeder, R.J. et al., 1998. Cholesterol and sphingolipid enhance the Triton X-100 insolubility of glycosylphosphatidylinositol-anchored proteins by promoting the formation of detergent-insoluble ordered membrane domains. *The Journal of Biological Chemistry*, 273(2), pp.1150–1157.
- Schübeler, D., 2015. Function and information content of DNA methylation. *Nature*, 517(7534), pp.321–326.

- Schwank, S., Sutherland, C.J. & Drakeley, C.J., 2010. Promiscuous expression of  $\alpha$ -tubulin II in maturing male and female *Plasmodium falciparum* gametocytes. *PloS One*, 5(12), p.e14470.
- Serricchio, M. & Bütikofer, P., 2012. An essential bacterial-type cardiolipin synthase mediates cardiolipin formation in a eukaryote. *Proceedings of the National Academy of Sciences of the United States of America*, 109(16), pp.E954–61.
- Serricchio, M. & Bütikofer, P., 2013. Phosphatidylglycerophosphate synthase associates with a mitochondrial inner membrane complex and is essential for growth of *Trypanosoma brucei*. *Molecular Microbiology*, 87(3), pp.569–579.
- Sharma, Arvind & Sharma, Amit, 2015. *Plasmodium falciparum* mitochondria import tRNAs along with an active phenylalanyl-tRNA synthetase. *The Biochemical Journal*, 465(3), pp.459–469.
- Shaw, W.R. & Catteruccia, F., 2018. Vector biology meets disease control: using basic research to fight vector-borne diseases. *Nature Microbiology*, 77, p.171.
- Sheffield, H.G. & Melton, M.L., 1968. The fine structure and reproduction of *Toxoplasma gondii*. *The Journal of Parasitology*, 54(2), pp.209–226.
- Sherman, I.W., 1979. Biochemistry of *Plasmodium* (malarial parasites). *Microbiological Reviews*, 43(4), pp.453–495.
- Sherman, I.W., 1977. Transport of amino acids and nucleic acid precursors in malarial parasites. *Bulletin of the World Health Organization*, 55(2-3), pp.211–225.
- Sherman, I.W., Prudhomme, J. & Tait, J.F., 1997. Altered membrane phospholipid asymmetry in *Plasmodium falciparum*-infected erythrocytes. *Parasitology Today*, 13(6), pp.242–243.
- Siddique, M.M. et al., 2012. Ablation of dihydroceramide desaturase confers resistance to etoposide-induced apoptosis *in vitro*. *PloS One*, 7(9), p.e44042.
- Simons, K. & Toomre, D., 2000. Lipid rafts and signal transduction. *Nature Reviews. Molecular Cell Biology*, 1(1), pp.31–39.
- Simões, A.P., Roelofsen, B. & Op den Kamp, J.A., 1992. Lipid compartmentalization in erythrocytes parasitized by *Plasmodium spp.* *Parasitology Today*, 8(1), pp.18–21.
- Sinclair, A.H. et al., 1990. A gene from the human sex-determining region encodes a protein with homology to a conserved DNA-binding motif. *Nature*, 346(6281), pp.240–244.
- Sinden, R.E., 1982. Gametocytogenesis of *Plasmodium falciparum in vitro*: an electron microscopic study. *Parasitology*, 84(1), pp.1–11.
- Sinden, R.E., 2017. Targeting the parasite to suppress malaria transmission. *Advances in Parasitology*, 97, pp.147–185.

- Sinden, R.E. et al., 1978. Gametocyte and gamete development in *Plasmodium falciparum*. *Proceedings of the Royal Society of London. Series B, Biological Sciences*, 201(1145), pp.375–399.
- Sinden, R.E., Hartley, R.H. & Winger, L., 1985. The development of *Plasmodium* ookinetes *in vitro*: an ultrastructural study including a description of meiotic division. *Parasitology*, 91 ( Pt 2), pp.227–244.
- Sinha, A. et al., 2014. A cascade of DNA-binding proteins for sexual commitment and development in *Plasmodium*. *Nature*, 507(7491), pp.253–257.
- Slater, A.F. & Cerami, A., 1992. Inhibition by chloroquine of a novel haem polymerase enzyme activity in malaria trophozoites. *Nature*, 355(6356), pp.167–169.
- Smalley, M.E. & Sinden, R.E., 1977. *Plasmodium falciparum* gametocytes: their longevity and infectivity. *Parasitology*, 74(1), pp.1–8.
- Smith, J.D. et al., 1995. Switches in expression of *Plasmodium falciparum* var genes correlate with changes in antigenic and cytoadherent phenotypes of infected erythrocytes. *Cell*, 82(1), pp.101–110.
- Snow, R.W., 2015. Global malaria eradication and the importance of *Plasmodium falciparum* epidemiology in Africa. *BMC Medicine*, 13(1), p.23.
- Sonda, S. et al., 2001. Cholesterol esterification by host and parasite is essential for optimal proliferation of *Toxoplasma gondii*. *The Journal of Biological Chemistry*, 276(37), pp.34434–34440.
- Sowunmi, A. et al., 2008. Activities of artemether-lumefantrine and amodiaquine-sulfalene-pyrimethamine against sexual-stage parasites in *falciparum* malaria in children. *Chemotherapy*, 54(3), pp.201–208.
- Sowunmi, A. et al., 2009. Population structure of *Plasmodium falciparum* gametocyte sex ratios in malarious children in an endemic area. *Parasitology International*, 58(4), pp.438–443.
- Spork, S. et al., 2009. An unusual ERAD-like complex is targeted to the apicoplast of *Plasmodium falciparum*. *Eukaryotic Cell*, 8(8), pp.1134–1145.
- Srivastava, A. et al., 2015. Host reticulocytes provide metabolic reservoirs that can be exploited by malaria parasites. *PLoS Pathogens*, 11(6), p.e1004882.
- Srivastava, A. et al., 2017. Metabolomics-based elucidation of active metabolic pathways in erythrocytes and HSC-derived reticulocytes. *Journal of Proteome Research*, 16(4), pp.1492–1505.
- Stone, W. et al., 2017. A molecular assay to quantify male and female *Plasmodium falciparum* gametocytes: results from 2 randomized controlled trials using primaquine for gametocyte clearance. *The Journal of Infectious Diseases*, 216(4), pp.457–467.

- Su, X.Z. et al., 1995. The large diverse gene family var encodes proteins involved in cytoadherence and antigenic variation of *Plasmodium falciparum*-infected erythrocytes. *Cell*, 82(1), pp.89–100.
- Sullivan, D.J., 2002. Theories on malarial pigment formation and quinoline action. *International Journal for Parasitology*, 32(13), pp.1645–1653.
- Sundararaman, S.A. et al., 2016. Genomes of cryptic chimpanzee *Plasmodium* species reveal key evolutionary events leading to human malaria. *Nature Communications*, 7(1), p.11078.
- Suplick, K. et al., 1988. Molecular cloning and partial sequence of a 5.8 kilobase pair repetitive DNA from *Plasmodium falciparum*. *Molecular and Biochemical Parasitology*, 30(3), pp.289–290.
- Suplick, K., Morrisey, J. & Vaidya, A.B., 1990. Complex transcription from the extrachromosomal DNA encoding mitochondrial functions of *Plasmodium yoelii*. *Molecular and Cellular Biology*, 10(12), pp.6381–6388.
- Sutherland, C.J. et al., 2010. Two nonrecombining sympatric forms of the human malaria parasite *Plasmodium ovale* occur globally. *The Journal of Infectious Diseases*, 201(10), pp.1544–1550.
- Tadesse, F.G. et al., 2018. Gametocyte sex ratio: the key to understanding *Plasmodium falciparum* transmission? *Trends in Parasitology*.
- Tao, D. et al., 2014. Sex-partitioning of the *Plasmodium falciparum* stage V gametocyte proteome provides insight into *falciparum*-specific cell biology. *Molecular & Cellular Proteomics : MCP*, 13(10), pp.2705–2724.
- Thanh, N.V. et al., 2017. Rapid decline in the susceptibility of *Plasmodium falciparum* to dihydroartemisinin-piperaquine in the south of Vietnam. *Malaria Journal*, 16(1), p.27.
- Tibúrcio, M. et al., 2015. Erythrocyte remodeling by *Plasmodium falciparum* gametocytes in the human host interplay. *Trends in Parasitology*.
- Tokumasu, F. et al., 2014. Inward cholesterol gradient of the membrane system in *P. falciparum*-infected erythrocytes involves a dilution effect from parasite-produced lipids. *Biology Open*, 3(6), pp.529–541.
- Torisawa, Y.-S. et al., 2014. Bone marrow-on-a-chip replicates hematopoietic niche physiology in vitro. *Nature Methods*, 11(6), pp.663–669.
- Trager, W. & Jensen, J.B., 1976. Human malaria parasites in continuous culture. *Science*, 193(4254), pp.673–675.
- Tran, P.N. et al., 2014. A female gametocyte-specific ABC transporter plays a role in lipid metabolism in the malaria parasite. *Nature Communications*, 5, p.4773.
- Tran, P.N. et al., 2016. Changes in lipid composition during sexual development of the malaria parasite *Plasmodium falciparum*. *Malaria Journal*, 15(1), p.73.



- Urao, T. et al., 1999. A transmembrane hybrid-type histidine kinase in arabidopsis functions as an osmosensor. *Plant Cell*, 11(9), pp.1743–1754.
- Vaidya, A.B., Akella, R. & Suplick, K., 1989. Sequences similar to genes for two mitochondrial proteins and portions of ribosomal RNA in tandemly arrayed 6-kilobase-pair DNA of a malarial parasite. *Molecular and Biochemical Parasitology*, 35(2), pp.97–107.
- van den Berghe, L., 1954. The history of the discovery of *Plasmodium berghei*. *Indian Journal of Malariology*, 8(4), pp.241–243.
- van den Brink-van der Laan, E., Killian, J.A. & de Kruijff, B., 2004. Nonbilayer lipids affect peripheral and integral membrane proteins via changes in the lateral pressure profile. *Biochimica et Biophysica Acta*, 1666(1-2), pp.275–288.
- Van der Schaft, P.H. et al., 1987. Phospholipid organization in monkey erythrocytes upon *Plasmodium knowlesi* infection. *Biochimica et Biophysica Acta*, 901(1), pp.1–14.
- van Dooren, G.G. & Striepen, B., 2013. The algal past and parasite present of the apicoplast. *Annual Review of Microbiology*, 67(1), pp.271–289.
- van Meer, G., Voelker, D.R. & Feigenson, G.W., 2008. Membrane lipids: where they are and how they behave. *Nature Reviews. Molecular Cell Biology*, 9(2), pp.112–124.
- Vance, J.E. & Steenbergen, R., 2005. Metabolism and functions of phosphatidylserine. *Progress in Lipid Research*, 44(4), pp.207–234.
- Vanderberg, J.P., 1975. Development of infectivity by the *Plasmodium berghei* sporozoite. *The Journal of Parasitology*, 61(1), pp.43–50.
- Vaughan, A.M. et al., 2009. Type II fatty acid synthesis is essential only for malaria parasite late liver stage development. *Cellular Microbiology*, 11(3), pp.506–520.
- Vieira, C.R. et al., 2010. Dihydrosphingomyelin impairs HIV-1 infection by rigidifying liquid-ordered membrane domains. *Chemistry & Biology*, 17(7), pp.766–775.
- Vielemeyer, O. et al., 2004. Neutral lipid synthesis and storage in the intraerythrocytic stages of *Plasmodium falciparum*. *Molecular and Biochemical Parasitology*, 135(2), pp.197–209.
- Vincke, I.H., 1954. Natural history of *Plasmodium berghei*. *Indian Journal of Malariology*, 8(4), pp.245–256.
- Visser, B.J. et al., 2013. Serum lipids and lipoproteins in malaria-a systematic review and meta-analysis. *Malaria Journal*, 12(1), p.442.
- Vivarès, C.P. et al., 2002. Functional and evolutionary analysis of a eukaryotic parasitic genome. *Current Opinion in Microbiology*, 5(5), pp.499–505.
- Vlachou, D. et al., 2004. Real-time, *in vivo* analysis of malaria ookinete locomotion and mosquito midgut invasion. *Cellular Microbiology*, 6(7), pp.671–685.

- Walliker, D. et al., 1987. Genetic analysis of the human malaria parasite *Plasmodium falciparum*. *Science*, 236(4809), pp.1661–1666.
- Walzer, K.A. et al., 2018. Single-cell analysis reveals distinct gene expression and heterogeneity in male and female *Plasmodium falciparum* gametocytes. *mSphere*, 3(2), p.E5.
- Wang, Zenglei et al., 2014. A flow cytometry-based quantitative drug sensitivity assay for all *Plasmodium falciparum* gametocyte stages. *PloS One*, 9(4), p.e93825.
- Wang, Zhensheng et al., 2009. Epitope mapping of monoclonal antibody 1B9 against *Plasmodium falciparum*-derived macrophage migration inhibitory factor. *Immunological Investigations*, 38(5), pp.422–433.
- Weber, J.H. et al., 2004. Adenylyl cyclases from *Plasmodium*, *Paramecium* and *Tetrahymena* are novel ion channel/enzyme fusion proteins. *Cellular Signalling*, 16(1), pp.115–125.
- Wein, S. et al., 2018. Contribution of the precursors and interplay of the pathways in the phospholipid metabolism of the malaria parasite. *Journal of Lipid Research*, 59(8), pp.1461–1471.
- Welte, M.A. & Gould, A.P., 2017. Lipid droplet functions beyond energy storage. *Biochimica et Biophysica Acta. Molecular and Cell Biology of Lipids*, 1862(10 Pt B), pp.1260–1272.
- White, N.J. et al., 2014. Malaria. *Lancet*, 383(9918), pp.723–735.
- Wiley, J.D. et al., 2015. Isoprenoid precursor biosynthesis is the essential metabolic role of the apicoplast during gametocytogenesis in *Plasmodium falciparum*. *Eukaryotic Cell*, 14(2), pp.128–139.
- Wilson, R.J. et al., 1996. Complete gene map of the plastid-like DNA of the malaria parasite *Plasmodium falciparum*. *Journal of Molecular Biology*, 261(2), pp.155–172.
- Witola, W.H. et al., 2006. Localization of the phosphoethanolamine methyltransferase of the human malaria parasite *Plasmodium falciparum* to the Golgi apparatus. *The Journal of Biological Chemistry*, 281(30), pp.21305–21311.
- Wolf, Y.I. & Koonin, E.V., 2013. Genome reduction as the dominant mode of evolution. *BioEssays : news and reviews in molecular, cellular and developmental biology*, 35(9), pp.829–837.
- World Health Organization, 2018. World Malaria Report.
- Yam, X.Y. et al., 2013. Proteomic analysis of detergent-resistant membrane microdomains in trophozoite blood stage of the human malaria parasite *Plasmodium falciparum*. *Molecular & Cellular Proteomics : MCP*, 12(12), pp.3948–3961.
- Yeoh, L.M. et al., 2017. Comparative transcriptomics of female and male gametocytes in *Plasmodium berghei* and the evolution of sex in alveolates. *BMC Genomics*, 18(1), p.734.
- Yin, Y. et al., 2017. Impact of cytosine methylation on DNA binding specificities of human transcription factors. *Science*, 356(6337), p.eaaj2239.

- Yoeli, M., 1965. Studies on *Plasmodium berghei* in nature and under experimental conditions. *Transactions of the Royal Society of Tropical Medicine and Hygiene*, 59, pp.255–276.
- Yokoyama, S., 2014. A potential screening factor for accumulation of cholesteryl ester transfer protein deficiency in East Asia: *Schistosoma japonicum*. *Biochimica et Biophysica Acta*, 1841(4), pp.495–504.
- Yu, M. et al., 2008. The fatty acid biosynthesis enzyme FabI plays a key role in the development of liver-stage malarial parasites. *Cell Host & Microbe*, 4(6), pp.567–578.
- Zhu, J. et al., 2012. Ikb- $\zeta$  plays an important role in the ERK-dependent dysregulation of malaria parasite GPI-induced IL-12 expression. *IUBMB Life*, 64(2), pp.187–193.
- Zhu, J. et al., 2009. MAPK-activated protein kinase 2 differentially regulates *Plasmodium falciparum* glycosylphosphatidylinositol-induced production of tumor necrosis factor- $\alpha$  and interleukin-12 in macrophages. *The Journal of Biological Chemistry*, 284(23), pp.15750–15761.
- Zuzarte-Luis, V. et al., 2017. Dietary alterations modulate susceptibility to *Plasmodium* infection. *Nature Microbiology*, 2(12), pp.1600–1607.